Measuring water surface width at the national scale for England and Wales using remote sensing and statistical modelling

Liam D. Clark, BA (Hons.), MSc

Thesis submitted to the University of Nottingham for the degree of Doctor of Philosophy

April 2018

Abstract

The vertical transport of CO_2 from rivers to the atmosphere has only recently been identified as a significant component of global greenhouse gas (GHG) budgets. Headwater streams are responsible for a disproportionately large quantity of total CO_2 evasion, yet are difficult to map comprehensively due to their width being smaller than the spatial resolution of most remotely sensed imagery that is currently used for this application. The need to capture these streams is further underlined by recent research that has identified water surface area as a key control of CO_2 evasion rate.

The challenge of extracting a complete representation of surface waters from remotely sensed imagery means that this critical component of CO_2 models is currently poorly understood. This thesis addressed this by applying the novel combination of fuzzy classification, one-class classification, and contouring to derive super-resolution maps of surface waters from high resolution colour infrared aerial imagery. The methodology produced maps of sufficient accuracy to capture a significant proportion of headwater streams, which were measured using a semi-automated GIS-driven technique.

Water surface width (WSW) was then estimated at the national scale using a predictive model that utilised widely available or readily calculable landscape variables in conjunction with image-based measurements of WSW. The multiple linear regression model accounted for a high proportion of the variation in WSW (adjusted $R^2 = 0.75$, $p < 0.01$), allowing the lack of a national-scale dataset of WSW for England and Wales to be addressed. The main explanatory variables included catchment area, hydrological source of flow, rainfall, relief,

and for the first time in a predictive model of WSW, a metric quantifying the extent to which the river has been modified.

WSW predictions were then applied to CO_2 evasion modelling to predict the quantity of CO_2 transferred from rivers to the atmosphere in England and Wales, based on previous research that identified the surface area covered by rivers to be a key control of vertical transport. Findings improved on previous attempts at modelling CO_2 evasion for England and Wales, and suggest that transfers are currently underestimated, with consequent ramifications for mitigation strategies in the future.

Acknowledgments

This research was supported by a three-year studentship from the School of Geography at the University of Nottingham, for which I will always be extremely grateful.

I would like to express my gratitude to Dr. Doreen Boyd for accepting me as her research student, and for providing me with both the opportunity to be part of this research and the guidance that was essential in seeing the thesis through to its completion. I would also like to thank Professor Giles Foody and Professor Colin Thorne at the University of Nottingham, and Dr. Barry Rawlins at the British Geological Survey, for their invaluable advice on a wide range of issues related to my thesis. I am also very grateful to the Internal Assessor, Dr. Simon Gosling, for providing numerous suggestions and insights as part of the annual review process.

I would also like to thank the School of Geography at the University of Nottingham as a whole. Having studied towards three different degrees within the school, the list of individuals who have made a substantial contribution both to my academic progression and overall enjoyment of my time in Nottingham is significant. In particular, thanks go to John Beaverstock (BA Geography tutor); and Gary Priestnall, Jeremy Morley, and Paul Aplin (MSc GIS contributors).

Finally, this research would not have been possible without the unwavering support of my family and friends. Thanks in particular go to Joseph Bailey for always being there to bounce ideas off and to celebrate/commiserate with throughout the inevitable ups and downs of life as a PhD student, and latterly as a member of staff in the School of Geography. I am also

grateful to those who were brave enough to simultaneously share a workplace and a house with me, namely Kate Whiston, Jeremy Rison, and Mark Stevenson.

Finally, my thanks go to my mum, for whom I do not have the words to express how I truly feel. You are my greatest inspiration and biggest supporter, and without your unwavering belief in me I am not entirely sure that I would have reached the point at which I felt capable of tackling the challenges that have faced me over the years, whether academic or personal.

Contents

Abstract ..... **i**

Acknowledgments ..... **iii**

Contents ..... **v**

List of Figures ..... **x**

List of Tables ..... **xv**

List of Equations ..... **xviii**

List of Abbreviations ..... **xix**

Chapter 1 ***Introduction*** **1**

1.1 Novel aspects of the research 5

1.2 Aims and objectives 5

1.3 Thesis structure 7

Chapter 2 ***Literature Review*** **11**

2.1 Estimating GHG evasion from rivers and streams 11

2.1.1 Evasion from headwater streams and the importance of spatial scale 14

2.2 Measuring water surface width 17

2.3 The controls of water surface width 21

2.3.1 Discharge and catchment area 22

2.3.2 Climate 23

2.3.3 Land cover 24

2.3.4 Channel boundary material and sediment transport 26

2.3.5 Hydrological source of flow 28

2.3.6 Channel gradient 29

2.3.7 Elevation 29

2.3.8 Human modification 30

2.4 The applicability of remote sensing 31

2.4.1 The spectral properties of inland surface waters 34

2.4.2 Extracting features from aerial imagery 37

2.5 Conclusion 43

Chapter 3 *Extracting surface waters from aerial imagery* 45

3.1 Study site 47

3.2 Aerial imagery 55

3.2.1 CIR aerial imagery for England and Wales 56

3.2.2 Contextualising aerial imagery with river flow data 57

3.2.3 Assessing intra-image variation in the spectral reflectance of water 60

3.2.4 The impact of spatial resolution on classification accuracy 61

3.3 Comparative analysis of classification techniques 64

3.4 Combining one-class classification, fuzzy classification, and contouring for super-resolution mapping 76

3.4.1 Setting appropriate parameters for fuzzy classification 76

3.4.2 Applying contouring to produce super-resolution maps of surface waters ... 77

3.4.3 Classification technique resource requirements 82

3.5 Assessing the accuracy of the extracted surface water features 85

3.5.1 Quantifying the impact of overhanging vegetation 87

3.6 Chapter summary 92

Chapter 4 *Image-based measurement of water surface width* 94

4.1 Post-processing to improve the accuracy of SRM-derived surface waters 96

4.2 Deriving centrelines from Ordnance Survey data 97

4.2.1 Current GIS-based methods for creating river centrelines 100

4.2.2 Methodology for centreline creation 104

4.3 Measuring perpendicular to the direction of flow 106

4.3.1 Existing methods for creating perpendicular measurements of width 106

4.3.2 Generating width measurements at specified points 107

4.4 Aggregating at-a-station measurements to derive maximum effective width 111

4.5 Validating image-based WSW measurements in the field 114

4.6 Chapter summary 118

Chapter 5 *Predicting water surface width for England and Wales* 121

5.1 The selection of explanatory variables to predict WSW 122

5.2 Using multiple linear regression to model and predict WSW 127

5.2.1 Testing MLR assumptions 129

5.2.2 Identifying second-order interactions between explanatory variables 132

5.2.3 Order of deletion 132

5.3 Model results 134

5.3.1 Model evaluation 136

5.4 Critical reflections on MLR 140

5.5 Predictions for England and Wales 142

5.6 Chapter summary 148

Chapter 6 *Estimating fluvial CO_2 evasion in England and Wales* 149

6.1 Methods for calculating fluvial CO_2 evasion 150

6.2 Field data for England and Wales 153

6.3 Model results 155

6.3.1 Full CO_2 evasion model 157

6.3.2 CO_2 evasion model with water surface area removed 160

6.3.3 Constraining CO_2 evasion both spatially and temporally 161

6.3.4 Model comparison 162

6.4 Spatial distribution of CO_2 evasion across England and Wales 164

6.5 Chapter summary 168

Chapter 7 *Discussion* 169

7.1 An assessment of study aims and objectives 169

7.1.1 Aim 1: Extract a high-resolution dataset of rivers and streams from aerial imagery for the chosen study area. 169

7.1.2 Aim 2: Make accurate, direct image-based measurements of WSW using a GIS-driven technique 173

7.1.3 Aim 3: Create a model capable of accurately predicting WSW for England and Wales 175

7.1.4 Aim 4: Determine the impact of incorporating WSW measurements into fluvial CO_2 evasion models for England and Wales 179

7.2 Future work 183

7.2.1 Addressing the issue of staticity 183

7.2.2 GHG evasion 185

7.2.3 Developments in remote sensing technologies 187

7.2.4 Global scale predictions of WSW 192

7.3 Conclusion 194

References **196**

Glossary of Terms **229**

Appendix **232**

A.1 Workflow Diagrams 232

A.2 R plot(lm) output for minimal adequate multiple linear regression model of WSW 238

List of Figures

Figure 1.1.1 The water surface width (WSW) geomorphological attribute of a river as viewed a) at a river cross-section and b) from an aerial perspective. 2

Figure 1.3.1 Overview of workflow with linkages and relationships between discrete methodological chapters identified 10

Figure 2.4.1 Spectral reflectance of natural land cover, with the CIR bands highlighted by the red shape (Aronoff, 2004; CIR emphasis added). 35

Figure 3.1.1 Location of chosen study site within Great Britain (bounding box coordinates are SW corner; 260000, 340000, and NE corner; 370000, 360000). 49

Figure 3.1.2 Major hydrological catchments across the study site. 51

Figure 3.1.3 Variation in explanatory variables of WSW across the study site (identified with bounding box). From top to bottom, these panels represent; a) catchment area for each IHU Group (Centre for Ecology and Hydrology, 2015b); b) rainfall in May 2009 (period of aerial imagery capture); c) land cover. 53

Figure 3.1.4 Variation in explanatory variables of WSW across the study site (identified with bounding box). From top to bottom, these panels represent; a) hydrological source of flow

(BFI); b) channel gradient; c) elevation; d) human modification of river channels (HMS score). 54

Figure 3.2.1 NRFA stations contained within the study area..... 57

Figure 3.2.2 A comparison of mean daily flow with gauged flow at time of data capture at NRFA gauging stations a) 67006 River Alwen at Druid, and b) 68004 Wistaston Brook at Marshfield Bridge. Red dashed lines indicate the date at which aerial imagery were obtained. 59

Figure 3.2.3 Visual comparison of surface waters from a) WorldView-2 imagery, and b) CIR imagery for a reach of the River Trent (WSW ≈ 80 m) in Nottingham, England; NE corner coordinate 455340, 336069. 63

Figure 3.3.1 Errors of omission (underprediction) and commission (overprediction) when measuring WSW using aerial imagery (adapted from Fisher *et al.*, 2013). Accurate field measurement of actual width is assumed. 67

Figure 3.3.2 Errors of commission caused by the comparable spectral signature of water, shadow, and roads 70

Figure 3.3.3 Errors of omission caused by the presence of overhanging vegetation and suspended material in the channel..... 71

Figure 3.3.4 A comparison of a) local and b) global approaches to classification. Local classification creates a separate training dataset for each image, whereas global classification creates and applies a single training dataset to the entire study area..... 72

Figure 3.4.1 Monotonically increasing sigmoid function with control points a, b, c and d. ... 77

Figure 3.4.2 Example of transect used to inform the selecting of a boundary value for the contouring process. Values range from 0 to 1 and represent the degree of membership to the water land cover class. ... 78

Figure 3.4.3 The impact of incorrectly specifying the threshold value for the contouring process, with contour values of 0.8 and 0.2 displayed. ... 80

Figure 3.4.4 Errors of commission resulting from the specification of an incorrect contouring threshold of 0.2. ... 81

Figure 3.4.5 The final product of the super-resolution mapping process (SRM). ... 81

Figure 3.5.1 Example of a classification uncertainty image used to perform in-process accuracy assessment of the classification approach ... 86

Figure 3.5.2 Overhanging vegetation limits the extent of the SRM-derived surface water dataset (red) and prevents the true extent of surface waters (purple line) from being captured. ... 88

Figure 3.5.3 Histogram depicting the NDVI values of WSW measurement points that were omitted from SRM-derived surface waters dataset. ... 90

Figure 3.5.4 The relationship between the total river length missing from each sub-catchment (n=398) and the mean NDVI score ($R^2 = 0.44$, $p < 0.05$). ... 91

Figure 4.2.1 Visual comparison of how surface waters are represented by the OS VectorMap District and OS Meridian 2 products. 99

Figure 4.2.2 A comparison of the OS VMD-derived centreline (blue) with SRM output (red). 106

Figure 4.4.1 aggregated WSW measurements for the study site using IHU Section data (Centre for Ecology and Hydrology, 2015b), showing a) variation in mean WSW, and b) variation in maximum WSW. White indicates an area with no WSW measurements due to no rivers being present. 113

Figure 4.5.1 Field validation measurement locations 116

Figure 4.5.2 Comparison of image-based and at-a-station field measurements of WSW (n = 51, RMSE = 0.87m, MAPE = 11.17%). 117

Figure 5.3.1 Comparison of observed and predicted values of MEW from the minimal adequate model (n – 237). 140

Figure 5.5.1 Predicted mean WSW in England and Wales (data visualised using IHU Group polygons and Jenks natural breaks). 143

Figure 5.5.2 Predicted range in WSW in England and Wales (data visualised using IHU Group polygons and Jenks natural breaks). 144

Figure 6.2.1 Location of $\boldsymbol{KCO2}$ field measurements (n = 28). 154

Figure 6.4.1 Predicted total CO_2 evasion in England and Wales (data visualised using IHU Group polygons and Jenks natural breaks) 165

Figure 6.4.2 Predicted total CO2 evasion in England and Wales (data visualised using IHU Group polygons and the same class breaks as Figure 6.4.1 to aid with direct comparison) 167

List of Tables

Table 2.4.1 Recommended methods for the classification of surface waters based on the varying spectral reflectance of differing water types (adapted from (Frenette *et al.*, 2012; Sun *et al.*, 2012). 36

Table 3.1.1 Summary statistics for the major hydrological catchments found in the study site. 51

Table 3.2.1 Descriptive statistics derived from flow hydrographs at all NRFA gauging stations within the study site (n = 10). All units for MDF are m^3 59

Table 3.3.1 Comparative analysis of classification accuracy for commonly applied techniques. 69

Table 3.3.2 comparison of image classification techniques 74

Table 3.4.1 resource requirements for each stage of the image classification process. 83

Table 4.2.1 Comparison of remote sensing and GIS-based programs for centreline derivation 101

Table 4.3.1 Comparison of techniques for measuring perpendicular to the direction of flow 108

Table 5.1.1 Initial selection of explanatory variables and proposed data source. 124

Table 5.2.1 methods for testing the assumptions of ordinary least squares linear regression 130

Table 5.3.1 Descriptive statistics for measurements of WSW and landscape data..... 134

Table 5.3.2 Summary of minimal adequate multiple linear regression model of WSW (n = 231) generated in R (R Core Team, 2017). 135

Table 5.3.3 Summary of multiple linear regression model of WSW with BFI and HMS excluded from process (n = 231) 137

Table 5.3.4 AIC diagnostics for selecting the most appropriate model for WSW prediction 138

Table 5.5.1 Size distribution of rivers in England and Wales as predicted by MLR WSW model 146

Table 6.3.1 Summary statistics of WSW and $\boldsymbol{KCO2}$ data used to model CO_2 evasion. 156

Table 6.3.2 $\boldsymbol{FCO2}$ model for England and Wales using water surface area (WSW) as an explanatory variable 157

Table 6.3.3 $\boldsymbol{FCO2}$ model for England and Wales with water surface area excluded from initial variable selection 160

Table 6.3.4 $\boldsymbol{FCO2}$ model for England and Wales constrained for seasonality.....162

Table 6.3.5 Fluvial CO2 evasion model comparison of R^2, adjusted-R^2, and AIC.....163

List of Equations

Equation 2.1 Power-law relationship between channel width ($\boldsymbol{W}$) and mean annual discharge ($\boldsymbol{Q}$) 22

Equation 3.1 Normalised Difference Vegetation Index (NDVI) calculation using near-infrared (NIR) and red image bands..... 88

Equation 5.1 Expression of multiple linear regression (MLR) modelling..... 128

Equation 6.1 Carbon mass balance; all units are the same (normally Pg C/yr) 150

Equation 6.2 Net carbon dioxide gas exchange ($\boldsymbol{FCO2}$) between rivers and the atmosphere 151

Equation 6.3 Gradient between fluvial CO_2 and atmospheric CO_2 ($\Delta\mathbf{CO2}$) 152

List of Abbreviations

AAS	at-a-station
AIC	Akaike information criterion
BIC	Bayesian information criterion
BFI	baseflow index
CA	catchment area
CH_4	methane
CIR	colour infrared
CO_2	carbon dioxide
DHG	downstream hydraulic geometry
DOC	dissolved organic carbon
DSWE	dynamic surface water extent
EU	European Union
F CO_2	'free' CO_2
GCOS	Global Climate Observing System
GIS	geographical information systems
GloRiCh	global river chemistry database
GME	Geospatial Modelling Environment
GWR	Geographically Weighted Regression

HMS	habitat modification score
HQA	habitat quality assessment
IHU	Integrated Hydrological Units
IRES	intermittent rivers and ephemeral streams
ISODATA	Iterative Self-Organizing Data Analysis Technique
K CO_2	gas transfer coefficient of CO_2
LDM	laser distance measurer
MAPE	mean absolute percentage error
MARS	multivariate adaptive regression splines
MAT	medial axis transform
MDF	mean daily flow
MEW	maximum effective width
MLC	maximum likelihood classification
MLR	multiple linear regression
N_2O	nitrous oxide
NIR	near infrared
NRFA	national river flow archive
OCC	one-class classification
OLS	ordinary least squares
OS	Ordnance Survey of Great Britain and Northern Ireland
p CO_2	partial pressure of CO_2

POC	particulate organic carbon
RHS	River Habitat Survey
RMSE	root mean square error
SRM	super-resolution mapping
SRTM	Shuttle Radar Topography Mission
VIF	variance inflation factor
WFD	water framework directive
WSW	water surface width
WV2	WorldView-2

Chapter 1
Introduction

Water surface width (WSW) – the width of a stream or river measured from one edge of the water to the other at the air-water interface, orthogonal to the direction of flow (Figure 1.1.1, p.2) – is of critical importance to a number of application areas. These include the management of river channels in response to natural geomorphological changes or land use change (Anderson *et al.*, 2004; Booker and Acreman, 2007), the quantification of water surface area for resource management and monitoring over time (Alsdorf *et al.*, 2003; Gleason and Smith, 2014), and the estimation of CO_2 effluxes from rivers and streams to the atmosphere (Butman and Raymond, 2011; Crawford *et al.*, 2013; Wallin *et al.*, 2013).

Despite this, the extent of surface waters is poorly characterised at all scales, both in terms of local to global levels of analysis and for narrow low-order headwaters to Earth's widest rivers (Raymond *et al.*, 2013; Ward *et al.*, 2017). Headwaters are especially significant, because despite exhibiting narrow

widths they comprise the majority of the river network globally in terms of length (70%; Lowe and Likens, 2005) and a significant quantity of river surface area (15%; Raymond *et al.*, 2013; Wallin *et al.*, 2011). Recent research into the role of inland waters in biogeochemical processes (Ward *et al.*, 2017) has identified the inability to adequately capture narrow streams in particular as a key barrier to fully understanding the role of surface waters in processes such as the carbon cycle, for example.

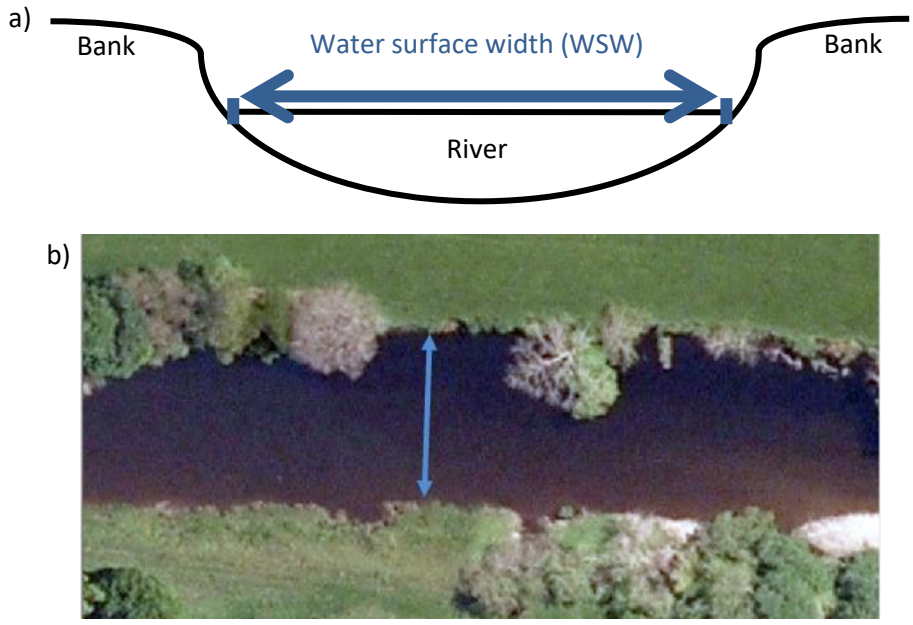


Figure 1.1.1 The water surface width (WSW) geomorphological attribute of a river as viewed a) at a river cross-section and b) from an aerial perspective.

Until recently, rivers have been conceptualised as 'neutral pipes' that transfer biogeochemical constituents from terrestrial sources to the world's oceans (Cole *et al.*, 2007), yet it is now understood that vertical transfer with the atmosphere takes places. This process is currently poorly understood at the national scale, with the majority of research focusing on estimating global CO_2 evasion (Lauerwald *et al.*, 2015; Raymond *et al.*, 2013; Wallin *et al.*, 2013) which requires a significant compromise in the resolution of data used to determine river surface area (Benstead and Leigh, 2012) – a critical component in CO_2 evasion models that ultimately relies on an accurate dataset of both river length and WSW. As a result, existing estimates potentially only account for half of the total transfer

(Downing *et al.*, 2012), while simultaneously failing to accurately monitor water resources at a time when climate change is placing them under increasing pressure.

Furthermore, CO_2 evasion occurs at a higher rate in headwater streams due to connectivity with carbon-rich terrain (Benstead and Leigh, 2012) and increased hydrodynamic turbulence, resulting in a comparatively high rate of transfer (Aufdenkampe *et al.*, 2011). However, these streams are routinely narrower than the spatial resolution of the majority of large format satellite imagery datasets used for global scale analysis, creating a requirement for national studies targeted at measuring both WSW and CO_2 evasion.

The main challenge currently facing those wishing to accurately measure WSW for use in applications such as the aforementioned is the lack of a method that is capable of providing reliable measurements at multiple spatial scales. There have been recent efforts to create a global-scale database of inland water size distribution (Andreadis *et al.*, 2013; Downing *et al.*, 2012; Verpoorter *et al.*, 2014; Yamazaki *et al.*, 2014), supported by local and national-scale studies for predicting WSW (Booker, 2010; Rawlins *et al.*, 2014a), which generally focus on establishing the statistical relationship between WSW and key explanatory variables, such as catchment area (Faustini *et al.*, 2009) and riparian land cover (Allmendinger *et al.*, 2005). A significant drawback of the majority of these studies is that they rely on measurements from hydrological gauging stations as a model input (Booker, 2010), despite these locations having limited coverage (Alsdorf and Lettenmaier, 2003; Revilla-Romero *et al.*, 2015), sampling bias (Booker and Dunbar, 2008) and an uncertain future (Alsdorf *et al.*, 2003). Meanwhile, large scale, high resolution surveys that directly quantify river width, such as that undertaken recently in North America (Allen and Pavelsky, 2015), are a comparatively new phenomenon, with the aforementioned capturing rivers wider than 30 m at mean discharge. As a consequence, there is currently no national scale WSW dataset for the UK that is adequate for use in the estimation of fluvial CO_2 evasion.

To address this, a novel process was created in this study for the estimation of WSW at the national scale for England and Wales. This was achieved through the creation of a predictive model that was based on the established relationship between factors such as catchment area, hydrological source of flow, and rainfall with WSW. Using freely available or easily derivable data for explanatory variables across a study site comprising the rugged terrain of northern Wales and the lowlands of central England – which is representative of the landscapes typically found throughout both nations – a model capable of providing accurate estimates of WSW for any catchment in England and Wales was created.

Model estimates were validated through the coupled use of remote sensing techniques to extract rivers and streams from aerial imagery covering the study area, and NRFA gauging station data to confirm that conditions when the imagery was captured were representative of normal flow conditions within the study area. A combination of one-class classification (OCC), fuzzy classification, and contouring enabled the production of super-resolution maps that captured headwaters narrower than the input resolution of 50cm, addressing the need for narrow stream to be better represented (Ward *et al.*, 2017). Direct image-based measurements were then made of the extracted surface water features parallel to the direction of flow using a semi-automated GIS-driven technique, which enabled the creation of a high resolution, large scale dataset of WSW.

Estimates of CO_2 evasion were then possible by calculating water surface area for catchments in England and Wales where *p* CO_2 (partial pressure of CO_2) data had previously been collected. While these locations are relatively few and constrain the extent to which broad conclusions can be drawn regarding the role of fluvial CO_2 evasion in England and Wales, the lack of a pre-existing benchmark that incorporated WSW measurements meant that the study was able to contribute to the advancement of the field. The key ways in which this was achieved are listed below.

1.1 Novel aspects of the research

- Previous WSW studies did not consider the role of human modification; this study marked the first time that an explanatory variable for this factor was successfully used in a predictive model of WSW.
- OCC, fuzzy classification, contouring, and local training data were combined to meet the specific needs of this study
- No viable method for delivering national scale estimates of WSW for England and Wales previously existed, addressed herein through the creation of a predictive model.
- The spatial distribution of surface waters across England and Wales was elucidated by identifying spatial patterns in WSW.
- WSW predictions were directly incorporated in the prediction of fluvial CO_2 evasion for England and Wales at the national scale.
- .

1.2 Aims and objectives

To address the overall research theme of creating and applying model-derived estimates of WSW in England and Wales, the following aims were devised, alongside subsidiary objectives geared towards signposting progress towards completion. These were:

i. Extract a high-resolution dataset of rivers and streams from aerial imagery for the chosen study area.
    - Conduct a comparative analysis of the different feature extraction techniques presented in the literature, in order to select the most appropriate for the specific context of this study, particularly the need to capture narrow low-order streams to as great an extent as possible.

- Appraise the selected methodology to identify potential sources of error, in order to limit this wherever possible, inform subsequent studies which may aim to reproduce or reapply the technique, and to understand the impact of error propagation through subsequent stages of the study.
- Assess the degree to which overhanging vegetation, emergent vegetation, and substrate limit the ability to derive a complete and accurate dataset of rivers and streams, and a recommendation of strategies for mitigating this.

ii. Make accurate, direct image-based measurements of WSW using a GIS-driven technique.

- Utilise widely available techniques to allow users to replicate the approach as easily as possible both spatially and temporally.
- Validate a representative subset of width measurements to establish the accuracy of the measurement technique.
- Use UK river flow data to ensure that the selected aerial imagery represents typical flow conditions in order to ensure non-biased measurements.

iii. Produce a model capable of accurately predicting WSW for England and Wales.

- Investigate the potential controls of WSW given the background literature and the specific context of the study area.
- Extract appropriate data for the chosen explanatory variables at the same points at which WSW measurements were derived.
- Produce a predictive model based on the statistical relationship between WSW and the explanatory variables across the study area.
- Validate the capability of the model to accurately estimate WSW at randomly selected sites beyond the study area.

iv. Determine the impact of incorporating WSW measurements into fluvial CO_2 evasion models for England and Wales.

- Adapt an existing statistical model to incorporate WSW estimates derived from the model produced in addressing aim ii (below).
- Compare model estimates of CO_2 evasion with previous studies to describe and explain any differences.

1.3 Thesis structure

This thesis is divided into chapters that relate to the four primary aims, as stated above, in addition to a review of the relevant literature, a synthesis of key research findings, and recommendations for future research. This allows for each of the stated aims and objectives to be addressed with clarity, as what could be considered as the 'traditional' empirical model – discreet chapters focusing on the methodology, followed by chapters focusing on results, discussion, and so on – would likely result in a less coherent and substantive argument due to the outcome of earlier stages of the research dictating choices made in subsequent analyses. Figure 1.3.1 (p.10) explains the purpose of each empirical chapter, as well as the linkages between chapters. In summary: -

- *Chapter 2: Literature Review* examines the 'state of the art' in relevant research fields, including studies relating to CO_2 evasion from inland waters, the role of WSW in CO_2 evasion, the hydrological and geomorphological controls of WSW, approaches to the measurement of WSW, and the role of remote sensing technologies and associated methodological approaches within the aforementioned fields. It critically assesses the above to identify areas requiring further research, and in doing so situates the aims of this study within the broader literature. Finally, the national-scale distribution of rivers and variation in WSW is disaggregated to identify national-scale patterns.
- *Chapter 3: Extracting surface waters from aerial imagery* introduces a methodology combining multiple remote sensing techniques to meet the requirement for the improved

integration of low-order streams in particular. The selection of high resolution colour-infrared (CIR) imagery is corroborated by an analysis of the impact of spatial resolution on the ability to capture watercourses, alongside a comparative analysis of multiple image classification and feature extraction techniques. The final method – a combination of fuzzy classification, OCC, and contouring – is rigorously tested to establish its utility in capturing streams and rivers, especially at lower orders.

- *Chapter 4: Image-based measurement of WSW* describes the process created to take perpendicular WSW measurements directly from the surface waters dataset derived from aerial imagery, as above. Covers the use of GIS analysis for dataset post-processing to remove errors of commission. Following is a discussion of the measurement workflow, from manipulating the surface waters dataset to make it more amenable to measurement, the creation of centrelines along which a sample of points can be defined at varying intervals, and most importantly, the use of Thiessen polygons to calculate a precise 90 degree angle at which measurements of WSW can be made. Finally, image-based measurements are presented alongside field measurements to establish overall accuracy.
- *Chapter 5: National-scale predictions of WSW for England and Wales* establishes the statistically significant explanatory variables of reach-scale WSW using widely available landscape data, followed by a discussion of how multiple linear regression is able to meet the demands of this study. Also includes a comparison of multiple applicable models to select that which was most applicable to being scaled up from the chosen study site to the national scale for England and Wales. Spatial variation in WSW is examined with an appraisal of the potential ramifications for both research and policy following.
- *Chapter 6: Estimating fluvial CO_2 evasion in England and Wales* begins by assessing previous modelling efforts for estimating the national-scale vertical transport of CO_2 before introducing WSW predictions for England and Wales made by the national scale model created previously

into CO_2 estimation models. National-scale patterns in CO_2 evasion are presented, and evasion values compared to previous estimates.

- *Chapter 7: Discussion* addresses the degree to which the stated aims and objectives of the study have been met by summarising the findings relevant to each. An appraisal of limitations is also presented, alongside the potential solutions to these issues. Finally, future research opportunities are highlighted within the context of present and future developments within the field of remote sensing, drawing on the availability of new techniques and technologies.

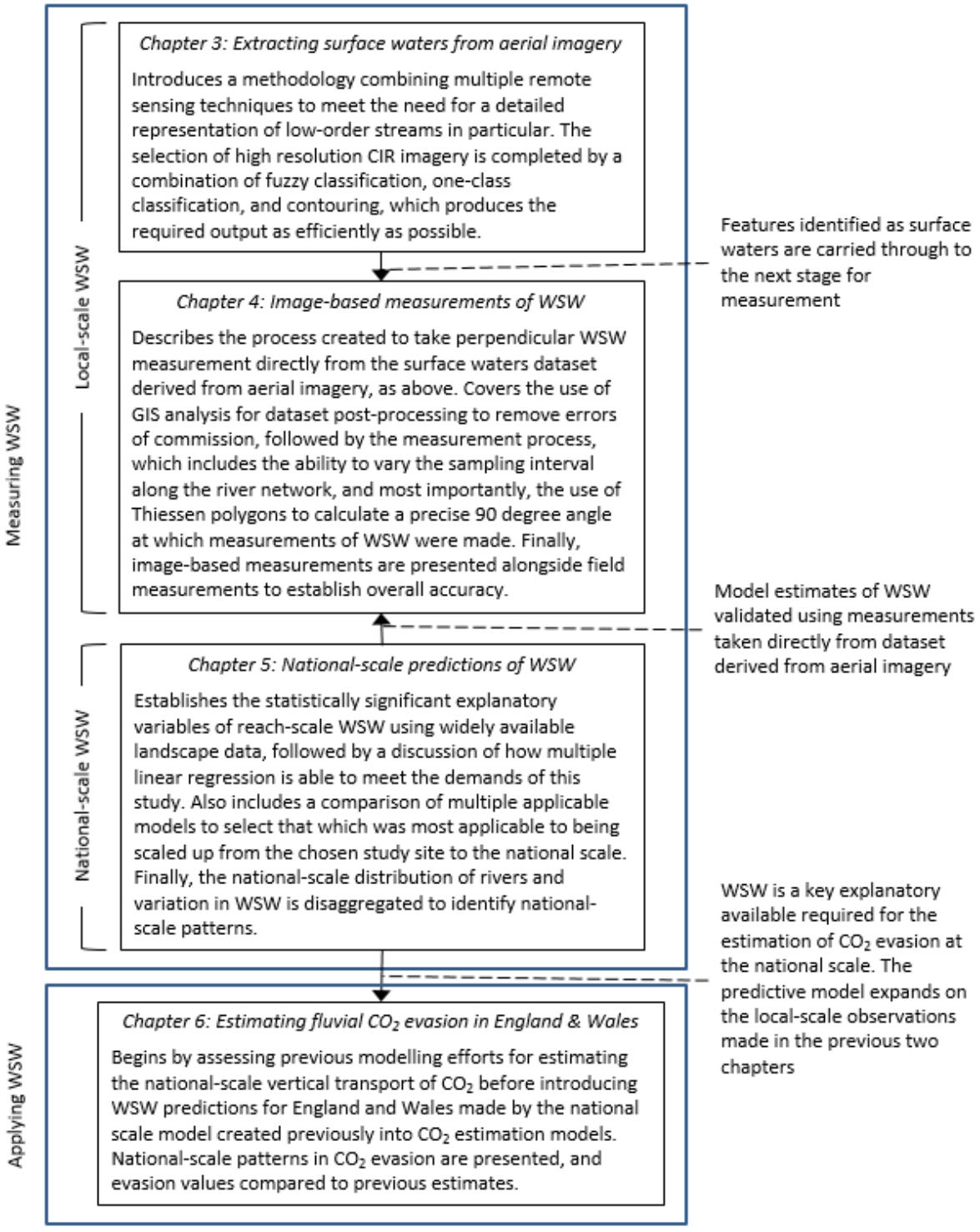


Figure 1.3.1 Overview of workflow with linkages and relationships between discrete methodological chapters identified

Chapter 2
Literature Review

In order to both situate this study within the context of previous and ongoing research, and to inform the design and execution of the selected methodologies, a thorough review of the relevant literature was undertaken.

An interest in WSW, while in itself a worthwhile area of research, is truly made relevant and timely by the areas within which measurements can be applied. This is most evident considering the importance of WSW to the ability to accurately predict the quantity of GHGs such as CO_2, CH_4, and N_2O transferred from inland waters to the atmosphere, which is the first research field examined below.

2.1 Estimating GHG evasion from rivers and streams

Inland waters (rivers, streams, lakes, and reservoirs) have long been hypothesised as net sources of CO_2 to the atmosphere (Kempe, 1982). However, lotic (flowing) freshwaters, such as rivers and streams, have been conceptualised until recent years as 'neutral pipes' (Cole *et al.*, 2007) which simply carried CO_2 from terrestrial sources to the world's oceans. It was not until the Fifth IPCC Assessment

Report (Ciais *et al.*, 2013) that vertical transport from rivers to the atmosphere was formally recognised as a significant component of the carbon cycle. This is despite the existence of a strong understanding of the biogeochemical processes that govern the way in which GHGs interact with inland waters, for example how organic matter is converted into CO_2; see the recent work undertaken by Ward *et al.* (2017) for a thorough review.

Inland freshwaters cover approximately 3% of the Earth's surface (Downing *et al.*, 2006), with lotic systems containing only 5% of these freshwaters. Understandably, this means that the contribution of rivers and streams to GHG evasion is poorly characterised when compared to the body of research on the larger lakes and reservoirs (Battin *et al.*, 2009; Cole *et al.*, 2007; Wallin *et al.*, 2011), yet the air-water interface between lotic systems and the atmosphere contributes significant fluxes of a number of important GHGs, including CO_2 (Butman and Raymond, 2011; Cole and Caraco, 1998; Richey *et al.*, 2002), CH_4 (Bastviken *et al.*, 2011; Cole *et al.*, 2007; Stanley *et al.*, 2016), and N_2O (Beaulieu *et al.*, 2011; Peterson *et al.*, 2001). A greater body of research exists for the evasion of CO_2 than other GHGs, which is due to CO_2 being acknowledged as playing the most significant role in the anthropogenic greenhouse effect (Ciais *et al.*, 2013). Consequently, this thesis focuses solely on the role played by rivers and streams in CO2 evasion specifically, driven by modelling approaches (Chapter 5, p.121) and field measurements existing in greater quantity (Section 6.2, p.153) and for a longer period of time than for CH4, and N2O, for example. That said, inland waters are still poorly integrated into the carbon cycle more generally when compared with research into the role of other habitats in carbon biogeochemistry (Tranvik *et al.*, 2018), which underlines the need not only for improved estimates of CO_2 evasion, but of the relative importance and magnitude of evasion when compared with sequestration or burial in sediments, for instance. Herein lies the problem; the role of processes such as sediment burial in inland water carbon fluxes is poorly understood due to the existence of very few estimates or direct measurements (*ibid*.), so while the research that exists indicates that evasion from inland waters is greater than burial in sediments (Hanson *et al.*, 2015), there is significant uncertainty due to a dearth of research, as well as a relative bias in research in favour of lakes, meaning that the

role of riverine environments in the carbon cycle is even more poorly understood. While it has long been established that organic carbon is present in rivers in dissolved (DOC) and particulate (POC) forms in the ratio of 10:1 (Schlesinger and Melack, 1981), supporting the focus of this study on the fluvial evasion component of the carbon cycle, the relative magnitude of evasion when compared with other components of the fluvial carbon cycle is poorly quantified.

For example, when compared with an estimated 1.8 Pg C yr−1 transferring from rivers to the atmosphere globally, 0.6 Pg C yr−1 is removed from rivers via storage in sediments and wetland soils as well as through sequestration by primary producers (Wehrli, 2013). However, significant disagreement exists with these figures, with even the comparatively better-constrained estimate of global CO_2 evasion varying significantly between papers as discussed below (and hence why this thesis focuses on the provision of data that can improve the parametrisation of fluvial CO_2 evasion models).

Recent estimates of global fluvial CO_2 evasion range from 0.26 Pg C yr−1 to 1.8 Pg C yr−1 (Aufdenkampe *et al.*, 2011; Cole *et al.*, 2007; Lauerwald *et al.*, 2015; Raymond *et al.*, 2013; Tranvik *et al.*, 2009), with the most recent research trending towards the upper limit. The divergence in estimates is largely a result of two factors that not coincidentally lie at the heart of this study; the lack of a comprehensive dataset of rivers (and thus WSW) at every scale, and the use of predictive models for CO_2 evasion that require further improvement for reasons outlined below.

WSW plays a critical role in estimating the evasion of GHGs from rivers and streams, as water surface area, in combination with knowledge of the rate of gas evasion between water and the atmosphere (Öquist *et al.*, 2009; Raymond and Cole, 2001), is a fundamental requirement without which estimates are incomplete. This is because the transfer of GHGs occurs at the air-water interface, so the greater the surface area – a product of river length and WSW – then the greater the potential transfer, assuming a constant rate.

Currently, addressing this issue is problematic because a framework for estimating inland water surface area at the regional or global scale does not exist (Cole *et al.*, 2007; Raymond *et al.*, 2013), making it difficult to reliably estimate CO_2 evasion in turn. Without this, our knowledge of global carbon cycling is incomplete, preventing effective strategies for quantifying current evasion, monitoring change over time, and mitigating the role of inland waters in climate change. This is further complicated by the important role that headwater streams play in this process, as they are far more difficult to capture using the available methodologies.

2.1.1 Evasion from headwater streams and the importance of spatial scale

Headwater streams – defined as stream orders 1 to 3 (Denfeld *et al.* 2013) – tend to be supersaturated in CO_2 (Halbedel and Koschorreck, 2013) as a result of closer connectivity with organic-rich soils than wider, higher order rivers (Benstead and Leigh, 2012; Crawford *et al.*, 2013; Dinsmore and Billett, 2008; Wallin *et al.*, 2011). Furthermore, the tendency for lower order streams to reside in comparatively more rugged terrain increases hydrodynamic turbulence within the channel (Aufdenkampe *et al.*, 2011; Downing *et al.*, 2012; Vachon *et al.*, 2010), resulting in increased gas transfer velocity. Thus, low order streams both contain significant amounts of CO_2, and transfer gas to the atmosphere at a high rate per unit area, resulting in exchanges of a comparable or higher intensity than larger rivers (Kling *et al.*, 1991; Mulholland *et al.*, 2008; Rantakari *et al.*, 2010). Disaggregated by stream size, fluxes from first and second order streams can be ~3x those from third to fifth order streams (Schelker *et al.*, 2016).

In addition to significantly higher evasion from headwaters, these streams can also account for a significant proportion of total river network length. In Sweden for instance, headwater streams (defined as having a catchment area <15 km^2) account for 90% of all streams in the country (Bishop *et al.*, 2008). Globally, headwater streams represent a disproportionately large (~15%) quantity of total global river surface area (Raymond *et al.*, 2013; Wallin *et al.*, 2011) and over 70% of river length

globally (Lowe and Likens, 2005), so capturing a complete representation of low order streams is essential to fully understanding fluvial CO_2 evasion.

The importance of evasion from low order streams is only able to be factored into local-scale studies at present, as current methods for measuring evasion – similarly to local-scale methods for measuring WSW – are not scalable due to their labour-intensive nature. Floating chambers, which directly measure evasion but generally underestimate gas exchange between the water and atmosphere due to reducing water surface turbulence (Dinsmore and Billett, 2008; Erkkilä *et al.*, 2017; Wallin *et al.*, 2011), and the tracer gas method, where an inert gas that does not occur naturally is injected into the water system (Cole and Caraco, 1998; Wanninkhof *et al.*, 1990), both require the researcher to carry out repeated field measurements. This means that making estimates beyond the local scale relies on establishing the statistical relationship between field measurements of evasion and controlling factors such as water temperature, pH, and alkalinity to create predictive models of CO_2 evasion (see Lauerwald *et al.*, 2015 for a recent example). However, few sites have data available for all of the aforementioned controlling factors globally, so focusing an investigation on the national scale results in very few measurements being available for the analysis of CO_2 evasion. Correcting for this lack of data would require an intensive and widespread field campaign in order to produce a usable dataset covering the expected range in both the controlling variables and CO_2 evasion for a given nation, which would be prohibitively resource intensive.

Large scale, global predictions predominate in much of the literature and are symptomatic of what has been termed a 'globalising instinct' in ecological and environmental research more broadly (Hulme, 2010). While such studies are hugely significant given the need to better understand this component of GHG budgets, it is perhaps at the expense of research at the national or regional scales, which occupy the middle ground between local measurements and global models.

At the global scale, the majority of recent studies that attempt to quantify CO_2 evasion globally rely on datasets of inland water size distribution that are relatively coarse and exclude headwater streams

entirely (Andreadis *et al.*, 2013; Aufdenkampe *et al.*, 2011; Downing *et al.*, 2012; Yamazaki *et al.*, 2014) or use interpolation methods to predict the abundance of these streams (Butman and Raymond, 2011; Lauerwald *et al.*, 2015) rather than measuring them directly. Most commonly, such studies rely upon the use of data for a selection of lotic freshwaters for which extensive hydrological monitoring has already taken place, biasing the selection of inland waters to the more widely-studied rivers across the globe. As a result, river-atmosphere efflux of CO_2 could be double previous estimates (Cole and Caraco, 1998; Cole *et al.*, 2007), mainly due to the way in which headwater streams are currently poorly accounted for

The combination of coarse spatial resolution and limited sampling inevitably causes significant problems when results are extrapolated to all inland waters on Earth as part of efforts to estimate CO_2 evasion (Butman and Raymond, 2011), as significant uncertainties exist that are as yet unchallenged due to the relative lack of national-scale studies. Raymond *et al.* (2013) produced a visualisation of the varying gas effluxes from rivers and streams for every country, with the UK, as a result of being classified (correctly) as a temperate environment with relatively high water surface area, revealed to be among the biggest contributors of CO_2 to the atmosphere in terms of evasion from inland freshwaters. Water surface area, however, was calculated using predetermined hydraulic equations, with only the influence of climate variables taken into consideration as a controlling factor, yet it has been established in the broader literature that numerous other controls exist (see Section 2.3, p.21).

However, this is not to question the validity of global-scale modelling, because such studies play a vital role in addressing the underrepresented contribution made by inland freshwaters to global-scale processes. However, with the degree of compromise that is necessary, it is evident why Hulme (2010) characterises global-scale knowledge as 'brittle'. It is therefore increasingly necessary to contextualise global observations with location-specific studies. Unfortunately, there seems to be a relative lack of national-scale analysis in particular, with a limited number of national studies of CO_2 evasion – for example, in the USA (Butman and Raymond, 2011) and Sweden (Bishop *et al.*, 2008) – situated in

between local-scale studies utilising methods that are not easily scalable, and the instinct of many researchers to focus on far-reaching global trends. This is in spite of the reality that it is often on the national scale that change is more readily achieved, given the lack of an international body with unilateral powers to dictate climate policy (Stavins, 1997).

Overall, the importance of headwater streams to CO_2 evasion, coupled with the relative lack of national scale research or a clear blueprint for those wishing to address this issue, provided a clear direction for this study.

2.2 Measuring water surface width

As well as being critical to biogeochemical processes such as CO_2 evasion, the quantification of total water surface area at various scales is in itself an important application of WSW, as it is key to understanding challenges in terms of water resource management, food security, ecosystem studies, flood forecasting, drought monitoring, and geopolitical conflicts over resource usage (Alsdorf *et al.*, 2003; Alsdorf and Lettenmaier, 2003; Brakenridge *et al.*, 2005; Engman and Gurney, 1991; Gleason and Smith, 2014).

However, recent estimates of global river surface area vary considerably, with examples including 485,000 km^2 (Lehner and Döll, 2004), 624,000 km^2 (Raymond *et al.*, 2013), 662,000 km^2 (Downing *et al.*, 2012), and 832,000 km^2 (Lauerwald *et al.*, 2015). This lack of certainty required an examination of existing methods for measuring WSW in order to ensure that an estimate for England and Wales was as accurate and complete as possible.

At the local scale, field surveys remain the method of choice, with techniques such as the use of a level and staff at channel cross-sections inherited from engineering practices as fluvial geomorphology underwent significant change in the 1950s (Lane, 2000). Manual measurements using a tape measure

or rangefinder continue to be used in contemporary studies (Booker, 2010), and can contribute to understanding local scale channel morphology within the framework of stream reconnaissance (Thorne, 1998a). However, while these measurements are easily repeatable and achieve a high degree of accuracy, there are obvious drawbacks when attempting to carry out measurements over a larger spatial extent as they require the researcher to be *in situ*.

Historically, the problem of scale has been addressed via the use of power-law relationships between discharge and WSW (Leopold and Maddock, 1953). The proliferation of gauging stations in countries such as the USA and the UK has allowed direct measurements of stream discharge to be used for predicting WSW at larger spatial scales (Beighley and Gummadi, 2011; Booker, 2010; Booker and Dunbar, 2008), but this in itself raises two key challenges. Firstly, the requirement for data relating to discharge means that the methodology is inapplicable to large-scale studies of locations without a gauging station network. Secondly, gauging sites are neither randomly nor consistently distributed spatially.

The reliance upon using data from gauged sites introduces a source of potential bias, because locations tend to be selected for accessibility and are often sited on straight, unaltered channel sections with no engineering structures (Booker and Dunbar, 2008) to simplify the collection of data (Booker, 2010; Rawlins *et al.*, 2014a). The spatial arrangement of the network may also be sparsely distributed (Alsdorf and Lettenmaier, 2003; Birkett, 1998; Westaway *et al.*, 2003), which means that channel variation in between stations is overlooked. Furthermore, while countries such as the UK have hydrological monitoring networks, factors such as funding pressure and a general lack of understanding as to the value of river flow data are placing the future of gauging stations in jeopardy (Alsdorf *et al.*, 2003; Hannah *et al.*, 2011). With continuity far from guaranteed, it is important that methodologies are developed that are capable of providing WSW estimates independent of discharge data from either field surveys or gauging stations, which would also address the issue of applicability in contexts where discharge data are not available to begin with.

Efforts to achieve this are already under way, with a number of studies using remotely sensed imagery to derive channel width or WSW (Birkett, 1998; Westaway *et al.*, 2003; Bjerklie *et al.*, 2003, 2005; Fisher *et al.*, 2013; Rawlins *et al.*, 2014a). This generally involves manual measurements using a GIS (Bjerklie *et al.*, 2005; Rawlins *et al.*, 2014a), but this is an extremely labour-intensive process and results in either sparse sampling or limited spatial extent in order to expedite the manual measurement process, a drawback of relying on gauged sites that a technique utilising remotely sensed imagery really should aim to correct, rather than consolidate. Therefore, the automation of the measurement process would appear to be the solution.

Recently, algorithm-driven approaches have been used to extract a river network from remotely sensed imagery. Most significantly, Pekel *et al.* (2016) used a combination of Landsat 5, 7 and 8 imagery to develop a dataset of not only rivers at the global scale, but temporal change in these surface waters, available online (European Commission Joint Research Centre, n.d.). This is currently the most detailed dataset available and required the analysis of petabytes of data, yet is severely limited in the ability to capture low-order streams due to the native resolution of Landsat being 30 m at best in the visible and NIR channels, and coarser still prior to the Landsat 4 mission. At the regional scale, the RivWidth program (Pavelsky and Smith, 2008) automates measurements at user-specified intervals perpendicular to the direction of flow within the channel, which reveals the potential for an automated approach. However, the coding of pixels using a binary classification relating to either the presence or absence of the river channel means that the accuracy of the final measurement is compromised by a combination of the mixed pixel problem (i.e. pixels routinely contain multiple classes yet membership is decided by the majority class) and the spatial resolution of the imagery used, especially as there is a pixel on either side of the river channel. Furthermore, where small streams fall within a single pixel, there is even greater potential for RivWidth to either fail to measure channel width at all, or to produce a measurement with high relative error. Additionally, braided channels are handled by assuming that the outer extent of the most distant channel strands represents the limits of a single channel, overestimating WSW as a result. Alternatives also suffer from

similar restrictions, for example by only functioning when applied to single braid channels (Fisher and Bookhagen, 2014), deriving measurements from an artificial river network from a DEM rather than taking a true river network as input (ESSA, 2014), or by placing stringent requirements on the format of input data that would require extensive manual editing (ESRI, 2014; Lauer, 2012; Roux *et al.*, n.d.; US Army Corps of Engineers Hydrologic Engineering Centre, n.d.), which is impractical for large datasets. A systematic analysis of the utility of these WSW measurement tools is presented in 4.3.1.

Ideally, to avoid having to make such assumptions about river channels, a semi-automated methodology would be utilised. This would strike a compromise between the need for limiting extensive and time-consuming manual user input (Bjerklie *et al.*, 2005; Rawlins *et al.*, 2014a) and preventing an unacceptably high degree of error. The latter would be achieved through the application of human expertise to the classification procedure, in order to take advantage of the merits of human cognition in recognising patterns with relative ease when compared with personal computers (Quackenbush, 2004). An entirely automated methodology has a tendency to result in errors of omission or commission (Baumgartner *et al.*, 1999) and, as has been noted, places limitations on how varied river channel morphology can be measured.

Overall, there is a need to improve upon the current reliance on either gauged sites or image-based measurements that require a significant degree of abstraction or simplification, such as the removal of braided channels. That said, the latter approach has great potential to capture narrow streams, with remote sensing technologies and methodologies assessed below (in Section 2.4, p.31) to determine whether any could realistically generate a comprehensive WSW dataset that addresses the need to capture headwater streams in particular. Before an appraisal of remote sensing in the context of this study, it is necessary to understand the physical controls of WSW, particularly as the environments within which headwater streams in particular predominate present specific challenges that remote sensing-driven methodologies need to address in order to be fit for purpose.

2.3 The controls of water surface width

The factors that shape river channel form have been the subject of study for decades, with the field of fluvial geomorphology codifying and formalising the scientific study of river channel processes and morphology. Despite its origins in the 1950s and 1960s in particular (see Leopold and Maddock, 1953; Leopold and Wolman, 1957; Leopold *et al.*, 1964; Schumm, 1967, 1977; Wolman, 1955), fluvial geomorphology is still an active and developing research field, as evidenced by a proliferation of review articles in recent years (Brierley *et al.*, 2013; Cudennec and de Lavenne, 2015; Everard and Quinn, 2015; Piégay *et al.*, 2015; Wohl, 2014), in addition to the continuation of applied research in the field (Alber and Piégay, 2011; Allen and Pavelsky, 2015; Kleinhans, 2010; Manners *et al.*, 2014; Martínez-Fernández *et al.*, 2015). Furthermore, hydromorphology – the synthesis of hydrology and geomorphology – is now considered a distinct science of its own (Newson and Large, 2006; Sear *et al.*, 2010; Vogel, 2011).

River width specifically is a vital component of channel flow equations, and as demonstrated throughout the discussion below, is crucial to estimating discharge, sediment transport, and potential erosion (Fisher *et al.*, 2013; Knighton, 1998; Leopold and Maddock, 1953; Pavelsky and Smith, 2008). Despite this importance, a national scale dataset of channel width or WSW does not exist for England and Wales, restricting the ability to undertake research in areas that require a comprehensive understanding of this attribute. The complexity of a potential solution to the current lack of headwater streams in particular in existing datasets, as discussed in the previous sub-section, indicated that an alternative approach may be necessary for estimating WSW at the national scale. The use of a predictive model, informed by the more comprehensive measurements taken from the remotely sensed imagery, was identified as a potential solution, necessitating an assessment of the landscape variables that could account for variation in WSW. What follows is a disaggregation of each controlling variable of WSW into a discrete section. However, it is acknowledged that there are multiple interactions and dependencies between these variables that will manipulate the relationships

explained below at varying spatial and temporal scales (Thorne, 1998b); it is in the pursuit of clarity that variables have been separated.

2.3.1 Discharge and catchment area

The role of discharge in shaping river channels has been the primary occupation of fluvial geomorphology as a field for over half a century (Leopold and Maddock, 1953; Wolman, 1955), with the impact upon hydraulic geometry of particular note, which explains characteristics such as width, depth, velocity, slope, and sediment transport both at-a-station (AAS) (a defined cross-section) and downstream using variation in discharge (Fryirs and Brierley, 2012; Gleason, 2015; Singh, 2003).

The strength of the relationship is such that WSW alone can be used to predict discharge. Channel width (W) scales in a power-law relationship with mean annual discharge (Q) to an exponent (b) multiplied by a constant (a), with these two terms being unique to a defined watershed or catchment. Equation 2.1 can also be stated with catchment area (A) in place of discharge (Q), although this changes the locally variable exponent that is used.

$$W = aQ^b$$

Equation 2.1 Power-law relationship between channel width (W) and mean annual discharge (Q)

Typically, width increases downstream as a function of discharge (Leopold and Maddock, 1953). However, direct measurement of discharge is problematic in that it generally requires in-situ monitoring, which generally occurs at sparsely distributed gauging stations. In lieu of discharge data, catchment area becomes the most significant control of WSW, as it is in itself strongly related to discharge (Beighley and Gummadi, 2011; Burgers *et al.*, 2013) while having the advantage of being readily calculable via GIS analysis of a digital elevation model (DEM).

Field surveys (e.g. Montgomery and Gran, 2001) have established the direction of the relationship between catchment area and channel width. Where all other variables are controlled, a point along a

river with a larger upstream catchment area will be wider than a point that has a smaller upstream catchment area. Additionally, recent efforts to model channel or WSW have aided in quantifying the strength of this relationship, with more recent studies showing that catchment area is able to account for somewhere in the range of 36% (Faustini *et al.* 2009) to in excess of 65% (Booker 2010) of variation in WSW, with Rawlins *et al.* (2014a) falling in between these two figures (0.54 coefficient of determination). The difference in these figures reflects the varying influence of catchment area depending upon the study site, as well as variation within each site in relation to other controls, including precipitation (Booker 2010) and catchment land cover (Faustini *et al.* 2009).

The variation in the influence of catchment area eventually gave rise to a paradigm shift in the field. As fluvial geomorphology progressed and essentially united with hydrology to become the field of hydrogeomorphology (Cudennec and de Lavenne, 2015; Grabowski and Gurnell, 2016; Sear *et al.*, 2010), the reductive view of channel form being predictable solely by discharge was expanded to include a more holistic representation of the river as an integrated 'system' (Piégay and Schumm, 2003; Schumm, 1977), with connectivity between physical, chemical, and biotic processes that together shape channel morphology. These additional controls are discussed below in relation to WSW.

2.3.2 Climate

The study of how fluvial environments respond to climatological forcing is a topical area of research at present, given the emphasis on projecting future climate conditions and their impact on rivers both internationally and in the UK (Arnell and Gosling, 2014; Arnell and Reynard, 1996; Coulthard and Macklin, 2001; Osborn *et al.*, 2015). There is a particular interest in the alteration of patterns of precipitation, runoff and discharge, which in turn would have a subsequent effect on channel geomorphology and WSW. However, such concerns are beyond the scope of this thesis, as future climate change cannot be practically integrated given the use of static remotely sensed imagery as a primary component of the methodology.

However, this limitation does not prevent the use of historical climate data relating to either the specific time that the remotely sensed imagery was captured, or data that are averaged over a specified time period for the study site. Of particular note is the role played by precipitation in controlling WSW, a component that is emphasised in previous efforts to model WSW as secondary in importance only to catchment area (Booker, 2010; Booker and Dunbar, 2008; Rawlins *et al.*, 2014a), or indeed as the primary controlling factor (Butman and Raymond, 2011). This is not especially surprising, given that both catchment area and precipitation directly control the absolute quantity of water entering the channel, although it is important to note that factors such as land cover – which in turn influences infiltration rates and surface runoff, for example – can alter the relationship between precipitation and WSW.

Additionally, atmospheric temperature has been shown to have a minor negative correlation with WSW (Raymond *et al.*, 2013) as a result of higher evapotranspiration rates reducing the quantity of water when all other variables are controlled. However, this trend is not observed in more local scale studies (Booker, 2010; Rawlins *et al.*, 2014a), where variation in temperature is unlikely to be substantial enough to yield statistically significant results when used as a control of WSW.

2.3.3 Land cover

The primary focus of research into land cover has been on the role of riparian vegetation in shaping river morphology and altering bank cohesion. Generally, the presence of vegetation on a river's banks helps to reinforce soil, reducing the rate of lateral erosion and thereby decreasing the width of a river over time (Eke *et al.*, 2014; Elliott, 2011). Particularly dense vegetation consolidates this trend by reducing soil moisture due to higher interception and evapotranspiration rates, reducing the frequency of saturation and bank collapse (Leopold and Wolman, 1957). As well as exhibiting narrower channels, rivers with cohesive banks are generally stable over time with little adjustment in width, whereas less cohesive banks result in both wider and more variable channels (Fryirs and Brierley, 2012). Furthermore, river planform can be altered entirely by riparian vegetation, with research

documenting how braided channels can be forced into a single channel (Tal and Paola, 2010), for example, as a result of the presence of vegetation.

In terms of quantifying whether the ability to control WSW is dependent on a simple presence-absence assessment of riparian vegetation or varies along a more expansive continuum of vegetation density, previous research has established that banks with >50% vegetation cover were narrower than banks with <50% vegetation cover (Thorne, 1998a), with dense riparian vegetation resulting in a river channel that is between 0.5 and 0.7 times the width of a channel with only grass on its banks (Fryirs and Brierley, 2012).

However, other studies have found the opposite effect, with riparian vegetation responsible for channel widening (Allmendinger *et al.*, 2005; Hession *et al.*, 2003).This is because while vegetation can aid in fixing unstable banks in place, it also contributes to an increase in woody debris in the channel itself, which can increase lateral erosion, thereby increasing WSW. Critically, the interaction of riparian vegetation with other morphological, geological, and biogeochemical factors changes both the strength and direction of its relationship with channel form (Gurnell, 2013; Montgomery, 1997), so in studies incorporating varied landscape and terrain, land cover could affect WSW in different ways.

Similarly, the presence of impervious surfaces such as concrete may also have a variable relationship with WSW, because while runoff is increased, which subsequently widens the river channel (Hession *et al.*, 2003), in areas where the channel itself has been modified, human disturbance correlates negatively with channel width (Faustini *et al.*, 2009) as lateral erosion is severely limited.

In addition to land cover immediately adjacent to the river, catchment scale land cover change has also been shown to directly affect channel geomorphology, for example via the alteration of processes of sediment supply, transport and deposition (Liébault *et al.*, 2005), as well as runoff rates (Dunjó *et al.*, 2004). For example, reforestation as a result of either direct human intervention or rural depopulation results in an absolute decrease in bedload sediment (Liébault and Piégay, 2001), causing

channels to narrow. The effect in upland regions is especially pronounced as a result of stronger coupling between the river channel and the surrounding hillslope (Liébault *et al.*, 2005), demonstrating the interaction of land use change with factors such as relative elevation (discussed below) and stream order.

2.3.4 Channel boundary material and sediment transport

Having considered the influence of the land surface adjacent to the river on WSW, the composition of the channel boundary (i.e. the section of the channel in contact with the water) itself is a logical next step to examine.

Rivers can be categorised using a binary approach which contrasts channels that are predominately comprised of either bedrock or alluvial substances. The former tend to occur in more mountains upland terrain and are relatively stable over time (Whipple *et al.*, 2000). However, alluvial rivers, by virtue of having a channel boundary (bed and banks) composed of mobile sediment, are more diverse in their form, as the quantity, grain size, and type of sediment all have an impact on channel forming processes at multiple scales. As a result, these rivers can be straight, meandering, or braided, and adjust in response to events of varying magnitude and frequency, whether it is the gradual adaption to the long-term adjustment of sediment supply or a sudden change in response to a flood event (Ashley *et al.*, 1988; Eaton and Rosenfeld, 2016; Leopold *et al.*, 1964; Schumm, 1967). While few rivers entirely fit into the bedrock or alluvial categories (Ferguson and Rennie, 2017), the most prevalent channel type has a clear impact on the dynamism and diversity of the river morphology.

An associated factor, sediment transport, is one of the key differences between bedrock and alluvial rivers, but does not influence WSW in a linear manner. An absolute reduction in the quantity of sediment results in narrower channels (Harvey, 1991; Liébault and Piégay, 2001), but this is highly dependent on the size distribution of this sediment. Studies have found that as sediment size increases from silt to clay and then sand, there is a systematic increase in channel width, yet this trend reverses

as size further increases to cobbles and boulders (Hjulstrom, 1939; Luke *et al.*, 2015; Nazir *et al.*, 2016), largely due to the trade-off between the energy required to initiate bedload motion in the first instance and the erosive potential of larger grains of sediment. In practice, rivers with a large proportion of boulders have significant erosive potential, but there is rarely adequate energy to initiate and maintain motion, and when this does occur, grains roll along the bed of the river and increase depth rather than width. Conversely, finer grains are more readily transported, and are comparatively easy to carry either in suspension or saltation, which is a more vigorous action that has greater lateral erosion potential.

In addition to sediment supply being directly related to processes of erosion and deposition (Lane and Richards, 1997), this control is heavily influenced by factors such as the presence of river engineering structures, for example the existence of an upstream reservoir (Shields *et al.*, 2000) or channelization works (Brookes, 1987). Consequently, the human modification of river habitats is addressed in Section 2.3.8 (p.30).

The overall influence of channel bed material on WSW is both direct and through the modification of other controls such as sediment availability (discussed above). Bedrock rivers are capable of supporting considerably higher wall stress than alluvial rivers (Faustini *et al.*, 2009; Finnegan *et al.*, 2005), so will have narrower channels where all other factors are controlled. However, as with many of the controls of WSW, the relationship is scale-dependent, because while a local-scale study may be able to place the river channel somewhere along the aforementioned continuum without too much difficulty, the same river reach may be given an entirely different classification within a regional scale study that utilises a mean to represent channel material. Even in cases where allowance is given for local variation in channel material, the spatial distribution of differing lithologies upstream or downstream of a location along the channel in itself has an impact on WSW, as areas of alternating hard and soft rock can create knickpoints, which correlate with a narrowing of the channel upstream (Allen *et al.*, 2013).

Ultimately, with the goal of this study being to quantify the impact of factors such as bed material, it may be that the difficulties in classifying the composition of a river's bed and banks can be mitigated by using an alternative dataset (see Section 2.3.5, p.28).

2.3.5 Hydrological source of flow

Due to the difficulty of gathering data over a large scale for WSW controls such as sediment transport or geology, a proxy indicator for these factors was sought. Hydrological source of flow is the ratio of long-term baseflow to total stream flow, so could potentially be used as a proxy indicator of surface geology and channel material as these are the predominant controls of baseflow (Bloomfield *et al.*, 2009). In addition, the role of groundwater baseflow has previously been identified as a significant control of channel morphology second only to catchment area and precipitation (Leopold, 1994).

River flow can be derived from multiple sources, including overland flow or from baseflow, which can be disaggregated into delayed shallow subsurface flow and deep subsurface flow (McGuire and McDonell, 2007). The overall contribution of baseflow to channel flow is quantifiable through the use of a baseflow index (BFI), which is a proportional measure of how much river flow is derived from stored sources i.e. baseflow, relative to other sources (Gustard *et al.et al.*, 1992). More permeable lithology, alluvial deposits, and soils within a channel will result in a higher BFI statistic (Beck *et al.et al.*, 2013; Bloomfield *et al.*, 2009), so BFI correlates strongly with geology.

There is a relative lack of research into the relationship between hydrological source of flow and WSW. However, Rawlins *et al.* (2014a) utilised the BFIHOST (baseflow index hydrology of soil types) dataset for the UK (Boorman *et al.*, 1995) to determine the degree to which BFI could account for variation in WSW across a study site comprising a varied landscape in northern Wales and central lowland England. When comparing a basic model of catchment area and WSW (R^2 = 0.54) with a model incorporating additional explanatory variables (R^2 = 0.76), the greatest increase in the ability to predict WSW was achieved through the addition of the interaction term between BFIHOST and catchment

area. A greater proportion of channel flow derived from baseflow was found to result in narrower channels when compared to channels with the same catchment area that had lower BFIHOST values. However, given the relationship between BFI and other WSW controls, such as sediment supply, further research is required in order to better understand the nature of this relationship.

2.3.6 Channel gradient

Channel gradient, expressed as either an arithmetic mean for slope across a catchment or as a more localised measure of slope within the river channel, has been shown to improve predictions of channel or WSW in previous studies (Booker, 2010; Faustini *et al.*, 2009; Rawlins *et al.*, 2014a). Steeper gradients increase flow velocity, resulting in smaller cross-sectional area (Finnegan *et al.*, 2005; Fryirs and Brierley, 2012), and WSW as a consequence. Given the relative ease with which slope can be calculated via GIS analysis of a DEM, this control is one of the more amenable to the modelling approach utilised in this study, although complex interactions between channel slope and factors such as channel bed material and land use may modify the observed relationship to a degree, as two channels with identical mean slope may have different widths due to variations in channel lithology and riparian vegetation, for example. These interactions were examined as a routine part of creating the predictive model.

2.3.7 Elevation

For a given study area, elevation can be used as a relative measure within WSW models to improve the accuracy of predictions (Faustini *et al.*, 2009). A channel section that is at a higher relative elevation will be narrower than a lower channel section, because as elevation decreases, discharge increases dependent on both drainage density and catchment area, resulting in wider channels in the downstream direction. This is corroborated by Strahler's theory of stream order (Strahler, 1956, 1957), with a decrease in elevation seeing a cumulative increase in discharge as streams combine. Similarly to the ease with which channel gradient can be computed, elevation requires only very simple GIS analysis to extract into a form usable in the predictive model. Further calculations can then yield relief

– the difference between the maximum and minimum elevations in a given area, such as a catchment – which can be used in place of elevation as a proxy for the relative change in stream order (Rawlins *et al.*, 2014b).

2.3.8 Human modification

The previous sections have covered the natural predictors of WSW, yet the reality is that these factors have been affected to varying extents by the role of human modification. Paradoxically, direct human intervention in fluvial environments is at times precipitated by width adjustment brought about by these natural controls, chiefly to protect human populations or infrastructure from channel erosion and accretion, and the consequent risk of bank instability causing landslides, for example.

Due to this dynamic and bi-directional relationship between humankind and river channels, it is no easy task to provide a concise summary. The role of human modification in the fluvial system is a topic that would require its own thesis to explain thoroughly; the impact of human modification on the natural environment has been considered in great depth by others, both within the context of the natural world in general (Vitousek *et al.*, 1997) and river channels specifically (Gregory, 2006). Ideally, because this influence has a direct impact on WSW, it would be accounted for in attempts to predict width. This is further reinforced when one considers that only 11% of rivers and streams in the UK are defined as 'near-natural' (Environment Agency, 2010a). However, there is limited information on the spatial distribution of river engineering projects and their specific impacts, for example, at the national scale for the UK, making it difficult to account for or incorporate human modification of the river channel into predictions of WSW.

Human intervention has likely modified other controls such as the sediment regime, for example, where increased sediment production and deposition occurs (leading to channel narrowing) in response to land use change and the implementation of engineering structures (Fryirs and Brierley, 2012; Latapie *et al.*, 2014), followed by a longer-term trend which potentially leads to channel

widening as a result of increased runoff causing channel scour (Chin, 2006). In this respect, human modification of the environment is partially accounted for (by land cover data), but a more explicit measurement, if available, would potentially increase the predictive ability of a statistical model, especially in urban areas where river channels are more heavily modified (Bernhardt and Palmer, 2007). Finally, human presence has also had an impact on the abundance of other species that themselves are capable of shaping river morphology. For instance, beavers have been preyed upon, forced from their natural habitats, and in some cases are now being reintroduced, for example in Scotland (Puttock et al, 2015) and North America (Curran and Cannatelli, 2014). This has a direct impact on river morphology, as documented by Wohl (2015), although one that for the purpose of this study is impractical to capture.

2.4 The applicability of remote sensing

It is only recently that the potential of remote sensing in river science and management applications has been acknowledged (Marcus and Fonstad, 2010), while recent review articles (Lettenmaier *et al.*, 2015; Tarolli, 2014) demonstrate the broad range of Earth surface applications that remote sensing is now able to support. This growth has been driven by factors such as the introduction of the EU WFD, which focuses on catchment scale management and thus necessitates the use of methods capable of capturing relevant data beyond the local scale, which invariably requires that remote sensing technologies be used (Dugdale *et al.*, 2009).

Remote sensing is particularly well situated to address the key inland surface water questions arising from the literature, specifically the need to quantify resource availability at various scales (Alsdorf *et al.*, 2003; Alsdorf and Lettenmaier, 2003; Brakenridge *et al.*, 2005; Gleason and Smith, 2014), the role of freshwaters in biogeochemical cycles (Alsdorf *et al.*, 2003), and the need to capture headwater streams more effectively (Bishop *et al.*, 2008; Crawford *et al.*, 2013; Schade *et al.*, 2016), with a

summary provided by Palmer *et al.* (2015). Given the emphasis on both a broad spatial scale and a fine spatial resolution, the use of remote sensing is both appropriate and necessary. This is because the utility of remote sensing lies predominately in the ability to improve the spatial coverage of data collection (Bjerklie *et al.*, 2005; Boyd, 2009), with geopolitical concerns regarding data sharing – or a lack of local data collection initiatives – negated via the use of satellites which can transcend national borders (Brakenridge *et al.*, 2005; Engman and Gurney, 1991). Furthermore, depending on the sensor and platform used (see Anderson, 2016; Gilvear and Bryant, 2003, p.136; Jensen, 2013a; Ünsalan and Boyer, 2011; for summaries of RS technologies), imagery from satellites (e.g. GeoEye-1 and WorldView-3) now have a sub-1 m spatial resolution (in the panchromatic band), so there is a minimal compromise in terms of the maximum achievable accuracy when substituting aerial imagery for field study. However, it is important to note that when using such imagery in the context of extracting a dataset of headwater streams, even a spatial resolution of tens of centimetres could still be too coarse to capture the narrowest streams.

However, the nature of this study's subject matter also introduces a number of challenges when using remote sensing. Rivers and streams are highly dynamic, yet a static image is captured. This could unknowingly be taken during a period of abnormally high flow conditions, for example after a period of heavy rainfall, which would result in the overestimation of both WSW and CO_2 effluxes if image-based measurements were used as the basis for a predictive model. Similarly, low-flow conditions would result in the underestimation of these metrics.

On the other hand, this is not a challenge that is exclusive to the use of remotely sensed imagery, as field observations are equally vulnerable to error if care is not taken to contextualise findings. Data from the UK's hydrological monitoring network are stored in the NRFA (National River Flow Archive), an online repository of hydrological data that, most importantly, contains flow data from a number of gauging stations (Centre for Ecology and Hydrology, 2015a). These data can be used to ensure that measurements are taken from aerial imagery representing river discharge at below mean daily flow

(MDF), as flow conditions show a strong positive skew due to the strong influence of high magnitude events such as periods of intense rainfall and flooding (Rawlins *et al.*, 2014a). Through the use of ancillary information, it is therefore possible to represent rivers and streams with a static image without needing to accept an unknown degree of uncertainty. For this reason, a deeper study of remote sensing methods was undertaken to identify those that were applicable to the specific objectives of this study.

However, before these methodologies are examined, it is important to recognise the diversity of approaches available for mapping water bodies from space. Section 2.4.1 (p.34) discusses optical data for reasons of practicality and applicability. Specifically, data accessibility at the inception of this study meant that optical aerial imagery, described in Section 3.2 (p.55), was the most likely source of waterbody information, hence why methods utilising optical imagery have been the predominant focus in the pages that follow. That said, a significant and highly relevant body of research on waterbody mapping exists that focuses on radar imagery. Most importantly, radar is daylight- and weather-independent, and offers the advantage of cloud penetration due to the use of comparatively 'long' wavelengths ranging from approximately 1 mm to 1 metre (Warner *et al.*, 2009), whereas the shorter wavelengths used by passive optical sensors mean that cloud cover poses significant problems i.e. the inability to collect data for obscured land surfaces.

More recent examples applied to the mapping of waterbodies include efforts to automate the extraction of inland surface waters from Radarsat-2 imagery using an algorithm-driven approach (Li and Wang, 2015), and the combination of pre-existing datasets to inform the extraction of surface water extent from Sentinel-1 data (Huang *et al.*, 2018). The strengths of these approaches relate to the aforementioned advantages of radar technology itself. However, significant drawbacks that are especially relevant to this thesis include the limitation of the spatial resolution of outputs, which tend to be in the region of 1 m to 30 m (Brown *et al.*, 2016) - which would fail to capture particularly narrow

headwaters – as well as high variation in classification accuracy (e.g. 79 to 93%) depending on whether ancillary datasets of known surface water locations are available (Huang *et al.*, 2018).

Despite the focus of this investigation from an early stage on extracting surface waters from optical aerial imagery specifically due to data accessibility and the use of the same imagery in a comparable study (Rawlins *et al.*, 2014a), the wealth of data available from sensors mounted to other platforms, as well as technologies such as radar, should not be overlooked in future investigations. The fitness for purpose of datasets is inherently context-specific and will vary particularly with the spatial and temporal extent of a study, and with constant developments in remote sensing seeing innovations on an almost annual basis (see Section 7.2.3, p.187 for developments relevant to this study), there is a place for both optical and radar-derived datasets (among others) from multiple platforms either separately or in combination.

2.4.1 The spectral properties of inland surface waters

Before considering the variety of techniques available for the extraction of surface waters from remotely sensed imagery, it is important to appreciate the spectral properties of surface waters, as this will have a direct impact on the suitability of any methodologies chosen. Previous studies have highlighted the near-infrared (NIR) and middle-infrared bands as being particularly effective when attempting to extract water from an image, as water absorbs the majority of light in this portion of the electromagnetic spectrum (Engman and Gurney, 1991; Jensen, 2013a). Conversely, vegetation has a high reflectance in the NIR band, allowing for these two classes to be separated. Given the temperate climate of England and Wales and the high likelihood of the imagery containing extensive rural areas, this was a significant benefit.

The NIR band is commonly combined with bands from the visible light spectrum to produce CIR imagery (Aronoff 2004), which specifically contains three bands – two from the visible light spectrum (green and red), and the critically important near-infrared band (NIR) that is invisible to the human

eye. In order to display the non-visible NIR band, the reflected colour of an object is shifted to a false colour in the CIR image as follows: -

- Blue objects appear black on the CIR imagery.
- Green colours are shifted to blue.
- Red colours are shifted to green.
- NIR reflectance is represented by red.

The conventional use of this imagery is for the identification of vegetation and the analysis of its health, as healthy vegetation has a high NIR reflectance (Figure 2.4.1), whereas stressed vegetation sees a reduction in NIR reflectance; thus, vegetation appears as varying shades of red on CIR imagery (Aronoff 2004, Paine and Kiser 2012).

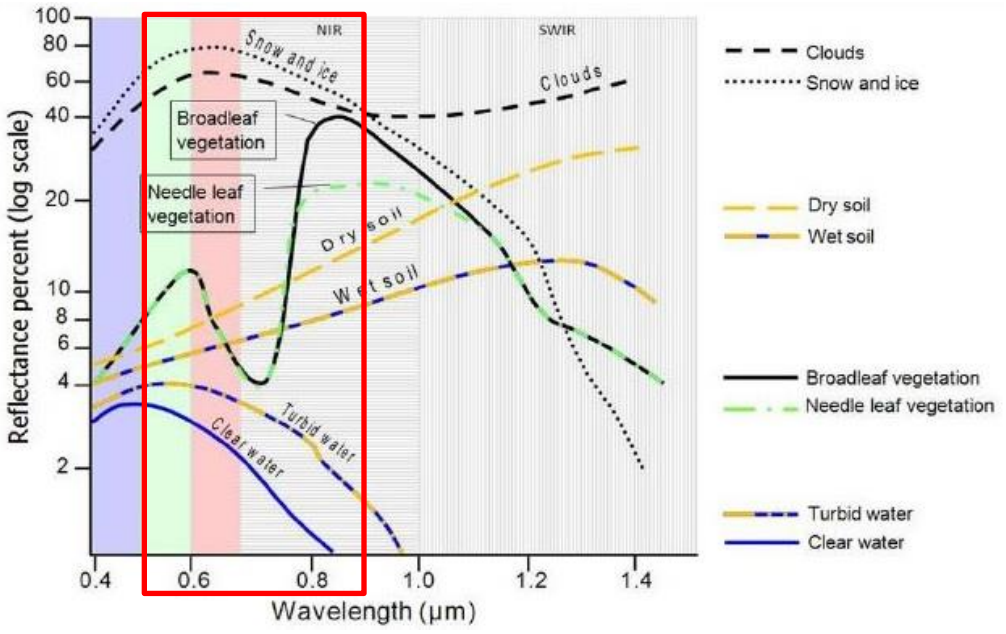


Figure 2.4.1 Spectral reflectance of natural land cover, with the CIR bands highlighted by the red shape (Aronoff, 2004; CIR emphasis added).

As shown above, water – whether turbid or clear – has a distinctive spectral reflectance at the wavelengths covered by CIR imagery, generally appearing jet black or dark blue (Legleiter and Fonstad, 2012; Sun *et al.*, 2012). The spectral separability of water is enabled largely by the NIR band (>0.75µm),

hence why CIR is an ideal medium for extracting surface waters. The main confounding factor for extracting surface waters from CIR imagery is that the environment both within the channel and immediately surrounding it can contain objects with a comparable spectral response (Sivanpillai and Miller, 2010). For example, suspended or floating vegetation can alter the spectral reflectance of water to such an extent that it is comparable to that of terrestrial vegetation, while suspended sediment or shallow stream depth – with the latter likely to be the case with the lower order headwater streams critical to this study – has a similar effect (Jensen, 2013b; Williamson, 1974) (see Table 2.4.1).

Table 2.4.1 Recommended methods for the classification of surface waters based on the varying spectral reflectance of differing water types (adapted from (Frenette *et al.*, 2012; Sun *et al.*, 2012).

Water type	Characteristics	Observed trend	Approach recommended
Clear	Little suspended sediment or vegetation.	Spectral reflectance decreases as wavelength increases.	MNDWI with threshold of '0'.
Green	Submerged or floating vegetation; presence of phytoplankton.	Maximum spectral reflectance occurs in the NIR band.	Threshold set to be lower than reflectance of vegetation, which also has high spectral reflectance in this band. NDVI used to differentiate between green water and paddy fields.
Turbid	Suspended sediment or low depth; presence of phytoplankton.	Maximum spectral reflectance occurs in the MIR band.	Threshold set to be lower than reflectance of bare soil, which also has highest spectral reflectance in this band.

In order to account for the varying spectral reflectance in surface waters, different training data sets could be created for each of the three stream types as described above. This approach is comparable to a technique where classification accuracy was improved by creating multiple sets of localised training sites in place of a single homogenous training dataset, in order to account for the local variation of spectral reflectance of the classes of interest across the study site (Muslim *et al.*, 2006). A

combination of the two approaches – disaggregating the selection of training sites based on both spectral and spatial variation in surface waters – could yield even greater improvements in classification accuracy.

2.4.2 Extracting features from aerial imagery

In order to measure WSW from aerial imagery, it is first necessary to identify where rivers and streams are located. There is an established body of literature concerning the identification of linear features from remotely sensed imagery, such as roads (Mnih and Hinton, 2010), hedgerows (Thornton *et al.*, 2007) and coastlines (Foody, 2005; Muslim *et al.*, 2006), as well as parameters for monitoring rivers and streams, such as bathymetry (Biancamaria *et al.*, 2016a; Iervolino *et al.*, 2015).

There are a number of techniques available for extracting the desired features from an image, with the use of an automated algorithm the simplest method for increasing the efficiency of the classification process (Güneralp *et al.*, 2014). An unsupervised classification method, such as k-means or ISODATA (Iterative Self-Organising Data Analysis Technique Algorithm), classifies remotely sensed imagery based on basic user inputs, namely the target number of land cover classes that should be in the output, the minimum size for an individual cluster of pixels to be attributed to a thematic class, and the number of iterations (Memarsadeghi *et al.*, 2007). However, the user is not able to guide the classification process by training the algorithm to recognise that a particular spectral reflectance relates to a specified class, hence the term 'unsupervised'. Supervised classification, on the other hand, allows for a greater degree of user input and more accurate representations of land cover as a result. The following sub-sections address the various techniques that fall into this category.

i. Hard classification

Perhaps the simplest method for extracting surface water without resorting to manual techniques is to apply a supervised classification. This is achieved by the user selecting training data that correspond to the classes contained within the image. For example, the user will select a sample of areas that

exclusively contain surface waters, then another subset that contains vegetation, and so on. The supervised classification method then applies the same thematic classes to unknown portions of the image, analysing the spectral reflectance of each individual pixel and applying the correct class based on the training data provided. This is commonly carried out for surface waters using the maximum likelihood classification (Sheng *et al.*, 2008; Sun *et al.*, 2012), or MLC, which determines the thematic class a pixel belongs to by calculating the probability of class memberships based on the training data provided, and then assigning, as the name suggests, the most likely class to the pixel.

The simplicity of the hard classification approach, however, has significant drawbacks that adversely affect the accuracy of the classification. Evidently, the reliance on a user-defined training dataset means that the outcome is affected by the accuracy of the initial classification process where the user identifies the range of land cover classes present in the image, which is in itself a time-consuming processing requiring a degree of expert knowledge. However, the automatic identification of classes in the remainder of the image is an improvement on the tendency for studies beyond the river reach scale to use manual extraction when delineating water boundaries (Birkinshaw *et al.*, 2014).

Furthermore, significant errors of omission occur as a result of the comparable spectral reflectance (in optical imagery) of surface waters and thematic classes such as coalfields, building roofs, asphalt, and shadows. Post-processing techniques are capable of removing some of these classification errors, but are context dependent. For instance, Armenakis (2005) and Sun *et al.* (2012) used elevation and slope data to differentiate between mountain shadows and surface water, yet did so by concluding that water bodies occurred in areas of low slope and low elevation. This approach, therefore, was not appropriate for use in this study, given the need to identify low order headwater streams, which occur in areas of relatively high elevation and slope. Without the ability to use this ancillary information to improve classification performance, a simple hard classification was not likely to yield the best results.

ii. Spectral indices

Spectral water indices are another common method for classifying surface waters from remotely sensed imagery. Building upon trends in the broader land cover classification literature, particularly the use of the Normalised Difference Vegetation Index (NDVI) (Fensholt and Proud, 2012; Rouse *et al.*, 1974; Tucker, 1979), to both classify vegetation and quantify its general health, such approaches have been shown to be capable of extracting over 99% of rivers and streams from an aerial image (Rodríguez-Cuenca and Alonso, 2014).

Of the indices that specifically aim to enhance the spectral contrast between land cover classes in a manner that allows the user to more readily differentiate between surface water and other classes, the Normalised Difference Water Index (NDWI), developed by (McFeeters, 1996), is commonly used as the reference method with which others are compared. In this instance, contrast is enhanced by finding the ratio between the green visible light band and the near infrared (NIR) band, with the downside being that water surface extent is overestimated in cases where there is a high degree of noise caused by the adjacency effect e.g. where a water pixel is adjacent to a comparatively 'bright' land surface. This problem is addressed by the Modified NDWI (Xu, 2006) which replaces the NIR band with mid-IR. This method is currently the most commonly used when attempting to classify surface waters from remotely sensed imagery (Feyisa *et al.*, 2014; Ji *et al.*, 2009; Sagin *et al.*, 2015; USGS, 2016).

However, misclassification is still common with the MNDWI, as non-water features such as shadows from trees, mountains, or cloud cover have a comparable spectral reflectance to surface waters. A recent method, named the Automated Water Extraction Index (AWEI), demonstrates that it is possible to suppress these non-water classes, thus minimising the extent of misclassification (Feyisa *et al.*, 2014), yet does so by utilising five separate Landsat bands, with two context-dependent equations applied to the imagery based on whether or not shadow is considered to have a great impact on the classification. This is a highly subjective process, and when combined with the comparatively high

resource demands (5 vs. 2 bands for other indices) of the methodology, the ease of classification allowed by the greater degree of automation is somewhat negated. Similarly, the application of $NDWI_{green}$ and $NDWI_{red}$ to improve water extraction accuracy, as discussed by Yan *et al.* (2017), is dependent entirely on *a priori* knowledge of where clear/green and brown water bodies are located, which is both subjective and unknown in many studies. Finally, the use of Landsat – common to all of the above approaches – is also a limiting factor, as the spatial resolution of the most recent Landsat 8 satellite is 30 m for the bands used in the aforementioned indices. While this is an improvement on previous iterations, it still falls short of being able to capture the critically important lower order streams.

A final index of interest, the Simple Water Index (SWI), utilises only two bands – the blue visible light and the shortwave infrared (SWIR) bands from Landsat 8 – and is the most promising in terms of producing accurate maps. In a recent comparison with MNDWI and AWEI, where classification accuracy of inland waters was 78.4% and 83.8% respectively, SWI had an accuracy of 91.9% (Malahlela, 2016). This index is, however, so recent that there have been no systematic tests to see whether there are certain environmental conditions in which it performs best. The sole study using SWI was conducted in arid and semi-arid conditions and on a local scale, so the temperate climate of the UK and the greater range of spectral responses present in large scale imagery may have reduced the accuracy considerably.

Furthermore, a problem common to all indices is the need to specify a threshold value which divides the class of interest from all others. While it is commonly stated that a threshold of zero adequately separates surface waters (values <0) from other land cover classes (Xu, 2006), this is an overgeneralisation, as this value is unstable and varies from one remotely sensed image to another as a result of the particular spectral reflectance of features in each image, with the threshold also varying depending upon which index is applied (Ji *et al.*, 2009). Although variation in the threshold value is an

order of magnitude lower with the AWEI method (Feyisa *et al.*, 2014), the input of an expert user is still required if the classification accuracy stated in previous studies is to be achieved.

iii. Spatial enhancement

While the techniques outlined above are limited by the spatial resolution of the input imagery, a number of methods exist that allow the user to derive outputs at a greater spatial resolution than the original imagery. This is of particular interest for this study, as headwater streams are potentially narrower than the spatial resolution of the available imagery sources.

Whereas hard classification techniques function by applying an individual class membership for each pixel, the reality is that a single pixel may be 'mixed' and contain multiple thematic classes (Fisher, 1997), so assigning it to a single class has the effect of shifting class boundaries to lie between pixels, when they may in fact run through a pixel. Soft, or fuzzy classification (Foody, 1996), allows for a pixel to belong to multiple classes, with the output of such a procedure creating fraction images that represent the relative class membership within a pixel (Foody, 2005), expressed as a percentage or as a decimal where the total is equal to 1.

However, soft classification is unable to provide any information regarding the spatial arrangement of the thematic classes, so while the output reveals the relative proportions of each class within a given pixel, it is not evident as to where these classes occur within the pixel. In the context of estimating WSW, this introduces a source of error proportional to the spatial resolution of the imagery.

Fortunately, a technique known as super-resolution mapping (SRM) directly addresses this fundamental problem by applying various post-processing techniques, effectively undertaking a hard classification at the sub-pixel level (Atkinson, 2004; Atkinson, 2005). There are limitations to these techniques though, with the use of a Hopfield neural network (HNN), for example, generally requiring multiple images of the same area in order to derive the *a priori* information that is vital to the success of this approach (Tatem *et al.*, 2002). In addition, pixel swapping, where each iteration of the method

swaps two sub-pixels if spatial correlation within the pixel can be improved (Atkinson, 2005), is heavily reliant on the accuracy of the initial soft classification. Thus, the use of SRM is highly dependent on the context in which such methods are to be applied, while it has also been acknowledged that using multiple SRM techniques in tandem further improves the final classification accuracy (Su *et al.*, 2012a, 2012b; Yu *et al.*, 2014).

The complementary use of soft classification and SRM to determine thematic class composition at the sub-pixel level for high resolution imagery has previously been used to extract linear features from aerial imagery. For example, in a study of shoreline extraction (Foody *et al.*, 2005; Muslim *et al.*, 2006), soft classification techniques were applied to 20 m resolution imagery to derive a more accurate and true-to-life classification, with a final RMSE of between 2.13 m and 1.51 m. The degree of error relative to the original resolution of the imagery is indicative of the extent to which imagery can be enhanced using SRM.

Within the context of WSW, studies using sub-1 m resolution imagery are able to demonstrate that imagery is already sufficiently accurate when compared to field validation (Rawlins *et al.*, 2014a). Being able to improve on this even further would provide clear benefits, especially in terms of addressing the need to better represent smaller headwater streams (Yang *et al.*, 2014) in both the initial measurements and within the context of applying WSW estimates CO_2 evasion estimates.

iv. Classifying a single feature of interest

The techniques discussed previously are capable of producing a land cover map that identifies every different surface present in an image. However, this study only requires data pertaining to rivers and streams, meaning that any time spent on defining training sites for non-water classes is unnecessary, and diverts valuable and limited resources away from the job at hand (Boyd and Foody, 2011).

A technique known as unary or one-class classification (OCC) does not require this superfluous work to be undertaken, significantly reducing training set size requirements (Li and Guo, 2010; Pal and

Foody, 2012) while also improving the ability to identify the particular class of interest (Silva *et al.*, 2017). Multi-class approaches such as MLC are optimised to identify all features within the landscape, which can result in lower classification accuracy for the single feature of interest when compared with approaches designed to classify a single specific class (Boyd *et al.* 2006, Foody *et al.* 2006, Sanchez-Hernandez *et al.* 2007a, Sanchez-Hernandez *et al.* 2007b). However, OCC intentionally creates an incomplete and unrepresentative reference dataset, making accuracy assessment extremely challenging (Mack *et al.*, 2014), something that must be addressed in studies utilising this approach.

Considering the acknowledgment that current methodologies for extracting inland waters from imagery and subsequently measuring WSW are very labour and resource-intensive (Rawlins *et al.*, 2014a), the use of OCC would directly address this fundamental problem and, when used in conjunction with sub-pixel classification, form the basis for an efficient and novel approach to surface water feature extraction capable of delivering an improved representation of headwaters.

2.5 Conclusion

The above examination of the relevant literature highlighted a number of areas worthy of further research. Chief among these is the need to quantify the impact of fluvial CO_2 evasion to the atmosphere, largely because the important of lotic inland waters to the carbon cycle has only recently been fully recognised. The result of this is that the spatial and temporal dynamics of fluvial CO_2 evasion are poorly understood at all scales, from local to global, and require significant research to elucidate.

A key barrier to future progress is the dependence on statistical models of fluvial CO_2 evasion that do not incorporate all possible explanatory variables. In the case of England and Wales, water surface area is an obvious omission, correcting which could also offer additional benefits beyond an improved understanding of biogeochemical processes, for instance in quantifying the spatial distribution of water resources and allowing for their long-term monitoring. While river network length is easily

calculable, the temporal dynamism of WSW presents significant problems in adequately capturing it. The literature concerning channel width, bankfull width, and WSW highlighted remote sensing as a viable solution, both in terms of offering improved spatial coverage and potentially high-resolution imagery. The latter is especially significant, as capturing narrow, low-order headwater streams has been highlighted by previous research as problematic, yet of vital importance, as these streams account for a disproportionately large proportion of both total river network length and fluvial CO_2 evasion.

The most immediate concern, and the focus of the preceding chapter, was to capture inland surface waters in the first instance, with a particular emphasis on meeting the requirement for a scalable approach capable of capturing narrow low-order streams.

Chapter 3

Extracting surface waters from aerial imagery

To address the need for a high-resolution dataset of WSW for England and Wales that was fit for purpose, surface waters were required from which measurements could then be taken. This chapter focuses on the process used for achieving this, beginning with the selection of an appropriate study site, imagery, and extraction method, before analysing the surface waters dataset produced to examine its quality considering that direct image-based measurements of WSW would subsequently be derived from this dataset (see Chapter 4, p.94).

In order to differentiate areas of surface water from other land cover types, it was first necessary to evaluate the performance of existing image classification and feature extraction techniques in this regard. This process would subsequently inform the selection of a methodology for identifying surface waters across the chosen study area. This was also required due to existing datasets representing surface waters in a manner that was not conducive to this study. For example, Ordnance Survey data

represents rivers at maximum winter flow using a single line for rivers narrower than 5 m, and dual lines for those that are wider (Ordnance Survey, 2016a, 2016b). The inconsistency of this representation and the requirement for a dataset capturing rivers at below MDF rendered existing products unusable.

Before commencing with a comparative analysis of techniques, it was first necessary to consider the ideal properties that a technique would have. Specifically, these were: -

1. The ability to produce as accurate a representation of surface water as possible, both in terms of traditional remote sensing accuracy assessment techniques (e.g. confusion matrices) and spatial data quality metrics (e.g. completeness when compared with an established reference dataset).
2. The capacity to capture as narrow a river or stream as possible, in line with the understanding that low order headwater streams play a significant role in CO_2 evasion due to being supersaturated, having a comparatively high gas transfer velocity, and being underrepresented in existing research beyond the local scale.
3. Applicability to subsequent analyses, as the classification of surface waters from the imagery was not the end product, as WSW measurements were subsequently made that had to be of sufficient quality to validate the predictive model.

These specific requirements, when combined with the use of high-resolution CIR imagery, meant that no baseline existed in terms of a recommended standard practice, thus necessitating the comparative analysis of existing techniques for feature classification.

3.1 Study site

The direct image-based measurement of WSW (Chapter 4, p.94), while ideal, was not feasible for the entirety of England and Wales due to the extensive resource requirements of the process, not least in terms of labour and computational power. This meant that for the dual purpose of deriving WSW inputs for use in a statistical model capable of scaling these measurements to the entirety of England and Wales, and the validation of the model estimates of WSW (Chapter 5, p.121), a smaller area was selected upon which the remote sensing methodology was applied. In order for the predictive model of WSW to be applicable to England and Wales, the study area had to be as representative as possible, necessitating an examination of a number of criteria.

The primary objective was to capture the full extent of the national-scale variation in the known predictors of WSW within a manageable area. This process took the predictors identified throughout the literature review as a starting point, which was followed by the analysis of the range of values specific to England and Wales, thus informing the selection of a representative site. The overall approach has a significant history, as the use of river typologies is a common tool for conceptualising the variation in the form of rivers over space and time. An extensive review is beyond the scope of this study, and can instead be found in Kondolf *et al.* (2003).

One of the more popular techniques, largely due its simplicity, is the Strahler stream order approach, or the Horton-Strahler number (Horton, 1945; Strahler, 1952, 1957), which applies a numeric value to a watercourse that increases by 1 when two streams of the same order converge, with a 1st order stream being a watercourse that has no tributaries. Thus, once two 1st order streams converge, a 2nd order stream is created, with the observed maximum being the Amazon at its mouth, which is a 12th order river. The popularity of this typology is arguably due to the ease with which it can be calculated within a GIS (Gleyzer et al, 2004), especially when compared with alternative approaches to measuring stream size that involve the availability and analysis of ancillary datasets such as discharge, cross-

sectional area, width, and depth, the main components of hydraulic geometry (Fryirs and Brierley, 2012; Gleason, 2015). However, while Strahler stream order is capable of providing a good approximation of stream size, there is a significant degree of error associated with this approach. Hughes *et al.* (2011) assessed the accuracy of Strahler stream order for predicting stream size in specific ecoregions and hydrological basins in the USA, with *r* ranging from 0.48 and 0.92 and showing a significant degree of variation dependent on both landscape type and spatial scale. While Strahler stream order was effective in mountainous areas, comparisons with actual stream size in lowland areas demonstrated high variability, with a single stream size occurring in up to 7 different Strahler stream orders at the national scale; local-scale variation was generally much lower. Based on these findings, it was decided that an alternative approach was required to capture the variation in rivers for England and Wales for this study.

Such an approach already exists, with the UK Technical Advisory Group for the Water Framework Directive (UKTAG) determining that a river should be identified as such if the catchment area is greater than 10 km^2 or if a water body is especially important as a source of drinking water or the location of significant ecological habitats (UKTAG, 2003a). Rivers with a catchment area less than 10 km^2 may also be included in the classification if they are especially prevalent in a given region. These rivers are then divided into classes based on a three-stage typology, with elevation (<200 m, 200-800 m, >800 m), catchment area (10-100 km^2, 100-1000 km^2, >1000 km^2), and dominant geology (siliceous, calcareous, organic) used to develop 27 unique categories, with 18 found to exist in significant quantities in the UK (UKTAG, 2003b).

However, even though typologies are frequently applied and that a UK-specific system has already been devised, they were of questionable use for this study. The primary objective of site selection in this case was to find a representative area that covered the range in the potential explanatory variables of WSW (as discussed in Section 2.3, p.21), so using a typology as a proxy instead of measuring the variables directly made little sense. The very notion of river channel classification is

based on the idea that distinct river types are found in areas with differing sets of geomorphological controls (Sear *et al.*, 2010). Therefore, by ensuring variation in these controls across the study area, a range of river typologies was captured by default.

Examination of landscape and geomorphological attributes for England and Wales identified a 20km x 110km study site that was representative of national-scale variation. Figure 3.1.1 shows the location of this area in Great Britain, comprising northern Wales and a small portion of central England.

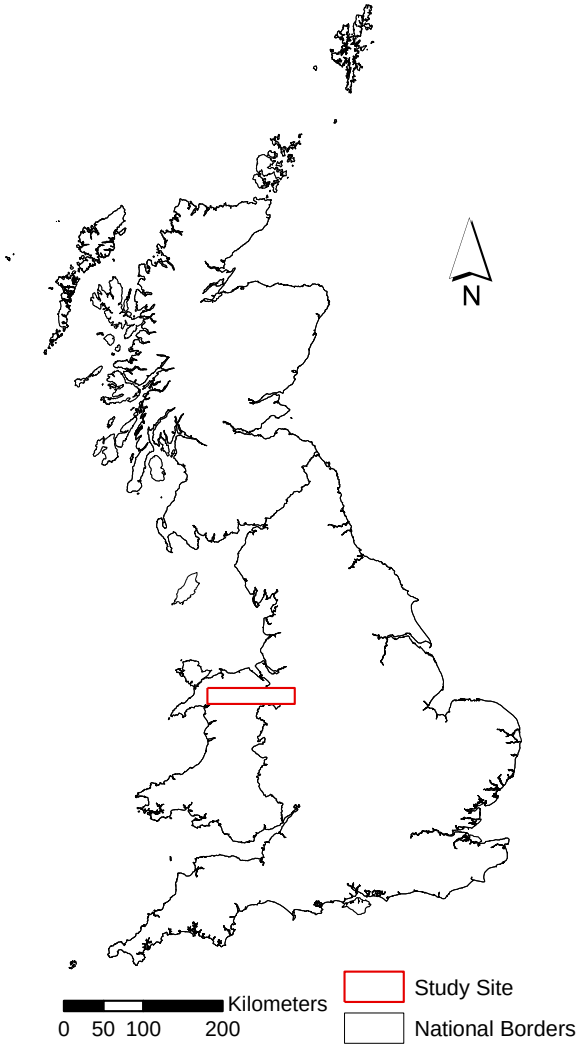


Figure 3.1.1 Location of chosen study site within Great Britain (bounding box coordinates are SW corner; 260000, 340000, and NE corner; 370000, 360000).

This region was selected for three key reasons in addition to containing representative variation in the controls of WSW. Firstly, the variation in elevation and slope (Figure 3.1.4 on p.54, panels B and C) ensures that the techniques used were able to address issues such as the varying spectral response of shallow channels, as well as the problems introduced by mountain shadows (Güneralp *et al.*, 2014), by incorporating both the rugged terrain of Snowdonia National Park and lowland areas in central England. These factors were considered to be of greater importance because of their potential impact on the ability to accurately identify surface waters; shallow channels may differ both visually and spectrally from the mean for surface waters in a given area due to channel bedrock being more visible, while mountain shadows similarly affect spectral response when they coincide with surface waters. By incorporating the highest peak in England and Wales in Mount Snowdon, the study site was sure to contain both shallow first-order streams and mountain shadows. Thus, if the extraction methodology was capable of achieving a high level of accuracy in these areas then the technique could potentially be more generalizable and applicable to any area of England and Wales.

Secondly, there was variation in drainage density across the study area (Figure 3.1.2 and Table 3.1.1 overleaf). Drainage density correlates with both sediment yield (Strahler, 1957) and erosion intensity (Strahler, 1956), so in addition to the aforementioned variation in topography, the study area represents different degrees of key fluvial processes which in turn affect channel morphology (see Section 2.3, p.21), and which are difficult to account for through other means due to the lack of existing datasets and the scale of the study site prohibiting meaningful and representative fieldwork to remedy this.

Thirdly, the study area provided an acceptable compromise between the competing factors of confirming that the range of landscapes found in England and Wales were adequately represented, ensuring that the predictive model based upon subsequent measurements is generalizable, while minimising the burden on the available computational resources. Processes such as thematic classification and the semi-automated measurement of WSW at densely packed sampling points were

intensive procedures and required a significant degree of refinement that meant an increase in study site extent would have increased resource requirements exponentially.

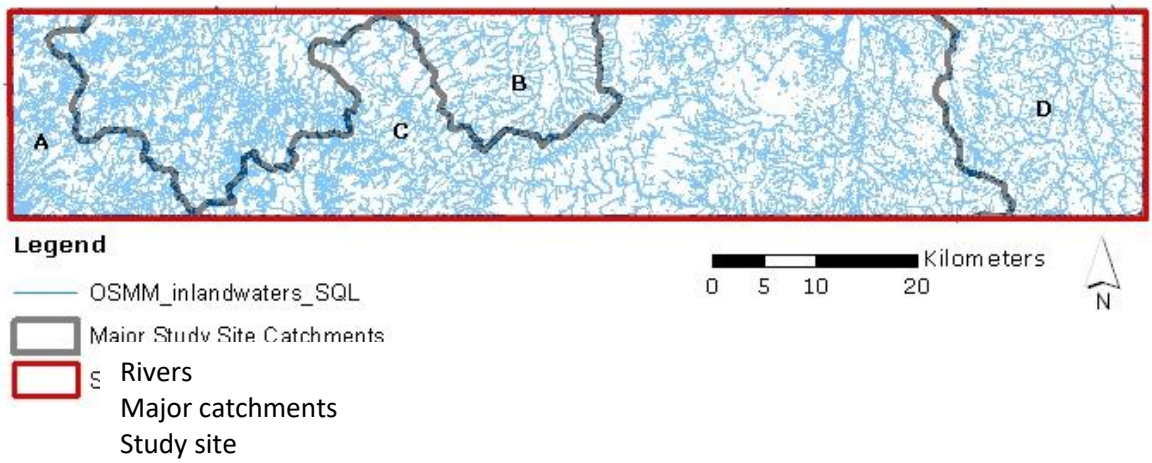


Figure 3.1.2 Major hydrological catchments across the study site.

Table 3.1.1 Summary statistics for the major hydrological catchments found in the study site.

Catchment	Length (km)	Area (km^2)	Drainage density (km/km^2)
Catchment A	1039.65	197.09	5.27
Catchment B	2391.93	571.93	4.18
Catchment C	3782.37	1072.87	3.53
Catchment D	1206.82	357.28	3.37

Figure 3.1.3 (p.53) and Figure 3.1.4 (p.54) display the variation in all remaining WSW explanatory variables across the study site. The key spatial trends are as follows: -

- Catchment area: the west of the study site generally contains rivers and streams with a smaller catchment area, with a progressive increase further east. This indicates a higher proportion of low-order streams in the west.
- Rainfall: the west of the study site experiences some of the highest rainfall levels in England and Wales while easterly areas have some of the lowest.

- Land cover: a very clear rural-urban gradient is observable running west to east. The study area includes a variety of woodlands and grasslands.
- Hydrological source of flow: BFI is generally varied across the study site, but does not exhibit a clear spatial trend. Low values for BFI are dispersed across the area, while higher values are more prevalent in the east.
- Channel gradient: slope is higher in the west around Snowdonia National Park (NW corner of study area), with the east comprising the lowlands of central England.
- Elevation: follows the same general pattern as channel gradient.
- Human modification of river channels: all HMS classes are represented in the study area, with channels in the east generally being more heavily modified than those in the west. Comparison with the spatial distribution of land cover shows that urban areas are generally limited to the east of the study site, and when compared with the larger catchment areas of rivers in the east justifies why management efforts, as well as inadvertent human impacts on the river channel, would exhibit the observed trend i.e. larger human populations, as well as larger rivers, means that there is a greater requirement for river channel management.

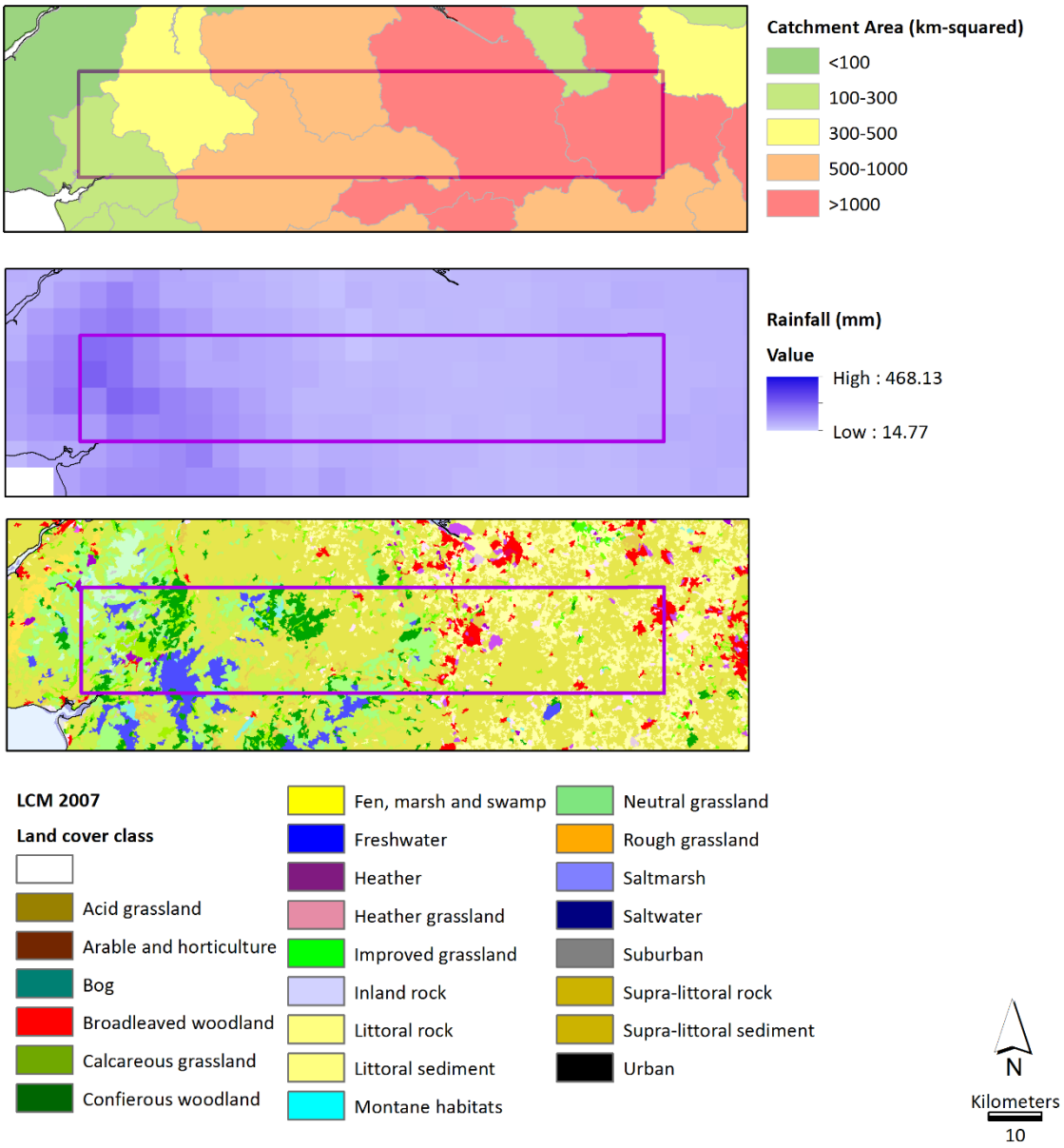


Figure 3.1.3 Variation in explanatory variables of WSW across the study site (identified with bounding box). From top to bottom, these panels represent; a) catchment area for each IHU Group (Centre for Ecology and Hydrology, 2015b); b) rainfall in May 2009 (period of aerial imagery capture); c) land cover.

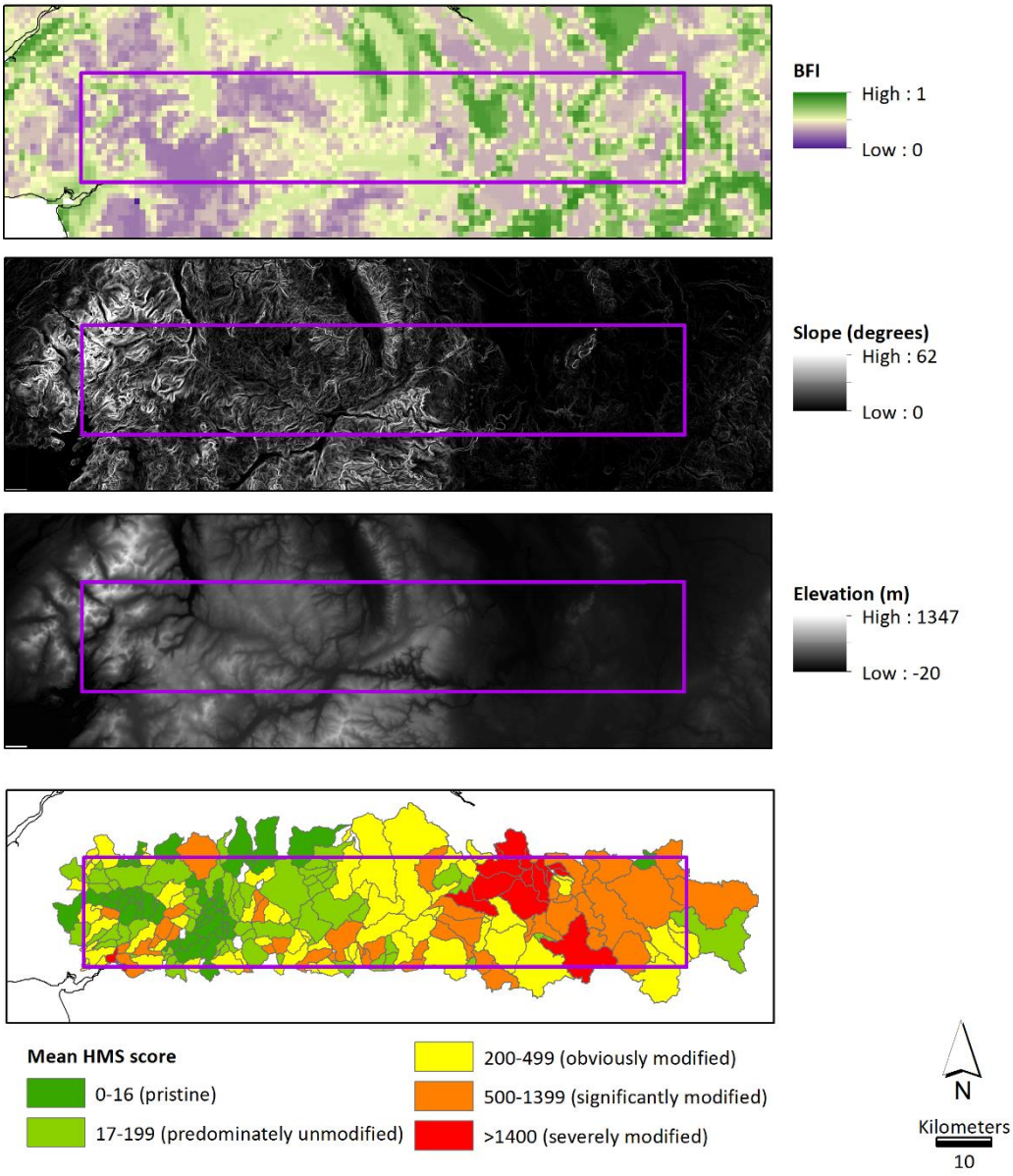


Figure 3.1.4 Variation in explanatory variables of WSW across the study site (identified with bounding box). From top to bottom, these panels represent; a) hydrological source of flow (BFI); b) channel gradient; c) elevation; d) human modification of river channels (HMS score).

Finally, this study site also had the advantage of containing a significant number of headwater streams, with 66.08% having a catchment area <15 km^2, compared with ~90% in a national scale study of Sweden which established this catchment area size as the threshold for identifying headwaters (Bishop *et al.*, 2008). Using this same threshold for England and Wales, GIS analysis of the widely available IHU catchment dataset (Centre for Ecology and Hydrology, 2015b) carried out as part of this study found that ~95% of rivers in England and Wales are headwaters. While this would suggest that headwaters are relatively underrepresented by the study site, this is likely due to the temporal and spatial resolution of the IHU data omitting a number of surface waters e.g. intermittent rivers and ephemeral streams (IRES) that exist seasonally, as well as catchments and/or streams below a certain size threshold.

Overall, the combination of the previously discussed factors meant that this study site was deemed suitable for the analysis, meaning that suitable data then had to be identified. The lack of a suitable pre-existing dataset meant that one had to be derived from scratch, making the application of remote sensing techniques to aerial imagery the most appropriate approach for addressing this objective.

3.2 Aerial imagery

With a key aim of this study being to quantify CO_2 evasion from rivers using the features extracted from the imagery, the need to capture the narrowest, super-saturated streams was at the forefront of the imagery selection process. This meant that high resolution imagery that was also amenable to further enhancement, if deemed necessary, was the ideal.

Firstly, the ability to clearly differentiate between water and other land cover classes was of the utmost importance, as this would help reduce errors of omission (waterbodies that have been overlooked) and commission (materials such as tarmac that have been misclassified as water) in the final product. The use of multispectral Landsat imagery is very common (Zhang 2000, Rover *et al.* 2011,

Verpoorter *et al.* 2012), as the combination of multiple bands can be used to easily distinguish different surface materials. However, the spatial resolution for the Operational Land Imager (OLI) sensor aboard Landsat 8 is limited to 30 m at best, which was considered to be too coarse for this study. Alternatives such as imagery gathered by Sentinel-2's MSI platform and the Pleiades constellation improve markedly by offering a spatial resolution of 10 m and 2 m respectively in RGB and NIR bands that are usable for surface water extraction, but despite this, these satellite platforms are still limited by another significant factor, namely cloud cover. The UK has an estimated 9.5 clear days per year (Mewse, 2016), and when combined with the 5-day return period for Sentinel-2 (versus 16days for Landsat and 26 days for Pleiades) the likelihood of having coverage for the entire study area was remote. One solution would be to create a cloud-free composite image using imagery taken at different times, but this could result in a high probability of river flow exhibiting a significant degree of variation across a small area, contrary to the desire to measure river flow at below MDF for the entire study site (discussed in Section 3.2.2, p.57).

3.2.1 CIR aerial imagery for England and Wales

Multispectral CIR imagery with a spatial resolution of 50cm, captured between 11th May and 3rd June 2009, was kindly provided by the British Geological Survey (BGS) for the study area. The imagery was originally captured by Getmapping for the entirety of Great Britain with the primary aim of being used to differentiate between vegetated and non-vegetated land surfaces (Getmapping, n.d.), but as discussed in Section 2.4.1 (p.34), CIR imagery can also be used effectively to identify inland surface waters.

In addition to being selected for accessibility reasons, the Getmapping CIR imagery was deemed suitable for this study due to striking an acceptable compromise between cloud-free coverage (aerial surveys were timed to coincide with comparatively cloud-free days) and a high spatial resolution (allowing for headwater streams to be identified and measured).

3.2.2 Contextualising aerial imagery with river flow data

National River Flow Archive, or NRFA, data (Centre for Ecology and Hydrology, 2015a) were used to provide context to the aerial imagery, which was captured between 11th May and 3rd June 2009. Gauging station data were not used as a direct input in predictions of WSW made in Chapter 4 due to the disparity between the 10 NRFA stations contained in the study site (Figure 3.2.1) and the several thousand locations at which WSW was predicted, so the data were instead used to offer a general picture of river discharge across the study site to ensure that any effects of flow on WSW were reduced. Specifically, conditions *below* MDF were desirable, as MDF is calculated as a long-term average of AAS discharge measurements, meaning that it is influenced by infrequent but high magnitude flood events, resulting in a positively skewed distribution. Hence, imagery representing river discharge at or above MDF would lead to both the overestimation of both WSW and factors such as CO_2 evasion that depend upon it.

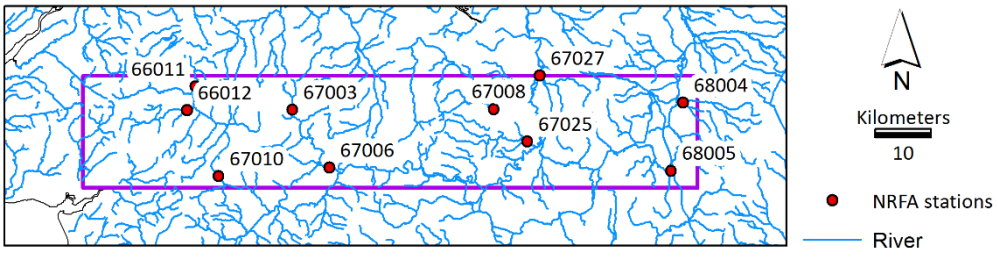
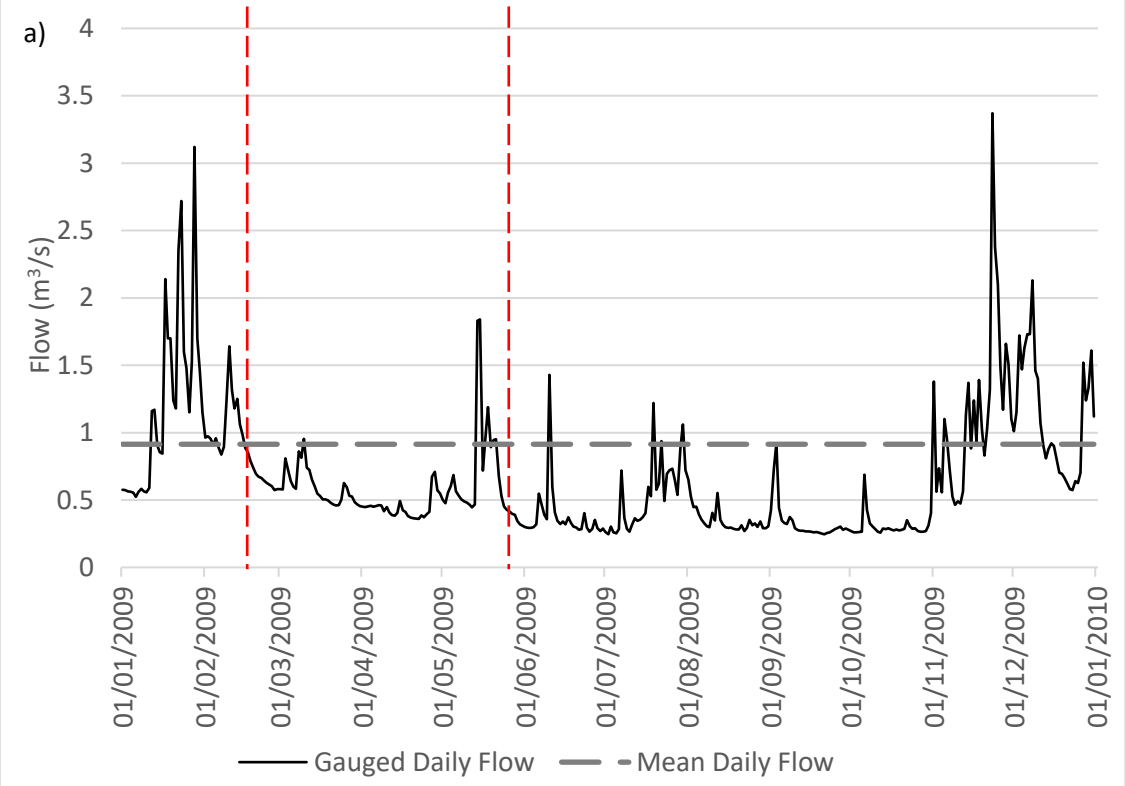


Figure 3.2.1 NRFA stations contained within the study area.

The flow hydrographs for each of the 10 NRFA stations in the study area were examined, and the raw data downloaded to ensure that flow conditions at the time of capture were both below long-term MDF, and broadly comparable to the second-quarter flow observed during other years, thereby controlling for both inter- and intra-annual variation. All hydrographs exhibited the same trend, with gauged flow at the time of image acquisition being below MDF (Figure 3.2.2, p.59). This is not altogether surprising, as the operational requirements for medium-format aerial surveys are that

cloud cover is at a minimum, so the wetter winter months where flow is more likely to be above MDF were avoided by default when capturing the CIR imagery.

Additional trends present in Table 3.2.1 show that gauged flow as present in the aerial imagery is largely suitable for the analysis of WSW. In two cases, mean second-quarter flow for 2009 (Q2 2009 MDF) exceeded the long-term second-quarter mean (Q2 MDF), but only marginally. Of greater significance is that Q2 2009 MDF was consistently lower than both MDF and 2009 MDF.



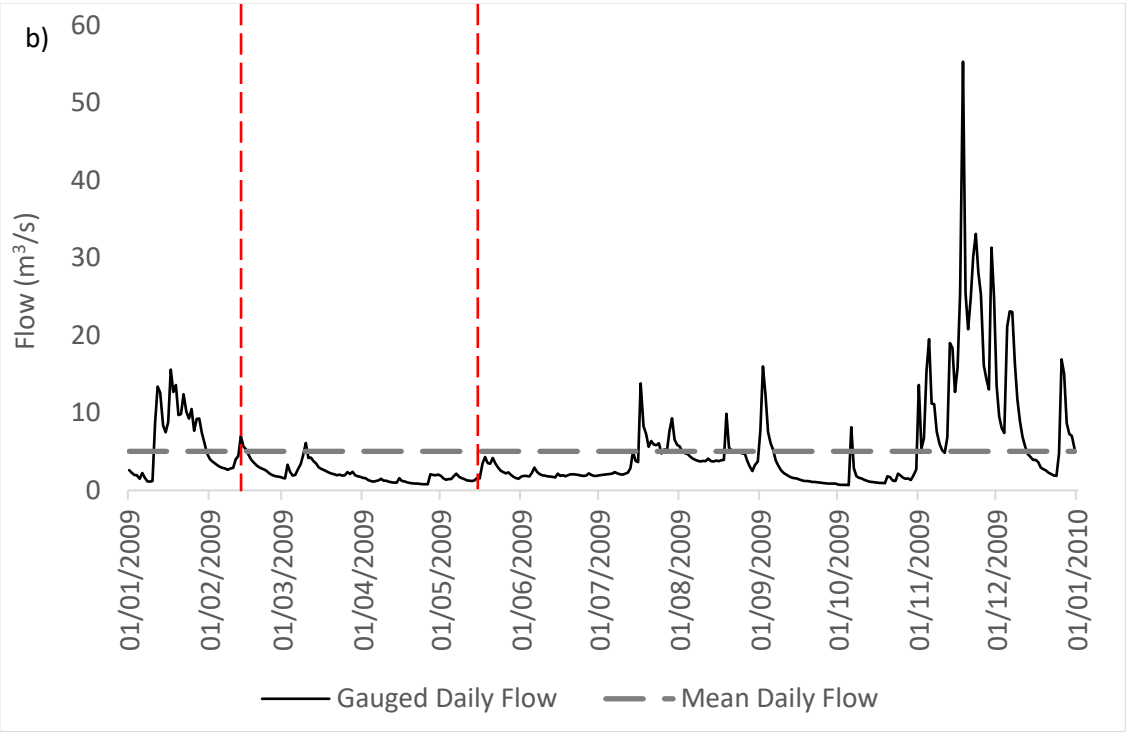


Figure 3.2.2 A comparison of mean daily flow with gauged flow at time of data capture at NRFA gauging stations a) 67006 River Alwen at Druid, and b) 68004 Wistaston Brook at Marshfield Bridge. Red dashed lines indicate the date at which aerial imagery were obtained.

Table 3.2.1 Descriptive statistics derived from flow hydrographs at all NRFA gauging stations within the study site (n = 10). All units for MDF are m^3.

Station ID	Station Name	MDF (long term)	Q2[1] MDF (long term)	2009 MDF	Q2[1] 2009 MDF
66011	Conwy at Cwmlanerch	18.88	10.75	18.02	5.99
66012	Lledr at Pont Gethin	4.95	2.90	5.23	2.98
67003	Brenig at Llyn Brenig outflow	0.58	0.39	0.72	0.59
67006	Alwen at Druid	5.04	2.94	4.91	1.79
67008	Alyn at Pont-y-Capel	2.38	1.76	2.07	0.87
67010	Gelyn at Cynefail	0.70	0.39	0.72	0.25
67025	Clywedog at Bowling Bank	1.35	1.07	1.22	0.60
67027	Dee at Ironbridge	38.53	23.87	34.89	13.42

68004	Wistaston Brook at Marshfield Bridge	0.91	0.72	0.66	0.50
68005	Weaver at Audlem	1.60	1.07	1.49	0.64

[1]Q2 = April, May, and June

3.2.3 Assessing intra-image variation in the spectral reflectance of water

The CIR imagery was originally provided in 1 km^2 sections. For a study site covering an area of 110kmx20km, this meant that there were 2,400 individual images. The reality was that some of these images did not contain water, and were therefore unnecessarily increasing the time taken for the analysis, as it was carried out on an image-by-image basis for reasons explained in 3.3. Therefore, the imagery was aggregated into a raster mosaic, with the result being 22 images that each covered 10 km^2.

Further grouping was not undertaken for two key reasons. Firstly, it has been established that raster operations are more efficient when a dataset is broken into segments (Whiteaker *et al.*, 2007). Secondly, and most importantly, each image was captured at a different time, so the spectral reflectance for each class may vary both within and between images. Realistically, natural variation would also cause such differences, for example where water is more turbid, has more suspended sediment, or varies in depth, but the difference in atmospheric conditions is the primary factor that can be controlled.

Amalgamating the imagery into a single continuous raster would likely result in decreased classification accuracy due to pixels belonging to the water class appearing increasingly different as the imagery is further combined. 10 km^2 mosaics were found to be a good compromise between practicality and limiting intra-image variation in spectral reflectance, which was important due to the classification process being applied to each image separately.

This was tested systematically by measuring the cross-sectional variation in spectral reflectance in every image. This was undertaken by using the 'Profile' tool in TerrSet to draw a perpendicular transect

line that covered the surface water from bank to bank. This was completed 30 times for every 10 km^2 image, with the image values for every pixel covered by each transect displayed to show variation in spectral response (see Figure 3.4.2, p.78). The 10 km^2 mosaics were sufficiently small that intra-image variation was minimal. However, significant inter-image variation was present, largely due to the imagery being captured on different dates. Also, there is a clear gradient across the study site with shallow headwater streams in the west and higher order rivers in the east, the latter of which are more likely to have alluvial beds, so a greater proportion of suspended sediment that can alter the spectral response of surface waters.

The consistency of the signature within each 10 km^2 image meant that the analysis could then be undertaken, but it was first necessary to establish which of a number of imagery classification approaches would yield the best results within the context of this study.

3.2.4 The impact of spatial resolution on classification accuracy

50cm CIR imagery was selected partly for the comparative ease with which rivers can be extracted from imagery containing the NIR band (refer to Section 3.2.1, p.56). However, the spatial resolution was also significant as it meant that headwater streams could be captured, particularly when the resolution was further enhanced using SRM, as headwater stream width can be sub-metre. To test the impact of spatial resolution on the ability to derive a complete dataset of surface waters, features extracted from CIR imagery were compared with those produced from WorldView-2 (WV2) multispectral imagery with a resolution of 1.85 m (DigitalGlobe, n.d.). This not only aided in comparison, but addressed the relative lack of research analysing what impact low magnitude changes in resolution have on classification accuracy, as the majority of studies compare sub-metre datasets against those with a significantly coarser resolution, normally >10 m (Chen *et al.*, 2014). This comparison was conducted with imagery of Nottingham using a simple MLC approach with training data from the same locations in both cases; the SRM technique developed in this study (Section 3.4, p.76) was not applied as the aim was to understand the impact of spatial resolution, so enhancing the

imagery would have made this problematic. However, because the focus was entirely on the ability to extract surface waters as opposed to accurately capturing all possible land cover classes, a binary water/non-water classification was undertaken.

Overall, the resultant output from both sources was highly accurate (>95% of surface waters captured), as one would expect from high resolution imagery. However, this alone was not adequate in identifying potential differences as the confusion matrix approach examines whether a pixel is assigned to the correct class, which in the case of MLC is that which is most prevalent within each pixel. This does not give a true reflection of how completely the surface water class is represented, demanding a further examination of the imagery. A visual comparison was therefore undertaken, and demonstrated that the impact of a low-magnitude change in resolution was especially significant at the edge of land cover classes (Figure 3.2.3, overleaf). This is especially noticeable on the footpath adjacent to the River Trent in this figure, which is more distorted in the WV2 imagery. With a width of a couple of metres, this is similar to the width of a low-order stream, demonstrating a clear advantage to using higher resolution CIR imagery when attempting to accurately represent comparatively narrow linear features.

However, the finer spatial resolution of the CIR imagery also made floating debris a bigger problem, as the smaller pixel size meant that surface waters were more likely to be misclassified when compared to the same quantity of floating debris being present in the WV2 imagery, as there was a higher probability that the debris would constitute the majority of a CIR pixel.



Figure 3.2.3 Visual comparison of surface waters from a) WorldView-2 imagery, and b) CIR imagery for a reach of the River Trent (WSW ≈ 80 m) in Nottingham, England; NE corner coordinate 455340, 336069.

In comparison with previous studies, Chen *et al.* (2014) showed that a low magnitude change of 1 m to 1.5 m in the resolution of the imagery had a negligible impact on overall accuracy in terms of total water surface area mapped, while Vanderbilt *et al.* (2007) determined that an increase in pixel size (i.e. a coarser resolution) could lead to an *increase* in classification accuracy due to there being a greater distance separating pure pixels containing only water or land. However, other studies have disaggregated the analysis of accuracy to examine the degree to which waterbodies of varying sizes were captured, which revealed that there was a clear impact on the ability to map smaller waterbodies, with finer resolution imagery producing greater accuracy (Enwright *et al.*, 2014).

Therefore, despite the exponential increase in resource requirements brought about by the difference in the spatial resolution of CIR and WV2 imagery (9 whole 50cm pixels fit into a single 1.85 m pixel, and this study utilises pixel-based classification techniques), the ability to capture headwaters is paramount, so this is a worthwhile concession. Logically, headwater streams can be narrower than 1.85 m, the WV2 resolution, so in catchments where these streams predominate, a threefold improvement in spatial resolution is likely to pay dividends, although this is difficult to quantify with imagery of Nottingham that does not include an abundance of low order streams.

3.3 Comparative analysis of classification techniques

Having selected appropriate imagery, a comparative analysis of different classification techniques was undertaken to determine which approach was most capable of capturing the full extent of surface waters. From a review of the literature, six general approaches were identified alongside specific techniques: -

- Unsupervised classification e.g. ISODATA algorithm
- Supervised hard classification e.g. maximum likelihood
- Supervised soft classification e.g. fuzzy classification
- Super resolution mapping (SRM) e.g. contouring
- One-class classification
- Local vs. global training datasets

ISODATA was selected to determine how readily the water land cover class could be identified by automatically applying an algorithm that separates classes based on the analysis of variation in spectral response in an image, after which classes are formed based on the number specified by the user.

MLC was used to establish a baseline in terms of how narrow streams in particular could be extracted with the resolution of 50cm. This technique is by far the most common in the field, with an estimated 32% of all studies that use an imagery classification utilising MLC (Yu *et al.*, 2014).

Fuzzy classification, like other soft classification techniques, expresses the degree of membership of a pixel to each user-defined class, rather than assigning the entire pixel to the most prevalent class, as in hard classification. The output generated assigns a value between 0 (non-membership) and 1 (full membership) for each class by comparing the distance, in terms of standard deviation, of pixel values from the mean values for each class, an approach known as fuzzy set theory (Zadeh, 1965). Where a pixel differs from the areas identified as representing a 'pure' form of a defined class, then the output value will be lower, indicating a lower degree of membership.

Contouring, meanwhile, is a relatively simple GIS surface analysis process, and is frequently used by mapping products to indicate a change of elevation with a vector line, primarily due to the inability to superimpose a continuous raster dataset of elevation over information such as land cover, particularly in hard copy. Just as an elevation raster can be converted into a line, so too can the raster output of the fuzzy classification process (Muslim *et al.*, 2006). In fact, because the output of the classification procedure was standardised to a common scale (zero to one) across all images, this made the application of contouring comparatively easy. The utility of the contouring technique is that it allowed the boundary between land cover classes to pass *through* pixels, rather than between them as in conventional hard classification. With the latter, the output would be restricted by the spatial resolution of the input image, with the ability to improve upon this generally referred to as super-resolution mapping. This allowed for a more accurate representation at the boundary of the identified rivers and streams.

By applying each of the above approaches to the specific problem of extracting surface water features from 50cm CIR imagery, the most appropriate technique for achieving the stated objectives of this study was identified. The first step in this process was to establish a desired level of accuracy and the

identification of suitable methods for the measurement of accuracy. A common accuracy target for classifications is 85% overall, with no single thematic class less than 70% accurate (Thomlinson *et al.*, 1999), yet there is a growing recognition that these standards may be inappropriate and arbitrary, particularly given the pessimistically-biased perspective of the remote sensing community in too readily declaring classification output as not being fit for purpose based entirely on these thresholds (Foody, 2008). Furthermore, sources of error are not limited to thematic classification error (Congalton and Green, 1993; Powell *et al.*, 2004), with factors such as sensor properties, the need to perfectly co-register images, and pre-processing techniques also having an impact (Foody, 2002).

While a variety of methods exist for accuracy assessment (Comber, 2013; Congalton and Green, 2009; Foody, 2002), error matrices, or confusion matrices, have been the most commonly used for some time (Congalton, 1991). This approach simply states the percentage of cases that are correctly assigned to the appropriate thematic class, displaying errors of omission or commission (Figure 3.3.1, overleaf) for each thematic class defined at the signature creation stage by comparing to a reference dataset.

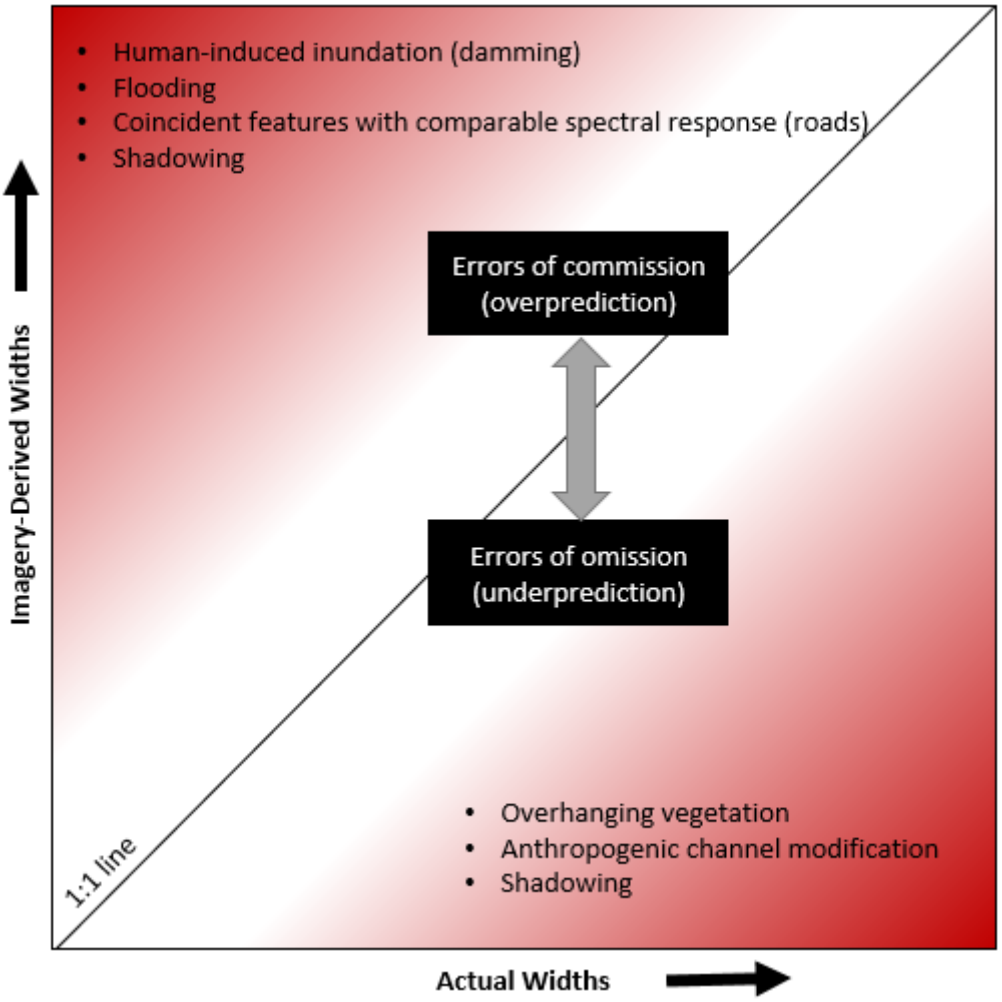


Figure 3.3.1 Errors of omission (underprediction) and commission (overprediction) when measuring WSW using aerial imagery (adapted from Fisher *et al.*, 2013). Accurate field measurement of actual width is assumed.

This is generally a set of points randomly distributed across the image, at which the user records the correct class of membership via fieldwork or other data sources (Congalton and Green, 2009), and then compares to the class assigned by the chosen classification process. The creation of the signature file is critical to the resultant accuracy of the classification, as the user is given an opportunity to define the range of spectral responses that can be assigned to each thematic class. If this process is completed poorly i.e. the signature for a class does not include examples of the full range of responses, or a signature file created for one image is applied to another, then misclassification will occur.

However, the accuracy of the classification in terms of errors of omission/commission for each thematic class in the image is not entirely relevant to this study. The only factor that is of interest is the accuracy of the classification for surface waters specifically. For this reason, a simplified form of the error matrix is presented, and relates exclusively to errors regarding the classification of surface waters for each of the above methods. Given that this generally goes against the recommendations of the remote sensing community for accuracy assessment (Foody, 2002), the opportunity has been taken to better integrate remote sensing and GIS techniques by adopting a method for assessing the accuracy of GIS-derived linear features (Goodchild and Hunter, 1997; Tveite, 1999), which utilises a 'reference dataset' of known quality to compare to another dataset, in this instance, rivers and streams extracted via a classification from aerial imagery. The reference dataset used was the Ordnance Survey VectorMap District product, which is available as Open Data and represents rivers less than 5 m in width as single lines, and those above this limit with two lines, representing the two river banks (Ordnance Survey 2014), differing clearly from WSW. By buffering these vectors and carrying out overlay analysis with the classification output, the extent of any overlap can be quantified. This provides an indication of errors of omission. Errors of commission, meanwhile, were calculated arithmetically by comparing the number of pixels that were assigned to the water land cover class across the study site against the total area covered by the buffered OS VMD dataset. It was assumed that a figure of 100% indicated zero errors of commission, although this is highly unlikely to be the case; even if both datasets covered the same extent, they may still differ across space i.e. a river reach can be omitted from the classification process while an area of shadow covering the same extent could be incorrectly classified as water. However, for the purposes of this comparison the method for quantifying errors of commission struck an appropriate balance between elucidating the differences between classification techniques while limiting resource requirements. The results of this analysis are presented in Table 3.3.1, overleaf; for a summary of the workflow used for the comparative analysis, see Figure A.1.1 in the Appendix.

Table 3.3.1 Comparative analysis of classification accuracy for commonly applied techniques.

Method	Errors of Omission[A]	Errors of Commission[B]
ISODATA	42%	523%
MLC (global)	38%	276%
MLC (local)	32%	275%
Fuzzy (global)	30%	213%
Fuzzy (local)	31%	187%

[A] % of reference dataset surface waters missing from classification. [B] number of pixels allocated to water thematic class vs. number of water pixels in reference dataset; 100% represents zero errors.

The figures for errors of commission initially appeared to be unacceptably high, but it is widely acknowledged that the spectral reflectance of shadows, roads and buildings is very similar to that of water for CIR imagery (Figure 3.3.2), hence why the errors decrease as the user is able to have greater control over the specification of signature files. The decrease in commission was much less pronounced when comparing the local and global MLC techniques, which is likely due to the limitations introduced by hard classification techniques; the ability to apply the more representative training data sets allowed by the local approach was only exploited fully by the fuzzy classification process.

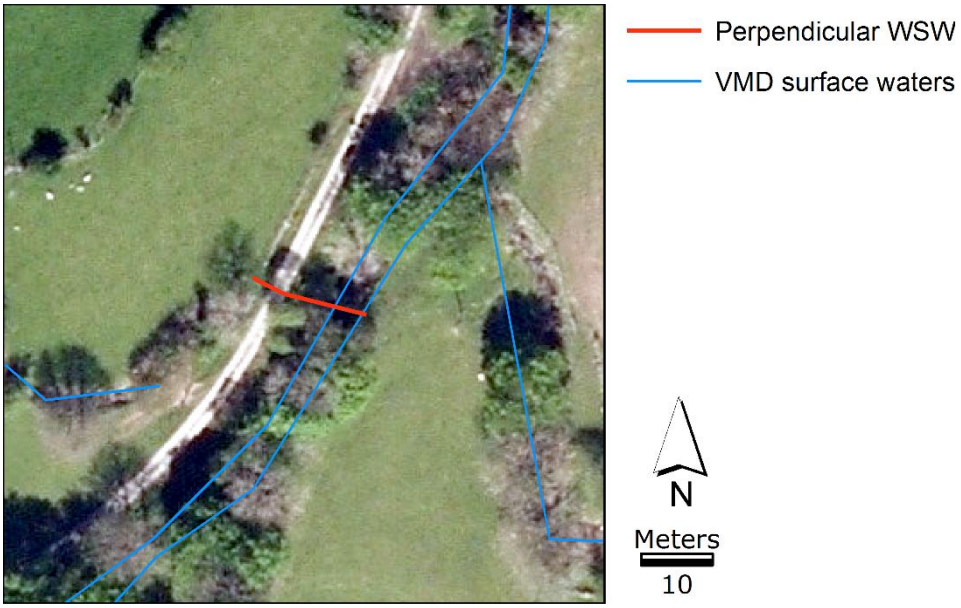


Figure 3.3.2 Errors of commission caused by the comparable spectral signature of water, shadow, and roads

Further visual analysis showed that errors of omission, meanwhile, tended to be related to tree cover obscuring the view of the river (Figure 3.3.3). As the uppermost thematic class, none of the above approaches are able to 'see through' the trees to the river below because of the very nature of the aerial imagery used, hence why the best outcome was that only 70% of rivers and streams could be extracted from the imagery.

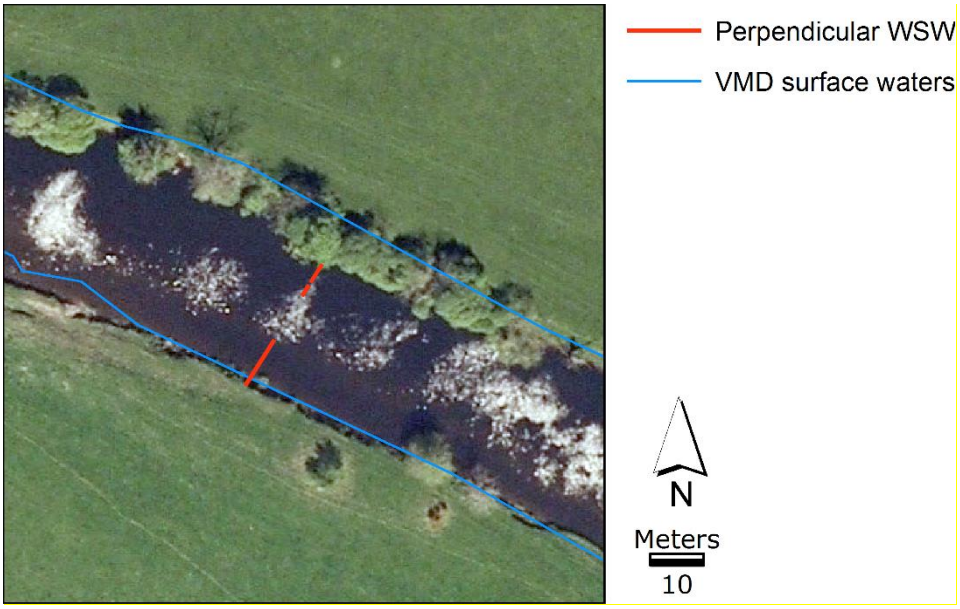


Figure 3.3.3 Errors of omission caused by the presence of overhanging vegetation and suspended material in the channel.

The overall poor performance of MLC is in line with previous research that finds accuracy to be lower than average, despite this being the most popular classification method (Yu *et al.*, 2014). Furthermore, the significant increase in errors for ISODATA can be linked to the difficulty in accurately automating the process when land cover classes such as water and shadow are especially difficult to distinguish without human input.

Finally, there was a pronounced difference in the performance of fuzzy classification trained using local datasets, with a clear improvement in classification accuracy. The approach taken to the global form of each classification approach was the amalgamation of the local training datasets, meaning that training sites for each image were identical in both cases. Figure 3.3.4 visualises the difference between the local and global approaches to classification. The difference in classification performance can therefore be attributed to the aforementioned issue of inter-image variation in the spectral response of the water land cover class. For the global approach, pixel values were further away from the mean, causing misclassification and hence lower overall accuracy.

This phenomenon was likely to be exaggerated for the full site considering the extent of the study area (2200 km^2) and that the full sample of aerial imagery for the study site was likely to contain an even greater range of spectral responses for water than the accuracy assessment subset. Therefore, local training areas e.g. separate datasets for every 10 km^2 area, were created in an effort to improve the ability to accurately classify surface waters.

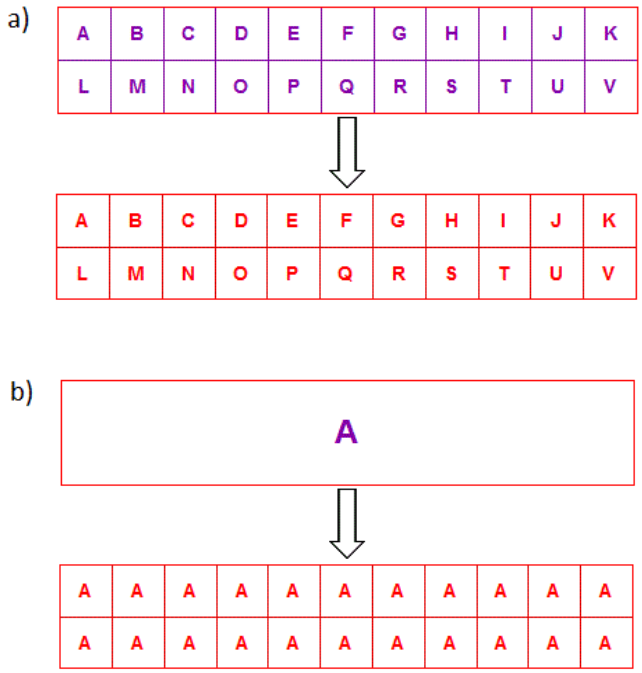


Figure 3.3.4 A comparison of a) local and b) global approaches to classification. Local classification creates a separate training dataset for each image, whereas global classification creates and applies a single training dataset to the entire study area.

This approach is supported by previous studies (Muslim *et al.* 2006) and also follows logically considering how classification techniques such as fuzzy classification work. In this case, (sub-) pixels are classified based on their deviation from the mean spectral reflectance of the training sites, so variation in this response across the entire study area will skew the mean. However, by deriving training statistics locally rather than globally, the mean is more likely to be representative of surface waters contained within a subset of the larger area.

Overall, a combination of techniques was found to produce results that were most fit for purpose within the context of this study, because the weaknesses of individual methods were compensated for to an extent, as also found by others undertaking research focusing on the extraction of surface waters from optical imagery (Li *et al.*, 2016; Su *et al.*, 2012a, 2012b; Yu *et al.*, 2014). In this instance, the inability of fuzzy classification to determine the spatial arrangement of sub-pixel classes was corrected for by using a contouring approach, which looks beyond the level of an individual pixel to analyse inter-pixel relationships in membership to the water land cover class. Based on the results of the comparative analysis, and the desire to capture headwater streams to as great an extent as possible, a local, one-class classification approach, combined with fuzzy classification, and enhanced using contouring to produce super-resolution output maps was recognised as the ideal approach for extracting surface waters from the chosen study site.

Table 3.3.2 comparison of image classification techniques

Technique	Description	Resource requirements per 10 km^2 image*
ISODATA (Iterative Self-Organising Data Analysis Technique Algorithm)	An automated, unsupervised technique that requires minimal user involvement, and is generally considered to be an efficient method for rapidly classifying imagery (Güneralp *et al.*, 2014).	1 hour 7 mins per 10 km^2 image; up to 3 iterations per image required due to redefinition of number of classes and class size parameters.
MLC (maximum likelihood classification) – global training sites	A hard classification approach that assigns each pixel to the class which is most prevalent; has a history of being applied to water body extraction (Sheng *et al.*, 2008; Sun *et al.*, 2012)	2 hours per image. Up to three iterations required for each image; redefinition of signature files can be undertaken for all 4 images simultaneously.
MLC (maximum likelihood classification) – local training sites	As above, but locally-trained. This means that resource requirements are considerably higher, as a separate signature file must be created and modified for each image.	Up to 4 hours and three iterations for each image.
Fuzzy classification – global training sites	Fuzzy classification allows for the proportion of different land cover classes within a pixel to be determined. Contouring places class boundaries	2.5 hours per image
Fuzzy classification – local training sites	As above, but locally-trained.	4.5 hours per image
Fuzzy classification and contouring – global training sites, one-class classification	Fuzzy classification allows for the proportion of different land cover classes within a pixel to be determined. Contouring places class boundaries through a pixel, producing a more accurate representation. OCC ignores all but the water class.	3.5 hours per image

Technique	Description	Resource requirements per 10 km^2 image*
Fuzzy classification and contouring – local training sites	As above, but locally-trained. The inclusion of OCC has obvious advantages when combined with local training sets, as separate signatures for non-water classes do not need to be redefined for each image.	4.5 hours per image.

*Assumes that data are already in an appropriate format for processing.
Specification of PC: Windows 7 Enterprise version 6.1.7601, Intel Core i3-3110M CPU @ 2.40GHz, 2400 MHz, 2 Core(s), 4 Logical Processors, 8GB single-channel RAM.

3.4 Combining one-class classification, fuzzy classification, and contouring for super-resolution mapping

To produce a super-resolution map of surface waters for the study area, a locally-trained one-class fuzzy classification was performed, with contouring subsequently applied to produce a super-resolution map of surface waters for the study site (see Figure A.1.2 in the Appendix for a summary of the workflow). The use of an ensemble approach, while having clear advantages (Su *et al.*, 2012a, 2012b), involved numerous user-defined options that had to be tested with a view to reducing error at each stage and creating output that was suitable for the subsequent process.

3.4.1 Setting appropriate parameters for fuzzy classification

The first parameter defined was the Z-score distance at which class membership became zero. Any pixel with a spectral response equal to the mean response for a class (as determined by the signature creation process) was given a membership grade of 1, denoting complete membership. The fuzzy set membership grade progressively decreases as the spectral response diverges from the mean, reaching 0 (no membership) at the z-score distance specified. This distance is specified as a standard score (z-score) to make it simpler to apply regardless of the imagery being used. For example, using the z-critical value for the 95th percentile (1.96) as the z-score distance would result in 5% of the pixels having a fuzzy membership grade for the water class of 1 or 0 (Zadeh, 1965).

The main ramification of the chosen z-score for the classification process was in determining the ease with which the contouring process could be carried out, as this selection altered the class membership values contained within the fuzzy classification output image. With this in mind, a sigmoidal curve (Figure 3.4.1, overleaf) was selected as the basis for the classification. When combining this with a higher z-score, a greater proportion of pixels were assigned class membership values for the water class at the two extremes of the scale (0 and 1). This meant that the fuzzy classification approach was

forced to assign a larger proportion of pixels to the 'water' class, with the critically important mixed pixels in the middle of the distribution left for the user to assess during subsequent analysis, specifically the contouring process.

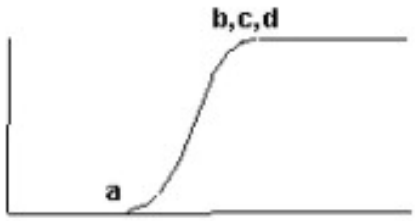


Figure 3.4.1 Monotonically increasing sigmoid function with control points a, b, c and d.

3.4.2 Applying contouring to produce super-resolution maps of surface waters

A super-resolution mapping technique was required to fully exploit the sub-pixel class membership information assigned to pixels by the fuzzy classification. Contouring was identified as being ideally suited due to previously being used for the extraction of shorelines (Muslim *et al.*, 2006). Rivers are also linear features, and because contouring only identifies the boundary between classes, it significantly reduced the amount of redundant data, as pixels within the river were not of interest; only the water's edge was required for WSW measurements. The main advantage, however, was that the contouring process allowed the class boundary between water and non-water to run *through* pixels, rather than around them as in conventional hard classification techniques.

In order to gather empirical evidence for the selection of contouring parameters, profiling was carried out to establish the appropriate boundary value to use for the contouring process. This entailed digitising a perpendicular transect across the river channel, and then identifying which pixels the line ran across. The fuzzy classification values associated with these pixels were then visualised, as in Figure 3.4.2 (overleaf), to determine the values that lay on the boundary of the water and non-water classes. This was repeated 30 times per 10 km^2 to account for the contouring threshold being locally variable, potentially even within an individual image, as the contouring process could only apply a single

threshold per image. In the event of substantial intra-image variation, the 10 km^2 mosaic would have been split into four 5 km^2 images, which would have been reclassified and re-profiled, but this proved unnecessary.

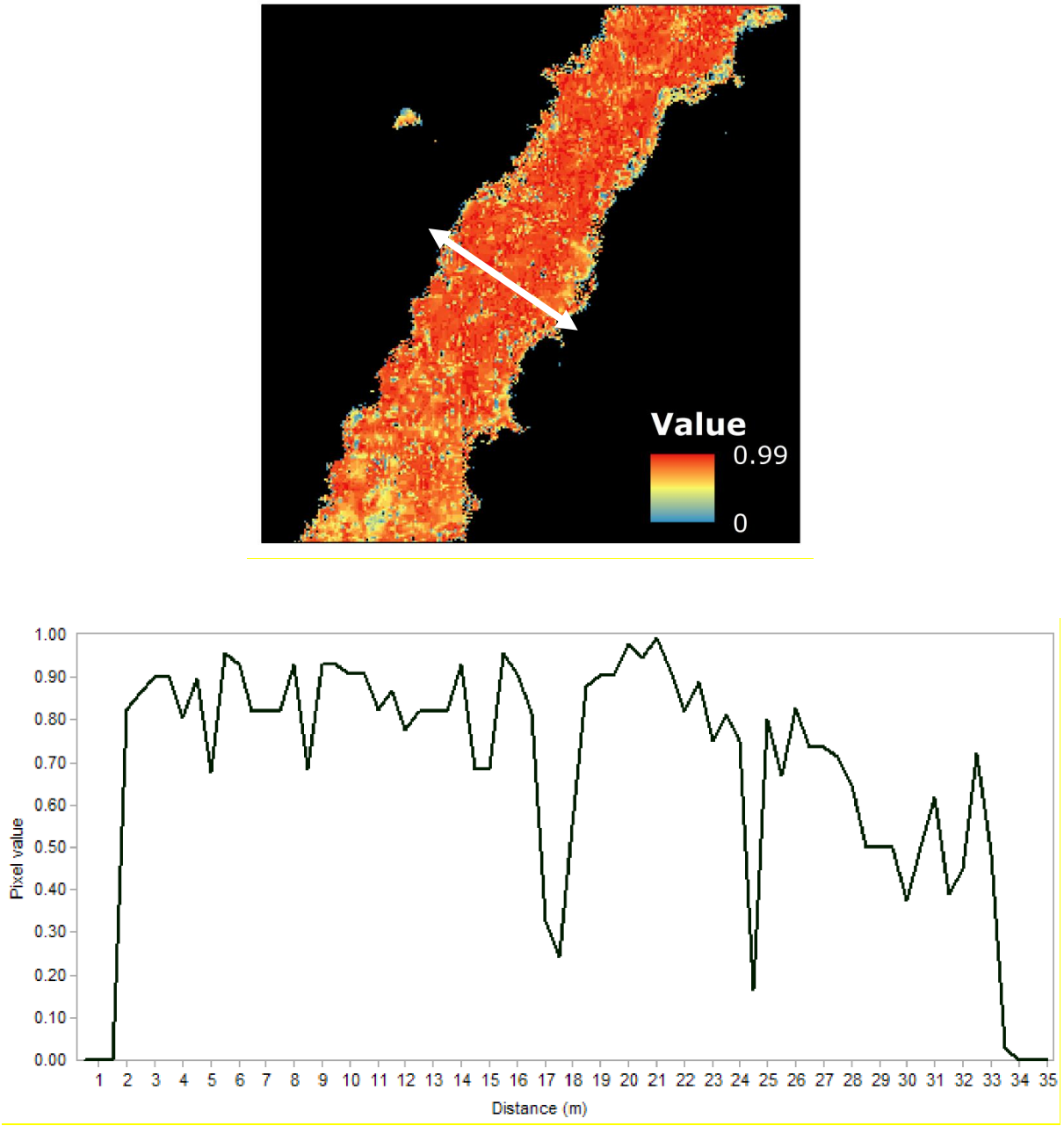


Figure 3.4.2 Example of transect used to inform the selecting of a boundary value for the contouring process. Values range from 0 to 1 and represent the degree of membership to the water land cover class.

Profiling also had the added advantage of indicating factors that could complicate the extraction process as a whole. For example, variation in the profiling values identified the presence of suspended sediment, floating woody debris, shallow depth, and the presence of shadow or overhanging vegetation as factors that caused the spectral reflectance to differ from that expected from 'pure' surface water. This means that there was a lower probability of a pixel being assigned to this land cover class during fuzzy classification due to variation from the class mean. Despite this, the profiling process still allowed for the clear identification of the class boundary between water and non-water, with in-channel variation, irrespective of cause, of little consequence.

Profiling generally showed that the starting threshold of 0.5 had to be reduced for the majority of the 10 km^2 images. This was expected, as the only fuzzy membership values of consequence to the extraction of rivers in this study were those at the water's edge, which were more likely to include a mixture of both water and non-water classes. Furthermore, a penalty was applied to class membership as a result of carrying out the fuzzy classification on unnormalised values, which was necessary due to the use of an intentionally unrepresentative training dataset containing only the water class. Consequently, membership values were reduced in pixels at the water's edge due to the existence of non-water land cover classes that had not been captured in the training data.

As part of the exploratory analysis, the contouring threshold for a single image was varied independent of the profiling results in order to understand the potential error in the event of an incorrect threshold being specified.

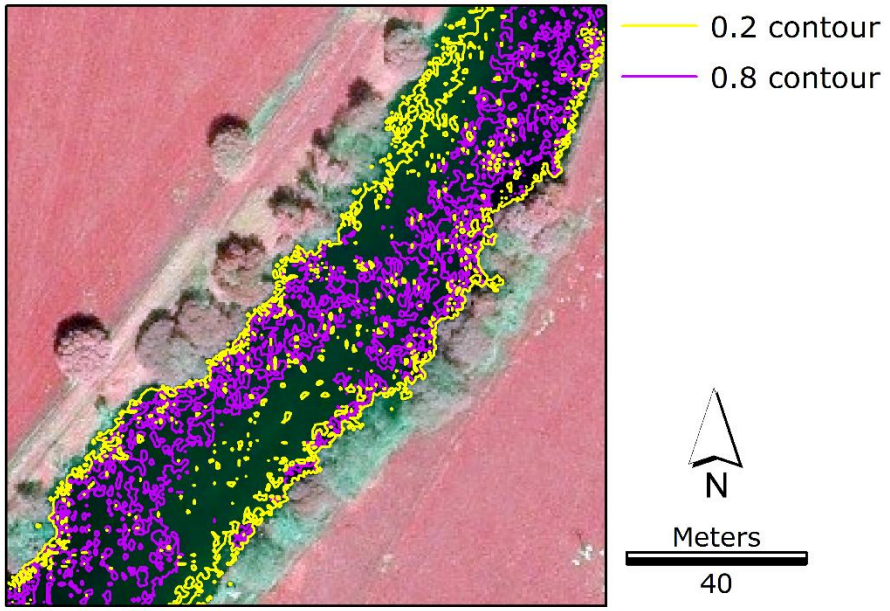


Figure 3.4.3 The impact of incorrectly specifying the threshold value for the contouring process, with contour values of 0.8 and 0.2 displayed.

At the widest point of the channel in the image used for exploratory analysis (Figure 3.4.3), the contour generated with a 0.8 threshold value estimated a width of 17 m, less than half the actual measurement (and that produced by a threshold of 0.2). However, while the value of 0.2 represented the channel more completely, errors of commission were increased, particularly in areas obscured by shadow (Figure 3.4.4, overleaf). This was due to the comparable spectral response of surface waters and shadows in CIR imagery. However, these errors of commission were limited by subsequent analysis (see Section 4.1, p.96). In addition, as demonstrated by the figure above, incorrectly specifying a threshold value of 0.8 resulted in errors of omission, in that areas that should have been classified as surface water were not adequately captured, showing that a careful compromise – and a representative sample of cross-sectional profiles – was vital to SRM accuracy.

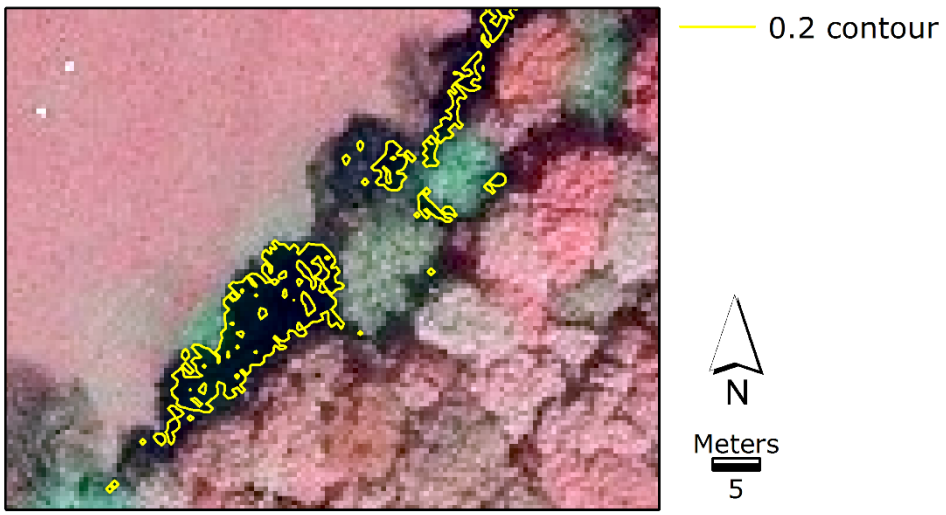


Figure 3.4.4 Errors of commission resulting from the specification of an incorrect contouring threshold of 0.2.

Once the process had been informed as fully as possible, contouring was applied to each image in the study site. The final output of the process was continuous polylines representing the class boundary between water and non-water land cover classes Figure 3.4.5.

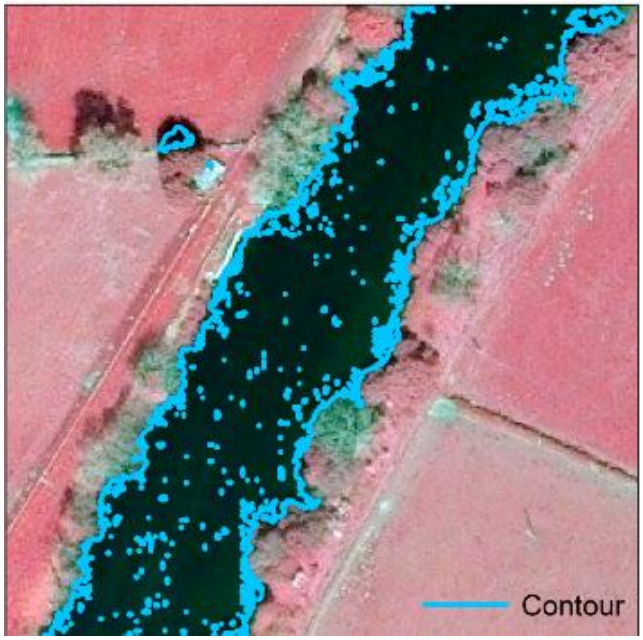


Figure 3.4.5 The final product of the super-resolution mapping process (SRM).

3.4.3 Classification technique resource requirements

Given that this research is primarily concerned with formulating a methodology that can be transferable to comparable studies, minimising resource requirements was a necessity. The national-scale focus of the study is accompanied by the caveat that England and Wales are comparatively small, meaning both that the classification-driven approach could feasibly be applied to the entire nation given improved computational resources, and the model-driven approach is able to be informed with a single study site, as England and Wales are small enough to have comparatively little variation in WSW controls when compared to, for example, the vastly different landscapes and climates present in continental-scale nations such as the USA and Australia. Table 3.4.1 (p.83) quantifies the resource requirements for the selected classification technique.

The time requirements are likely to have been underestimated in various places. For example, the time stated for processes such as contouring does not include the time spent qualitatively appraising the fit of the contours generated – only the time spent processing the images and changing contouring intervals manually.

Queuing processes is possible in TerrSet, but results in a disproportionate increase in processing time as well as increasing the possibility of errors occurring. This is because all queued processes initiate concurrently, so run simultaneously, putting computational resources under greater demand than if each process was allowed to complete before the next was started manually. For example, creating a composite of the three image bands in Idrisi took, on average, five minutes and twenty seconds per image. Initiating fifteen of these tasks at once resulted in a total run time in excess of eleven hours.

Table 3.4.1 resource requirements for each stage of the image classification process.

Process	Purpose	Primary 'driver' of process	Processing time per 10 km^2 image (one iteration*)	Typical number of iterations (average)	Total per Process (all iterations for all images+)
Mosaicking	Allows greater area to be processed at once in subsequent analyses	Automatic (Erdas Imagine)	1 hour	1	**24 hours**
Conversion from .img to. rst format	Idrisi cannot process .img format	Automatic (Idrisi)	2 min 30 sec	1	**1 hour**
COMPOSITE module	Joins three image bands together to make digitizing easier	Automatic (Idrisi)	4 min 20 sec	1	**1 hour 44 mins**
Digitizing	Identifies areas of interest (i.e. surface water) for subsequent signature creation	Manual	1 hour 30 mins	2	**72 hours**
Signature creation	Identification of training areas	Automatic (Idrisi)	6 minutes	2	**4 hours 48 minutes**
FUZCLASS module	Performed fuzzy classification technique	Automatic (Idrisi)	17 min 30 sec	2	**14 hours**
PROFILE module	Inform contouring process	Manual (Idrisi) – only a single profile can be graphed at a time	1 hour (30 profiles)	1	**24 hours**

Process	**Purpose**	**Primary 'driver' of process**	**Processing time per 10 km^2 image (one iteration*)**	**Typical number of iterations (average)**	**Total per Process (all iterations for all images$^+$)**
CONTOUR module	Placed contours at user-defined intervals around output fuzzy classification output	Automatic (Idrisi)	27 min 25 sec	3	**32 hours 54 mins**
Total					**154 hours 4 mins**

*processes such as digitizing and signature creation required iterative modification after accuracy assessment.

$^+$n = 24.

Specification of PC: Windows 7 Enterprise version 6.1.7601, Intel Core i3-3110M CPU @ 2.40GHz, 2400 MHz, 2 Core(s), 4 Logical Processors, 8GB single-channel RAM.

3.5 Assessing the accuracy of the extracted surface water features

A common approach to validating and assessing the accuracy of a sub-pixel classification is to use a finer resolution image as a reference (Myint, 2006). This was problematic in this case, as the highest resolution imagery available was selected with the express purpose of capturing the narrowest streams possible.

Furthermore, the oft-used error matrix is perhaps inappropriate for use with OCC as the user intentionally creates an unrepresentative and incomplete reference dataset. This makes accuracy assessment problematic, particularly as the traditional error matrix approach is somewhat redundant when only a single class is present in the output. Therefore, in order to ensure the accuracy of the output, alternative methods were required. Mack *et al.* (2014) directly addressed the problem of how the user confirms the reliability of OCC, recommending that in-process classification in particular be undertaken. This was especially pertinent given the use of multiple classification techniques in the case of this study, as each required a degree of user input and came with potential sources of error.

One of the in-process methods is described on p.60, where transects were drawn across river channels in each image to establish intra- and inter-image variation in the spectral response of the water land cover class. This process was repeated on the one-class fuzzy classification output in an effort to understand the membership values, which were then used to inform the parameters chosen for the contouring process on a local, per-image basis (p.77).

In addition to this, the classification uncertainty image proved vital for classification assessment. This output applies a number between 0 (low uncertainty) and 1 (high uncertainty) to every image pixel based on the confidence that the pixel belongs to the assigned class (Figure 3.5.1). Due to the use of OCC, the overall likelihood of poor training data is lower, as time and labour can be spent focusing on

digitising a representative selection of training sites for this single class of interest. However, because all non-water classes were an unknown, high uncertainty existed across the majority of each image

This meant that with the uncertainty image, areas of high uncertainty were only of interest if they coincided with the water land cover class. A random sample of points was created for areas classified as water for each image, and the classification uncertainty values displayed on a graph. Combined with a manual exploration of the uncertainty image, this allowed for the accuracy of the fuzzy classification process to be tested. Where high uncertainty existed in locations where surface water was present, signature creation was redone and the fuzzy classification procedure run again. This was repeated until classification uncertainty was reduced to an acceptable level, allowing for class definition errors to be limited.

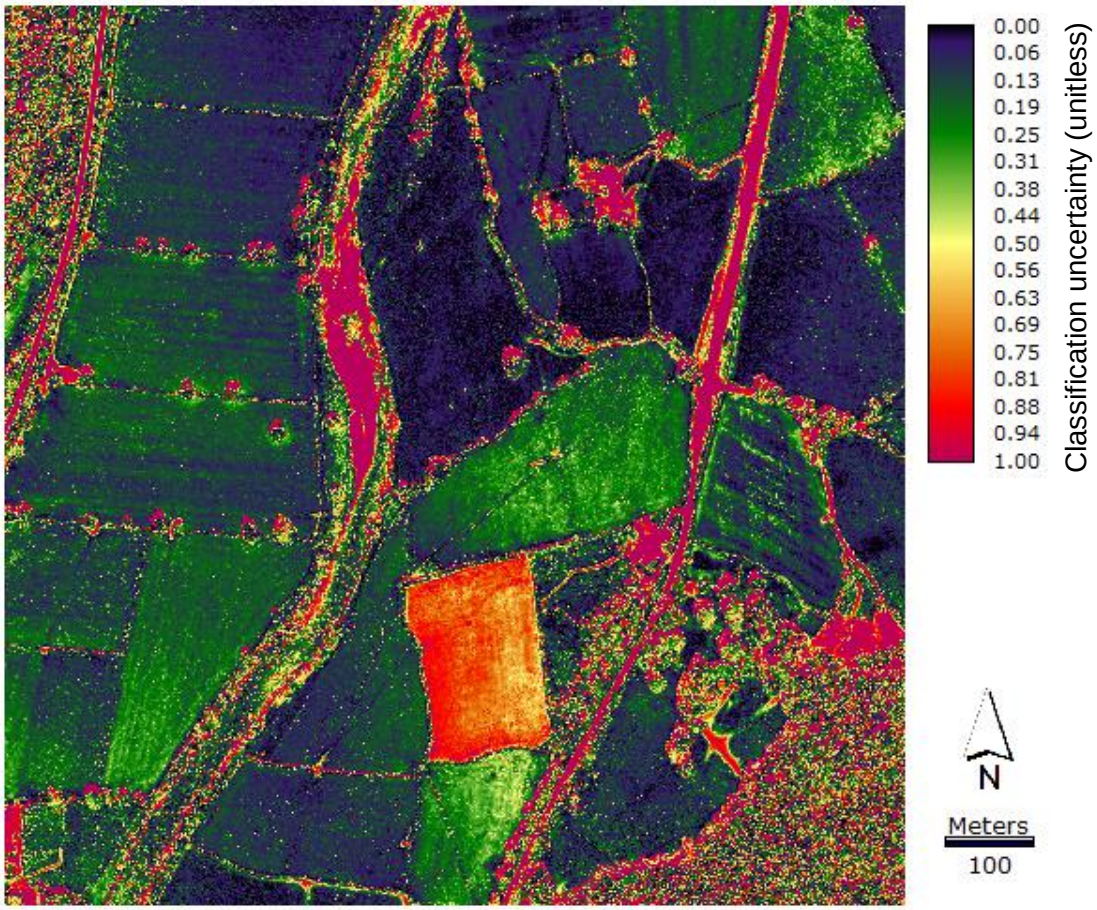


Figure 3.5.1 Example of a classification uncertainty image used to perform in-process accuracy assessment of the classification approach

In addition to questions of accuracy, the completeness of that extracted dataset was also of interest. Riparian vegetation, overhanging trees (Güneralp *et al.*, 2014), and shadows (Filippi and Güneralp, 2013; Verpoorter *et al.*, 2012) all act to obscure the boundary between surface water and land. In addition, low-albedo non-water surfaces such as asphalt roads, building roofs and shadows can have a similar spectral reflectance to surface waters (Feyisa *et al.*, 2014), resulting in misclassification.

The total river length in the study site is 6174.19km. The length of the river network captured by the classification procedure was 3379.75km, meaning that 54.74% of the river network is present in the contouring output. If this figure related to classification accuracy in the traditional sense, then it would be indicative of significant problems that required correcting before any measurements could be taken from the output. However, this is an indicator of completeness rather than accuracy, and this is more than a trivial semantic difference. The notion of accuracy in remote sensing relates to how well *visible* features have been captured, whereas this measure of dataset completeness reveals the proportion of rivers that *cannot* be captured using CIR aerial imagery in the first instance due to overhanging vegetation obscuring the aerial view.

3.5.1 Quantifying the impact of overhanging vegetation

While it was always understood prior to commencing the extraction process that overhanging vegetation would lead to sections of surface water being omitted from the final dataset, the extent of this was an unknown. Therefore, the extent to which surface waters and overhanging vegetation intersected was quantified by applying the Normalised Difference Vegetation Index (NDVI) to identify the presence of vegetation across the entire study site in the first instance, with areas identified as vegetation then compared with a river centreline created from Ordnance Survey data (Ordnance Survey, 2016b). By examining where vegetation intersected with the river centreline (represented by pixels that both intersected the centreline and exhibited a comparatively high NDVI value), it was hoped that an impression of the overall impact of vegetation on the ability to see surface waters from the air could be created.

While alternatives to NDVI, such as the enhanced vegetation index (Jiang *et al.*, 2008) and soil-adjusted vegetation index (Huete, 1988), offered a more refined approach, these indices could not be calculated from the 3-band CIR imagery selected for this study.

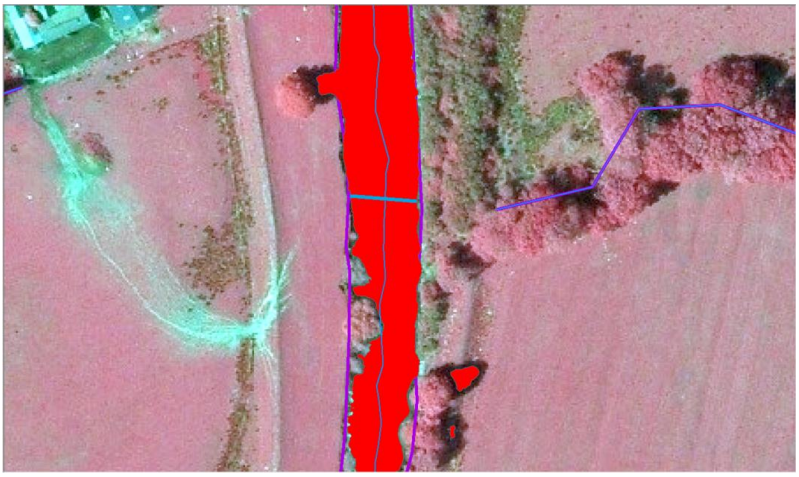


Figure 3.5.2 Overhanging vegetation limits the extent of the SRM-derived surface water dataset (red) and prevents the true extent of surface waters (purple line) from being captured.

NDVI has been applied extensively for a number of decades, originating in work such as that undertaken by Rouse *et al.* (1974) and Tucker (1979). NDVI uses the visible and near-infrared (NIR) portions of the electromagnetic spectrum to quantify the presence of healthy, photosynthetically active green vegetation, using Equation 3.1. Both of the required bands were present in the CIR imagery used for the extraction of surface waters.

$$NDVI = \frac{NIR - RED}{NIR + RED}$$

Equation 3.1 Normalised Difference Vegetation Index (NDVI) calculation using near-infrared (NIR) and red image bands

Healthy vegetation absorbs the majority of visible (red band) light while reflecting the majority from the NIR band. Unhealthy vegetation reflects more visible light and less NIR light. Bare earth reflects both of these bands to a moderate degree. Therefore, by calculating the difference between these

two bands, one is able to determine the presence of healthy vegetation, in this case on a per-pixel basis. In practice, what this means is that values closer to +1.0 indicate healthy vegetation, while those closer to -1.0 show that an area or pixel is not vegetated.

After completing the process for producing the NDVI data, it was then necessary to relate this to the river network covering the study site, which presented a number of options. The focus was on determining the extent to which overhanging vegetation resulted in the misclassification of known surface water features, so the centrelines derived from Ordnance Survey topographical mapping (Ordnance Survey, 2016b) were used in place of the SRM output, which only contained areas of visible surface water by design. The centreline dataset was clipped so that it only contained areas of surface water (as represented by the centreline derived from OS data) that were not captured by the SRM process. Therefore, the remaining centreline that was compared with intersecting NDVI values was from areas known to contain surface waters based on OS data, so in analysing the presence of vegetation along these line segments, the inability of the SRM process to capture these areas could potentially be attributed to the presence of vegetation (i.e. where a pixel with a high NDVI value intersected with the centreline dataset, it was assumed that the SRM process could not capture surface waters at this location due to overhanging (or suspended) vegetation).

As well as giving a measure of overall dataset completeness by quantifying how much of the OS data-derived centreline the SRM process failed to capture, the NDVI values were then used to determine the proportion of the missing features that were absent due to the potential influence of vegetation i.e. that had a high NDVI score, indicating the presence of vegetation overhanging the river centreline (Figure 3.5.3). Therefore, if overhanging vegetation was responsible for the omission of significant sections of the watercourse, then a histogram of the NDVI value should reveal a distribution that is predominately concentrated towards the upper end of the positive side of the x-axis.

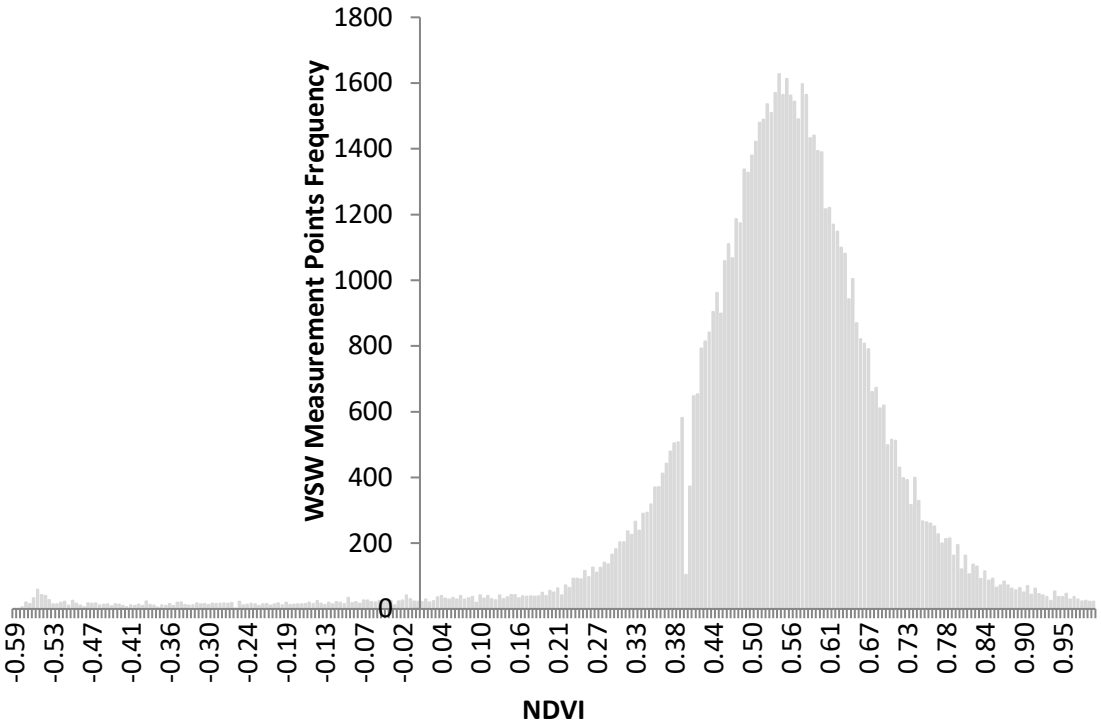


Figure 3.5.3 Histogram depicting the NDVI values of WSW measurement points that were omitted from SRM-derived surface waters dataset.

This distribution is strongly skewed towards higher NDVI values with very few of the surface waters missing from the SRM output having a value in the negative portion of the histogram. This demonstrates that overhanging vegetation is likely to be the primary reason why the SRM process failed to capture features that are known to be surface waters based on ancillary datasets, such as OS VMD and the centrelines derived herein. The range of NDVI values around the mode could also indicate that riparian vegetation in the study area is composed of a combination of shrubs, grasses, and trees, although in practice this distinction matters little as the end result is still an inability to capture the full cross-section of the river in these locations.

There was also a clear spatial pattern in the influence of overhanging vegetation, with a clear gradient from west to east. Streams located in the higher altitude slopes of Snowdonia National Park are comparatively well represented in the dataset of surface waters, whereas the more heavily urbanised lowland areas of central England see the worst performance. This stands to reason, as cooler

temperatures and steep, rocky terrain are less conducive to the growth of large trees. To ensure that missing features were indeed the result of overhanging vegetation, the relationship between the missing river reaches and NDVI values was analysed statistically (Figure 3.5.4).

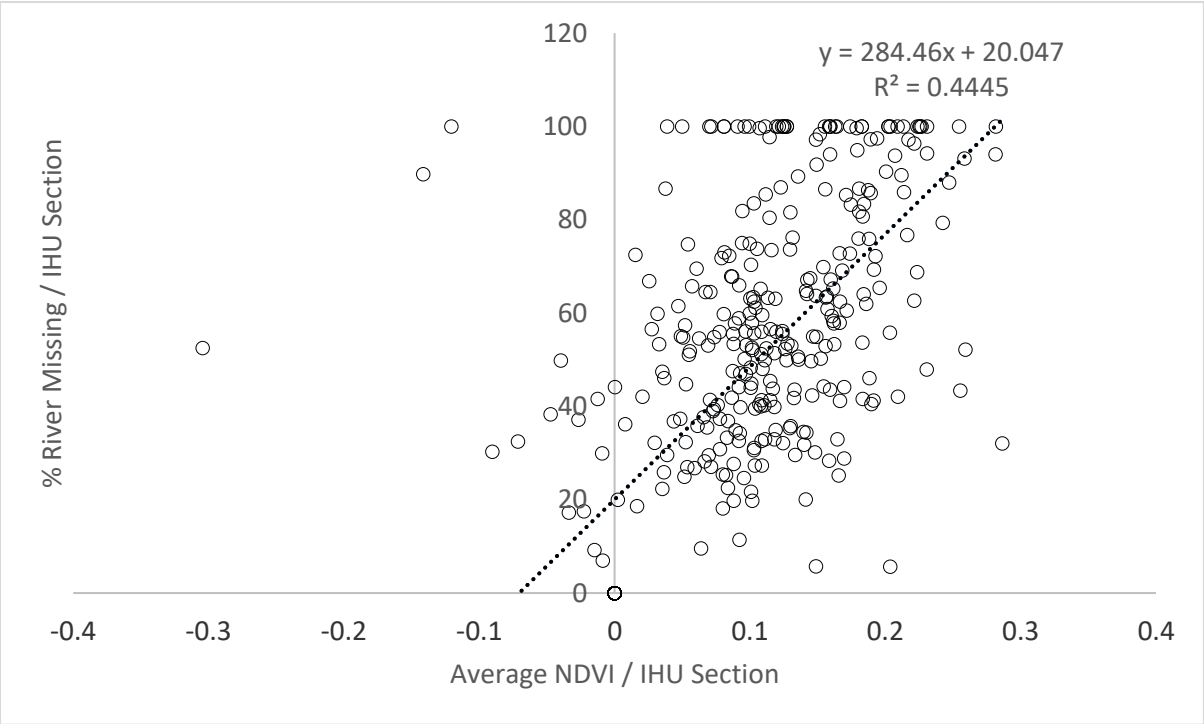


Figure 3.5.4 The relationship between the total river length missing from each sub-catchment (n=398) and the mean NDVI score (R^2 = 0.44, $p < 0.05$).

A positive relationship is observable between missing river length per catchment and the mean NDVI value per catchment. This means that a significant proportion of centreline features that were not extracted from the CIR imagery coincide with a high NDVI score, indicating the presence of vegetation.

Furthermore, the influence of vegetation is potentially underestimated, as this analysis addresses centreline completeness as the sole measure by which overhanging vegetation is quantified. Assuming that the centreline is exactly half way between each edge of the watercourse, then all calculations are focused on where >50% of a river is covered by vegetation at a given cross-section, with no consideration given to where <50% of a river is obscured despite the reality that WSW measurements taken in these locations will still be inaccurate, and potentially even more so as the influence of

vegetation is unquantified and unknown. However, knowing the degree to which overhanging vegetation obscures the aerial view of the watercourse, and removing or accounting for this influence, are two entirely different challenges. A more nuanced approach to assessing the influence would ultimately not aid in improving the completeness of the surface water dataset, as there is nothing that can be done with the available CIR imagery to make these locations visible or measurable, irrespective of the proportion of cross-sectional width that is obscured.

Regardless of the precise effect of overhanging vegetation, previous research has found that discharge can be accurately predicted (6.7% RMSE) from width data derived from aerial imagery with only 20% of watercourses visible (Pavelsky, 2014). While this is not directly comparable, it does point to spatial discontinuity being an issue that can be managed. By ensuring that the locations captured still cover the variation in WSW and its controls, and by carefully accounting for measurements that may be artificially reduced, an accurate account of WSW can still be gained.

3.6 Chapter summary

This chapter has shown that: -

- The combination of multiple remote sensing techniques allowed for the large-scale, fine-resolution extraction of surface waters.
- Local training datasets produced superior results to a global approach. This was due to the large spatial extent of the study site combined with aerial imagery being captured on different dates, causing the spectral response of the water land cover class to differ between images.
- OCC reduced the need to capture redundant information while maintaining classification accuracy.
- Fuzzy classification allowed the boundary between the water and non-water land cover classes to run through pixels, allowing for a more accurate representation of the water's edge.

- SRM (contouring) was capable of enhancing the resolution of classification output, resulting in increased accuracy. By applying this technique to imagery that was high resolution to being with (50cm), the proportion of headwater streams captured was increased.
- Overhanging vegetation obscured a significant proportion of rivers for the study site. However, a representative dataset was still extracted from the imagery.
- Areas requiring improvement in future studies utilising this or comparable techniques include the degree of manual work required, particularly when creating training classes and analysing the variation of spectral response within and between images.

The rivers and streams identified using the methodology detailed in this chapter were then exported to a GIS, where WSW was measured; the process designed to achieve this is discussed in the following chapter.

Chapter 4
Image-based measurement of water surface width

Having completed the mapping of inland surface waters from the CIR aerial imagery, the next stage was deriving accurate measurements of WSW from these features. This process achieved two objectives, namely the creation of a method capable of making direct image-based measurements from aerial imagery, and the validation of WSW estimates made by the multiple linear regression (MLR) model devised in Chapter 5. The end result was that the work described in this chapter directly addressed the second stated aim of the study and the accompanying objectives, namely the use of pre-existing or easily repeatable techniques to allow for repeat measurements both spatially and temporally, and the field validation of image-based WSW measurements to quantify the degree of accuracy (see Section 4.5, p.114).

A four-stage procedure was designed to take WSW measurements:

1. The generation of points along river vectors to guide the measurement process.

2. The measurement of WSW orthogonal to the direction of flow at the aforementioned points, using river and stream features previously extracted from CIR aerial imagery to constrain the extent of the measurement process.
3. The statistical aggregation of point measurements for defined river sections to derive 'effective width' (Smith *et al.*, 1996). This limits the influence of any errors, such as the impact of overhanging vegetation, still present from the classification process that may result in inaccurate point measurements.
4. The field validation of measurements to quantify the accuracy of the measurement process.

The use of a GIS, specifically ArcGIS, allowed for a degree of automation. Approximately 85% of manual labour can be saved by utilising a fully automated procedure (Merwade, 2007), yet such techniques have also been found to be less effective for removing human cognition from the process completely (Baumgartner *et al.*, 1999). A semi-automated procedure was therefore preferred to combine accurate measurements with the ability to gather a larger sample than is possible using a manual approach, particularly for a study area covering such an extensive area. Secondly, there is a growing need to provide potential users with an understandable, repeatable technique that does not require advanced knowledge of programming languages, for example (Marcus and Fonstad, 2010). The aim was therefore to use as much standard functionality of ArcGIS as possible.

Finally, the ability to automatically generate points at which to measure WSW was desirable, as sampling frequency could then be altered at will which would make the technique applicable at multiple scales. This required a method for constraining the locations where points were generated, with a requirement for each of them to lie within the bounds of the river dataset derived from the SRM technique. The most logical way to achieve this, and to subsequently ensure that WSW measurements were made perpendicular to the direction of flow, was to create a centreline dataset that accounted for the complex geometry of the river network.

However, before commencing with the measurement of WSW, the dataset of surface waters produced by the remote sensing methodology covered in the previous chapter was further examined to determine whether it required post-processing to make it more amenable to the selected measurement technique.

4.1 Post-processing to improve the accuracy of SRM-derived surface waters

The use of ancillary data has previously been shown to improve the accuracy of the feature extraction process (Agouris *et al.*, 2001; Armenakis, 2005; Khan *et al.*, 2012; Quackenbush, 2004; Sun *et al.*, 2012). In these examples, GIS analysis is carried out to correct misclassification when the classification technique or source imagery reduces the opportunity to do so during the classification process itself. For instance, surface waters are known to have a comparable spectral response to shadows in the NIR band, so the extraction of rivers from CIR imagery will inevitably include errors of commission. Consequently, the spectral signature alone is not adequate to separate water from other classes, an observation mirrored in a previous study using multispectral Landsat 7 ETM+ 8-band imagery (Armenakis, 2005) which used slope data to remove areas classified as water that intersected with a steep gradient, increasing classification accuracy markedly in doing so.

The contouring output, which was known to include errors of commission (see Section 3.5, p.85), was clipped using OS VectorMap District data, which contains the most complete and geometrically accurate representation of the river network at the regional scale (Ordnance Survey, 2016b). The use of an authoritative dataset to verify one of unknown quality is frequently undertaken in GIS (Goodchild and Hunter, 1997; Haklay, 2010), and by amending this approach, errors of commission were reduced. The primary modification made to the technique was that rather than simply comparing descriptive statistics for the two datasets, such as the percentage overlap, the VMD dataset was used to directly clip the contouring output, so that any areas classified as water that occurred a certain distance away

from the VMD river network were removed. By buffering the VMD river network prior to clipping, it was ensured that WSW was still being measured based on the contouring process, rather than the OS data. Due to the VMD dataset representing average winter conditions that were likely in excess of those present in the imagery to begin with, applying a buffer left adequate margin for error to account for the possibility that the contouring output included rivers that fell outside the boundaries of the OS dataset.

With the accuracy of the surface water dataset improved, the WSW measurement process was then executed.

4.2 Deriving centrelines from Ordnance Survey data

In order to measure WSW in a semi-automated manner, a point of origin was required that was located between the two lines delineating the extent of the water's surface. This required the creation of a centreline, along which a sample of points could later be generated. Before beginning this process, the following related factors had to be considered: -

1. The term 'centreline' is vague and does not have a universally accepted definition.
2. As a result of the above, existing GIS-driven methods for creating river centrelines do not deliver identical outputs.
3. Differences in these outputs mean that particular techniques are not universally applicable as they may not be fit for purpose, as was the case with a number of pre-existing methods for WSW measurement attempted during this study.

For the first of these factors, two broad conceptualisations of a river channel's centreline were considered, namely the thalweg, which is the point of lowest elevation in a channel's cross-section, and the geometric centre at the water's surface. While they can appear to be identical from an aerial

perspective for regularly-shaped channels, this is not the case for an irregular channel. Given the use of the centreline for guiding the subsequent sampling and measurement processes, this was a non-trivial distinction that required careful thought. This is corroborated by a recent analysis of the geometry of morphological features that found that a poor centreline representation resulted in unreliable width measurements (Nyberg *et al.*, 2015).

One benefit of using the thalweg is that it is more likely to remain constant in the short-term, barring any significant tectonic events or landscape modification by humans, whereas the geometric centreline at the water's surface can migrate laterally across the channel, depending on conditions such as flow and channel morphology. For this reason, using existing datasets that represent the centreline as the latter is impractical, because the extent of the water's surface is likely to be represented under different flow conditions than those present in the aerial imagery being used as the basis for this study. For example OS products represent surface water extent at winter maximum flow (Ordnance Survey, 2016a, 2016b), so the centreline could potentially be outside the extent of the water's surface as defined by the SRM process, especially considering both the narrow extent of some of the streams captured and the potential for error, making the automation of subsequent measurements impossible. Furthermore, different products have different levels of abstraction in the way that surface waters are represented (Figure 4.2.1).

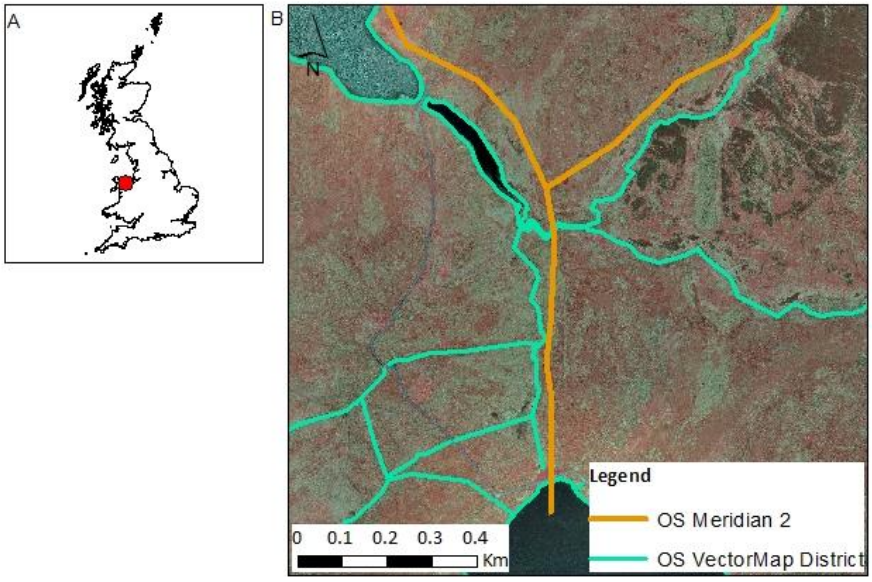


Figure 4.2.1 Visual comparison of how surface waters are represented by the OS VectorMap District and OS Meridian 2 products.

On the other hand, despite the temporal migration of the geometric centreline, it has the advantage of requiring no additional data, whereas the thalweg is calculated from a DEM. This introduces both an additional resource requirement and another source of error, depending on the spatial resolution of the data. Additionally, while the process of finding the geometric centreline requires constant measurement of the distance from the central point to each polyline representing the extent of the river, in order to ensure that the line is equidistant, the thalweg can be produced independently of any knowledge regarding the surface extent of a river or stream. Therefore, using the use of the geometric centreline is capable of measuring WSW – the intended goal – as a by-product of the centreline creation technique, with the only subsequent analysis required being to capture this measurement and store it in an attribute table or a text file, for example. The measurement stage using a thalweg, however, would require additional processing in order to generate a WSW measurement. For example, the perpendicular line generated to measure the width would need to have a maximum value defined by the user, with this line then clipped to the extent of the SRM, in order to derive a measurement. This would require *a priori* knowledge of the maximum WSW across the study site, which would be, at best, a highly subjective estimate informed by the user's knowledge

alone, while also requiring that the SRM output be converted to either a polygon or a raster, depending on the approach used to clip the perpendicular polylines. Evidently, there are advantages and disadvantages with both approaches.

Overall, two key factors influenced the final selection of which conceptualisation would be carried forward. Firstly, it was essential that any centreline fell, at all times, between the two polylines representing the extent of the surface water generated by the SRM process. Secondly, it was intended for the subjectivity and error of the later measurement process to be reduced to as great a degree as possible. Consequently, it was decided that a geometric centreline derived directly from the SRM output was the most appropriate. With this established, the next stage was to examine existing GIS tools to see if any would be fit for purpose.

4.2.1 Current GIS-based methods for creating river centrelines

Various approaches already exist for creating geometric centrelines. An exploratory analysis was undertaken with one of the study objectives in mind, that is, the creation of a method that was as easily repeatable as possible. However, ease of use had to be balanced with fitness for purpose i.e. meeting the overall study aim of deriving accurate measurements of WSW. The focus on WSW as opposed to channel or bankfull width meant that some existing techniques were inapplicable, while others did not provide measurements with a suitable degree of accuracy given the desire to capture narrow headwater streams (see Table 4.2.1, p.101). Additionally, a number of these approaches required a DEM for stream network calculation that could not be bypassed, meaning that the known locations of surface waters, as extracted from aerial imagery in the previous chapter, could not be taken into account, which made little sense.

Table 4.2.1 Comparison of remote sensing and GIS-based programs for centreline derivation

Technique	Advantages	Disadvantages	Comments
RivaMap (Isikdogan *et al.*, 2017)	▪ Open source ▪ Capable of automating centerline and width extraction	▪ Requires Landsat imagery as an input, immediately limiting the ability to extract low-order streams	Despite demonstrating the potential of an automated approach to centerline and width extraction, the approach is currently only compatible with Landsat imagery. Adapting this technique for finer resolution imagery would exponentially increase computational requirements to an extent that would currently be unfeasible.
'FluvialCorridor' – ArcGIS extension (Roux *et al.*, n.d.)	▪ Does not require extensive additional data e.g. DEM data ▪ Modular nature of toolbox allows individual process to be run independently	▪ Poor compatibility with multipart features (i.e. shapefiles containing more than one unique feature) ▪ Infrequently updated	This toolbox offers a ready-made approach to deriving river centrelines without the need for additional data. However, as the toolbox is not regularly maintained, compatibility is a significant problem, with the most recent version of the toolbox being incompatible with the current version of ArcGIS. Access to other versions of ArcGIS was not possible while undertaking the comparative analysis.
'Collapse dual lines to centerline' – standard ArcGIS tool (ESRI, 2014)	▪ Uses the standard functionality of ArcMap, so is widely available ▪ Well documented and regularly updated	▪ Severely limited functionality; lines must be close to parallel, and complex channels e.g. braided channels cause process to fail.	Originally designed for road network centerline creation, the tool is unable to effectively process the greater variation found in the natural world, where feature edges are less uniform than those found at the edge of an urban road.

Technique	Advantages	Disadvantages	Comments
HEC-GeoRAS – toolbox for ArcGIS (US Army Corps of Engineers Hydrologic Engineering Centre, n.d.)	▪ Well documented in online tutorials ▪ Frequently revised and updated due to tool being used regularly in real-world applications ▪ Powerful suite of tools	▪ Centreline must be manually digitized ▪ Centreline must be digitized from upstream to downstream in order for process to run properly, requiring *a priori* knowledge ▪ Requires DEM	Tool is intended for local-scale analysis, and for using the stream centreline in subsequent analyses e.g. cross-section creation, rather than as a ready-made approach for deriving a centerline in the first instance.
River Bathymetry Toolkit – extension for ArcGIS (ESSA, 2014)	▪ Regularly updated	▪ Requires a high-resolution DEM for all analyses	The requirement of a DEM introduces both an additional resource requirement and a potential source of error. Most importantly, the tool does not consider the location of surface waters as indicated by the fuzzy classification, and calculates centerlines exclusively from DEM-derived bank and thalweg datasets.
Channel planform statistics toolbox – extension for ArcGIS (Lauer, 2012)	▪ No additional data (DEM) required ▪ Produces a relatively smooth centerline ▪ Includes functionality for measuring width between lines	▪ Requires roughly parallel polylines ▪ Requires each bank to be a separate feature	Given that the tool includes the ability to measure width as part of the centerline creation process, it initially appears to be very promising. However, requiring each bank (or the edge of the surface water) to be a separate feature would require extensive and time consuming manual processing of the contour vector data.

Technique	Advantages	Disadvantages	Comments
FME 'CenterLineReplacer' tool	▪ Easy to batch process large quantities of polygons and replace them with centerlines. ▪ Works with a wide variety of input and output file formats.	▪ Replaces polygons with an overly simplified medial axis / straight skeleton, losing significant channel geometry.	FME is available as a short-term free trial, but thereafter purchase is required.
ArcGIS Data Interoperability extension (developed by FME – see above)	▪ (See above)	▪ (See above)	Does not come as standard with any version or license level of ArcGIS. (See above)

4.2.2 Methodology for centreline creation

The significant drawbacks of existing techniques meant that an alternative method was created for deriving a centreline dataset from widely available data. Ordnance Survey data were used for this purpose as it was desirable to create centrelines from observed rather than predicted river data, as would be the case if using a DEM. This approach has a tendency to underestimate both channel sinuosity and total length, with higher resolution alternatives enabled by the development of LiDAR affected by the opposite trend due to the characteristic 'bumpiness' of the LiDAR-derived land surface (Passalacqua *et al.*, 2012).

A review of previous studies found that the use of polygon skeletonisation algorithms for creating centrelines is relatively widespread (Haunert and Sester, 2007; McAllister and Snoeyink, 2000; Mioc *et al.*, 2004; Regnauld and Mackaness, 2006; Smith *et al.*, 2007), with the main advantage of this approach being that gaps in the river network caused by the presence of a bridge, for example, can be joined using this technique to create a continuous dataset (Regnauld and Mackaness, 2006). Conversely, this approach is known to leave artefacts at the end of line segments in the form of additional polylines that do not represent the centreline or medial axis (Smith *et al.*, 2007). Considering that WSW measurements were made perpendicular to the skeleton and that the dataset was too extensive to check manually, this was an unacceptable compromise.

An alternative approach utilised advanced functionality in ArcGIS is to use a Thiessen polygonisation to extract a skeleton (Alber and Piégay, 2011; García Balboa and Ariza López, 2007; Manners *et al.*, 2014; Nickerson, 1988). The relative ease with which this method can be carried out – an objective of this study – and the degree of geometric accuracy possible, led to the technique being selected. The full workflow for this process can be found in Figure A.1.3 and Figure A.1.4 in the Appendix.

The simplification of the initial Thiessen polygon was essential yet highly subjective. Due to subsequent analysis using this centreline dataset as a reference from which measurements were taken

at a 90-degree angle, artefacts that were not representative of the centreline had to be removed. However, this involved repeated use of the Wang- Müller bend simplification algorithm (Wang and Müller, 1998) in ArcGIS, which aims to eliminate insignificant components (very minor changes in line orientation) while staying true to the overall line geometry of the input data, thereby producing a simpler, more generalised centreline. It was only through exploratory analysis after each iteration of the Wang-Müller algorithm that the suitability of the centrelines for subsequent analyses could be confirmed. Too few iterations resulted in artefacts that were not parallel with the water's edge remaining, which would compromise the ability to make perpendicular measurements, while too many iterations resulted in portions of the centreline being removed entirely from the dataset.

Despite the labour-intensive nature of this process, the result was a centreline that allowed a key issue of previous studies to be addressed, namely the inability to accurately measure width for braided channels, as discussed in the next section. The primary drawback of the methodology was that by using an ancillary dataset to derive a centreline, there were occasions where it fell outside the bounds of the SRM output (Figure 4.2.2). However, this was due to factors such as overhanging vegetation preventing the SRM process from capturing a complete representation of the river, as discussed previously. In summary, the use of optical imagery meant that where the river was obscured by vegetation, an incomplete cross-section was captured by the SRM process, whereas Ordnance Survey data, although using winter maximum extent contrary to the aim of this study to focus on below mean daily flow, represented the full cross-section. Hence, when combining the centrelines derived from the latter with the output of the former, these two datasets were not always spatially contiguous.

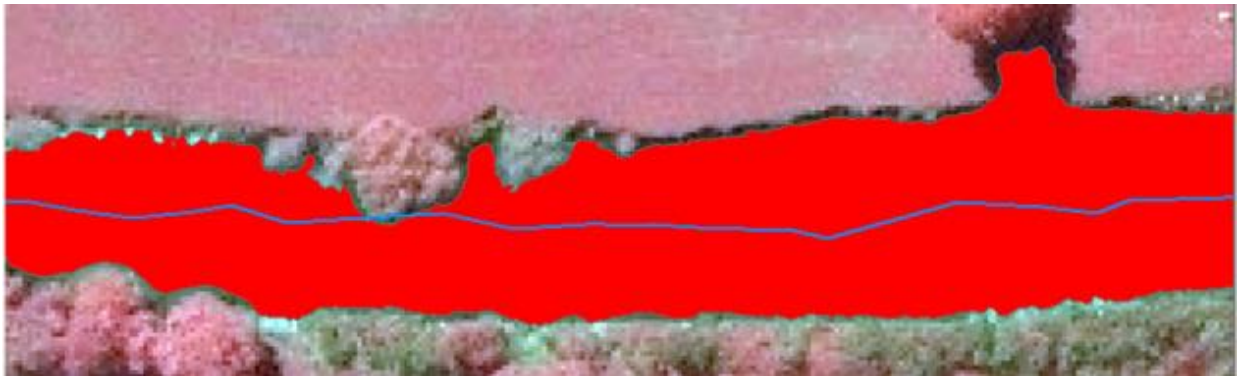


Figure 4.2.2 A comparison of the OS VMD-derived centreline (blue) with SRM output (red).

4.3 Measuring perpendicular to the direction of flow

The creation of a detailed centreline dataset was then complemented with a technique to measure WSW perpendicular to the direction of flow.

4.3.1 Existing methods for creating perpendicular measurements of width

An analysis of existing techniques for making perpendicular measurements yielded similar results to the previous work that focused on tools used for deriving centrelines. As can be seen from Table 4.3.1 (p.108) there is no established technique for generating perpendicular lines that was applicable to this study, compatible with the current version of ArcGIS, or usable without substantial ancillary data.

Purpose-built tools for measuring width, such as RivWidth (Pavelsky and Smith, 2008) and ChanGeom (Fisher and Bookhagen, 2014), use a raster mask of surface water extent and require a minimum number of pixels across the channel before measurements are made, which significantly decreases the ability to capture headwater streams, though this is dependent on the resolution of the imagery used. The surface water mask generated by both tools removes features between the outermost riverbanks, including both morphological features such as sand bars and multi-thread channels, causing WSW to be overestimated. The advantage of using vector data as an input in this study is that complex channel geometry can be maintained, allowing for more accurate WSW measurements.

4.3.2 Generating width measurements at specified points

To exploit the comparatively high quality of the centreline representation created in the previous stage of the analysis, an alternative method for WSW measurement was devised. An additional program – Geospatial Modelling Environment (GME) (Spatial Ecology, 2014) – was used in combination with ArcMap functionality to create a novel approach for WSW measurement. With the importance of reducing the resource requirements associated with manual measurements (Rawlins *et al.*, 2014a), two key parts of the technique should be emphasised. Firstly, GME is freely available and allows for the rapid generation of points perpendicular to line features at user-defined intervals, allowing for more frequent sampling than with manual measurements. Secondly, WSW measurements are automated to an extent, meeting the aim of repeating the process as easily as possible.

The latter is achieved because the GME output is easily converted into transect lines that take the perpendicular points as endmembers. This creates lines that are perpendicular to the direction of flow, which can then be clipped to the extent of the contouring output. Finally, by using the 'calculate geometry' command in ArcGIS, the length of these lines i.e. WSW is automatically appended to the attribute table.

In addition to the ease with which WSW measurements can be made with this method, the exploration of the final measurements dataset showed that rivers <50cm had been accurately captured, meeting the stated objective of capturing low order headwater streams. Furthermore, by using a 500 m sampling interval, 43,428 measurements were taken along rivers in the study site, demonstrating the utility of the GIS-driven technique relative to the impracticality of undertaking such measurements manually.

Table 4.3.1 Comparison of techniques for measuring perpendicular to the direction of flow

Technique	Advantages	Disadvantages	Comments
The Global River Width Algorithm (Yamazaki *et al.*, 2014)	▪ Capable of calculating both bankfull width and effective width (i.e. by excluding islands)	▪ Relatively high resource demands (water body mask, flow direction map, drainage area map) ▪ Water body mask and flow direction data may not match, resulting in the need for the former to be modified to match; introduces error relative to resolution of mask ▪ Narrow channels represented by a single pixel are changed to land.	Despite the flexibility afforded by the ability to measure both bankfull and effective width, the inability to measure channels of a single pixel is contrary to the stated aim of this study to capture the narrowest channels possible.
Spatially Continuous Riverbank Erosion and Accretion Measurements, or SCREAM (Rowland *et al.*, 2016)	▪ Flexibility in how inputs are generated ▪ IDL-based algorithms allow for transferability	▪ Determines bankfull width according to limit of riparian vegetation; no ability to measure WSW	These algorithms offer a powerful set of techniques that directly address the limitations of some of the earlier efforts listed in this table. However, the inability to measure WSW significantly reduces applicability to this study.
Fluvial Information System (APEM, n.d.; Dugdale *et al.*,	▪ Extracts a wide range of hydromorphological data directly from aerial imagery including grain size, channel cross	▪ Proprietary ▪ Offered more as a service than as a standalone product	This is potentially a very powerful platform, but is not accessible as a standalone product.

Technique	Advantages	Disadvantages	Comments
2009; Carbonneau *et al.*, 2012)	sections, bathymetry and habitat maps.	▪ Requires additional data e.g. DEM	
'Segment deflection' – standard ArcGIS tool (ESRI, 2012a)	▪ Built-in functionality in ArcMap. ▪ High degree of customisation.	▪ Lack of automation ▪ Requires manual selection of line, creation of new segment, and selection of angle.	This option is available while in an active Edit session, triggered by selecting 'Create New Feature' and then right-clicking on the polyline (i.e. channel centerline).
RivWidth – IDL based program (Pavelsky and Smith, 2008)	▪ Automation ▪ Established in the academic literature ▪ Uses simple trigonometry to create perpendicular line	▪ Works with a raster mask as input, which is not directly compatible with the contouring approach used. ▪ Expertise in IDL required.	Due to the unavailability of an ENVI or IDL license, this program was not a viable option for use during this study. Regardless, the requirement of a raster mask for input is inappropriate given the use of a contouring approach to delineate river extent, as converting to raster would compromise the geometry of this boundary.
ChanGeom – Matlab algorithm (Fisher and Bookhagen, 2014)	▪ Automation of process. ▪ Demonstrated in the literature (Fisher *et al.*, 2013, 2012)	▪ Requires manual digitization of the channel or surface water boundary. ▪ Less effective than RivWidth in areas of complex channel topography e.g. braided channels (Fisher *et al.*, 2013). ▪ Requires a minimum of three pixels across the channel in order to ensure	Comparable to RivWidth in terms of execution, but is again limited by requiring Matlab, the cost of which could be prohibitive in some cases, especially as the algorithm also requires the Matlab Image Processing Toolbox. The requirement for a minimum of three pixels in order to measure width limits its applicability to this study, given the need to capture as narrow a stream as possible.

Technique	Advantages	Disadvantages	Comments
		WSW measurements are accurate.	
'Transect' – extension for ArcGIS IS (Ferreira, 2014)		▪ Unable to include *a priori* knowledge i.e. extent of surface water in process ▪ Developed by a single user, so updates are unpredictable	
Create perpendicular lines – Python script (Gabrisch, 2008)	▪ Relatively simple to execute ▪ Does not require ArcGIS	▪ No GUI ▪ Creates perpendicular lines at the centre point of existing line segments, limiting sampling frequency	
'Measure' – standard ArcGIS tool (ESRI, 2012b)	▪ Full control of measurement process ▪ Very simple to execute	▪ Must be operated manually, meaning angle of measurement across channel and judgement of extent is extremely subjective ▪ Result must be manually recorded	This approach, as used by Rawlins, Clark and Boyd (2014a), is capable of producing accurate measurements of WSW, but is dependent on the judgement of the user. Furthermore, the manual nature of the process makes it impractical for studies such as this, where a large area must be sampled extensively.

4.4 Aggregating at-a-station measurements to derive maximum effective width

The impact of overhanging vegetation results in AAS WSW measurements being of limited accuracy (Section 3.5.1, p.87). To address this, measurements were aggregated for river reaches. Previous studies have used a mean width for a river reach, a metric known as 'effective width' (Smith *et al.*, 1996), which would aid in reducing the influence of measurements limited by overhanging vegetation. This technique is commonly undertaken by using a single WSW measurement for a reach and then multiplying by reach length, or by dividing reach surface area by length (Birkinshaw *et al.*, 2014), but is equally achievable by averaging a number of WSW measurements for a defined section of a river.

Ideally, measurements would have been aggregated by creating a 'moving window' that followed river geometry and divided the network based on user-defined parameters, such as the number of point measurements or river length for which a single value of WSW should be created. However, the complexity of the river network geometry, particularly where multiple confluences or braided channels existed, made this more labour intensive to achieve than was acceptable given the time frame of the study. An approach using ArcGIS Network Analyst (ESRI, 2016; Okabe and Satoh, 2009), which is normally applied to road routing analysis, has the potential to deliver this, but specific requirements of river network routing, such as flow being unidirectional at any given point, introduced too great a degree of complexity.

As a compromise, a pre-existing dataset was used which contained catchment polygons at varying scales. Called Integrated Hydrological Units (IHU), the dataset contains a fine-resolution layer (IHU Sections) that disaggregates the river network into discrete sections on every occasion that two watercourses converge (Centre for Ecology and Hydrology, 2015b). This has the effect of delineating separate river reaches into polygons that cover the area that drains into the section. With 398 IHU

Sections either wholly or partially in the study area, a degree of granularity was still present while expediting the measurement process considerably.

The IHU Sections polygons were used to aggregate the AAS measurements of WSW. It was possible to aggregate measurements using a variety of statistical measurements (e.g. mean, maximum, minimum, standard deviation). The choice of summary statistic was crucial, as the resultant values would be used as the basis for the predictive model of WSW. Despite the tendency for the mean to be used (Sear *et al.*, 2010; Smith *et al.*, 1996; Thorne *et al.*, 1996), this was considered inappropriate within the specific context of this study due to overhanging vegetation skewing the mean value. This was particularly concerning as the IHU Sections were not of uniform size, as places along the river network had multiple tributaries in a small area, resulting in several small river reaches within which few AAS WSW measurements had been taken. This meant that even a single inaccurate measurement would have exerted significant influence over the mean in these locations, which would in turn compromise the statistical modelling undertaken.

As a result, maximum WSW per reach was used to derive 'maximum effective width' (MEW). Even though overhanging vegetation could still influence MEW, this was statistically less likely by selecting a single WSW measurement to represent many AAS values, as opposed to calculating a mean using every value in each IHU Section that almost certainly included inaccurate measurements due to the aerial view of the river being obscured. Figure 4.4.1 visualises the different spatial patterns in WSW when using mean WSW or maximum WSW.

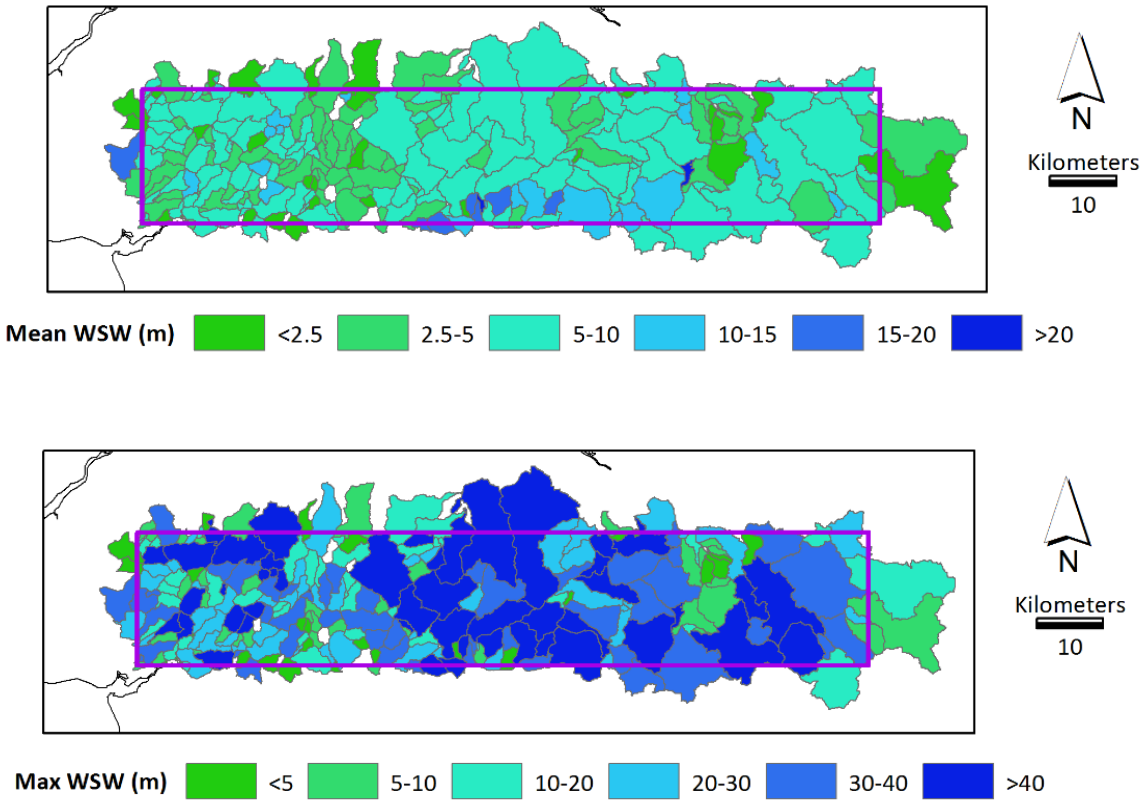


Figure 4.4.1 aggregated WSW measurements for the study site using IHU Section data (Centre for Ecology and Hydrology, 2015b), showing a) variation in mean WSW, and b) variation in maximum WSW. White indicates an area with no WSW measurements due to no rivers being present.

Mean WSW varied across the study site to a lesser degree than maximum WSW, with a significant skew also evident, with the majority of areas having mean WSW <10 m. This contrasts with maximum WSW, which had a greater range and better coverage across all categories. While this is not altogether surprising given that there is an inverse relationship between stream order and the proportion of rivers within each order, in that low-order streams are more numerous than higher-order rivers (Strahler, 1957), it must be remembered that the units used to aggregate measurements were IHU Sections (Centre for Ecology and Hydrology, 2015b). These areas delimit a single river section between confluences, so the measurements that were used to produce both the mean and maximum were theoretically from a single river reach. While there would have been an element of natural WSW variation, the extent of the discrepancy between the mean and maximum WSW suggested that an external factor may have exerted an influence. Based on previous analyses (see Section 3.5.1, p.87),

this was most likely due to overhanging vegetation obscuring the aerial view of WSW, reducing the measurable width. When these inaccurate WSW measurements were aggregated with those that *did* accurately capture width for the reach, this resulted in mean WSW that misrepresented real-world conditions by presenting a significantly lower WSW. Therefore, the use of maximum WSW, or MEW, is further corroborated, particularly considering that techniques to limit errors of commission were applied (see Section 4.1, p.96), so MEW is unlikely to be overpredicted as a result.

4.5 Validating image-based WSW measurements in the field

Quantifying the accuracy of the image-based measurements was critically important in itself (and a stated aim of the study), but was also necessary for clarifying the degree of error that could propagate through to the predictive model of WSW that used these measurements as the response variable. Ensuring that any observed differences between the two sets of measurements could be attributed to the image-based measurement process was challenging, because ideally field measurements would be taken synchronously as the aerial imagery was captured. This was impossible due to the use of aerial imagery captured a number of years prior to the commencement of the research, while the infrequent return period for large-scale aerial surveys meant that there were no further opportunities to address this. Even then, a large field team would be required to match the speed and range of an aerial survey to capture a significant number of synchronous measurements.

In order to ascertain whether image-based and field measurements were taken in comparable conditions, a number of safeguards were put in place. Firstly, NRFA gauging station data – previously used to confirm that the imagery from which measurements were derived represented rivers at below MDF (Section 3.2.2, p.57) – were analysed for both time periods, and demonstrated that conditions were generally comparable i.e. below MDF.

Secondly, field validation was targeted at channels that were more likely to have remained consistent in form. This was necessary because both natural and anthropogenic factors will have altered river geomorphology over time, potentially altering WSW even when controlling for flow conditions. Consequently, intentionally biasing validation towards channels where width was more likely to be consistent and controlled over a period of time was both justifiable and necessary, as the intent was not to discover where channel adjustment had taken place in the intervening years, but to quantify the difference between the two datasets caused by limitations in the image-based measurement process alone. Used in combination with NRFA gauging station data to ensure that flow was also controlled for, this approach presented the best opportunity for quantifying the degree of error in the semi-automated image-based measurement technique.

The most reliable approach to ensuring that channel form had remained consistent was to take field measurements only at cross-sections where the river channel had been modified using techniques such as embankments or revetments due to the bank stability that such modifications afford the river channel. These locations were identified using the RHS dataset (Environment Agency, 2010a; Raven *et al.*, 1998, 2010) to constrain the initial search to heavily modified reaches, with a visual analysis of the aerial imagery then identifying specific measurement points. Locations adjacent to public footpaths or roads were also preferred to allow for accessibility, achieved by examining OS data. The final locations selected for the collection of field measurements of WSW are shown in Figure 4.5.1.

Controlling for both flow and channel geomorphology when comparing between image-based and field measurements expands on existing research. For instance, Fisher *et al.* (2013) identified river reaches that were free of tree cover and shadow when comparing their ChanGeom technique with field measurements, comparable to the use of MEW as opposed to AAS measurements in this study, and while the distinction between WSW and channel width meant that controlling for flow was not a

necessity, the additional use of an intentionally biased sampling approach as in this study offers a further guarantee that measurements are being compared like-for-like.

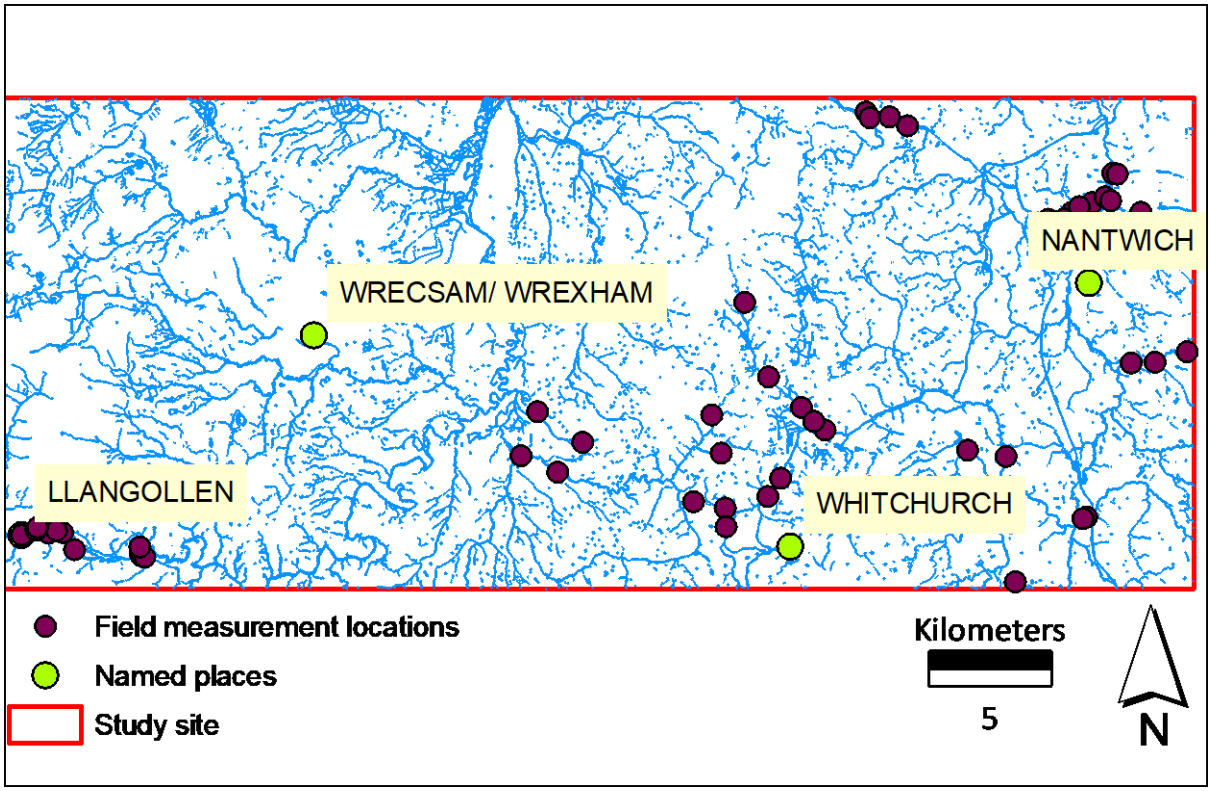


Figure 4.5.1 Field validation measurement locations

A Leica DISTO D210 laser distance measurer (LDM) was used to calculate WSW in the field, with a tape measure used at a number of narrower cross-sections to confirm the accuracy of the LDM. Stated accuracy was ±1 mm up to 80 m distances, but the challenges of measuring both vertical and oblique surfaces outdoors, some of which were partially covered in vegetation, meant that confirmation of accuracy was still required. Although difficulties were encountered when attempting to measure as close to the surface of the river as possible, with some repeat measurements required, the LDM accuracy was sub-centimetre.

The results of the field validation are presented in Figure 4.5.2. The degree of absolute error was consistent across rivers of different widths, indicating the consistency of the measurement method for rivers of different scales. The coefficient of determination was 0.95 with an RMSE of 0.87 m and a MAPE of 11.17%. The RMSE appears to be high when compared with the input resolution of the CIR

imagery (50 cm) and the efforts to further enhance the resolution of the imagery via SRM, but further analysis (beginning overleaf) revealed that overhanging vegetation was largely responsible for error. Similarly, MAPE is higher than anticipated for similar reasons, and is inflated by two measurements in particular when absolute percentage error exceeded 40% (relative error was between 30 cm and 40 cm, as both streams had WSW <2 m), which is particularly significant given that sample size was comparatively small (n = 51).

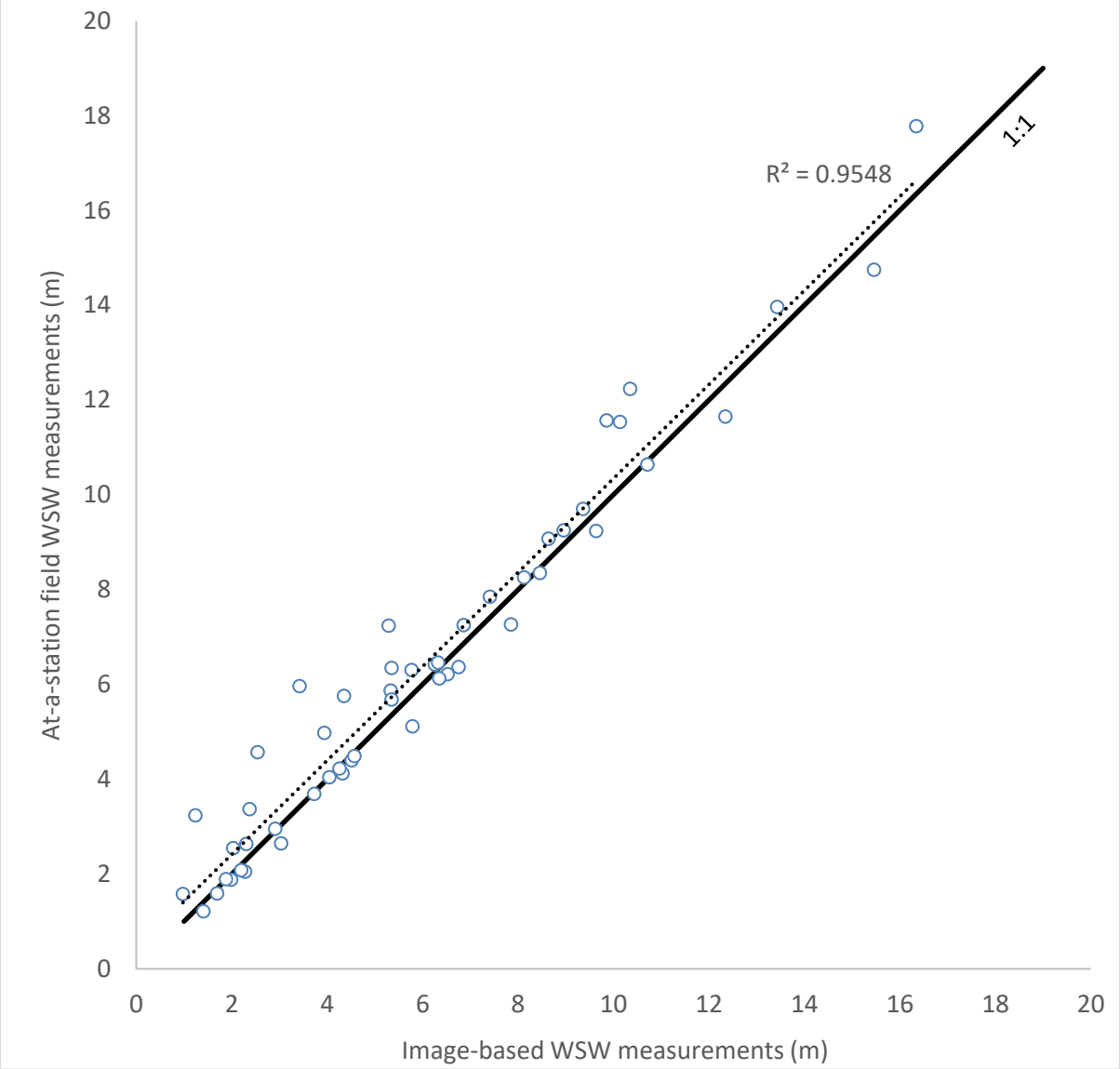


Figure 4.5.2 Comparison of image-based and at-a-station field measurements of WSW (n = 51, RMSE = 0.87m, MAPE = 11.17%).

The semi-automated image-based WSW measurement process was most effective in areas where the channel was comparatively simple geometrically, with an absence of overhanging vegetation, shadow, and in-channel landforms. Where these features did exist, WSW was consequently measured incorrectly, albeit to a small degree. The overall trend was for the image-based measurements to underestimate WSW, with the highest magnitude absolute error being an underprediction of 2.53 m, and the highest relative error standing at an underestimation of 44.4%. These errors were both for narrow streams of between 4 m and 6 m in width. The extent of relative error was initially concerning, but still only equated to approximately 2 m difference; this was high in comparison to the spatial resolution of the imagery, but was explained by significant floating debris at this cross-section. In terms of overestimation, the most significant absolute and relative errors were 71.23 cm and 16.1% respectively, the latter once again for a narrow stream (<2 m), which results in even a minor absolute difference appearing significantly larger in relative terms.

Underestimation of WSW occurred, as anticipated, where image-based measurements were obscured by overhanging vegetation. This was especially noticeable at the measurement locations based in rural areas, which had a higher incidence of overhanging vegetation and floating debris, the latter a result of the higher prevalence of organic matter along the riverbanks, be it vegetation or soil. The highest magnitude overestimation was due to the presence of tarmac alongside the river, which has a comparable spectral signature to surface waters. The GIS post-processing did not eliminate this overestimation due to the water and tarmac being in such close proximity, and lying within the winter extent of the river surface water as indicated by OS data.

4.6 Chapter summary

This chapter has shown that: -

- The use of GIS enabled a combination of high-frequency, large-scale measurements to be made using a semi-automated approach that exceeded the capabilities of both manual measurement strategies and pre-existing algorithms or GIS tools. This directly addressed one of the aims of the study to deliver accurate image-based measurements of WSW.
- The use of ancillary data is capable of significantly improving the accuracy of datasets extracted from aerial imagery, demonstrated by the reduction in errors of commission achieved by clipping the extracted surface water features to the bounds of an authoritative river network dataset.
- The influence of overhanging vegetation can be compensated for by aggregating AAS measurements of WSW into MEW for a defined river reach, limiting the degree of measurement error propagating through to subsequent analysis.
- The study objective to create an easily replicable method was hampered by the inapplicability of existing approaches for reasons such as unacceptably low accuracy, high ancillary data demands, and being designed for bankfull or channel width, as opposed to WSW. The objective was instead addressed by repurposing existing GIS tools to create a repeatable workflow (see Figure A.1.3 and Figure A.1.4 in the Appendix) that can be applied in any location, and at any time.
- Field validation has shown that the accuracy of the image-based measurement process is sufficiently high (R^2 = 0.95, RMSE = 0.87m, MAPE = 11.17%) that the stated aim – to make accurate, direct image-based measurements of WSW – was achieved.

Despite the ability of the WSW measurement process to yield accurate results, the methodology currently has very high resource requirements that prevent its effective application to the entirety of

England and Wales. While this may change in the future as the cost of high resolution remotely sensed imagery decreases and computer processing power improves, an alternative method is currently required. Hence, the subsequent chapter explains how the direct image-based WSW measurements generated herein were upscaled through the use of statistical modelling, allowing for WSW to be estimated for the entirety of England and Wales while still taking advantage of the enhanced capabilities of the image-based measurement process, particularly the ability to capture narrow headwater streams.

Chapter 5
Predicting water surface width for England and Wales

Despite the ability to take WSW measurements directly from aerial imagery being demonstrated in the previous chapter, the resource intensive nature of this process made it impractical to apply this method at the national scale, even for what are comparatively small regions (England and Wales).

Therefore, in order to deliver on the stated aim of creating a national-scale dataset of WSW, an alternative approach was required that could combine the advantages of the image-based measurement process (e.g. the ability to incorporate low order streams into the WSW dataset) with the ability to scale these measurements up. Consequently, a modelling approach was selected, as this allowed *a priori* knowledge of channel-shaping fluvial processes to be incorporated into the analysis (see Section 2.3, p.21 for an overview of factors that shape river morphology). Similar approaches have previously been applied at the national scale (Booker, 2010; Rawlins *et al.*, 2014a), revealing explanatory variables that may be relevant to such a model. However, the use of direct image-based WSW measurements in this process is limited to gauging station locations or a small number of manual

measurements, something that this study aimed to improve upon by creating a method where the user could define a regular interval along the river network at which to take measurements, allowing for a sampling frequency that would be impractical to match using manual measurements and that exceeds the number of gauging stations. However, an element of compromise was also necessary, as models that contain greater complexity when compared to traditional width scaling approaches that use discharge or catchment area alone to predict river width (Leopold and Maddock, 1953) have been criticised for introducing greater demands in terms of additional knowledge of model parameters and sources of error (Fisher *et al.*, 2013), as this knowledge may be incomplete or difficult to incorporate into a model. By using widely available, easily interpretable, and well-supported landscape data as explanatory variables in a predictive model that was kept as simple as possible, these concerns were addressed. With this aim in mind, multiple objectives were devised to set clear waypoints towards completion. The objectives can be found in full in Section 1.2 (p5). In brief, these relate to investigating which controls of WSW can be used as explanatory variables given the context of the study; the collection of appropriate data for the explanatory variables identified; the creation of a predictive model of WSW informed by the image-based measurements taken previously; and finally, the validation of the final model to ascertain its accuracy and applicability beyond the north Wales/central England study site.

5.1 The selection of explanatory variables to predict WSW

A review of the relevant literature identified a number of factors that could be of potential use in predicting WSW (see Section 2.3, p.21). These were:

- Discharge, or catchment area
- Climate, including precipitation
- Land cover

- Channel boundary material, and subsequent effects on sediment transport
- Hydrological source of flow
- Channel gradient
- Elevation
- Human modification of the river channel and the surrounding environment.

However, the local-scale dynamism of river systems immediately meant that some of these controls had to be omitted due to the incongruity of modelling WSW at the national scale and current theory. Bed material size, which affects the erosive potential of a given river, and vegetation species type and root system density were among the factors that were not included, chiefly due to the lack of an existing dataset for these factors. Field surveys are by far the most effective way of assessing these variables (Sear *et al.*, 2010; Thorne, 1998a; Thorne *et al.*, 1996) yet are impractical given the extent of the study site, reinforcing that this study and similar approaches to modelling WSW (Booker, 2010; Rawlins *et al.*, 2014a) are a complement to existing methodologies, rather than a direct replacement. The most appropriate technique, as alluded to here, depends upon the scale of the investigation and the desired precision.

Table 5.1.1 (overleaf) details the factors that were selected as explanatory variables for the predictive model, reasons for inclusion, the data source(s) identified as most appropriate, and finally, issues with either the variable itself or the data sources that presented difficulties.

Table 5.1.1 Initial selection of explanatory variables and proposed data source.

Variable	Rationale	Data Source	Confounding Factors
Catchment area	Area upstream of a given point is a key explanatory variable from previous studies (Booker, 2010); proxy for discharge, which is only available in England and Wales at gauging stations.	Derived from a DTM using ArcHydro.	Accuracy is relative to the resolution of the DTM used, yet the national scale of the investigation meant that the exponential increase in computational storage requirements introduced by an increase in spatial resolution made the use of the finest scale data difficult.
Rainfall	Key variable from previous studies (Booker, 2010); related to runoff.	5 km^2 May 2009 rainfall dataset from EA – CP09. Total rainfall from centre of each 5x5 cell. Converted .txt to raster in ArcMap.	Relatively coarse spatial resolution of data means that rainfall may occur over a diverse landscape in terms of slope, aspect, and land cover, among other factors, so unlikely that all recorded rainfall will flow into river. Coarse temporal resolution is acceptable given that imagery is captured on different days, so extracting multiple different daily rainfall datasets and associating them with measurements taken from images captured on different dates is extremely complex.
Land cover	Riparian vegetation stabilizes river banks and encourages deposition (Allmendinger *et al.*, 2005; Leopold and Wolman, 1957; Liébault *et al.*, 2005), and also reduces the rate of widening over time (Elliott, 2011). Land cover in	100 m resolution CORINE raster dataset; contains most prevalent land cover class	Despite having the finest resolution representation of land cover available at this spatial scale, the assignment of a single land cover class per pixel obscures landscape variation that is potentially very important to channel morphology.

Variable	Rationale	Data Source	Confounding Factors
	the catchment affects runoff (Piao *et al.*, 2007).		
Channel material	Composition of channel (lithology and structure) affects erodibility of banks and sediment availability (Finnegan *et al.*, 2005).	Various BGS data available via EDINA Digimap.	Very little data explicitly addresses the surface material of channels in a way that is interpretable using established fluvial geomorphology theory e.g. the differences in sediment transport and deposition in alluvial and bedrock channels (Ashley *et al.*, 1988; Finnegan *et al.*, 2005).
Hydrological source of flow	The proportion of river runoff from stored sources indicates underlying geology and soil type (Beck *et al.*, 2013; Bloomfield *et al.*, 2009; Gustard *et al.*, 1992)	1km resolution BFIHOST dataset (Boorman *et al.*, 1995)	1km spatial resolution is coarse compared to the level of detail possible with both the sampling frequency for measurements along the watercourse and the precision of the image-based WSW measurements. Therefore, the statistical relationship between BFIHOST and WSW could be obscured.
Slope / channel gradient	Key control of channel width (Finnegan *et al.*, 2005)	Derived from DTM using ArcMap Spatial Analyst toolbox.	Calculable at a variety of scales, such as a catchment area, or more locally with either a focal or zonal mean i.e. slope around a specified measurement point, or along the course of the river for a specified distance upstream or either side of the measurement point along the watercourse.
Elevation	Potential proxy for stream order.	Values extracted to points from DTM.	Ability to capture variation in terrain is relative to the spatial resolution of the DTM.

Variable	Rationale	Data Source	Confounding Factors
Relief	Difference between maximum and minimum elevation in a given area (Rawlins *et al.*, 2014b)	Made catchment and section measurements using zonal statistics.	Correlation with slope and/or elevation
Human modification	Alterations to the channel or surrounding area affect natural response (Chin, 2006; Gregory, 2006)	HMS score from RHS dataset (Environment Agency, 2010a; Riverdene Consultancy, 2016). RHS is UK-specific and has been revised repeatedly over the better part of two decades (Newson *et al.*, 1998; Raven *et al.*, 2010, 1998; Sear *et al.*, 2010). Habitat Quality Assessment (HQA) is included in this dataset and was also tested.	By representing a wide array of river channel management strategies quantitatively as a single number, two measurement locations with significantly different features – with significantly different impacts – may be represented by the same number due to the system used.
Sinuosity	The ratio between distance covered by a meander and the straight-line distance of the meander (Leopold and Wolman, 1957; Williams, 1986; Zolezzi *et al.*, 2012). Meander wavelength is approximately ten times channel width.	Meander wavelength and amplitude can be predicted as a function of channel width using GIS analysis	Human modification of channel can include strategies for straightening, particularly in flood defence schemes where increasing conveyance speed is a priority. Calculations are complicated by multi-threaded channel planform.

5.2 Using multiple linear regression to model and predict WSW

There were numerous options when it came to creating a predictive model, each with different requirements and assumptions. Of the more traditional statistical modelling approaches, the continuous nature of both the explanatory and response variables meant that regression was most likely to produce a model that best fit the data (Chatterjee and Hadi, 2009; Crawley, 2013; Everitt and Hothorn, n.d.; Field *et al.*, 2012). The process is also reasonably straightforward to communicate, an advantage when a requirement of the study is to create a methodology that can be utilised by an external stakeholder. This line of thinking stems from the principle of parsimony, or Occam's razor. In this context, the model should be as simple as possible, a theory expressed more specifically in this context as the 'minimal adequate model' (Crawley, 2013). In layman's terms, this means that even though a number of models may be viable, the most preferable is one that performs well while also being as simple as possible. This principle applies to both the number of explanatory variables used as well as the overarching approach. Thus, a balance was struck between a simple observation-driven empirical model and a highly complex physics-driven physically-based model by opting for a conceptual model. This approach accounts for potential relationships without assuming that knowledge of the underlying physical principles is complete, as with physically-based models, while avoiding the oversimplification inherent in some empirical models that limits predictive ability. The selection of regression as the preferred method also allowed for the generation of probabilistic model output, allowing for a fresh examination of the relationships between the explanatory and response variables without assuming that there exists a definitive answer, as with deterministic modelling (Mount and Stott, 2008).

Multiple linear regression (MLR) was undertaken using the ordinary least squares (OLS) method, which minimises the sum of squared deviations (squared residuals) from the regression line.

The regression model can be expressed as follows: -

$$Y_i = (b_0 + b_1X_1 + b_2X_2 + b_nX_n) + \varepsilon_i$$

Y_i is the response variable (WSW)

b_0 is the y-intercept

$b_nX_n$are the coefficients (b) for the explanatory variable values (X)

ε_i is the error (residual)

Equation 5.1 Expression of multiple linear regression (MLR) modelling

The application of MLR is in line with previous attempts to model WSW beyond the local scale (Booker, 2010; Rawlins *et al.*, 2014a), which were expanded upon by sampling at a higher frequency than was possible with gauging station and manual measurements, respectively. Furthermore, particular emphasis was placed on examining the role of human modification in controlling WSW. This was achieved by including River Habitat Survey (RHS) results in the model, specifically the habitat modification score (HMS), which quantifies the extent of modification on a consistent, standardised scale across the UK. The inclusion of a metric quantifying human modification in estimating WSW is truly novel, in that no existing studies attempt to account for human influences, or quantify them relative to the established 'natural' controls of WSW e.g. catchment area. Given that only 11% of rivers and streams in the UK are defined as 'near-natural' (Environment Agency, 2010a), human modification of the river channel is an important aspect that is worth addressing.

The complete range of explanatory variables that were selected for inclusion in the initial model are shown in Table 5.1.1 (p.124). The relevant datasets were imported into ArcMap and extracted for the locations where AAS WSW measurements were taken as part of the image-based measurement process discussed in Section 4.3.2 (p.107), and then aggregated using IHU Section polygons. The use

of these polygons allowed for a semi-distributed modelling approach, which struck a balance between the assumption of total spatial heterogeneity of lumped models, which would conceal the variation in the very processes that are being modelled, and the significantly higher data requirements of distributed models that could not be met due to the varying spatial resolutions of the available data (see Table 5.1.1, p.124). Where there were no immediate data underlying the AAS measurement locations, such as in the case of the RHS dataset which is presented as points which do not frequently intersect the WSW measurement points, the nearest available value was extracted based on Tobler's first law, which states that more proximal locations are more related than distal locations (Tobler, 1970).

5.2.1 Testing MLR assumptions

As with any statistical test, MLR comes with a set of assumptions that must not be violated in order for model output to be verified. The assumptions that were tested, and the methods for doing so, were derived from a number of texts on statistical theory (Crawley, 2013; Field *et al.*, 2012; Zuur *et al.*, 2010), and are presented in Table 5.2.1. Depending on the assumption in question, it may be tested prior to, during, or after running the MLR process.

Table 5.2.1 methods for testing the assumptions of ordinary least squares linear regression

Assumption	Test (and associated threshold)	Remedial action if violated
1. Data are a random sample	Analysis of data collection strategy	Collect data again
2. Data are independent i.e. no perfect multicollinearity	Correlation >0.8 and/or VIF (Variance Inflation Factor) >5 require further examination	Use of alternative technique e.g. robust regression, or removal of variables
3. Relationship is linear	Graph of response variable vs. each explanatory variable, and residuals vs. explanatory variable	Transformation of explanatory or response variable, and/or inclusion of quadratic term
4. Residuals are normally distributed	Q-Q plot and Shapiro-Wilk test, for which a small p-value indicates that the residuals are not normally distributed	Transformation of variables
5. Variance of the residuals is homogenous (heteroscedasticity)	Residual vs. fitted plot, and Levene's test where p-value < 0.05 indicates that the assumption is violated	Transformation, or use of non-parametric methods
6. No influential cases	Cook's statistic >1 cause for concern; scatterplot reveals outliers	Omission of offending data
7. Explanatory variables are relevant	Initial selection grounded in literature. Tested using t-tests. Relevant second-order interactions also included.	Removal of irrelevant variables

The majority of assumptions were met, with a few important exceptions. Multicollinearity refers to the phenomenon where explanatory variables are strongly correlated with one another. A variance inflation factor, or VIF, with values >5 (Zuur *et al.*, 2009) or >10 (Field *et al.*, 2012) are of concern and require further investigation, and this applied in some cases. Model standard errors can become inflated if collinearity is present, making estimates of the coefficients unstable.

The multicollinearity diagnostics identified an element of collinearity in some of the model variables. These were HQA and HMS; drainage density and catchment area; elevation and relief. In the first two cases, there was a strong theoretical basis for omitting one of the related variables in particular. HQA and HMS both attempt to quantify the 'naturalness' of the river channel, with the former assigning a

value based on the diversity of the environment and the latter measuring the impact of human modification. A higher HMS value correlates with a higher HQA value, showing that a greater degree of human interference leads to a less diverse habitat. It was decided that the HMS variable was more relevant to the analysis, as human modification was a factor of interest that was not accounted for in any other way, whereas HQA – a measure of habitat diversity – was partially accounted for by other variables, such as land use and channel gradient, and was in itself less likely to shape channel geomorphology directly when compared to the strong body of literature hypothesising the impact of human modification on WSW. Habitat diversity, while critically important as an indicator of ecological health and quality, is more of a proxy measurement in this scenario that would be useful only if the HMS score was not available, as it is a consequence of other landscape variables, many of which were already accounted for.

Secondly, drainage density was omitted in favour of catchment area, as the latter is consistently the most significant variable in WSW models (Booker, 2010; Rawlins *et al.*, 2014a) and was preserved as a result. Using drainage density may also be somewhat specious due to IHU Sections being used to aggregate data. The subdivision of the river network into polygons delineating single channels between confluences meant that drainage density within these areas was more a measure of polygon area, which captures a very limited and often unrepresentative impression of total catchment area. As a result, the catchment area explanatory variable was maintained.

Finally, elevation and relief were correlated, which is not surprising as the latter is a calculation of spatial variation in the former (the differences between maximum and minimum elevation within a catchment area). Both of these variables were significant predictors of WSW in previous studies. VIF was greater than 5, but less than 10 for these variables, and with no obvious case for omitting one variable over the other, both were therefore maintained in the model despite this being a borderline case. Future studies would therefore require a re-examination of this trend to discover whether the degree of correlation is consistent in space and time, and if not, to determine which variable most

commonly accounts for greater variation in WSW, although this is likely to vary with scale and the units of WSW used (i.e. aggregated measurements for a reach versus AAS WSW).

5.2.2 Identifying second-order interactions between explanatory variables

An assumption of MLR is that all relevant variables are included in the model, so the *tree* R package (Ripley, 2016) was used to visually identify second-order interactions between explanatory variables. Longer branches on the regression tree identified the variables that explained the most variance in WSW, and these were included in the first MLR model run.

5.2.3 Order of deletion

Having fitted the maximal model i.e. forcing all of the available explanatory variables into the model, stepwise deletion was used to systematically reduce the model until only significant variables remained and no assumptions were violated. The single most non-significant explanatory variable was removed, the model re-run, and the process repeated until completion. This process required several dozen iterations as a variety of methods were used to aggregate AAS values for the explanatory variables to the reach scale (e.g. mean, minimum, maximum, range) in order to assess which was the most appropriate predictor of WSW, necessary due to a number of the variables affecting WSW at varying spatial scales. The variables that were completely removed from the final model were: -

1. Second-order interactions
2. Sinuosity
3. Relief
4. Land cover
5. Elevation

Second-order interactions were not found to be significant, with the exception of the interaction between BFI and catchment area (identified as a significant predictor of WSW in the UK by Rawlins *et al.*, 2014a). This is somewhat surprising, as the two models differ in the way that WSW measurements

are used (AAS vs. reach-aggregated). While additional research would be required to offer anything more than a tentative conclusion, the fact that the interaction between BFI and catchment area has proven to be a statistically significant predictor of both AAS and reach-aggregated WSW could potentially indicate the existence of an underlying mechanism, although this is caveated by the existence of the BFI dataset existing for the UK alone.

Sinuosity and relief were not significant, likely due to the scale of the IHU Sections dataset. For the former, variation is likely to occur at a coarser resolution than the dataset derived for this study i.e. by calculating sinuosity for IHU Section polygons of varying size, rather than at uniform intervals along the river network (e.g. every 1km), the relationship with maximum WSW was obfuscated to the point where sinuosity was no longer a significant explanatory variable in later model runs.

Finally, the omission of land cover was most likely due to the dataset used, as this assigned the most substantial land cover class rather than the proportions of multiple classes for pixels of 100 m resolution. Given the potential for there to be a significant number of different land cover types in an area covering 100 m^2, the most prevalent land cover may in reality have represented a small proportion in the case of pixels that contained a wider variety of land cover classes. For instance, a pixel with 10 different land cover types within it could theoretically assign the entire pixel to a land cover class that covers fractionally more than 10%, with all others covering fractionally less than 10%. This inability to account for heterogeneity in land cover meant that a statistically significant relationship with WSW was unlikely to be observed. Furthermore, while more detailed datasets such as 25 m resolution LCM vector data were available (Centre for Ecology and Hydrology, 2017), the improved spatial resolution meant that the water land cover class was often assigned to each measurement point as the river itself formed the most dominant land cover class. 100 m resolution CORINE data were selected partly for this reason, as alternatives such as extracting land cover within a certain radius of each measurement location, for example, had no theoretical justification and would ultimately still result in the most prevalent class being assigned.

5.3 Model results

Table 5.3.1 Descriptive statistics for measurements of WSW and landscape data

	WSW (m)	BFI:CA	Maximum HMS Survey	Mean HMS Survey	Maximum slope (local) (degrees)	Mean slope (local) (degrees)	CA (km^2)	Mean monthly rainfall (mm)	Range BFI
Minimum	0.14	0.41	0	0	0.49	0.34	1.29	44.65	0
Mean	24.45	53.95	720.69	406.22	13.68	5.22	101.95	109.83	0.22
Median	23.61	6.49	430	230.71	12.77	4.92	13.73	91.97	0.22
Max	65.06	1140.81	3800	3050	47.39	31.26	1671.38	249.96	0.54
SD	15.07	142.56	913.14	564.20	9.08	3.75	256.78	57.11	0.16

The minimal adequate model of WSW (BFI:CA, HMS score, slope, catchment area, rainfall, and BFI) had an adjusted R^2 of 0.75 (Table 5.3.2). The *p*-value associated with the F-statistic is sufficiently small that the model can be described as a significantly better predictor than the mean alone, while the descriptive statistics for the residuals, presented at the top of the aforementioned figure, are relatively symmetrical, suggesting normality. Model results are shown in Table 5.3.2, below.

Table 5.3.2 Summary of minimal adequate multiple linear regression model of WSW (n = 231) generated in R (R Core Team, 2017).

Residuals:

Min	1Q	Median	3Q	Max
-6.33	-1.71	-0.40	1.71	5.57

Coefficients	Estimate	Std. Error	t value	Pr(>t)[1]
(Intercept)	7.99	0.23	4.29	<0.01
BFI:CA	7.95e-02	1.43e-02	5.54	<0.01
Max HMS score	4.30e-03	1.62e-03	2.66	<0.01
Max slope (local)	6.76e-01	1.32e-01	5.12	<0.01
Max slope (catchment)	1.11e+01	3.85	2.87	<0.01
Mean CA (km^2)	-2.28e-05	6.23e-06	-3.66	<0.01
Mean HMS score	-5.90e-03	1.47e-03	-2.39	0.02
Mean rainfall	-5.27e-02	0.93e-02	-2.73	<0.01
Mean slope (local)	-7.81e-01	1.06e-01	-2.56	<0.01
Mean slope (catchment)	-1.10e+01	2.86	-2.85	<0.01
Range BFI	4.53e+01	0.72e+02	5.57	<0.01

[1]Probability of observing value equal to or larger than the t value

Residual standard error: 1.16 on 220 degrees of freedom
Multiple R-squared: 0.77
Adjusted R-squared: 0.75
F-statistic: 226.19 on 10 and 220 DF
p-value: 2.2e-16

Some of these variables initially appear to be extraneous with a high potential for multicollinearity. For example, the use of both the maximum and mean HMS score for a river reach seems unnecessary, but was justified as the inclusion of both did not violate any assumptions and was supported by the background literature. The mean HMS score gave a general impression of channel modification, whereas maximum HMS score indicated the presence or absence of an especially significant modification – for which the HMS methodology would have assigned a high score, even in lieu of any additional 'minor' modification (Riverdene Consultancy, 2016) – which had the potential to exert a significant influence on channel morphology independent of any other proximal modifications. Additionally, the use of multiple slope parameters, including maximum and mean measurements of slope both locally (for each IHU Section) and at the catchment scale, seems excessive. However, slope is significant at multiple scales when considering the way in which channel width, or WSW, is controlled, and relates to the differing – although not necessarily competing – theories of downstream

hydraulic geometry and AAS hydraulic geometry. In summary, these theories consider river morphology as a function of reach-scale or cross-sectional processes at a specific point. These two theories relate to the catchment-scale slope and local slope explanatory variables respectively, so the inclusion of so many apparently similar parameters in fact reflects current understanding of river processes.

Analysis of the model residuals showed no clear pattern in residual errors versus their fitted values (random distribution of residuals), a Q-Q plot with little deviation from horizontal, a scale-location plot with no obvious trend, and a Cook's distance plot with distances well below 1, all of which suggest that the model suitably explains the input data (see Chapter A.2, p.238) in the Appendix for outputs exported from R).

5.3.1 Model evaluation

The minimal adequate model of WSW had an adjusted R^2 of 0.75, compared with a model using catchment area alone to predict WSW which had an adjusted R^2 of 0.46. Summary plots and statistics were generated for the MLR model using the *plot(modelname)*, *summary.lm*, and *summary.aov* commands in R (see R Core Team, 2017 for a description of each of these commands). Scatterplots of the residuals against each predictor in the model were also generated; no pattern was observed in any of these plots, confirming that the minimal adequate model was accurately representing a linear relationship.

However, one downside of the final model is that it used a number of datasets that only exist for the UK, and while a model with these removed would still not be generalisable beyond the UK due to WSW varying less than in other nations (i.e. the UK's widest river is substantially narrower than those found globally), and extrapolating beyond this width would be to misuse the model, the impact of removing these datasets was still a valuable exercise. Specifically, BFI and the RHS datasets were excluded, and the model run from the beginning using the same methodology as outlined above

(stepwise deletion of a single explanatory variable at a time). While it would have been far simpler to remove the remaining UK-specific variables from the final model discussed previously, the underlying relationships and interactions between the remaining explanatory variables would be different from the outset, changing the order of deletion and likely the form of this more generalisable minimal adequate model of WSW. The ability of catchment area to explain a significant proportion of variance in WSW meant that the new model performed well, with slope, rainfall, and relief also contributing (see Table 5.3.3), raising the question as to which model should be used for the national-scale prediction of WSW. While the omission of BFI and HMS from the predictive model shown below results in a reduction in the adjusted R^2, for example, the direct comparison of different models demands for more than a basic comparison of numerical values.

Table 5.3.3 Summary of multiple linear regression model of WSW with BFI and HMS excluded from process (n = 231)

Residuals:

Min	1Q	Median	3Q	Max
-7.89	-1.86	-0.85	1.33	8.43

Coefficients	**Estimate**	**Std. Error**	**t value**	**Pr(>t)[1]**
(Intercept)	6.76	0.44	3.91	<0.01
Max slope (local)	7.33e-01	1.03e-01	3.24	<0.01
Max slope (catchment)	1.17e+01	3.82	2.10	<0.01
Mean CA (km^2)	-1.48e-03	4.33e-05	-4.36	<0.01
Mean rainfall	-2.27e-02	0.83e-02	-2.21	<0.01
Mean slope (local)	-8.77e-01	0.23	-1.65	0.03
Mean slope (catchment)	-3.69e+01	3.42	-2.22	0.04
Mean catchment relief	3.41	0.76	2.17	0.03

[1]Probability of observing value equal to or larger than the t value

Residual standard error: 2.26 on 223 degrees of freedom
Multiple R-squared: 0.62
Adjusted R-squared: 0.60
F-statistic: 189.01 on 7 and 223 DF
p-value: < 2.2e-16

Each of the MLR models of WSW was compared using a diagnostic designed to select the most appropriate model, called the Akaike Information Criterion, or AIC (Schelker *et al.*, 2016). The AIC test penalises the inclusion of a greater number of model parameters, unlike R^2 or adjusted R^2 which are more liable to being inflated with the addition of further explanatory variables. Results are presented in Table 5.3.4, and demonstrated that the full model of WSW, inclusive of RHS and BFI, was the most appropriate for predicting WSW in England and Wales (lower AIC scores are preferable), although the model with BFI and HMS data removed outperformed the use of catchment area alone, revealing that the remaining explanatory variables enhance the predictive ability of the model. This remained the case despite the AIC test penalising the more complex models, suggesting that the inclusion of the additional variables was justified on the grounds that they made a genuine contribution to the model, and were not simply inflating the R^2.

Table 5.3.4 AIC diagnostics for selecting the most appropriate model for WSW prediction

Model	**AIC[1]**
Catchment area model	1888.16
Minimal adequate model	1747.91
Model with BFI and HMS data removed	1765.54

[1]Lower AIC value represents the most appropriate model

As this study was focused on the national scale from the outset, the inclusion of RHS and BFI as explanatory variables was justified. Nonetheless, the other models were demonstrably effective enough to raise the possibility of predicting WSW at the continental or global scale, dependent on the availability of appropriate remotely sensed imagery (see Section 7.2.4, p.192 for a discussion of possible approaches to global-scale WSW modelling).

In order to test the predictive capacity of the selected model, K-folds cross-validation was undertaken. This method splits data randomly into a user-defined number of subsets, or k-folds, of roughly equal size. One fold is reserved for model validation, while the chosen model (e.g. OLS MLR) is fit using all

other subsets (k - 1 folds). For example, in 10-fold cross-validation, nine subsets are used to fit the model, with the one remaining subset used for model validation. This process is repeated until each subset has acted as the validation dataset. Model accuracy is calculated using the mean prediction error from each model run. K-fold cross-validation is most frequently performed with k = 5 or k = 10 as these values do not tend to introduce high bias or high variance (James et al., 2013; Kuhn and Johnson, 2013).

10-fold cross-validation was performed for the minimal adequate model. The adjusted R^2 for the minimal adequate model was 0.75, with an RMSE of 1.14 m and a MAPE of 13.41%. The extent of error as expressed by the RMSE can be explained by the influence exerted by outliers displayed in Figure 5.3.1, which plots observed values of MEW against predicted values of MEW. Errors appear to be normally distributed overall, although where MEW is less than 30 m the model seems to over-predict values more frequently than not. Observed values, as discussed in Section 3.5.1 (p.87), are potentially impacted by the presence of overhanging vegetation, which would potentially cause over-prediction and the error represented by the RMSE and MAPE figures above.

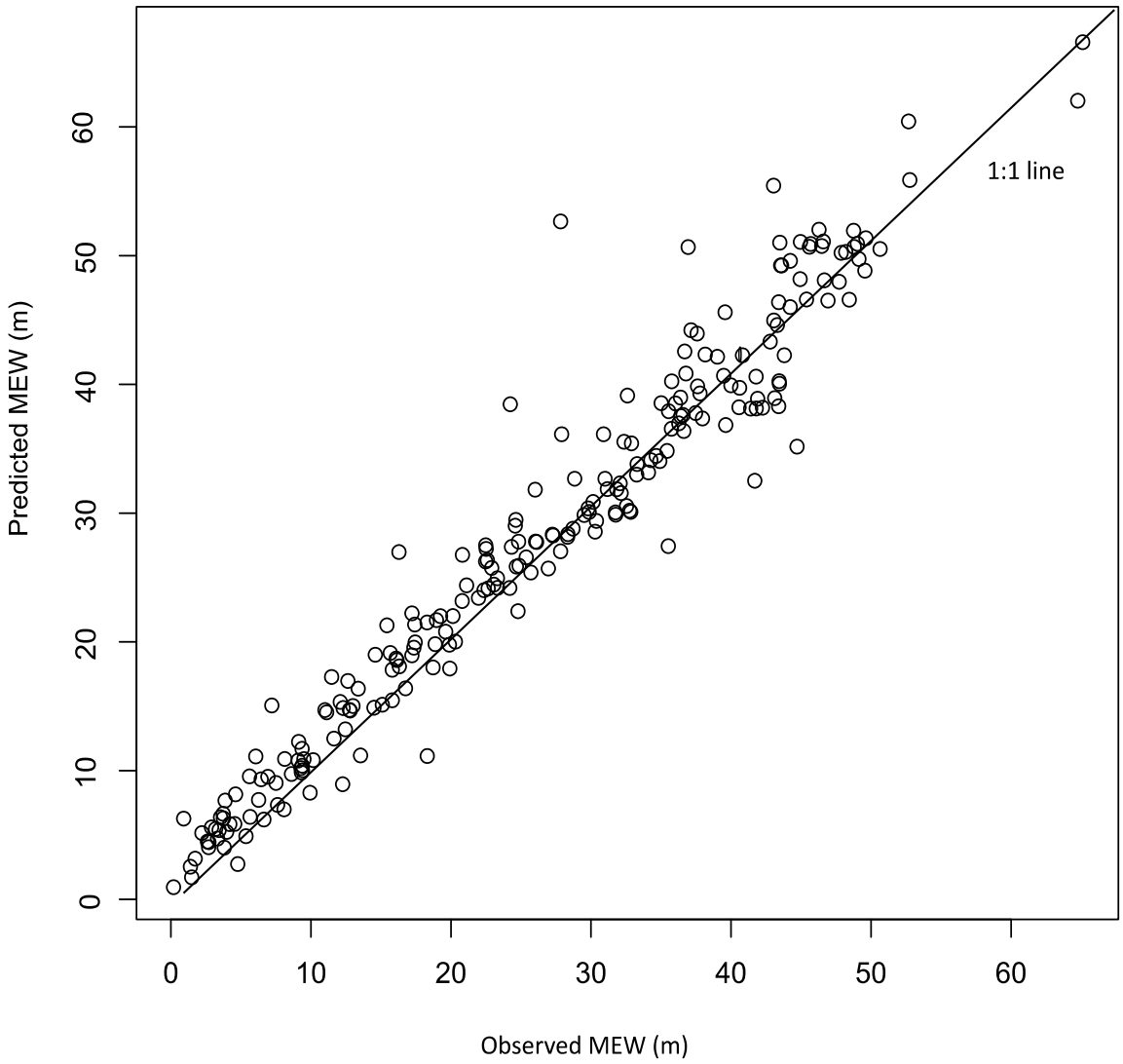


Figure 5.3.1 Comparison of observed and predicted values of MEW from the minimal adequate model (n – 237).

5.4 Critical reflections on MLR

In addition to quantitatively testing the MLR models, a more subjective assessment was made of their applicability. One potential issue identified was that when aggregating point values for selected explanatory variables to a single reach-scale value, the direction of flow was not considered (and could

not be due to the absence of this data). This is especially relevant for the HMS scores, as local scale river reconnaissance would arguably show a difference in the response upstream and downstream of a feature such as a weir (Sear *et al.*, 2010; Thorne, 1998a). Upstream, flow velocity is likely to be reduced, causing the deposition of sediment and channel narrowing. In the downstream direction, an initial increase in hydrodynamic turbulence as flow passes over the weir would cause channel deepening and lateral incision if the bed and banks are not protected, leading to an increase in WSW. This is a simplistic and purely theoretical account of highly dynamic processes, but one that illustrates the importance of flow direction. While GIS tools such as ArcHydro are capable of calculating flow direction, this generally relies on deriving a stream network from a DEM (ESRI, 2011), which would not intersect with the surface waters dataset extracted from the aerial imagery that was so significant in capturing the width of narrow headwater streams.

Secondly, a regression method capable of accounting for spatial variation could increase the predictive ability of the model. Geographically weighted regression (GWR) is a potential alternative to MLR that determines where locally-weighted regression coefficients diverge from their global values (Brunsdon *et al.*, 2010; Comber, 2013; Fotheringham *et al.*, 1997; Mennis, 2006). Initial analysis of the explanatory variables revealed clear spatial trends in rainfall and relief in particular across the study site, but GWR modelling failed to find any significant relationships, in part because some of this spatial variation is obscured and altered in the process of converting AAS measurements to reach averages, for example. A future analysis of GWR may pay dividends in producing a more effective predictive model of WSW, but only if the accuracy of AAS measurements can be improved by either accounting for or removing the influence of overhanging vegetation, for instance, which was the primary reason why measurements were aggregated.

An additional avenue that may yield further improvements to the model in future is the exploration of multivariate adaptive regression splines (MARS), a technique also known as ‘Earth’ in open source implementations. This is a non-parametric variant of regression analysis conceived by Jerome

Friedman (Friedman, 1991) that automatically models any interactions and nonlinearities between variables. The technique was not selected in this instance as a greater degree of manual control was preferred in light of certain interactions between the explanatory variables having a stronger theoretical basis for inclusion than others, but with a better understanding this alternative could be investigated in future.

5.5 Predictions for England and Wales

With the MLR model finalised, predictions of WSW for every IHU Section in England and Wales were made by extracting the required landscape variable data and aggregating to the reach scale (the IHU Sections dataset). Predicted WSW was then visualised to determine the spatial distribution of rivers and water resources in England and Wales. However, for the purposes of data visualisation, coarser spatial units were used, as there are more than 200,000 IHU Sections in England and Wales, but only 277 IHU Groups. In the process of aggregating IHU Sections to the IHU Group level, multiple metrics were derived. Presented below are the mean IHU Section WSW within each group (Figure 5.5.1), and the range in WSW within each group (Figure 5.5.2).

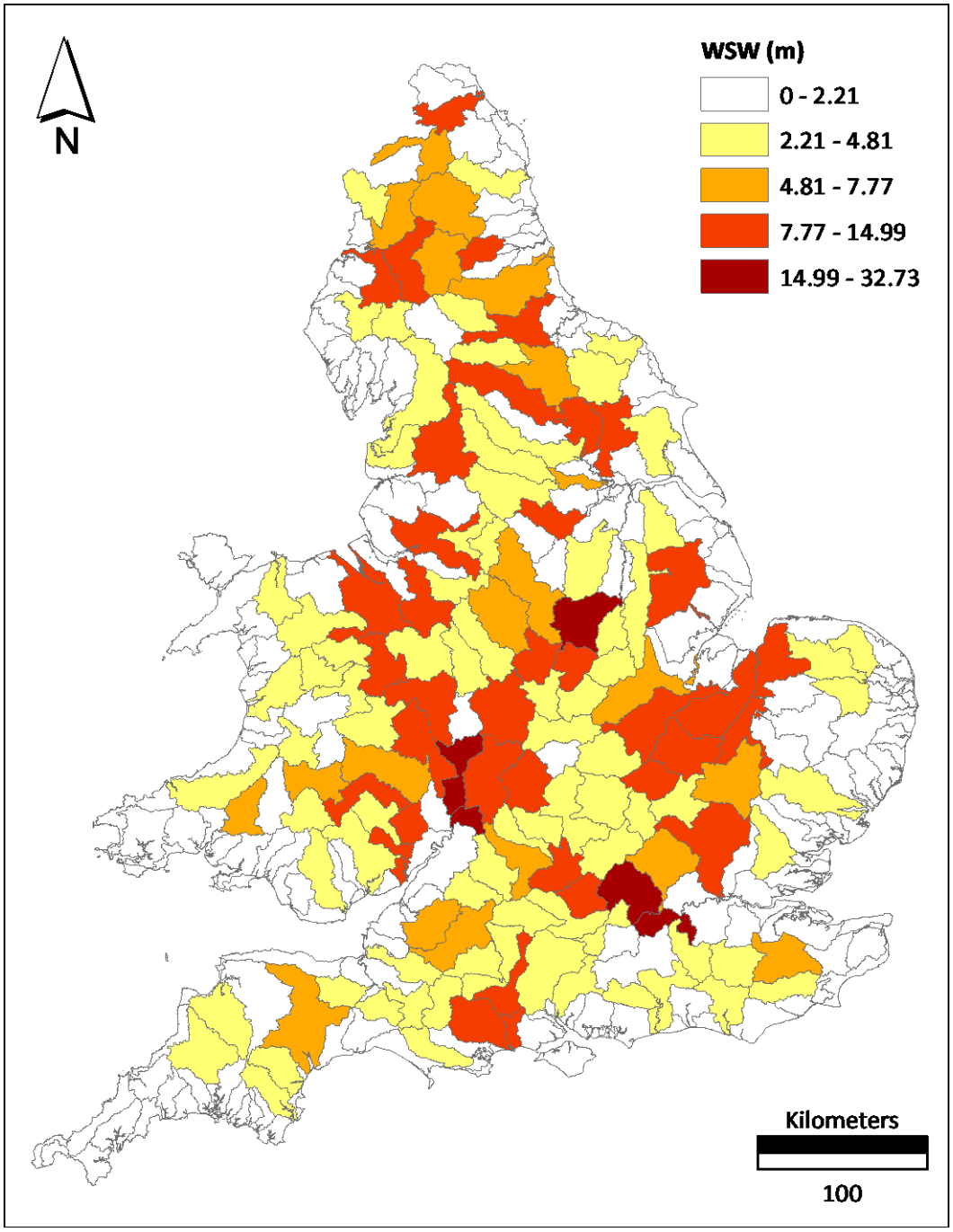


Figure 5.5.1 Predicted mean WSW in England and Wales (data visualised using IHU Group polygons and Jenks natural breaks).

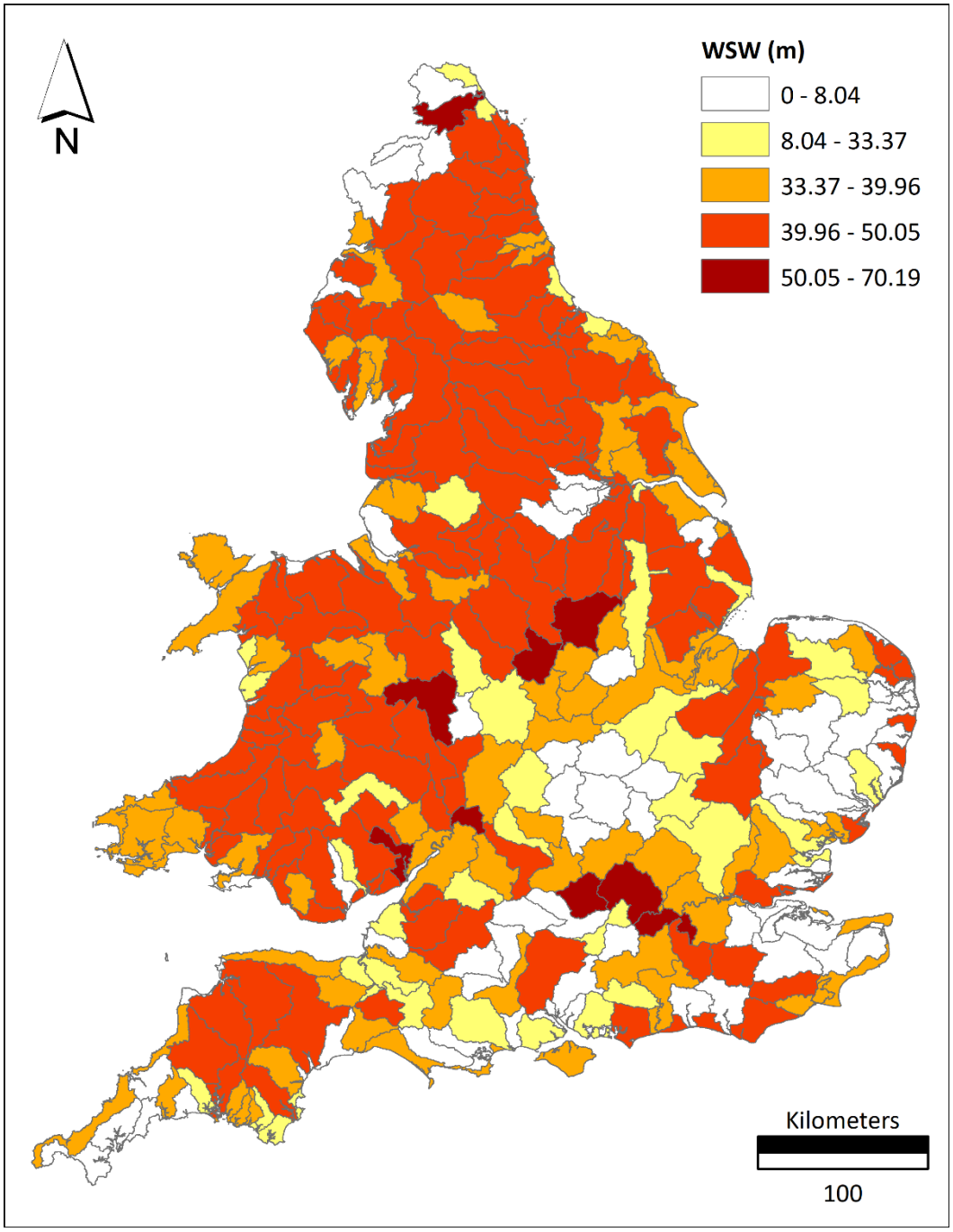


Figure 5.5.2 Predicted range in WSW in England and Wales (data visualised using IHU Group polygons and Jenks natural breaks).

Areas with the highest predicted mean WSW match closely with the three largest (in terms of length from source to mouth) rivers in England and Wales. Moving from north to south, the units shaded in

dark blue represent reaches of the River Trent, River Severn, and River Thames respectively. The general agreement between river length and mean WSW suggests that the model performs well, although it must be noted that these same rivers exhibit a comparatively low mean predicted WSW where they meet the sea. The likelihood is that there may be a number of IHU Sections within each of the IHU Groups that exhibit a significantly lower WSW, and by aggregating to the coarser scale the expected mean WSW of these long rivers has been averaged out.

The modal group is that representing the narrowest predicted mean WSW, which agrees with previous research (Downing *et al.*, 2012) that established the relative prevalence of narrow, low order rivers. The use of Jenks natural breaks to visualise classes has resulted in a classification of the data that matches closely with Downing *et al.*'s (2012) chosen threshold for low order rivers – 2.21 m and 1.8 m respectively – so IHU Group polygons belonging to the class shaded in yellow in Figure 5.5.1 can generally be stated to contain a high proportion of headwater streams. Due to the loss of granularity in using IHU Group polygons, IHU Section scale data were presented instead in Table 5.5.1, below, to elucidate the predicted size distribution of rivers in England and Wales.

For the range in reach-scale WSW within each IHU Group (Figure 5.5.2), the majority of spatial units exhibited a high degree of variation (between 39.96 m and 50.05 m). Once again, the three major rivers of England and Wales (in terms of length) dominate the widest WSW class. This suggests that the theory presented above that other sections of these same rivers that exhibit an unexpectedly low mean predicted WSW are affected by proximal IHU Sections containing much narrower rivers is generally correct.

Table 5.5.1 Size distribution of rivers in England and Wales as predicted by MLR WSW model

Stream order	WSW threshold[1] (m)	*n* in England and Wales[2]	Proportion of rivers in England and Wales (%; 2 dp)
1	0.8	170916	73.54
2	1.8	46537	20.02
3	3.7	12326	5.30
4	8.3	2441	1.05
5	29.3	111	0.05
6	73.3	74	0.03

[1]Stream order thresholds taken from Downing *et al.*, 2012, with those above stream order 6 omitted. [2]*n* represents the number of IHU Section polygons with a predicted width below the appropriate WSW threshold, independently of river length.

Table 5.5.1 shows the proportion of rivers in England and Wales belonging to each stream order as predicted by the WSW MLR model. Note that Downing *et al.*'s (2012) stream order thresholds were used in this study, but were not created to work explicitly with the maximum predicted width for a river reach (MEW), as this study calculates. Therefore, findings are necessarily tentative, yet still find general agreement with the literature in terms of 1st order streams being in the majority, and significantly so, as can be seen in Figure 5.5.1.

These WSW data were then analysed to determine the size distribution of rivers across England and Wales using parameters identified in the literature. The most comprehensive analysis of the relationship between stream order and WSW was undertaken by Downing *et al.* (2012), who combined a meta-analysis of figures published in previous studies with additional field measurements to derive descriptive statistics for each stream order, and most significantly, width thresholds for each. For instance, 1st order streams were thought to account for 52% of total river length globally despite having a mean width of just 0.8 m. When the same width thresholds were applied to the England and Wales predictions of WSW and multiplied by river length, 45% of rivers in England and Wales were classified as 1st order. This is not too dissimilar to the global mean, but is potentially an underprediction

based on the difficulty in capturing low-order rivers, as discussed previously; it is unlikely that all headwater streams have been captured in their entirety due to issues such as overhanging vegetation obscuring the aerial view of the river.

Globally, estimates for river water surface area vary, with examples including 485,000 km^2 (Lehner and Döll, 2004), 624,000 km^2 (Raymond *et al.*, 2013), 662,000 km^2 (Downing *et al.*, 2012), and 832,000 km^2 (Lauerwald *et al.*, 2015). This equates to 0.30–0.56% of Earth's land surface (Downing *et al.*, 2012). Using WSW predictions for every IHU Section in England and Wales and multiplying by the total river length of the OS VectorMap river network provided an estimate for England and Wales of 1012.74 km^2. When compared with a terrestrial surface area of 151,156 km^2 (calculated in ArcMap from the GB National Outlines dataset (Ordnance Survey, 2005)), river surface area accounted for 0.67% of the total terrestrial area of England and Wales. This is beyond the upper limit for the proportion of surface waters predicted by both Downing *et al.* (2012) and Lauerwald *et al.* (2015), but this is likely a legitimate deviation given the UK's temperate maritime climate likely resulting in a higher proportion of land surface area being covered by water relative to the global mean. Even so, it must be acknowledged that there are potential sources of error when calculating the estimate for England and Wales. For instance, the river network used to establish length at the national scale is likely to be incomplete, leading to underestimation. Conversely, the WSW model was parameterised using maximum WSW for defined river reaches (MEW), which meant that overestimation may have occurred, especially for IHU Sections covering a large area where river channel geomorphology varied considerably. The solution to this uncertainty is ultimately rooted in the need to better control for the influence of overhanging vegetation, as discussed in Section 3.5.1 (p.87), which would potentially remove or at least reduce the need for reach-aggregated measurements to be used in place of AAS cross-sectional measurements of WSW.

5.6 Chapter summary

This chapter has shown that: -

- Widely available landscape variables are capable of explaining 78% of variation in WSW.
- For data-poor regions, catchment area alone can explain just under 50% of variation in WSW and may be able to establish a useful benchmark.
- Human modification plays a small but significant role in predicting WSW at the reach scale; this is the first time that a metric directly quantifying this variable has been successfully applied to the prediction of WSW.
- There is an estimated water surface area of 1012.74 km^2 in England and Wales, which fits well within the context of previous global scale studies.

The WSW dataset produced by the methodology presented in this chapter was then used to calculate water surface area, a critical component of fluvial CO_2 evasion models as it is at the air-water interface that vertical transport to the atmosphere occurs. The next chapter details the process of creating a model for England and Wales in an effort to quantify the impact of WSW on the ability to accurately predict fluvial CO_2 evasion.

Chapter 6

Estimating fluvial CO_2 evasion in England and Wales

With a national dataset of reach-scale WSW produced, predictions of WSW were applied to the estimation of CO_2 evasion from rivers to the atmosphere in an effort to improve the parameterisation of national-scale CO_2 models, which currently use approximations of water surface area or coarse resolution datasets that fail to account for headwater streams. It is at this point that the national scale focus became most relevant, as previous studies tend to focus on field-based techniques applicable only at the local scale or on the estimation of global-scale fluxes. While studies have already attempted to address this gap in the research (Butman and Raymond, 2011; Rawlins *et al.*, 2014b), significant issues such as exhaustive dataset requirements or a high degree of uncertainty limit the viability of these efforts. Considering that it is at the national scale that climate change-related factors are most likely to be engaged with and potentially mitigated (Giddens, 2009; Turnpenny *et al.*, 2005), the need for further research is evident.

Critically, the methodological design of this study to this point was intended to address the need for improved models by specifically aiming to capture narrow headwaters, due to their significant contribution to CO_2 evasion. In fact, river–atmosphere efflux of CO_2 could be more than double previous estimates (Cole *et al.*, 2007; Cole and Caraco, 1998), CH_4 evasion 50% higher than recent assessments (Bastviken *et al.*, 2011), and N_2O emissions 20% higher (Beaulieu *et al.*, 2011), owing simply to the larger area that rivers and streams cover compared to those accounted for by published research.

The focus on CO_2 alone was due to the better-established theory regarding the controls of evasion, and the more common practice of measuring such variables in the field. For the UK, the availability of $K\mathrm{CO}_2$ data allowed for the creation of a model to estimate fluvial CO_2 evasion (see Section 6.2, p.153 for a description of these data).

6.1 Methods for calculating fluvial CO_2 evasion

The overall carbon mass balance can be simplified as shown in Equation 6.1 (Cole at al., 2007; Marx *et al.* 2017), with all factors represented in the same units (normally Pg C/yr):

$$I = G + S + A$$

I is carbon imported from the catchment

G is net carbon gas exchange between the stream and atmosphere

S is carbon storage in sediments and soils

A is losses due to runoff

Equation 6.1 Carbon mass balance; all units are the same (normally Pg C/yr)

Of these factors, both I and G are poorly understood (Marx *et al.*, 2017). G occurs predominately in the form of CO_2 evasion, although carbon is also lost to the atmosphere in the form of CH_4. In practice, G – represented henceforth as $F\mathrm{CO}_2$ – is estimated by calculating evasion from the gradient between fluvial CO_2 and atmospheric CO_2 (Lauerwald *et al.*, 2015: Marx *et al.*, 2017; Raymond *et al.*, 2012) as below in Equation 6.2.

$$F\mathrm{CO}_2 = WSA \times k \times \Delta\mathrm{CO}_2$$

WSA is river water surface area

k is the gas transfer velocity

$\Delta\mathrm{CO}_2$ is the gradient between fluvial CO_2 and atmospheric CO_2

Equation 6.2 Net carbon dioxide gas exchange ($F\mathrm{CO}_2$) between rivers and the atmosphere

Water surface area is the component that this study has attempted to estimate with as much accuracy as possible, by deriving a WSW dataset for England and Wales that was then combined with the more easily calculable river length parameter. $F\mathrm{CO}_2$ is driven primarily by discharge (Liu *et al.*, 2017; Marx *et al.*, 2017), but due to the low sampling resolution and siting bias of NRFA gauging stations across the UK – which directly measure discharge – water surface area is used as a proxy.

The remainder of the explanatory variables, while measurable at the local scale using field techniques such as the gas tracer method (Cole and Caraco, 1998; Marx *et al.*, 2017; Raymond and Cole, 2001; Wanninkhof *et al.*, 1990) or floating chambers (Dinsmore and Billett, 2008; Erkkilä *et al.*, 2017; Wallin *et al.*, 2011), are themselves commonly estimated using predictive models. For instance, $\Delta\mathrm{CO}_2$ is calculated using Equation 6.3. The fluvial $p\mathrm{CO}_2$ (partial pressure of CO_2) component of this model, in turn, is measured using statistical models that combine factors such as alkalinity, pH, and water temperature (Parkhurst and Appelo, 1999), using data from repositories such as the global river chemistry database (GloRiCh; Hartmann *et al.*, 2014), an approach documented by a number of recent

studies (Lauerwald *et al.*, 2015; Marx *et al.*, 2017; Raymond *et al.*, 2013). However, such studies tend to focus on the global scale, and even then encounter significant challenges in sourcing adequate data to produce reliable annual averages of $p\mathrm{CO}_2$ for use in predictive models. Consequently, this approach was not viable for a national scale study confined to England and Wales, necessitating a different technique.

$$\Delta\mathrm{CO}_2 = K\mathrm{CO}_2 \times (p\mathrm{CO}_2 - p\mathrm{CO}_{2\mathrm{atmos}})$$

$K\mathrm{CO}_2$ is the Henry's law constant

$p\mathrm{CO}_2$ is the partial pressure of CO_2 in rivers

$p\mathrm{CO}_{2\mathrm{atmos}}$ is the partial pressure of CO_2 in the atmosphere (assumed as being 390 µatm; Lauerwald *et al.*, 2015)

Equation 6.3 Gradient between fluvial CO_2 and atmospheric CO_2 ($\Delta\mathbf{CO_2}$)

An alternative is therefore required for the provision of the fluvial $p\mathrm{CO}_2$ component for this study, with previous research modelling the variable based on landscape predictors that can be derived for England and Wales. Precipitation affects CO_2 concentration in water by effectively limiting the proportion available to the evasion process (Rawlins *et al.*, 2014b; Smits *et al.*, 2017); slope (Lauerwald *et al.*, 2013; Smits *et al.*, 2017) controls carbon accumulation and the gas transfer velocity at the air-water interface; and ambient air temperature (Lauerwald *et al.*, 2013; Weyhenmeyer *et al.*, 2017) affects the gradient between the atmosphere and water. In England and Wales specifically, $p\mathrm{CO}_2$ has previously been calculated by Rawlins *et al.* (2014b). Their study identified slope, elevation, relief, and land cover class as significant explanatory variables of log $p\mathrm{CO}_2$ ($R^2 = 0.24$), allowing a dataset of $p\mathrm{CO}_2$ to be created for England and Wales that covers a greater geographical extent than would be possible by using GloRiCh, for example. What is immediately apparent is that the predictive ability of this model appears to be low, yet this is explained by the authors as indicative of the state of current knowledge

regarding the processes controlling $p\mathrm{CO}_2$ relative to the dynamism and variability in $p\mathrm{CO}_2$ in the real world, particularly seasonally. Similarly, Lauerwald *et al.* (2013) found that mean air temperature, mean catchment slope gradient, and mean annual precipitation accounted for 43% of the variation in the negative logarithm of mean $p\mathrm{CO}_2$, demonstrating that current models have plenty of room for improvement across the board.

$K\mathrm{CO}_2$ itself can also be modelled, with stream slope and stream width (including its standard deviation) the most significant predictors (R^2 = 0.52; Schelker *et al.*, 2016). However, field measurements were made available that removed the need to introduce further uncertainty by modelling another parameter (see Section 6.2 below for a description of these data).

For the model of CO_2 evasion created herein, $F\mathrm{CO}_2$ was converted to potential evasion by using, for the first time in England and Wales, water surface area data produced by multiplying model-derived WSW predictions with river length. This directly tested the substantial body of theory stipulating that the contact area between water and the atmosphere is a critical component of fluvial CO_2 evasion, as it is at this air-water interface that the vertical export of CO_2 occurs.

6.2 Field data for England and Wales

A total of 28 samples of $\boldsymbol{K\mathrm{CO}_2}$ were taken in the field between November 2013 and November 2015 (data collected and provided by the British Geological Survey). These are distributed across the UK (Figure 6.2.1) and include measurements taken within the study area in north Wales. A gas tracer method was used to determine the $K\mathrm{CO}_2$ values, a process documented by Schelker *et al.* (2016). The use of gas tracers is believed to be the most accurate method of determining the rate of evasion when compared with alternatives such as the floating chamber technique (Marx *et al.*, 2017), as the natural state of the river is disturbed to a minimal extent when used gas tracers.

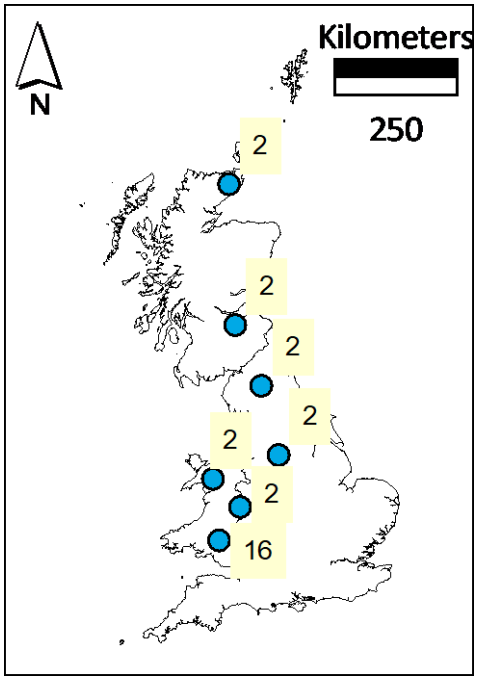


Figure 6.2.1 Location of $K\mathrm{CO}_2$ field measurements (n = 28).

A limitation of these data is that they only covered streams with widths ranging from 0.46 m to 1.64 m (mean = 1.006 m, n = 28), largely because the collection of water chemistry data required access to the middle of the stream, so practicality prevented wider rivers from being sampled. Furthermore, the established theory of headwater streams being the most significant sites of fluvial CO_2 evasion to the atmosphere likely played a role in the selection of field measurement locations. Furthermore, 16 measurements were taken at a single site, while the remaining 12 measurements were taken at 6 other locations. This reflects that there were two different rationales for collecting the measurements, namely an examination of site-specific $K\mathrm{CO}_2$ (16 measurements in south Wales), and an examination of headwaters across Great Britain (2 measurements at 6 separate headwaters upstream and downstream of a selected location). These factors presented a number of challenges, as the WSW model created previously was capable of predicting widths an order of magnitude greater than those present in the $K\mathrm{CO}_2$ dataset. The low number of measurements also presented issues in attempting to establish statistically significant relationships with the explanatory variables, although this is a

frequent problem as both pCO_2 and KCO_2 are poorly constrained in the majority of studies (Regnier *et al.*, 2013; Ward *et al.*, 2017), primarily due to the lack of available field data at present. Note that the sample size of 28 is for those collected in England and Wales; those displayed in Figure 6.2.1 as being available for Scotland have been excluded from this number, and indeed from the study, as river network data, and subsequently WSW measurements and predictions, were not available.

6.3 Model results

As with the WSW model, OLS MLR was again selected as the method of choice. This was because the majority of previous research attempting to model fluvial CO_2 evasion has applied this technique, not least because the physical processes that control the inputs and outputs of the carbon mass balance are generally poorly understood (Marx *et al.*, 2017). This prevented the application of more sophisticated techniques such as the numerous machine learning approaches, as the 'black box' nature of these methods was deemed counterintuitive given that there are potentially multiple explanatory variables and interactions that we cannot currently capture.

When applying the OLS MLR method, the same procedure was followed as described in Section 5.2 (p.127), which discussed the tests available for checking the assumptions inherent in MLR modelling. In the case of predicting fluvial CO_2 evasion for England and Wales, this process was repeated for a number of different approaches. Firstly, a 'full' model of CO_2 evasion was created that included all possible explanatory variables. Secondly, WSW was omitted to quantify the value of its inclusion as an explanatory variable, in order to directly test the objective of the study that aims to achieve the very same (see Section 1.2, p.5). Finally, two separate models were created that were constrained either spatially or temporally. For the former, reaches with a WSW greater than the upper limit sampled in the field when the KCO_2 data were collected – 1.64m – were omitted, resulting in the application of the 'full' CO_2 model to the prediction of evasion from low-order headwaters alone (see Table 6.3.1 for

full summary statistics of both WSW and $K\mathrm{CO}_2$ at the sample locations). This was to discover whether extrapolating beyond the upper limit of the known $K\mathrm{CO}_2$ values when predicting national-scale evasion undermined the model in any way, which could occur if the relationship between WSW and fluvial CO_2 evasion becomes non-linear in reality for rivers beyond a certain width, which were not captured during the collection of $K\mathrm{CO}_2$ data. For the second of the more constrained models, $K\mathrm{CO}_2$ data were omitted where they were collected in differing seasons to when the aerial imagery was captured ($K\mathrm{CO}_2$ was measured in summer, autumn, and winter; the aerial imagery is a static representation). Fluvial CO_2 evasion is dynamic and changes significantly both diurnally and seasonally (a limitation discussed in Section 7.2, p.183), yet the WSW predictions that were used to generate the water surface area component of the evasion model were made based on aerial imagery taken at a very specific point in time. It has already been shown that the imagery were representative of conditions below MDF, making it prudent to examine whether this limited the capability of the MLR model to predict CO_2 evasion based on $K\mathrm{CO}_2$ data gathered throughout the seasons.

Table 6.3.1 Summary statistics of WSW and $K\mathrm{CO}_2$ data used to model CO_2 evasion.

Variable	Mean	Median	Max	Min	SD
WSW (m)	1.01	0.96	1.64	0.46	0.31
$K\mathrm{CO}_2$	0.20	0.10	1.47	0.01	0.32

Finally, note that an assumption was made for all of the stated approaches; that all of the available dissolved $p\mathrm{CO}_2$ in the river had sufficient time to reach equilibrium with the atmosphere. This was based on the estimated timescale for equilibrium presented by Morel and Hering (1993), which is approximately 100 hours for large river systems. The water residence time for large rivers in England and Wales – the period of time that water is carried within the channel between source and mouth – is also approximately 100 hours (Rawlins *et al.*, 2014b), so this assumption, while also simplifying the MLR process and interpretation of results significantly, was justified by existing knowledge of the physical processes being modelled.

6.3.1 Full CO_2 evasion model

Before applying water surface area to the calculation of $F\mathrm{CO}_2$ (as in Equation 6.2), the gradient between fluvial CO_2 and atmospheric CO_2 ($\Delta\mathrm{CO}_2$), a required input to the $F\mathrm{CO}_2$ equation, was calculated using the approach documented in Rawlins *et al.* (2014b), who used slope, elevation, relief, and land cover class to calculate fluvial $p\mathrm{CO}_2$. The $K\mathrm{CO}_2$ data described in Section 6.2 (p.153) were then used in combination with atmospheric and fluvial $p\mathrm{CO}_2$ to produce $\Delta\mathrm{CO}_2$. For the final calculation of $F\mathrm{CO}_2$, WSW was used to calculate the water surface area component. Additionally, previous research was used to inform the choice of a gas transfer velocity (Beaulieu *et al.*, 2012; Borges *et al.*, 2004; Raymond and Cole, 2001). In combination, these three factors – water surface area, the gradient between fluvial and atmospheric CO_2, and the gas transfer velocity – were used to calculate $F\mathrm{CO}_2$.

To establish a baseline for comparison, the first model run included all available explanatory variables. Due to these being small in number – the result of both limited knowledge of the carbon mass balance at present and the unavailability of data pertaining to additional predictors of fluvial CO_2 evasion – the end result was that there were zero occurrences of multicollinearity. Further assumption testing confirmed that the OLS MLR model of fluvial CO_2 evasion could be executed without the need for further amendments. The model output is presented in Table 6.3.1, below:

Table 6.3.2 $F\mathrm{CO}_2$ model for England and Wales using water surface area (WSW) as an explanatory variable

Residuals:

Min	1Q	Median	3Q	Max
-7.55	-3.72	-2.67	3.10	10.46

Coefficients	Estimate	Std. Error	t value	Pr(>t)[1]
(Intercept)	3.31	2.33	5.89	0.03
Water surface area (m^2)	5.48e-9	5.32e-10	3.86	0.04
Gas transfer velocity (cm/hr)	0.04	0.02	4.44	0.04
Gradient between fluvial and atmospheric CO_2	3.86e-07	7.32e-08	5.21	0.35

[1]Probability of observing value equal to or larger than the t value

Residual standard error: 1.54 on 24 degrees of freedom
Multiple R-squared: 0.33
Adjusted R-squared: 0.31
F-statistic: 19.32 on 3 and 24 DF
p-value: 1.98e-4

A number of key observations can be made from the model output. Model residuals were not perfectly symmetrical, suggesting that the model predictions fall outside of the observed values. Tests for normal distribution were undertaken, and while far from perfect, the transformation of variables did not aid in significantly improving this. Meanwhile, the F-statistic (19.32) is generally expected to exceed the number of data points (28), yet in this case does not. This raises the question as to whether the null hypothesis can genuinely be rejected, yet the values for model coefficients are sufficiently far from 0 relative to standard error in general. 10-fold cross-validation was performed to validate the model (for a description of k-fold cross-validation, refer to Section 5.3.1, p.136), and the relatively large RMSE of 1.54 indicates that predicted values may diverge from observed values by a significant degree; evidently, a model that performs well would perhaps not indicate such a relationship, but the reality is that a number of explanatory variables and interactions may be missing from the $F\mathrm{CO}_2$ model, yet knowledge of the relevant physical processes in the real world is limited. The RMSE reflects this lack of knowledge. Finally, the influence of water surface area appears to be small, but the units of measurement – m^2 – are responsible for what initially appears to be a small value. The low standard error for water surface area relative to the estimated coefficient shows that for a given $F\mathrm{CO}_2$, water surface area varies comparatively little, suggesting that a clear relationship exists between water surface area and fluvial CO_2 evasion, although there are a number of caveats for this conclusion that are discussed below.

Overall, the adjusted-R^2 of 0.31 suggests a model that is not especially well parameterised or optimised, but in light of the complexity of the processes being modelled, the potential for the propagation of error from the predictive models used to derive inputs to the $F\mathrm{CO}_2$ model, and the small sample size of $K\mathrm{CO}_2$ field measurements, this was perhaps to be expected. Furthermore,

previous models have exhibited comparably low figures, with Rawlins *et al.* (2014b) reporting that their model accounted for 24% of spatial and temporal variation in $F\mathrm{CO}_2$. While direct comparison is problematic due to the differing nature of the models – that created herein used reach-averaged WSW measurements to derive water surface area – this is indicative that the result achieved here is not abnormally low. This also reflects the reality that current knowledge of the processes governing fluvial CO_2 evasion is incomplete.

The model of $F\mathrm{CO}_2$ could be improved by expanding upon the subsidiary models used to generate the water surface area and gas transfer velocity models respectively. The former is discussed throughout this study, yet the latter is equally relevant. An examination into improving the parameterisation of the gas transfer velocity model was beyond the remit of this study – the focus was entirely on meeting the need for WSW measurements that could generate the water surface area component, as it was comparatively poorly represented, especially in England and Wales – yet could equally yield an overall improvement in our understanding fluvial CO_2 evasion.

The statistical significance of the gas transfer velocity is in itself an important finding, and corroborates previous research. However, the successful inclusion of water surface area – derived from WSW – is arguably the most important finding of the $F\mathrm{CO}_2$ modelling process. This is perhaps a given, as it has already been established that the surface area of water in contact with the atmosphere is where evasion takes place, hence an increase or decrease in area has an impact. However, the importance of water surface area to fluvial CO_2 evasion in England and Wales has not previously been quantified. Ultimately, the objective of this study was not to simply generate another prediction of CO_2 evasion for England and Wales – although corroborating or challenging previous findings is in itself a valuable exercise – but to clarify the potential role of WSW in accounting for variation in evasion. In order to achieve this, a second model with water surface area removed was created to quantify the impact of this component on the overall predictive ability of the model.

6.3.2 CO_2 evasion model with water surface area removed

Table 6.3.3 FCO_2 model for England and Wales with water surface area excluded from initial variable selection

Residuals:

Min	1Q	Median	3Q	Max
-8.82	-4.79	-2.07	4.27	9.66

Coefficients	Estimate	Std. Error	t value	Pr(>t)[1]
(Intercept)	4.52	2.72	6.69	0.04
Gas transfer velocity (cm/hr)	0.09	0.08	3.43	0.04
Gradient between fluvial and atmospheric CO_2	4.62e-07	7.35e-08	5.73	0.23

[1]Probability of observing value equal to or larger than the t value

Residual standard error: 3.49 on 25 degrees of freedom
Multiple R-squared: 0.25
Adjusted R-squared: 0.24
F-statistic: 12.75 on 2 and 25 DF
p-value: 0.37e-1

Assumptions were tested once again before commencing with the model, as removing explanatory variables can alter the resonance between those that remain. In this case however, all assumptions were met. With a resultant adjusted-R^2 of 0.24, removing water surface area had an impact on the goodness of fit of the MLR model and the consequent ability to predict CO_2 evasion with precision. The increase in uncertainty that this reduced model exhibits is a clear indication that WSW is an important predictor at the national scale for England and Wales and offers an improvement in predictive ability over that achieved by previous efforts for England and Wales. While this conclusion is necessarily caveated by the reality that the relationship between water surface area and fluvial CO_2 evasion requires further investigation, not least in terms of collecting additional KCO_2 data to confirm whether the relationship is indeed linear beyond a certain limit, the findings described above are a good foundation upon which future research can build. The collection of data for additional explanatory variables for fluvial CO_2 evasion, such as pH and turbidity, would also aid in clarifying the true importance of water surface area by contextualising it among a more comprehensive set of factors, as it cannot currently be said with any certainty whether water surface area is the single most

important variable, or if others make a more significant contribution within the context of fluvial CO_2 evasion in England and Wales.

6.3.3 Constraining CO_2 evasion both spatially and temporally

Due to the nature of the available data, specifically that only narrow rivers were sampled in the field and that measurements were taken in three different seasons, the full model (inclusive of WSW) was adapted to restrict the analysis spatially and temporally respectively. However, the latter of these efforts at ensuring model validity resulted in statistically non-significant results, as shown below in Table 6.3.4.

Table 6.3.4 FCO_2 model for England and Wales constrained for seasonality

Residuals:

Min	1Q	Median	3Q	Max
-11.03	-5.39	-2.33	3.04	14.64

Coefficients	Estimate	Std. Error	t value	Pr(>t)[1]
(Intercept)	5.35	3.93	1.79	0.85
Water surface area (m^2)	0.02	0.53	1.53	0.60
Gas transfer velocity (cm/hr)	0.04	0.22	0.73	0.42
Gradient between fluvial and atmospheric CO_2	5.96e-07	10.11e-08	2.12	0.66

[1]Probability of observing value equal to or larger than the t value

Residual standard error: 8.79 on 4 degrees of freedom
Multiple R-squared: 0.10
Adjusted R-squared: 0.09
F-statistic: 9.32 on 3 and 4 DF
p-value: 0.47

The seasonal dynamics of CO_2 evasion are complex, because despite in-stream concentrations being higher in the summer months in England and Wales due to rainfall-driven winter flows leading to dilution, evasion is driven primarily by discharge, so is therefore lower in drier summer months (Liu *et al.*, 2017; Rawlins *et al.*, 2014b). In contrast, WSW measurements were taken from a single image (see Section 7.2.1, p.183 for an extensive discussion of this issue and its impacts on the study as a whole); consequently, the application of KCO_2 data collected in different seasons to these measurements was

counterintuitive. However, due to the already small sample size (n = 28), limiting the $K\mathrm{CO}_2$ dataset to only those measurements collected within three months of the CIR image acquisition date – to control for seasonality – resulted in a sample of only 8 measurements. It is therefore not surprising that the trend in the data is not strong enough to produce statistically significant results, the solution being to either accept the overall model of evasion described above or to collect significantly more field data (see Section 7.2, p.183 for future recommendations). This was also the case when expanding the selection of measurements to a greater number of months.

However, in the case of constraining the analysis spatially, this was achieved not by reparameterising the model, but by applying it only to river reaches where MEW was less than the maximum sampled width during the collection of $K\mathrm{CO}_2$ field data. This was undertaken to reflect the inherent danger in extrapolating beyond the upper limit of the observed data, with results visualised in Section 6.4 (p.164).

6.3.4 Model comparison

In order to determine the importance of WSW to the new model of potential fluvial CO_2 evasion, a second model was created that excluded WSW as an explanatory variable. Akaike Information Criterion, or AIC (Schelker *et al.*, 2016), was calculated for the models. This allowed for a more advanced analysis of the models that moved beyond a comparison of the R^2 by penalising models where explanatory variables were added.

Table 6.3.5 Fluvial CO2 evasion model comparison of R^2, adjusted-R^2, and AIC

Model	No. of $K\mathrm{CO}_2$ samples	R^2	Adjusted-R^2	AIC
Full	28	0.33	0.31	1245.56
Full – WSA removed	28	0.25	0.24	1515.87
Seasonally constrained	8	N/A[1]	N/A[1]	1647.14

[1]Model was not statistically significant

The full model above exhibits the strongest outcomes across the range of analytics, with the highest R^2 and adjusted- R^2, and the lowest AIC. The latter suggests that the addition of explanatory variables – in this case water surface area, derived from WSW – made a genuine contribution to the model and achieved more than an artificial inflation of model R^2. Furthermore, Fisher's z-score test, or *R* to *Z* transformation, was undertaken on the full model and the model with water surface area removed so that the model z-scores could be compared and the significance of the difference calculated. The result was a *Z* of 2.4175, significant at the 0.05 level, so it can be stated that the two models – despite the presence of overlapping confidence intervals – are significantly different.

Further comparisons were attempted with a model that was constrained for both the maximum limit of WSW sampled while measuring $K\mathrm{CO}_2$ and seasonality, but the low sample size to begin with (n = 28) resulted in statistically non-significant relationships once the sample was reduced further. Additional field data are required to clarify whether this outcome is the result of sample size alone, or if there is genuine difficulty in modelling the dynamism of CO_2 evasion in such a constrained manner. The long-term viability of the statistical models to produce accurate estimates of CO_2 evasion must also be assessed. One predicted consequence of climate change, for example, is an increase of 30% in outgassing of CO_2 from rivers due to increased flooding (Langerwisch *et al.*, 2016), which could change the nature of the statistical relationships within the current models. The greatest challenge here, in addition to the uncertainty inherent in projecting future change, is that knowledge of the carbon mass balance in the fluvial environment is incomplete (Marx *et al.*, 2017), meaning that critical components may be missing from the model.

However, while it is evident that significant research is needed in this area, this study of England and Wales has nonetheless aided in clarifying previously observed trends and moving knowledge forwards. Most significantly, the application of WSW had a clear impact on the ability to predict CO_2 evasion at the reach scale. This expands on the body of research that previously determined that discharge is the dominant component of this process (Liu *et al.*, 2017), providing a more easily quantifiable but

statistically related measure that can be used as an alternative in investigations where extensive gauging station data are not available, which is likely to be the majority of studies outside of the US and a small number of other nations.

6.4 Spatial distribution of CO_2 evasion across England and Wales

With the model of fluvial CO_2 evasion inclusive of water surface area as an explanatory variable selected for use, national-scale evasion was predicted for England and Wales. This produced a figure of 74.6 kt C/yr, greater than a previous estimate of 65.4 kt C/yr (Rawlins *et al.* 2014b). However, the confidence intervals of the two estimates overlap - lower and upper 95% confidence intervals of 63.5 kt C and 85.7 kt C for this study and 56.1 kt C and 77.2 kt C for Rawlins et al. (2014b) respectively – so it cannot be stated that the predictions differ due to the potential uncertainties in each model. However, on balance of probability, CO_2 evasion is likely to be higher than the previous estimate, supported by the outcome of Fisher's z-score test. This is due to the new model's ability to account for water surface area, which plays a crucial role due to the proportion of surface water in contact with the atmosphere being the interface at which CO_2 transfer occurs.

Figure 6.4.1 disaggregates the aforementioned value spatially across England and Wales at the IHU Group level, and largely supports previous findings that CO_2 concentrations tend to decline as catchment area increases (Butman and Raymond, 2011; Rawlins *et al.*, 2014b). However, a significant caveat is that the displayed spatial trends do not account for temporal variation, and are based on field data for which the upper WSW limit is an order of magnitude lower than that being modelled.

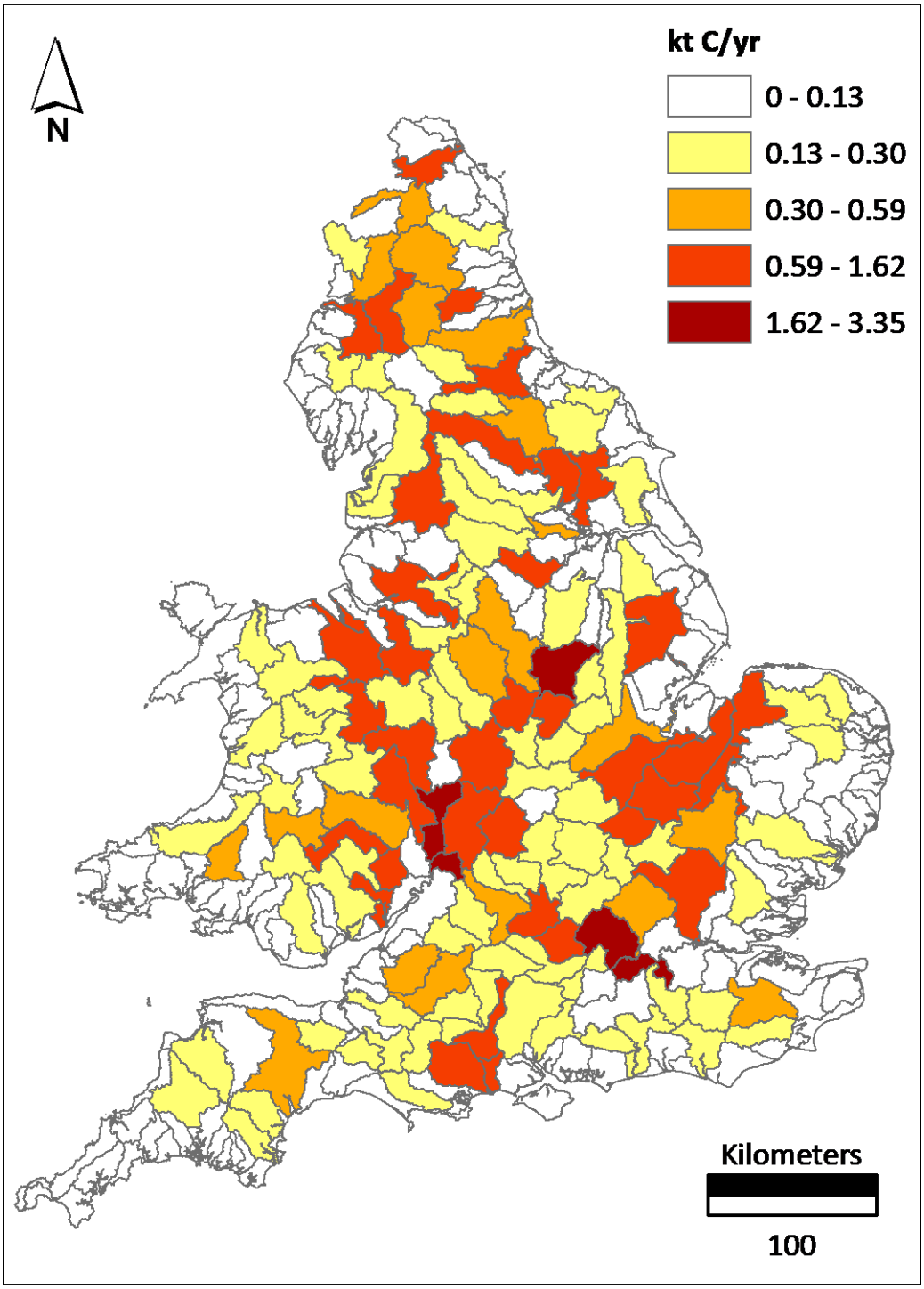


Figure 6.4.1 Predicted total CO_2 evasion in England and Wales (data visualised using IHU Group polygons and Jenks natural breaks)

There does not appear to be an especially strong spatial trend in terms of an east-west gradient across the country, which contrasts with the findings of Rawlins *et al.* (2014b) who note a higher concentration of fluvial CO_2 in the east. However, this difference can be explained for two reasons; i)

Rawlins *et al.* (2014b) consider seasonal differences in CO_2 concentrations, an approach that was unsuccessful in this study; and ii) water surface area, derived from WSW, has been included in the fluvial CO_2 model generated in this study. The latter point is especially apparent when visually comparing Figure 6.4.1 with Figure 5.5.1 (the spatial distribution of WSW across England and Wales), with clear similarities existing, particularly in terms of areas of higher WSW values matching areas of greater fluvial CO_2 evasion. The similarity suggests that the spatial distribution in fluvial CO_2 evasion observable in Figure 6.4.1 is due to the influence exerted on model output by the water surface area explanatory variable. In combination with the verification of the model from which the above figure was derived, it can tentatively be suggested that WSW is capable of improving the performance of fluvial CO_2 evasion models, yet due to a number of caveats and limitations outlined previously and in Section 7.1.4 (p.179), significant future research is required to establish the legitimacy and accuracy of this observation.

Predicting CO_2 evasion with the model that excluded WSW (described in Section 6.3.2, p.160) produced the spatial distribution visualised in Figure 6.4.2. In comparison with Figure 6.4.1, coastal areas exhibit a greater range in values, caused by the removal of WSW measurements that are likely to exhibit a greater degree of inaccuracy in coastal areas due to the IHU data used in this study only including freshwater reaches. Further research is required into both of the models used to produce estimates of national-scale CO_2 evasion visualised in this chapter.

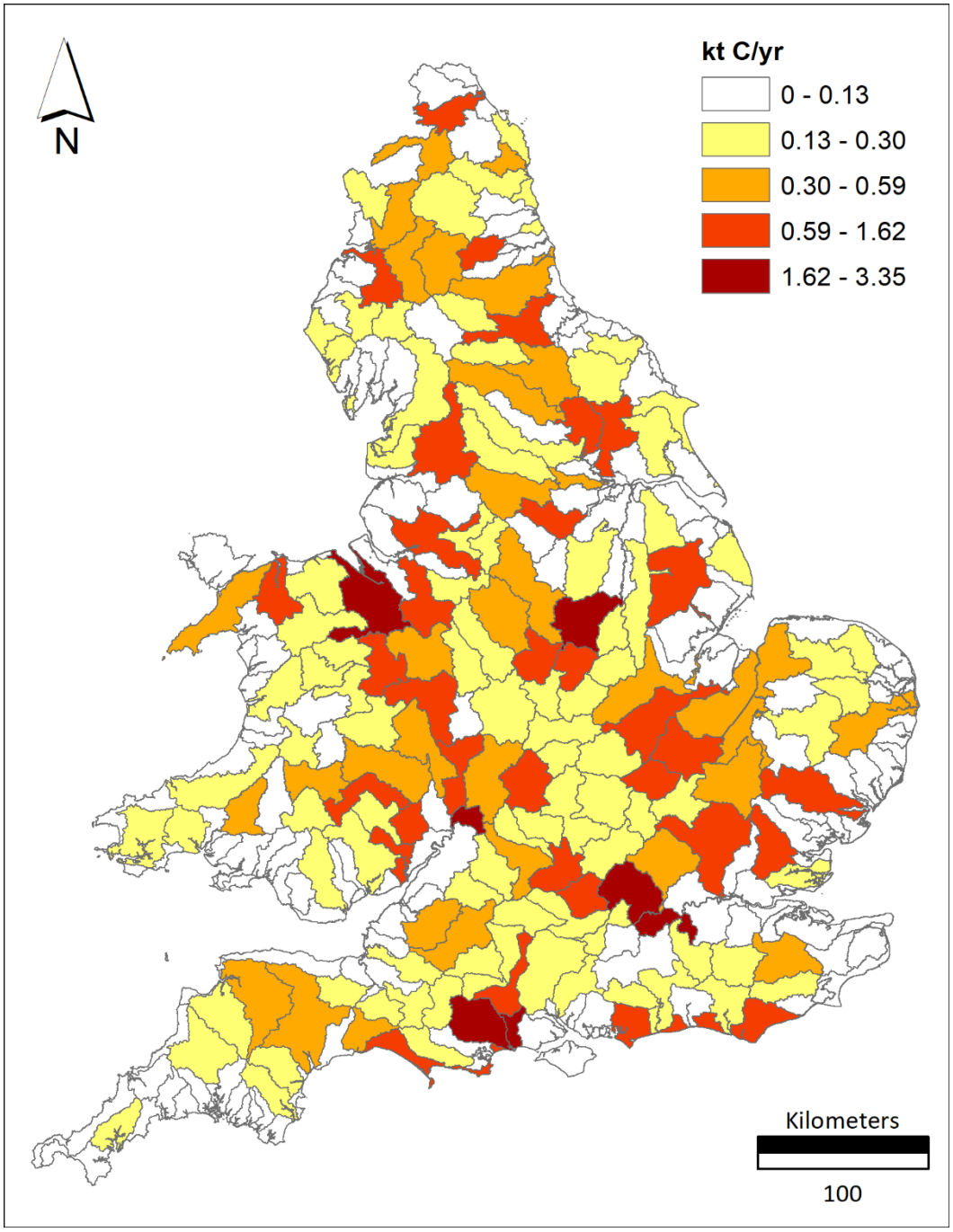


Figure 6.4.2 Predicted total CO2 evasion in England and Wales (data visualised using IHU Group polygons and the same class breaks as Figure 6.4.1 to aid with direct comparison)

6.5 Chapter summary

This chapter has shown that: -

- For England and Wales, there is a potential predicted fluvial CO_2 evasion of 74.6 kt C/yr, higher than a previous estimate of 65.4 kt C/yr (Rawlins *et al.*, 2014b). While it cannot be stated that the estimates differ due to the confidence intervals overlapping, the likelihood is that the new estimate exceeds the previous figure.
- The addition of water surface area, derived from WSW, improved the ability to model evasion at the national scale for England and Wales.
- Model parameterisation could be further improved by expanding on the limited field data currently available, including the predictors of fluvial CO_2 evasion such as discharge, pH, conductivity, and alkalinity, in addition to $K\mathrm{CO}_2$ – the gas transfer coefficient – measurable using gas tracers and the floating chamber method.
- The limited sample of field measurements of $K\mathrm{CO}_2$ is a key area requiring improvement in future, both because the observed relationships require corroboration and confidence with the predictive model is currently limited to headwater streams. Their importance cannot be understated, but failing to account for evasion from wider rivers provides an incomplete and uncertain picture of national-scale transfer to the atmosphere.

The completion of work towards meeting the final aim and related objectives, as discussed in this chapter, marked the end of the methodological part of this study. Following is a discussion of the key themes and findings from the research, alongside recommendations for future work informed by the challenges and opportunities faced throughout the research process.

Chapter 7
Discussion

Through the course of the research, a number of key findings were established. This chapter presents these, alongside a final assessment of each of the stated aims and objectives, synthesising the findings from each chapter. Furthermore, key recommendations for future research are made with the aim of corroborating and consolidating the research findings found herein.

7.1 An assessment of study aims and objectives

7.1.1 Aim 1: Extract a high-resolution dataset of rivers and streams from aerial imagery for the chosen study area.

The first aim of the study was devised to address the primary barrier to applying WSW measurements to national-scale applications in England and Wales: the lack of a suitable WSW dataset. The fitness-for-purpose of existing surface water data, whether directly related to river WSW or capable of being used as the basis for these measurements, was judged chiefly against the requirement to capture

rivers and streams at below MDF. As discussed in Rawlins *et al.* (2014a), high magnitude flows resulting from heavy rainfall skew the mean, so that it does not represent what could be considered 'typical' flow conditions. Due to the WSW measurements forming the basis of all subsequent analyses, capturing a non-biased representation of rivers and streams was paramount. Combined with the lack of such a dataset – OS maps represent rivers at their maximum winter extent, for example, and display rivers that are narrower than 5 m with a single line rather than a polygon (Ordnance Survey, 2016a, 2016b) – it was immediately clear that a new method for WSW measurement had to be devised. The extraction of rivers from high-resolution aerial imagery – from which measurements could then be taken – was identified as the preferred approach within the context established by the literature review, particularly that narrower streams are both underrepresented and disproportionately important to processes such as CO_2 evasion.

However, a number of different imagery classification techniques exist that were capable of meeting the stated aim. Therefore, a comparative analysis was undertaken to elucidate which technique, or combination thereof, was capable of delivering a high-resolution representation of rivers and streams. The result was that a novel combination of OCC, fuzzy classification, and contouring was the most effective, with the advantages offered by each technique making a clear contribution. For instance, OCC was established by previous studies as significantly reducing resource requirements (Li and Guo, 2010; Pal and Foody, 2012) while improving accuracy when targeting a single class of interest (Silva *et al.*, 2017), so with this study focusing on surface waters alone it came as little surprise that OCC was beneficial. Meanwhile, fuzzy classification and contouring used in tandem allowed for the already high resolution of the aerial imagery to be further enhanced, by allowing the class boundary between water and non-water pixels to pass through, rather than around the boundary of, individual pixels. In doing so, streams narrower than the image spatial resolution were captured (see Section 4.3, p.106), directly addressing the first objective towards meeting the overall aim.

However, the use of the combination of the approaches discussed above was not without its problems. One factor that limited the effectiveness of the above techniques, even when applied to high resolution imagery, is the reality that a number of features obscured the true extent of water either spectrally or spatially. For example, while the use of CIR imagery was beneficial in enhancing the contrast between rivers and the majority of other land cover classes, it did not allow for the spectral separation of surface waters from shadow and concrete surfaces. This resulted in widespread errors of commission that required rigorous post-processing in a GIS to limit (Section 4.1, p.96), and while the technique was ultimately beneficial, errors were not completely eradicated, so WSW is likely to have been overestimated in locations where shadow and concrete are contiguous with surface waters, because post-processing involved the use of a buffer within which all features classified as surface waters were maintained in order to preserve areas that had been correctly identified. This was a necessary compromise, but is something that may be addressed in future research with the use of additional wavebands that are capable of separating water and concrete surface features (e.g. Landsat-8 SWIR bands were used by Malahlela (2016) alongside RGB and NIR bands), or the application of shadow removal techniques (Adeline *et al*., 2013; Filippi and Güneralp, 2013).

Secondly, when considering the factors that limited the ability to extract a representative dataset of WSW from the CIR imagery, one issue in particular was a persistent problem. The influence of overhanging vegetation, as highlighted on numerous occasions in previous chapters, was arguably the most significant barrier that this research faced. Quite simply, the ability to accurately measure or predict WSW is made impossible when the full extent of the river is not visible. Therefore, an approach to account for or exclude this influence was required to ensure WSW measurements and predictions were reliable and representative.

To accomplish this, the study both excluded reaches where >50% of cross-sectional width was obscured, and used MEW for a river reach in place of AAS measurements of WSW. The former was achieved by identifying points along a geometric centreline at which WSW was subsequently measured, so if vegetation obscured more than half of cross-sectional width, based on OS data which

used the maximum winter extent of surface waters (Ordnance Survey 2016a, 2016b), then a centreline was not created in the first instance. For the latter, the influence of overhanging vegetation where <50% of cross-sectional width was covered had to be accounted for to improve the predictive ability of the MLR model created to meet the third aim of the study. The theoretical basis for using MEW was that instead of using multiple AAS measurements of WSW, many of which could individually be affected by overhanging vegetation, a single measurement for a river reach would be less likely to introduce error into the model. Maximum width was chosen over mean width for similar reasons, as the aggregation of multiple WSW measurements, each potentially affected by overhanging vegetation, would produce a mean value unrepresentative of real-world conditions, whereas selecting the single greatest value minimised this risk.

Gap filling is a potential solution where overhanging vegetation is present for a limited length of the rivers reach and for channels with simple planforms, but the assumption of a straight line between the sections of 'known' WSW is unlikely to fully represent true width, particularly where variation in WSW is naturally high due to poor bank cohesion, for example. Moreover, the gap filling method would require an exhaustive dataset identifying all locations where overhanging vegetation is present in order to avoid the 'correction' of channel sections where high width variability occurs naturally, for example due to the presence of a boulder at the edge of the channel that is resistant to erosion. If such a dataset existed or was simple to derive from the available data then this could be used to exclude these areas entirely, rendering gap-filling unnecessary.

It was also found to be extremely difficult to incorporate the presence of overhanging vegetation into the model. The presence of trees, particularly those that have reached the age of maturity for the particular species, is likely to impede the aerial view of the river to a greater degree than a sapling or grasses would, assuming that the vegetation is positioned in the same location. This suggests that species data could potentially be used to quantify the potential impact of riparian vegetation on width. However, this is a broad generalisation that is extremely difficult to represent adequately for modelling purposes, and is hugely impractical for a study site as extensive as that used in this thesis.

Furthermore, and most significantly, the measurement approach and predictive model are designed to address *real-world* WSW rather than simply WSW as visible from the air, so attempting to 'explain' WSW as a function of a factor that prevents the accurate measurement of width in the first place is hugely contradictory. Thus, the exclusion of affected reaches as carried out in this study, in lieu of the availability of LiDAR data for example (see Section 7.2.3, p.187), is arguably the most appropriate approach to the problem of overhanging vegetation.

Overall, despite encountering a number of difficulties, the overall aim of extracting a high-resolution dataset of rivers and streams for a representative study site in England and Wales was achieved. The combination of complementary image classification techniques, supported with subsequent post-processing GIS techniques, later allowed for accurate WSW measurements to be derived, which is the focus of the second study aim.

7.1.2 Aim 2: Make accurate, direct image-based measurements of WSW using a GIS-driven technique

Building upon the previous results, this aim was designed to establish best practice for exploiting the high-resolution surface waters dataset in order to take WSW measurements directly from the extracted features. The use of widely available techniques was preferred when working towards this aim so that the approach designed could be easily repeated both in other locations and to monitor changes in WSW over time. This was achieved by combining existing ArcGIS functionality, which took advantage of the extensive body of training and support resources available for the tools used to expedite the measurement process, while also delivering sufficiently accurate image-based measurements.

Accuracy was judged primarily by validating measurements derived from the imagery with those taken in the field. For this purpose, the measurement strategy was intentionally biased towards only measuring rivers contained within heavily modified channels, identified using the RHS dataset (Environment Agency, 2010a; Raven *et al.*, 1998, 2010). The theoretical underpinnings of this choice

were that both natural and anthropogenic factors were likely to have altered channel geomorphology in the years between the capturing of the CIR aerial imagery from which WSW was measured and the undertaking of field validation. Hence, WSW itself could have changed even when observing flow conditions in the field that were identical to those present when the aerial imagery was captured, established by comparing the available NRFA flow data for both periods. For this reason, the selection of modified river channels with stable banks was necessary to allow for any observed differences in image-based and field measurements of WSW to be attributed to potential flaws in the image measurements process designed in this study, rather than simply natural variation in WSW caused by channel geomorphology alterations. While few examples could be found in the literature that explicitly stated that a similar strategy was used, the lack of a viable alternative when collecting non-simultaneous measurements, and the application of a comparable approach to field validation by one especially relevant paper (Fisher *et al.* 2013) was felt to be enough justification to proceed.

The outcome of field validation was that the image-based measurements were found to offer a high degree of accuracy (RMSE = 0.87m, MAPE = 11.17%), with the highest magnitude differences explainable by the presence of factors such as overhanging vegetation and floating debris in the field. Despite this, the overall level of accuracy was largely unaffected. However, the comparatively low sample size of field measurements (n = 51) and the relative lack of measurements in the west of the study site, where lower-order streams are more prevalent, are aspects in clear need of improvement. The latter can be explained both by practical issues involving terrain that is harder to navigate in Snowdonia National Park and the surrounding region limiting the number of measurements able to be collected in the time available, and the sampling strategy that targeted modified channels, which are more prevalent in the more urbanised areas in the study site, which lie to the east.

Overall, the GIS-based image measurement technique met the aim of providing accurate measurements of WSW within the context of needing to capture low order streams. However, the labour-intensive nature of the process meant that the technique was not easily scalable, necessitating

the use of a predictive model for the provision of WSW measurements at the national scale for England and Wales.

7.1.3 Aim 3: Create a model capable of accurately predicting WSW for England and Wales

The third research aim was designed in recognition of the labour-intensive nature of the remote sensing and GIS-driven methodologies used previously to derive WSW measurements directly from remotely sensed imagery, with a view to upscaling the WSW dataset from the study site to the entirety of England and Wales, thus allowing for applications such as fluvial CO_2 evasion estimation at the same scale. It is important to emphasise that depending on future developments in areas such as the cost of high-resolution, sub-metre remotely sensed imagery (to aid in capturing headwaters), the availability of computational resources, and the potential for direct image-based measurements to be automated to a greater extent, the use of a model to deliver estimated WSW measurements for England and Wales may not be necessary. However, during the period in which this research was carried out, image-based measurement was not viable at the scale, necessitating an alternative. In this case, OLS MLR was selected as the favoured method as it struck a good compromise between simplicity – allowing the model to be more easily transferred and used by others – and predictive ability, while also allowing for the controls of WSW to be better understood for England and Wales.

After formulating a model of WSW through an investigation of a number of possible explanatory variables, as highlighted by previous research (see Section 2.3, p.21), a number of key findings came about. In terms of the overall predictive ability of the minimal adequate model, an adjusted R^2 of 0.75 compares well with previous findings (Rawlins *et al.*, 2014a) and proved to be sufficiently accurate enough to subsequently be used to generate WSW estimates for use in the modelling of fluvial CO_2 evasion (Chapter 6, p.149). This is based on both the verification of the mathematical functionality of the model, achieved by an examination of outputs that tested the assumptions inherent in MLR modelling, and the validation of model estimates with field data. While additional work on the latter

is required to aid in making conclusions more definitive, a good foundation was established in meeting the stated aim of the study.

Moving beyond an appraisal of the WSW model as a whole, a number of additional observations were possible for specific model parameters. A novel finding of this research is that for the first time, the role of human modification of the river channel was successfully incorporated into the prediction of WSW. While the HMS score proved to have the smallest effect on the model out of all the statistically significant explanatory variables, a number of caveats suggest that this impact may in fact be underestimated. For instance, previous research suggests that the study site chosen contained a lower proportion of heavily modified streams, as the south-east of England is where the majority of engineering projects have taken place over the past few decades, with a gradual reduction further north (Gregory, 1997). This was corroborated by an examination of the RHS dataset (Environment Agency, 2010a), which showed a comparatively low degree of modification both in terms of extent (the number of heavily engineered river reaches) and intensiveness (the degree to which individual teaches had been modified) in north Wales and central lowland England. While it is perhaps encouraging that the MLR model has still identified human modification as a significant predictor of WSW despite the study site being less than ideal for doing so, the potential significance of this finding necessitates re-examination to determine the true extent of the influence of human modification on WSW in England and Wales.

Furthermore, there is the potential to enhance understanding further by incorporating flow direction to determine whether modification is upstream, downstream, or contiguous with a WSW estimate. Knowledge of flow direction would aid in clarifying the role of a number of explanatory variables, including land cover, as upstream changes such as afforestation are known to have a significant impact on downstream river geomorphology. The more simplistic approach used in this study was to take the closest datum point from the RHS dataset, with the values extracted to the WSW measurement point in question, with no consideration of whether the data were taken from upstream or downstream.

However, this was for good reason; the primary barrier to incorporating flow direction information is that methods such as ArcHydro take a DEM-derived vector dataset as input, so further work must be undertaken to adapt such techniques to use a river network derived from imagery. However, a DEM would still be required in the calculation of flow direction, which raises the possibility of a mismatch both positionally and in terms of the resolution of the DEM used being significantly coarser than that of the river network. Nonetheless, this is something that is still worth pursuing in future research because knowledge of flow direction would also allow spatial scale to be investigated in respect of the impact of human modification on WSW. For example, if several reaches upstream of a measurement location have been heavily modified, then this could potentially exert greater influence over WSW than if a single modified reach follows a number of near-natural reaches. This study only accounted for the modifications present for the single nearest reach, so is an examination of human impacts at the local scale only.

Additional challenges were presented by the resolution of the data available for the chosen explanatory variables. Rainfall was a monthly total presented at a spatial resolution of 5km, larger than some of the catchment areas used to aggregate measurements, while thematic resolution was an issue in the case of land cover data, which captured only the single most prevalent land cover class. While the former was still a statistically significant predictor of WSW, the latter – despite a strong body of literature establishing its importance – was not, so improving upon this by sourcing alternative data could be a comparatively simple way of improving the predictive ability of the MLR model.

This also applies to the inclusion of additional explanatory variables that were either not considered or excluded from the minimal adequate model, such as data concerning channel bed material and sediment supply, transport, and deposition. These are perhaps the most obvious omissions within the context of the background literature and theory concerning the factors that shape river channel morphology, but are unfortunately difficult to quantify beyond the local scale, particularly for a study site as extensive as that used in this study. Channel bed material is likely to have been included by

proxy through the BFI:HOST dataset, but the remainder concerning sediment dynamics has not. A simple way of classifying these processes is to apply the binary that distinguishes alluvial from bedrock channels. However, this classification is strongly scale dependent, because when observing a river reach rather than a single cross-section, channel material may change significantly. Even in the case of AAS WSW predictions where channel type may be more easily established, an understanding of processes upstream would still prove beneficial.

Finally, but perhaps most significantly, one issue with producing an accurate model of WSW was in how WSW itself was represented, as AAS measurements of width were of limited use due to the significant issue of overhanging vegetation. Without a (semi-)automated method for systematically removing the influence of vegetation or excluding the affected river cross-sections, MEW had to be used as the response variable in the MLR model, contrary to comparable studies (Booker, 2010; Rawlins *et al.*, 2014a). This somewhat undermined an advantage of the image-based WSW technique developed in this study, in that the high and user-definable sampling frequency at which WSW measurements were taken was eventually consolidated into only a few hundred MEW measurements. This begs the question as to why the measurement technique was necessary in the first instance, as a visual analysis of the study area could also have yielded several hundred measurements of width with a far lower requirement for technical expertise.

However, as the first attempt at applying this semi-automated technique to WSW measurement, the inability to subsequently model AAS WSW only came to light after the fact. Furthermore, the automated technique was still effective in capturing MEW by stipulating a very high measurement frequency, removing the potential for user error in manually identifying the widest section of a river reach. Finally, there is still significant potential in a method capable of providing AAS measurements, and while a solution to overhanging vegetation has thus far proved elusive, this study provides a strong foundation upon which to build. With the integration of LiDAR data that is able to penetrate the tree canopy, for example, this technique could be adapted to address both of the traditional paradigms in

fluvial geomorphology, namely AAS and downstream measurements of morphological parameters, rather than the latter alone. In future, it will become increasingly important to have a technique that can be adapted to both of these conceptualisations due to the potential increase in overhanging vegetation due to its role in reducing flood risk (Barnes *et al.*, 2016; Collentine and Futter, 2016), mitigating water temperature increases caused by climate change (Environment Agency, 2010b), and providing an ecological niche for organisms requiring shade (Sturt *et al.*, 2011). All of these advantages of riparian vegetation, among others, are compelling reasons as to why afforestation along river channels could increase in the coming years and decades. The method devised in this study, with further adaption, could one day meet the need for an approach that could be adapted to provide either AAS or reach-scale WSW.

7.1.4 Aim 4: Determine the impact of incorporating WSW measurements into fluvial CO_2 evasion models for England and Wales

The final aim of the study was intended to demonstrate arguably the most topical and relevant application for the newly-created WSW dataset for England and Wales, by assessing the contribution of WSW to fluvial CO_2 evasion models. Water surface area, generated by multiplying WSW with river network length, is a key control of CO_2 evasion due to the water's surface being the site at which the vertical transfer of CO_2 occurs; the greater the area of contact between water and atmosphere, the higher the potential flux of CO_2. However, despite the theoretical background of the process being well established, the practicality of directly measuring or modelling the influence of water surface area is comparatively limited. At the global scale, accounting for water surface area is complicated by factors such as the difficulty in accurately capturing surface waters at this extent – which fundamentally underpins the work undertaken for this thesis – yet even at more limited spatial extents, the lack of a usable dataset of WSW prevents the examination of the relationship between fluvial CO_2 evasion and water surface area. Exceptions such as the research undertaken by Butman and Raymond (2011) demonstrate that it is possible to address the current lack of analysis, but the

absence of an established WSW dataset is the main limitation to expanding the approach to England and Wales, for example. Consequently, by establishing a WSW dataset as part of this study, the impact of WSW on fluvial CO_2 evasion could be examined, for the first time, in England and Wales. The result was a predicted evasion of 74.6 kt C/yr, higher than a previous estimate of 60.8 kt C/yr (Rawlins *et al.* 2014b), which did not take WSW into account. Despite overlapping confidence intervals between the two estimates, there is a high probability that fluvial CO_2 evasion is underestimated by previous studies that omit the WSW component.

However, it is very difficult to make direct comparisons with previous studies due to the usage of reach-scale WSW measurements herein – described with the term MEW – as opposed to those taken AAS. The decision to generalise WSW to the reach scale rather than AAS reflects the existence of a number of different paradigms within the field of fluvial geomorphology, but in reality was necessitated by the difficulty in controlling for the influence of overhanging vegetation when using AAS measurements of WSW (Section 3.5.1, p.87). Regardless of the motivation behind this decision, the end result was the same; the use of MEW, calculated by determining the maximum WSW along a reach, had the potential to overestimate fluvial CO_2 evasion when these WSW predictions were used in turn to predict CO_2 evasion. Despite previous studies contending that fluvial CO_2 evasion is widely underestimated (Cole *et al.*, 2007; Cole and Caraco, 1998), this is a result of failing to capture the full range of explanatory variables adequately, as opposed to the choice of reach-scale or AAS WSW measurements. What can be stated, however, is that the model created in this study was less effective at predicting fluvial CO_2 evasion when WSW was removed, which corroborates the existing theory that water surface area acts as a control of fluvial CO_2 evasion. The caveats highlighted above remain significant, and results need to be reproduced and improved upon by future research, but early findings are promising.

Furthermore, while the difficulty in comparing fluvial CO_2 evasion models that use AAS WSW measurements with the use of MEW, as in this study, makes inter-model comparisons problematic, it

must also be recognised that the two approaches are not in competition; AAS and reach-scale processes are represented, and indeed contrasted and compared, throughout fluvial geomorphology research for the very reason that controls can vary based on which scale an investigation is based on. Therefore, while the models differ in their approaches, they are in fact complementary and demonstrate that it is possible to account for both conceptualisations of WSW – reach-scale and AAS – providing those researching fluvial CO_2 evasion with multiple viable options. Further research indicating which scenarios each approach is most relevant to would aid in developing existing knowledge of both fluvial CO_2 evasion and the way in which rivers are approached in fluvial geomorphology, with the model incorporating reach-averaged WSW, developed in this thesis, potentially more applicable at larger spatial scales where variation in channel morphology is potentially greater, with an AAS model perhaps more usable if a study is limited to the traditional river reconnaissance scale of a single reach, particularly if channel morphology is homogenous. This latter point is especially relevant as it relates not only to natural variation in river planform, but also the *visible* planform from the air; where vegetation cover is significant, the reach-scale approach using MEW is favourable, yet where vegetation is not present or its influence can be accounted for, the AAS conceptualisation of WSW would be most appropriate for subsequently modelling fluvial CO_2 evasion.

Somewhat paradoxically though, it is discharge that ultimately determines the quantity of CO_2 exported to the atmosphere (Liu *et al.* 2017; Marx *et al.*, 2017), with WSW acting as a proxy. The limited spatial coverage of both $K\mathrm{CO}_2$ measurements (Figure 6.2.1) and discharge gauging stations in England and Wales raises the question as to which approach is more viable when creating a fluvial CO_2 evasion model; creating a dataset of $K\mathrm{CO}_2$ contiguous with existing NRFA gauging stations – at which discharge measurements are available, removing the need for WSW entirely – or gathering $K\mathrm{CO}_2$ measurements at field locations independently of gauging station sites with a view to covering a representative range of river typologies, and then requiring the measurement or modelling of WSW in place of discharge data. The most sensible approach to resolving the two potential approaches outlined above would be to compare fluvial CO_2 evasion models derived from each; one that utilises

discharge measurements, and a second that uses WSW, both at the same locations (NRFA gauging stations).

In the event that WSW can be demonstrated as the most viable of the two options, or at the very least as a useable alternative in locations where discharge data are unavailable, then the limited river width covered when measuring $K\mathrm{CO}_2$ requires expansion, not only to increase the sample size but also to reaffirm whether the relationship between fluvial CO_2 evasion and WSW is linear beyond the current WSW limit captured in the field. Without these data, predictions are either limited to headwater streams or require predictive relationships to be extrapolated beyond the range of the observed data, which severely limits the confidence in, and certainty of, model predictions.

Furthermore, the collection of data for additional explanatory variables of fluvial CO_2 evasion, such as pH and turbidity, would aid in clarifying the true importance of water surface area by contextualising it among a more comprehensive set of factors. Despite the removal of WSW from the model in this study resulting in a decrease r-squared, it cannot currently be said with any certainty whether WSW is the single most important explanatory variable, or if others make a more significant contribution within the context of fluvial CO_2 evasion in England and Wales. Additional data collection for the aforementioned variables (pH and turbidity) could occur concurrently with the gathering of additional $K\mathrm{CO}_2$ measurements, and also the field validation of the WSW predictions generated as part of this study, so would be beneficial in a number of ways to the enhancement of this research and for developing knowledge in the fields of biogeochemistry, remote sensing, and fluvial geomorphology.

The expanded collection of field data to enhance fluvial CO_2 modelling predictions is one of many future directions that are identifiable as a result of this study, and are discussed in detail in the following section.

7.2 Future work

A number of potential directions for research became evident while undertaking this study, some of which form a natural progression from the discussion of caveats and limitations found throughout the thesis. Following is a brief synopsis of potential solutions to these problems, followed by an overview of anticipated future developments that may also contribute to methodological developments.

7.2.1 Addressing the issue of staticity

Firstly, as this research uses aerial imagery from a single point in time, it is necessary to address the issue of staticity. This is especially relevant given the highly dynamic nature of river systems, with the concept of equilibrium stating that a given system is undergoing constant change in response to events over a variety of spatial and temporal scales, in response to a multitude of forcings (Schumm, 1977). This is underlined by WSW specifically, which can vary on a timescale as short as hours, dependent on factors such as rainfall. As demonstrated by the predictive model of WSW, precipitation is second only to catchment area in controlling WSW, yet the latter is comparatively stable. For precipitation to exert a significant influence over WSW yet to vary so significantly on short timescales stands in stark contrast to the way rivers are represented by aerial imagery. Future modelling efforts could attempt to address this, though sourcing usable data for a number of decades could be problematic. However, recent advances in the field of ecology have met with some success in incorporating the concept of lag time into the modelling of plant and ecosystem processes (Ogle *et al.*, 2015). Relatively short-term changes in explanatory variables such as rainfall and land use are comparatively well documented, so could be examined in future efforts of modelling WSW.

This would go some way in acknowledging the critical role of river equilibrium in shaping channel morphology, including width. Disequilibrium in a river channel is known to be commonplace, with timescales of 1 to 10-ky mooted as the potential lag time between significant changes in discharge and channel adaption (Stark, 2006). This study already improves on existing methodologies where

power-law relationships are used, as the simplicity of these approaches is undermined by a particular inability to reflect river response to disequilibrium conditions (Whittaker *et al.*, 2007). While addressing timescales of thousands of years is unrealistic, short-term changes in the explanatory variables is something that can certainly be studied to improve on this further.

An additional issue posed by the use of a static representation of watercourses is that the time of imagery capture affects the degree to which non-permanent watercourses, known as intermittent rivers and ephemeral streams (IRES), are represented, as they are strongly dependent on seasonal rainfall and snowmelt. This is pertinent because river science research predominately addresses perennial rivers despite the preponderance of IRES; at least 30% - and potentially more than half – of rivers experience a dry phase where flow ceases completely at some point during the year (Acuña *et al.*, 2014; Datry *et al.*, 2016a, 2016b, 2014; Leigh *et al.*, 2016; Sheldon *et al.*, 2010). IRES are also more likely to take the form of low- order headwaters (Lowe and Likens, 2005), meaning that they are also likely to occur in mountainous terrain where connectivity with carbon-rich landscapes is strongest (Crawford *et al.*, 2013; Hotchkiss *et al.*, 2015; Wallin *et al.*, 2011), turbidity is highest (Aufdenkampe *et al.*, 2011), and despite the comparatively small interface between the water and the atmosphere, rates of CO_2 evasion are disproportionately high (Mulholland *et al.*, 2008; Rantakari *et al.*, 2010).

The need to incorporate IRES is all the more urgent considering that an increasing number of watercourses are predicted to become intermittent due to water extraction, land use, and climate change (Datry *et al.*, 2014). Further complicating matters is that the dry phase and the initial period of rewetting of IRES contribute significant volumes of CO_2 to the atmosphere (Corti and Datry, 2012; Gómez-Gener *et al.*, 2015; von Schiller *et al.*, 2014), the latter as a result of an initial surge in biogeochemical processes due to the disturbance of accumulated organic material along the section of dry river.

The need to capture IRES in studies of both water resources and applications such as GHG evasion is therefore clear. However, IRES are difficult to capture by their very nature, as they are both non-

permanent features of the landscape and potentially narrower than the spatial resolution of sensors attached to contemporary satellites. While medium-format aerial surveys such as that which captured the imagery used in this study could address the latter, low cloud conditions are an operational requirement; periods of low cloud are more likely in warmer months, or the exact time when a large proportion of IRES will be experiencing their dry phase in a climate such as the UK's which has clear seasonal trends. In any case, an objective of this study from inception was to obtain imagery that correlated with a period of below MDF in order to provide a non-biased estimate of WSW (and to control for the aforementioned seasonal variability). It is therefore unlikely that this study would ever have been able to elucidate the poorly understood contribution of IRES to water surface area or biogeochemical cycling (Benstead and Leigh, 2012). Consequently, future work should build on the baseline provided herein and investigate the temporal dynamics of WSW and CO_2 evasion, particularly in winter months when IRES are in flow, by utilising remotely sensed imagery from platforms with a more frequent return period than is realistically achievable with aerial surveys (see Section 7.2.3, p.187 for a discussion of recent developments in satellite and UAV platforms, for example). Once identified, both the wet and dry phases of IRES can be incorporated to build a more complete understanding of freshwater and biogeochemical dynamics over both space and time.

7.2.2 GHG evasion

This is both the most significant aspect of this research and the area in need of further development within the research community. While this study has established a baseline measurement of CO_2 evasion from headwaters in England and Wales, this estimate was based on a small number of field measurements of the landscape variables that control CO_2 evasion that captured a limited sample of headwater streams. This dataset can be expanded further by repeating the use of gas tracers and grab samples in the field (see Rawlins *et al.*, 2014b for an account of a similar procedure); a particular emphasis should be placed on expanding the sample to include measurements of evasion from wider rivers throughout the year, because even though headwaters are more significant contributors,

confounding factors such as catchments with peat-rich soils can result in wider rivers exporting large quantities of CO_2 to the atmosphere (Raymond *et al.*, 2013). Direct in-situ measurements of CO_2 are becoming increasingly cost-efficient (Bastviken *et al.*, 2015; Hunt *et al.*, 2017), so the synchronous collection of actual evasion alongside the measurements of relevant predictors can both improve upon and better validate and constrain existing models.

Field spectroscopy could also play a significant role in addressing the knowledge deficit, with both discrete surveys and the use of automated, in-situ optical sensors (Grayson and Holden, 2016; Jollymore *et al.*, 2012), such as fluorometers and spectrophotometers to measure water quality components such as DOC (Ruhala and Zarnetske, 2016), having the potential to contribute to knowledge. Additional measurements of the other controls of CO_2 at the same sites would also improve the parameterisation of models, as measurements of conductivity, turbidity, pH, and alkalinity are also relatively infrequent in England and Wales (see Rennie *et al.*, 2015a, 2015b, for details). The advent of new remote sensing technologies such as Landsat 8 may help to address this need at larger spatial scales, as recent efforts have shown that it is possible to create models to retrieve estimates of turbidity, for example (Sharaf El Din *et al.*, 2017), with a high degree of accuracy (R^2 = 0.991). An additional factor that both complicates matters further and necessitates a better understanding of the controls of CO_2 is the seasonal and diurnal variation in evasion. While the former has been referred to at various stages, particularly when considering the use of aerial imagery representing a single point in time at the foundation of the research undertaken, previous studies demonstrate that potential evasion can also vary from one hour to another. This trend typically shows that $p\,CO_2$ is higher at night due to an increase in biological respiration (Schelker *et al.*, 2016; Teodoru *et al.*, 2015) by as much as 1.8 times (Peter *et al.*, 2014), suggesting that we may currently be underestimating CO_2 evasion due to studies necessarily being undertaken during the hours of daylight.

One way in which both the temporal and spatial resolution of field datasets can be improved is through citizen science, which has significant potential to address this need (see Ward *et al.*, 2017). An example

of a potential approach was recently demonstrated by Weyhenmeyer *et al.* (2017) who reported the outcome of a project involving 3,500 high school students in Sweden, who were able to provide accurate measurements of the temperature differential between water and air while significantly improving on the spatial and temporal coverage that is usually achievable by a smaller research team. The application of this approach in England and Wales would provide significant benefits, especially if additional explanatory variables of CO_2 evasion were also measured.

Finally, analysis of other GHGs such as methane and nitrous oxide is required to fully understand the role of inland waters in England and Wales GHG budgets. While CO_2 is the most abundant GHG transferred to the atmosphere, CH_4 has a global warming potential 28 times that of CO_2 (Myhre *et al.*, 2013), so its relevance should not be overlooked. However, projected climate change could *reduce* GHG transfer from inland waters to the atmosphere due to the temperature differential between water and the overlying air becoming increasingly negative (Weyhenmeyer *et al.*, 2017), although there is also a potential increase of up to 30% in fluvial CO_2 evasion due to increased flooding (Langerwisch *et al.*, 2016). Headwaters in England and Wales specifically are predicted to become warmer, with lower summer and increased winter streamflows alongside either reduced or absent inputs from snowmelt (Curtis *et al.*, 2013), resulting in the alteration of both spatial and diurnal trends in evasion. However, regardless of future trends in GHG evasion and the uncertainty in predictions, it is still necessary to improve the parameterisation of models for the national scale to enable policymakers to devise appropriate and proportionate measures for mitigating the far-reaching impacts of an increase in atmospheric GHG concentration.

7.2.3 Developments in remote sensing technologies

The nature of any remote sensing research is that developments inevitably continue apace while work is underway. This is especially evident in the proliferation of satellite launches that took place during the course of this research, and continue to do so. Of particular note is ESA's Sentinel-2 mission, with Sentinel-2A launched on 23rd June 2015, followed by the identical Sentinel-2B satellite on 7th March

2017. The thirteen spectral channels include four visible and near-infrared bands that approximate those combined to create the data used in this study, only with a coarser spatial resolution of 10 m (ESA n.d.-a, ESA n.d.-b). The main benefit is the return period of five days, because while the spatial resolution is some way behind that of the 50cm CIR imagery, the repeat capture and global scale of observations would make the data suitable for national, continental, or even global-scale studies into both WSW and CO_2 evasion, while also allowing intermittent rivers to be captured. When combined with the ability to enhance the spatial resolution of the imagery via SRM (which is already an improvement on previous global datasets such as the 30 m resolution Landsat), an assessment of the viability of the imagery for this research's study area would be of great interest, and potentially allow for the temporal dynamics of WSW to be better understood at multiple scales. Such studies are already possible (see Tulbure and Broich, 2013), but are based on coarse resolution imagery and tend to exclude lower order rivers.

Looking further ahead, the Global Climate Observing System (GCOS) has recently devised a number of Essential Climate Variables (ECVs) based on the data gathered by the Landsat missions, one of which relates to the surface area of water bodies. Attempts to monitor surface area include an ongoing USGS project examining a metric known as 'Dynamic Surface Water Extent' (DSWE) (Jones, 2015, p.201; USGS, 2016). As well as codifying the importance of monitoring surface waters, the intention is to produce a 30-year, 30 m resolution dataset of inland waters which could be used to further address the issue of staticity, although development of an appropriate extraction algorithm is ongoing.

The contributions of other sub-disciplines within remote sensing could also aid in mapping WSW. Inundation mapping is a relatively mature field due to the obvious importance of identifying locations affected by flooding, and while the priority in such cases is the rapid dissemination of findings to aid organisations, the techniques used to identify surface waters are still potentially relevant. These are possibly notable in their absence from this study, but it must be acknowledged that there is a distinct difference in flood mapping, in that the simplest and perhaps most effective technique is using

imagery for two time periods – pre and post-inundation – to make a map of the difference in these two scenes (Dumitru *et al.*, 2015; Ticehurst *et al.*, 2014). This approach cannot be easily integrated with this study as the requirement for two separate images is not compatible with the desire for high resolution data, as the need for a return period limits the search for data to satellites, which would not provide adequately detailed imagery. However, there is the potential for flood mapping techniques, if applied to imagery that strikes an acceptable compromise between spatial and temporal resolution, could aid in addressing the aforementioned issue of staticity, as mapping the difference between WSW maps for multiple time periods could aid in understanding seasonal dynamics while also addressing the need to better integrate IRES into existing studies.

Additional sensor technologies would also lend themselves to further refining this study. While the CIR dataset provided an effective medium for the extraction of surface waters, alternatives exist that could offer clear advantages when used either in tandem with, or in place of, this dataset. For example, higher resolution (25cm) RGB imagery was captured synchronously with the CIR imagery, and could as a result capture an even greater proportion of narrow streams. Despite water being more difficult to separate from other classes in RGB imagery, the ability to use GIS techniques to remove errors of commission may be able to correct for this, although this became evident only with hindsight and would fail to address the likelihood of extensive errors of omission i.e. surface waters being missed entirely.

However, looking beyond medium-format aerial remote sensing surveys could yield clearer and more tangible benefits. For instance, radar platforms such as SAR (including ASAR, Sentinel-1, and TerraSAR-X) are able to penetrate the atmosphere and operate independently of solar illumination, addressing two inherent drawbacks of optical imagery. SAR has most commonly been applied to flood mapping (Brown *et al.*, 2016; Martinis *et al.*, 2015; Pulvirenti *et al.*, 2011), in part due to the aforementioned benefits allowing for more rapid processing and dissemination, essential in such time-critical application areas. However, this platform could also be used for the more routine mapping of surface

waters (Li and Wang *et al.*, 2015), although the output would require systematic testing for the study site of interest against results derived from, for example, CIR imagery with a comparable spatial resolution. Realistically, this is likely to be in the range of 1 m to 30 m for most radar data (Brown *et al.*, 2016), with examples such as the SWOT Ka-band radar interferometer only capturing rivers wider than 100 m due to the focus on water depth rather than width exponentially increasing data volume (Biancamaria *et al.*, 2016b; Miller *et al.*, 2014; NASA, 2012). Even so, the reality that many countries have comparatively few cloud-free days per year could make radar imagery a usable alternative, particularly when attempting to make numerous intra-annual or seasonal measurements, as this makes it far more likely that the area of interest will be obscured by cloud on at least one occasion when using optical imagery.

In addition to radar, river science research has already utilised other sensors to improve knowledge of inland waters. These include LiDAR (Biron *et al.*, 2013; McKean *et al.*, n.d.; Passalacqua *et al.*, 2012), microwave (Engman and Gurney, 1991) as well as VNIR, SWIR, and TIR (Nath and Deb 2010). LiDAR in particular could address a significant problem of this research, specifically the influence of overhanging vegetation on direct image-based measurement accuracy. By combining two wavelengths – IR and green – bathymetric LiDAR is able to capture the water's surface and the river bed simultaneously (Passalacqua *et al.*, 2012) while also penetrating the tree canopy, but the maximum achievable spatial resolution is poor when compared to the width of a typical first-order stream, and differentiating between returns from land and water requires *a priori* information (Alsdorf *et al.*, 2007). Nonetheless, if used as an additional dataset alongside the CIR-derived surface waters developed in this study and land cover data, LiDAR has the potential to at least allow for partially obscured river reaches to be measured more accurately, if not allowing for entirely covered river reaches to be measured, as achieved for a limited river reach by Sofia *et al.* (2015).

This is especially relevant within the context of current policy on flood management, as natural alternatives to hard engineering are increasingly being sought to deliver catchment-scale flood

resilience (Collentine and Futter, 2016; Pearson *et al.*, 2015; Salazar *et al.*, 2012). Within the UK, a number of studies have investigated the potential of targeted afforestation to support this goal (Barnes *et al.*, 2016; Marshall *et al.*, 2009; Sharp, 2014), raising the possibility that overhanging vegetation may become more prevalent in future, especially in proximity to low order streams as the majority of studies focus on the potential of upland catchment management to mitigate flooding downstream by intercepting precipitation and fixing river banks. Additionally, shading from vegetation mitigates the impact of climate change-induced water temperature increases (Environment Agency, 2010b), and provides an ecological niche capable of supporting diverse communities of invertebrates, which in turn can help to limit the quantity of algae (Bunn *et al.*, 1998; Köhler *et al.*, 2010; Sturt *et al.*, 2011). Overall, there exists a strong motivation for maintaining and further expanding the incidence of riparian vegetation, meaning that future WSW measurement methods must be able to contend with overhanging vegetation, with LiDAR holding great potential.

Finally, the growing applicability of unmanned aerial vehicles (UAVs) and more widespread availability of the required equipment offer a number of benefits. The primary advantage is in further enhancing the temporal resolution of even satellite platforms, as both professional and 'hobbyist' UAVs can be mounted with a camera of sufficient quality to gather imagery at will. The spatial resolution of such imagery can also be at the sub-centimetre scale, offering significant improvements on medium-format aerial surveys, with a number of papers applying the technology within a river hydrology and morphology context (Casado *et al.*, 2015; Flener *et al.*, 2013; Tamminga *et al.*, 2015). This would arguably be over-elaborate for this study, as well as being hugely impractical given the study area size, but could be extremely useful if applied to field validation and to the quantification of the impact of vegetation cover, as the UAV could be flown beneath the treeline in some locations.

There are still a number of barriers to the more widespread use of UAVs for research, such as training, safety and privacy requirements, the spectral resolution of UAV-mounted sensors being comparatively poor due to payload weight considerations, and the potential for aviation rules to be tightened

considerably as UAV use becomes more common (Civil Aviation Authority, 2015). However, the use of UAVs as a complement to medium and large format surveys has the potential to improve research into rivers, mainly by compensating for the drawbacks of these approaches.

Overall, studies aimed at accurately mapping the spatial extent of surface waters may soon be achievable using a combination of small (UAV) and large format (satellite) surveys, which could address two of the significant drawbacks of medium format aerial surveys in cloud cover and the expense of repeat surveys respectively, while offering constantly improving spatial, spectral, and temporal resolution through the combination of platforms. Ongoing developments are likely to offer numerous opportunities to improve and expand upon this study through the technologies described above, among others, in order to further enhance our understanding of spatially and temporally dynamic lotic surface waters.

7.2.4 Global scale predictions of WSW

An overview of current approaches for estimating global scale WSW and river surface area is presented in Section 2.2 (p.17). In summary, these techniques derive a river network from imagery that is limited by a coarse spatial resolution, resulting in divergent inventories of river surface area of 485,000 km^2 (Lehner and Döll, 2004), 624,000 km^2 (Raymond *et al.*, 2013), 662,000 km^2 (Downing *et al.*, 2012), and 832,000 km^2 (Lauerwald *et al.*, 2015). Approaches to create a global-scale database specifically for width are also impacted adversely by the use of coarse spatial resolution imagery. Yamazaki *et al.* (2014) found that the accuracy of their method decreased significantly when measuring rivers with a width of below 700 m due to a combination of the algorithm used for width measurement and the use of comparatively coarse data from the SRTM Water Body Database, which contains rivers with a width of 183 m and greater. As a consequence, the majority of studies predicting global fluvial CO_2 evasion exclude headwater streams entirely (Andreadis *et al.*, 2013; Aufdenkampe *et al.*, 2011; Downing *et al.*, 2012) despite their importance. This is unlikely to improve significantly in the near future, as obtaining even a coarse-resolution dataset of rivers at the global scale is a relatively

recent achievement. Studies have developed from a 250 m spatial resolution (Carroll *et al.* 2009) to the use of 30 m-resolution Landsat data (Verpoorter *et al.*, 2014; Feng *et al.*, 2015) in a short period of time. The expansion of this analysis to account for temporal change in surface water coverage is currently the state of the art (Pekel *et al.*, 2016; Yamazaki and Trigg, 2016), and provides valuable insights into long-term trends and seasonal patterns. A daily record of inland waters termed Global WaterPack is now available (Klein *et al.*, 2017) that utilises 250 m MODIS imagery, achieving an accuracy of 96.3% for pure water pixels. Incorporating super-resolution mapping techniques may enhance this further to help account for the presence of inland waters in mixed pixels, although significant challenges currently prevent this from being feasible. The reality is that these techniques (Klein *et al.*, 2017; Pekel *et al.*, 2016; Yamazaki and Trigg, 2016) required petabytes of information to be processed using automated algorithms, which contrasts with current methods, such as the image-based measurement approach developed in this study, designed to derive a dataset that incorporates low-order streams, which rely on a degree of user input that is currently not possible at the global scale.

Modelling would therefore appear to offer a potential solution. When applying MLR to the prediction of WSW at the national scale, a less resource-intensive model was also created that removed UK-specific datasets (BFI and HMS) to determine the viability of a model using only widely available landscape parameters for the estimation of WSW (Section 6.3.2, p.160). Catchment area, slope, rainfall, and relief were less effective at predicting national-scale WSW for England and Wales in comparison to the alternative that utilised BFI and HMS as explanatory variables, but still produced a model that, if expanded, could potentially address the need for a methodology capable of representing headwater streams at the global scale. Substantial further research would be required to determine the ease with which the explanatory variable data could be obtained, while it is also necessary to recreate, retest, and re-validate a global-scale variant of the model due to the inherent danger of extrapolating the current version beyond the limit of the explanatory and response (WSW) variables found in England and Wales. However, with catchment area alone capable of accounting for

as much as 50% of variation in WSW in some cases (Booker, 2010; Rawlins *et al.*, 2014a), it would take only a smaller contribution from additional variables to produce a more complete inventory of global-scale river width and water surface area, helping to improve the parametrisation of fluvial CO_2 evasion in the process.

7.3 Conclusion

Overall, this study has largely been successful in meeting its stated aims and objectives, but with limitations that apply caveats to key findings, which can be addressed through further research designed not only to expand on the work undertaken herein, but in the many fields that exist at the intersection of the thesis.

The primary limitation that applies to the first two aims relating to the extraction and measurement of surface waters from aerial imagery (as assessed in Section 7.1, p.169) is the degree of user involvement required throughout the process. While parts of the methodology are semi-automated (e.g. the production of WSW measurements at regular intervals along the river channel), accuracy assessment was only truly achieved through extensive exploratory analysis of the output generated. Furthermore, the full automation of the methodology is hampered by the competing conceptualisations of river width (channel width, bankfull width, WSW) that exist in the literature, reinforced by the tendency to take measurements AAS or in the form of MEW.

The second pair of aims stated in this study, relating to the modelling of WSW and fluvial CO_2 evasion respectively, are limited to differing extents by data availability. The WSW model, while providing estimates that were sufficiently accurate, relied on the use of datasets that are currently only available within the UK, namely BFI and HMS, which severely limits the generalisability and transferability of the overall approach used for this study. The fluvial CO_2 evasion model is inhibited by data availability somewhat differently, in that the primary limitation is a significant lack of field observations that can

be used for parametrising the model. In fact, with only 28 samples of $K\mathrm{CO}_2$ available at present, significant uncertainty exists as to the true role of riverine carbon in the carbon cycle as a whole in England and Wales. This is exacerbated by $K\mathrm{CO}_2$ field measurements being taken for streams ranging from 0.46 m to 1.64 m. While headwater streams have justifiably been a key focus of this study, the long-term aim should be to incorporate rivers of all scales in order to fully understand fluvial CO2 evasion, a pre-existing limitation of existing research that this study has only addressed in part due to the omission of $K\mathrm{CO}_2$ data for wider rivers.

By addressing the aforementioned limitations of the study as a whole, in combination with the potential for further research as discussed in Section 7.2 (p.183), the implications of the key findings from the research can be fully realised. In summary, these key findings are i) the generation of a WSW dataset for England and Wales that captured headwater streams to an extent not previously achieved, supported by novel remote sensing and GIS techniques; ii) the creation of a predictive model of WSW that corroborated existing knowledge of the controls of WSW while quantifying the role of human modification of the river channel in a model for the first time; and iii) water surface area, derived from WSW, improves the parameterisation of fluvial CO_2 evasion models, providing a foundation upon which further advancements can be made in the future.

Overall, the research has aided in establishing good practice when quantifying WSW and fluvial CO_2 evasion. By building upon this foundation with advances in areas such as the automation of the image-based measurement process, accounting for the influence of overhanging vegetation, an improved understanding of the temporal dynamics of WSW, and expanding the current field measurements of CO_2 evasion across both space and time, our understanding of these critically important fields can be enhanced further, developing not only theoretical knowledge, but also practical implementations capable of having a very real impact upon current policy.

References

Acuña, V., Datry, T., Marshall, J., Barceló, D., Dahm, C.N., Ginebreda, A., McGregor, G., Sabater, S., Tockner, K., Palmer, M.A., 2014. Why Should We Care About Temporary Waterways? Science 343, 1080. doi:10.1126/science.1246666

Adeline, K.R.M., Chen, M., Briottet, X., Pang, S.K., Paparoditis, N., 2013. Shadow detection in very high spatial resolution aerial images: A comparative study. ISPRS Journal of Photogrammetry and Remote Sensing 80, 21–38. https://doi.org/10.1016/j.isprsjprs.2013.02.003

Agouris, P., Stefanidis, A., Gyftakis, S., 2001. Differential Snakes for Change Detection in Road Segments. Photogrammetric Engineering & Remote Sensing 67, 1391–1399.

Alber, A., Piégay, H., 2011. Spatial disaggregation and aggregation procedures for characterizing fluvial features at the network-scale: Application to the Rhône basin (France). Geomorphology 125, 343–360. doi:10.1016/j.geomorph.2010.09.009

Allen, G.H., Barnes, J.B., Pavelsky, T.M., Kirby, E., 2013. Lithologic and tectonic controls on bedrock channel form at the northwest Himalayan front. Journal of Geophysical Research: Earth Surface 118, 1806–1825. doi:10.1002/jgrf.20113

Allen, G.H., Pavelsky, T.M., 2015. Patterns of river width and surface area revealed by the satellite-derived North American River Width (NARWidth) dataset. Geophysical Research Letters 42, 395–402. doi:10.1002/2014GL062764

Allmendinger, N.E., Pizzuto, J.E., Potter, N., Johnson, T.E., Hession, W.C., 2005. The influence of riparian vegetation on stream width, eastern Pennsylvania, USA. Geological society of America bulletin 117, 229–243. doi:10.1130/b25447.1

Alsdorf, D., Lettenmaier, D., Vörösmarty, C., 2003. The need for global, satellite-based observations of terrestrial surface waters. Eos, Transactions American Geophysical Union 84, 269–276. doi:10.1029/2003EO290001

Alsdorf, D.E., Lettenmaier, D.P., 2003. Tracking Fresh Water from Space. Science 301, 1491–1494. doi:10.1126/science.1089802

Alsdorf, D.E., Rodriguez, E., Lettenmaier, D.P., 2007. Measuring surface water from space. Reviews of Geophysics 45.

Anderson, K., 2016. Integrating multiple scales of remote sensing measurement – from satellites to kites. Progress in Physical Geography 40, 187–195. doi:10.1177/0309133316639175

Anderson, R.J., Bledsoe, B.P., Hession, W.C., 2004. Width of streams and rivers in response to vegetation, bank material, and other factors. Journal of the American Water Resources Association 40, 1159–1172. doi:10.1111/j.1752-1688.2004.tb01576.x

Andreadis, K.M., Schumann, G.J.P., Pavelsky, T., 2013. A simple global river bankfull width and depth database. Water Resources Research 49, 7164–7168. doi:10.1002/wrcr.20440

APEM, n.d. Fluvial Information System (FIS).

Armenakis, C., 2005. A semi-automated approach for the recognition and extraction of water features from Landsat 7 imagery in northern Canada, in: Agouris, P., Croitoru, A. (Eds.), Next Generation Geospatial Information: From Digital Image Analysis to Spatiotemporal Databases, ISPRS Book Series. Taylor & Francis, London, pp. 59–68.

Arnell, N.W., Gosling, S.N., 2014. The impacts of climate change on river flood risk at the global scale. Climatic Change 1–15. doi:10.1007/s10584-014-1084-5

Arnell, N.W.W., Reynard, N.S.S., 1996. The effects of climate change due to global warming on river flows in Great Britain. Journal of Hydrology 183, 397–424. doi:10.1016/0022-1694(95)02950-8

Aronoff, S., 2004. Remote sensing for GIS managers. Environmental Systems Research.

Ashley, G.M., Renwick, W.H., Haag, G.H., 1988. Channel form and processes in bedrock and alluvial reaches of the Raritan River, New Jersey. Geology 16, 436–439. doi:10.1130/0091-7613(1988)016<0436:cfapib>2.3.co;2

Atkinson, P.M., 2005. Sub-pixel target mapping from soft-classified, remotely sensed imagery. Photogrammetric Engineering and Remote Sensing 71, 839.

Atkinson, P.M., 2004. Super-Resolution Land Cover Classification Using the Two-Point Histogram, in: Sanchez-Vila, X., Carrera, J., Gómez-Hernández, J. (Eds.), geoENV IV — Geostatistics for Environmental Applications. Springer Netherlands, pp. 15–28.

Aufdenkampe, A.K., Mayorga, E., Raymond, P.A., Melack, J.M., Doney, S.C., Alin, S.R., Aalto, R.E., Yoo, K., 2011. Riverine coupling of biogeochemical cycles between land, oceans, and atmosphere. Frontiers in Ecology and the Environment 9, 53–60. doi:10.1890/100014

Barnes, M., Quinn, P., Bathurst, J., Birkinshaw, S., 2016. Catchment scale afforestation for mitigating flooding. Presented at the EGU General Assembly Conference Abstracts, p. 987.

Bastviken, D., Sundgren, I., Natchimuthu, S., Reyier, H., Gålfalk, M., 2015. Technical Note: Cost-efficient approaches to measure carbon dioxide (CO_2) fluxes and concentrations in terrestrial and aquatic environments using mini loggers. Biogeosciences 12, 3849–3859. doi:10.5194/bg-12-3849-2015

Bastviken, D., Tranvik, L.J., Downing, J.A., Crill, P.M., Enrich-Prast, A., 2011. Freshwater Methane Emissions Offset the Continental Carbon Sink. Science 331, 50. doi:10.1126/science.1196808

Battin, T.J., Luyssaert, S., Kaplan, L.A., Aufdenkampe, A.K., Richter, A., Tranvik, L.J., 2009. The boundless carbon cycle. Nature Geoscience 2, 598–600.

Baumgartner, A., Steger, C., Mayer, H., Eckstein, W., Ebner, H., 1999. Automatic road extraction based on multi-scale, grouping and context. Photogrammetric Engineering & Remote Sensing 65, 777–785.

Beaulieu, J.J., Shuster, W.D., Rebholz, J.A., 2012. Controls on gas transfer velocities in a large river. Journal of Geophysical Research: Biogeosciences 117.

Beaulieu, J.J., Tank, J.L., Hamilton, S.K., Wollheim, W.M., Hall, R.O., Mulholland, P.J., Peterson, B.J., Ashkenas, L.R., Cooper, L.W., Dahm, C.N., 2011. Nitrous oxide emission from denitrification in stream and river networks. Proceedings of the National Academy of Sciences 108, 214–219.

Beighley, R.E., Gummadi, V., 2011. Developing channel and floodplain dimensions with limited data: a case study in the Amazon Basin. Earth Surface Processes and Landforms 36, 1059–1071. doi:10.1002/esp.2132

Benstead, J.P., Leigh, D.S., 2012. An expanded role for river networks. Nature Geoscience 5, 678–679. doi:10.1038/ngeo1593

Bernhardt, E.S., Palmer, M.A., 2007. Restoring streams in an urbanizing world. Freshwater Biology 52, 738–751. doi:10.1111/j.1365-2427.2006.01718.x

Biancamaria, S., Frappart, F., Leleu, A.-S., Marieu, V., Blumstein, D., Desjonquères, J.-D., Boy, F., Sottolichio, A., Valle-Levinson, A., 2016a. Satellite radar altimetry water elevations performance over a 200 m wide river: Evaluation over the Garonne River. Advances in Space Research. doi:10.1016/j.asr.2016.10.008

Biancamaria, S., Lettenmaier, D.P., Pavelsky, T.M., 2016b. The SWOT Mission and Its Capabilities for Land Hydrology. Surveys in Geophysics 37, 307–337. doi:10.1007/s10712-015-9346-y

Birkett, C.M., 1998. Contribution of the TOPEX NASA Radar Altimeter to the global monitoring of large rivers and wetlands. Water Resources Research 34, 1223–1239. doi:10.1029/98WR00124

Birkinshaw, S.J., Moore, P., Kilsby, C.G., O'Donnell, G.M., Hardy, A.J., Berry, P.A.M., 2014. Daily discharge estimation at ungauged river sites using remote sensing. Hydrological Processes 28, 1043–1054. doi:10.1002/hyp.9647

Biron, P.M., Choné, G., Buffin-Bélanger, T., Demers, S., Olsen, T., 2013. Improvement of streams hydro-geomorphological assessment using LiDAR DEMs. Earth Surface Processes and Landforms 38, 1808–1821.

Bishop, K., Buffam, I., Erlandsson, M., Fölster, J., Laudon, H., Seibert, J., Temnerud, J., 2008. Aqua Incognita: the unknown headwaters. Hydrological Processes 22, 1239–1242. doi:10.1002/hyp.7049

Bjerklie, D.M., Lawrence Dingman, S., Vorosmarty, C.J., Bolster, C.H., Congalton, R.G., 2003. Evaluating the potential for measuring river discharge from space. Journal of Hydrology 278, 17–38. doi:10.1016/s0022-1694(03)00129-x

Bjerklie, D.M., Moller, D., Smith, L.C., Dingman, S.L., 2005. Estimating discharge in rivers using remotely sensed hydraulic information. Journal of Hydrology 309, 191–209. doi:10.1016/j.jhydrol.2004.11.022

Bloomfield, J.P., Allen, D.J., Griffiths, K.J., 2009. Examining geological controls on baseflow index (BFI) using regression analysis: An illustration from the Thames Basin, UK. Journal of Hydrology 373, 164–176. doi:http://dx.doi.org/10.1016/j.jhydrol.2009.04.025

Booker, D.J., 2010. Predicting wetted width in any river at any discharge. Earth Surface Processes and Landforms n/a–n/a. doi:10.1002/esp.1981

Booker, D.J., Acreman, M.C., 2007. Generalisation of physical habitat-discharge relationships. Hydrol. Earth Syst. Sci. 11, 141–157. doi:10.5194/hess-11-141-2007

Booker, D.J., Dunbar, M.J., 2008. Predicting river width, depth and velocity at ungauged sites in England and Wales using multilevel models. Hydrological Processes 22, 4049–4057. doi:10.1002/hyp.7007

Boorman, D.B., Hollis, J.M., Lilly, A., 1995. Hydrology of soil types: a hydrologically-based classification of the soils of the United Kingdom. Institute of Hydrology, Wallingford.

Borges, A.V., Vanderborght, J.-P., Schiettecatte, L.-S., Gazeau, F., Ferrón-Smith, S., Delille, B., Frankignoulle, M., 2004. Variability of the gas transfer velocity of CO2 in a macrotidal estuary (the Scheldt). Estuaries 27, 593–603. https://doi.org/10.1007/BF02907647

Boyd, D.S., 2009. Remote sensing in physical geography: a twenty-first-century perspective. Progress in Physical Geography 33, 451–456. doi:10.1177/0309133309346645

Boyd, D.S., Foody, G.M., 2011. An overview of recent remote sensing and GIS based research in ecological informatics. Ecological Informatics 6, 25–36. doi:http://dx.doi.org/10.1016/j.ecoinf.2010.07.007

Brakenridge, G.R., Nghiem, S.V., Anderson, E., Chien, S., 2005. Space-based measurement of river runoff. Eos, Transactions American Geophysical Union 86, 185–188. doi:10.1029/2005EO190001

Brierley, G., Fryirs, K., Cullum, C., Tadaki, M., Huang, H.Q., Blue, B., 2013. Reading the landscape: Integrating the theory and practice of geomorphology to develop place-based understandings of river systems. Progress in Physical Geography 37, 601–621. doi:10.1177/0309133313490007

Brookes, A., 1987. River channel adjustments downstream from channelization works in England and Wales. Earth Surface Processes and Landforms 12, 337–351. doi:10.1002/esp.3290120402

Brown, K.M., Hambidge, C.H., Brownett, J.M., 2016. Progress in operational flood mapping using satellite synthetic aperture radar (SAR) and airborne light detection and ranging (LiDAR) data. Progress in Physical Geography 40, 196–214. doi:10.1177/0309133316633570

Brunsdon, C., Fotheringham, A.S., Charlton, M.E., 2010. Geographically Weighted Regression: A Method for Exploring Spatial Nonstationarity. Geographical Analysis 28, 281–298. doi:10.1111/j.1538-4632.1996.tb00936.x

Bunn, S.E., Davies, P.M., Kellaway, D.M., Prosser, I.P., 1998. Influence of invasive macrophytes on channel morphology and hydrology in an open tropical lowland stream, and potential control by riparian shading. Freshwater Biology 39, 171–178. doi:10.1046/j.1365-2427.1998.00264.x

Burgers, H.E., Schipper, A.M., Jan Hendriks, A., 2013. Size relationships of water discharge in rivers: scaling of discharge with catchment area, main-stem length and precipitation. Hydrological Processes n/a–n/a. doi:10.1002/hyp.10087

Butman, D., Raymond, P.A., 2011. Significant efflux of carbon dioxide from streams and rivers in the United States. Nature Geoscience 4, 839–842. doi:10.1038/ngeo1294

Casado, R.M., Gonzalez, B.R., Kriechbaumer, T., Veal, A., 2015. Automated Identification of River Hydromorphological Features Using UAV High Resolution Aerial Imagery. Sensors 15. doi:10.3390/s151127969

Centre for Ecology and Hydrology, 2015a. Search for gauging stations [WWW Document]. National River Flow Archive. URL http://nrfa.ceh.ac.uk/data/search (accessed 7.7.16).

Centre for Ecology and Hydrology, 2015b. Integrated Hydrological Units of the United Kingdom.

Centre for Ecology and Hydrology, 2017. LCM2015 [WWW Document]. URL https://www.ceh.ac.uk/sites/default/files/LCM2015_Dataset_Documentation_22May2017.pdf (accessed 4.7.17).

Chatterjee, S., Hadi, A.S., 2009. Sensitivity analysis in linear regression. John Wiley & Sons.

Chen, C., Qin, Q., Zhang, N., Li, J., Chen, L., Wang, J., Qin, X., Yang, X., 2014. Extraction of bridges over water from high-resolution optical remote-sensing images based on mathematical morphology. International Journal of Remote Sensing 35, 3664–3682. doi:10.1080/01431161.2014.915437

Chin, A., 2006. Urban transformation of river landscapes in a global context. Geomorphology 79, 460–487. doi:http://dx.doi.org/10.1016/j.geomorph.2006.06.033

Ciais, P., Sabine, C., Bala, G., Bopp, L., Brovkin, V., Canadell, J., Chhabra, A., DeFries, R., Galloway, J., Heimann, M., 2013. Carbon and other biogeochemical cycles, in: Climate Change 2013: The Physical Science Basis. Contribution of Working Group I to the Fifth Assessment Report of the Intergovernmental Panel on Climate Change. Cambridge University Press, pp. 465–570.

Civil Aviation Authority, 2015. Unmanned Aircraft System Operations in UK Airspace – Guidance (No. CAP 722). Safety and Airspace Regulation Group.

Cole, J.J., Caraco, N.F., 1998. Atmospheric exchange of carbon dioxide in a low-wind oligotrophic lake measured by the addition of SF6. Limnol. Oceanogr. 43.

Cole, J.J., Prairie, Y.T., Caraco, N.F., McDowell, W.H., Tranvik, L.J., Striegl, R.G., Duarte, C.M., Kortelainen, P., Downing, J.A., Middelburg, J.J., Melack, J., 2007. Plumbing the Global Carbon

Cycle: Integrating Inland Waters into the Terrestrial Carbon Budget. Ecosystems 10, 172–185. doi:10.1007/s10021-006-9013-8

Collentine, D., Futter, M. n., 2016. Realising the potential of natural water retention measures in catchment flood management: trade-offs and matching interests. J Flood Risk Management n/a-n/a. doi:10.1111/jfr3.12269

Comber, A.J., 2013. Geographically weighted methods for estimating local surfaces of overall, user and producer accuracies. Remote Sensing Letters 4, 373–380. doi:10.1080/2150704X.2012.736694

Congalton, R.G., 1991. A review of assessing the accuracy of classifications of remotely sensed data. Remote Sensing of Environment 37, 35–46. doi:http://dx.doi.org/10.1016/0034-4257(91)90048-B

Congalton, R.G., Green, K., 2009. Assessing the accuracy of remotely sensed data: principles and practices. CRC press.

Congalton, R.G., Green, K., 1993. A practical look at the sources of confusion in error matrix generation. Photogrammetric Engineering and Remote Sensing 59, 641–644.

Corti, R., Datry, T., 2012. Invertebrates and sestonic matter in an advancing wetted front travelling down a dry river bed (Albarine, France). Freshwater Science 31, 1187–1201. doi:10.1899/12-017.1

Coulthard, T.J., Macklin, M.G., 2001. How sensitive are river systems to climate and land-use changes? A model-based evaluation. Journal of Quaternary Science 16, 347–351. doi:10.1002/jqs.604

Crawford, J.T., Striegl, R.G., Wickland, K.P., Dornblaser, M.M., Stanley, E.H., 2013. Emissions of carbon dioxide and methane from a headwater stream network of interior Alaska. Journal of Geophysical Research: Biogeosciences 118, 482–494. doi:10.1002/jgrg.20034

Crawley, M.J., 2013. The R Book, 2nd ed. Wiley.

Cudennec, C., de Lavenne, A., 2015. Editorial: Hydrogeomorphology – a long-term scientific interface. Hydrology Research 46, 175. doi:10.2166/nh.2015.100

Curran, J.C., Cannatelli, K.M., 2014. The impact of beaver dams on the morphology of a river in the eastern United States with implications for river restoration. Earth Surf. Process. Landforms 39, 1236–1244. doi:10.1002/esp.3576

Curtis, C.J., Battarbee, R.W., Monteith, D.T., Shilland, E.M., 2014. The future of upland water ecosystems of the UK in the 21st century: A synthesis. Ecological Indicators, Threats to upland waters 37, Part B, 412–430. doi:10.1016/j.ecolind.2013.10.012

Datry, T., Fritz, K., Leigh, C., 2016a. Challenges, developments and perspectives in intermittent river ecology. Freshw Biol 61, 1171–1180. doi:10.1111/fwb.12789

Datry, T., Larned, S.T., Tockner, K., 2014. Intermittent Rivers: A Challenge for Freshwater Ecology. BioScience. doi:10.1093/biosci/bit027

Datry, T., Pella, H., Leigh, C., Bonada, N., Hugueny, B., 2016b. A landscape approach to advance intermittent river ecology. Freshwater Biology n/a–n/a. doi:10.1111/fwb.12645

Dawson, J.J.C., Soulsby, C., Hrachowitz, M., Speed, M., Tetzlaff, D., 2009. Seasonality of ep CO_2 at different scales along an integrated river continuum within the Dee basin, NE Scotland. Hydrol. Process. 23, 2929–2942. doi:10.1002/hyp.7402

DigitalGlobe, n.d. The DigitalGlobe constellation [WWW Document]. URL https://dg-cms-uploads-production.s3.amazonaws.com/uploads/document/file/223/Constellation_Brochure_forWeb.pdf (accessed 5.15.16).

Dinsmore, K.J., Billett, M.F., 2008. Continuous measurement and modeling of CO_2 losses from a peatland stream during stormflow events. Water Resources Research 44, W12417. doi:10.1029/2008WR007284

Downing, J.A., Cole, J.J., Duarte, C.A., Middelburg, J.J., Melack, J.M., Prairie, Y.T., Kortelainen, P., Striegl, R.G., McDowel, W.H., Tranvik, L.J., 2012. Global abundance and size distribution of streams and rivers. Inland Waters 2, 229–236. doi:10.5268/iw-2.4.502

Downing, J.A., Prairie, Y.T., Cole, J.J., Duarte, C.M., Tranvik, L.J., Striegl, R.G., McDowell, W.H., Kortelainen, P., Caraco, N.F., Melack, J.M., 2006. The global abundance and size distribution of lakes, ponds, and impoundments. Limnology and Oceanography 51, 2388–2397.

Dugdale, S.J., 2016. A practitioner's guide to thermal infrared remote sensing of rivers and streams: recent advances, precautions and considerations. WIREs Water 3, 251–268. doi:10.1002/wat2.1135

Dugdale, S.J., Carbonneau, P., Clough, S., 2009. The Fluvial Information System, in: AGU Fall Meeting.

Dumitru, C.O., Cui, S., Faur, D., Datcu, M., 2015. Data Analytics for Rapid Mapping: Case Study of a Flooding Event in Germany and the Tsunami in Japan Using Very High Resolution SAR Images. Selected Topics in Applied Earth Observations and Remote Sensing, IEEE Journal of 8, 114–129. doi:10.1109/JSTARS.2014.2320777

Dunjó, G., Pardini, G., Gispert, M., 2004. The role of land use–land cover on runoff generation and sediment yield at a microplot scale, in a small Mediterranean catchment. Journal of Arid Environments 57, 239–256. doi:http://dx.doi.org/10.1016/S0140-1963(03)00097-1

Eaton, B., Rosenfeld, J., 2016. Mechanisms of flow and sediment transport in fluvial ecosystems: physical and ecological consequences, in: Johnson, E.A., Martin, Y.E. (Eds.), A Biogeosciences Approach to Ecosystems. Cambridge University Press, UK, pp. 347–382.

Eke, E., Parker, G., Shimizu, Y., 2014. Numerical modeling of erosional and depositional bank processes in migrating river bends with self-formed width: Morphodynamics of bar push and bank pull. J. Geophys. Res. Earth Surf. 119, 2013JF003020. doi:10.1002/2013JF003020

Elliott, C.M., 2011. Geomorphic classification and evaluation of channel width and emergent sandbar habitat relations on the Lower Platte River, Nebraska. USGS.

Engman, E.T., Gurney, R.J., 1991. Remote Sensing in Hydrology. Chapman and Hall, London.

Environment Agency, 2010a. River habitats in England and Wales: current state and changes since 1995-96. Environment Agency, Bristol, UK.

Environment Agency, 2010b. Our river habitats - The state of river habitats in England, Wales and the Isle of Man: a snapshot.

Enwright, N.M., Jones, W.R., Garber, A.L., Keller, M.J., 2014. Analysis of the impact of spatial resolution on land/water classifications using high-resolution aerial imagery. International Journal of Remote Sensing 35, 5280–5288. doi:10.1080/01431161.2014.938181

Erkkilä, K.-M., Mammarella, I., Bastviken, D., Biermann, T., Heiskanen, J.J., Lindroth, A., Peltola, O., Rantakari, M., Vesala, T., Ojala, A., 2017. Methane and carbon dioxide fluxes over a lake: comparison between eddy covariance, floating chambers and boundary layer method. Biogeosciences Discuss. 2017, 1–29. doi:10.5194/bg-2017-56

ESRI, 2016. What is the ArcGIS Network Analyst extension? [WWW Document]. URL http://desktop.arcgis.com/en/arcmap/latest/extensions/network-analyst/what-is-network-analyst-.htm (accessed 6.22.16).

ESRI, 2014. Collapse dual lines to centreline: ArcGIS help page.

ESRI, 2012a. Creating a segment at an angle from another segment: ArcGIS help page.

ESRI, 2012b. Measuring distances and areas: ArcGIS help page.

ESRI, 2011. ArcHydro Tools Tutorial.

ESSA, 2014. River Bathymetry Toolkit (RBT), 3.7.5. ed.

European Commission Joint Research Centre, n.d. Global Surface Water Explorer [WWW Document]. URL https://global-surface-water.appspot.com/ (accessed 15.4.16).

Everard, M., Quinn, N., 2015. Realizing the value of fluvial geomorphology. International Journal of River Basin Management 1–14. doi:10.1080/15715124.2015.1048457

Everitt, B.S., Hothorn, T., n.d. Simple and Multiple Linear Regression: How Old is the Universe and Cloud Seeding, in: A Handbook of Statistical Analyses Using R.

Faustini, J.M., Kaufmann, P.R., Herlihy, A.T., 2009. Downstream variation in bankfull width of wadeable streams across the conterminous United States. Geomorphology 108, 292–311. doi:http://dx.doi.org/10.1016/j.geomorph.2009.02.005

Feng, M., Sexton, J.O., Channan, S., Townshend, J.R., 2016. A global, high-resolution (30-m) inland water body dataset for 2000: first results of a topographic–spectral classification algorithm. International Journal of Digital Earth 9, 113–133. doi:10.1080/17538947.2015.1026420

Fensholt, R., Proud, S.R., 2012. Evaluation of Earth Observation based global long term vegetation trends — Comparing GIMMS and MODIS global NDVI time series. Remote Sensing of Environment 119, 131–147. doi:http://dx.doi.org/10.1016/j.rse.2011.12.015

Ferguson, S.P., Rennie, C.D., 2017. Influence of alluvial cover and lithology on the adjustment characteristics of semi-alluvial bedrock channels. Geomorphology 285, 260–271. doi:10.1016/j.geomorph.2017.01.040

Ferreira, M., 2014. Transect tool for ArcGIS, 1st ed.

Feyisa, G.L., Meilby, H., Fensholt, R., Proud, S.R., 2014. Automated Water Extraction Index: A new technique for surface water mapping using Landsat imagery. Remote Sensing of Environment 140, 23–35. doi:http://dx.doi.org/10.1016/j.rse.2013.08.029

Field, A., Miles, J., Field, Z., 2012. Discovering Statistics Using R. SAGE Publications, London.

Filippi, A.M., Güneralp, I, 2013. Influence of shadow removal on image classification in riverine environments. Optics Letters 38, 1676–1678. doi:10.1364/OL.38.001676

Finnegan, N.J., Roe, G., Montgomery, D.R., Hallet, B., 2005. Controls on the channel width of rivers: Implications for modeling fluvial incision of bedrock. Geology 33, 229–232. doi:10.1130/g21171.1

Fisher, G.B., Amos, C.B., Bookhagen, B., Burbank, D.W., Godard, V., 2012. Google Earth and Virtual Visualizations in Geoscience Education and Research, Geological Society of America Special

Papers, Geological Society of America Special Papers. Geological Society of America. doi:10.1130/9780813724928

Fisher, G.B., Bookhagen, B., 2014. ChanGeom.

Fisher, G.B., Bookhagen, B., Amos, C.B., 2013. Channel planform geometry and slopes from freely available high-spatial resolution imagery and DEM fusion: Implications for channel width scalings, erosion proxies, and fluvial signatures in tectonically active landscapes. Geomorphology 194, 46–56. doi:http://dx.doi.org/10.1016/j.geomorph.2013.04.011

Fisher, P., 1997. The pixel: A snare and a delusion. International Journal of Remote Sensing 18, 679–685. doi:10.1080/014311697219015

Flener, C., Vaaja, M., Jaakkola, A., Krooks, A., Kaartinen, H., Kukko, A., Kasvi, E., Hyyppä, H., Hyyppä, J., Alho, P., 2013. Seamless Mapping of River Channels at High Resolution Using Mobile LiDAR and UAV-Photography. Remote Sensing 5. doi:10.3390/rs5126382

Foody, G.M., 2008. Harshness in image classification accuracy assessment. International Journal of Remote Sensing 29, 3137–3158. doi:10.1080/01431160701442120

Foody, G.M., 2005. Local characterization of thematic classification accuracy through spatially constrained confusion matrices. International Journal of Remote Sensing 26, 1217–1228. doi:10.1080/01431160512331326521

Foody, G.M., 1996. Approaches for the production and evaluation of fuzzy land cover classifications from remotely-sensed data. International Journal of Remote Sensing 17, 1317–1340. doi:10.1080/01431169608948706

Foody, G.M., Muslim, A.M., Atkinson, P.M., 2005. Super-resolution mapping of the waterline from remotely sensed data. International Journal of Remote Sensing 26, 5381–5392. doi:10.1080/01431160500213292

Foody, G.M.G.M., 2002. Status of land cover classification accuracy assessment. Remote Sensing of Environment 80, 185–201. doi:http://dx.doi.org/10.1016/S0034-4257(01)00295-4

Fotheringham, A.S., Charlton, M., Brunsdon, C., 1997. Measuring Spatial Variations in Relationships with Geographically Weighted Regression. Springer Berlin Heidelberg, pp. 60–82.

Frenette, J.-J., Massicotte, P., Lapierre, J.-F., 2012. Colorful Niches of Phytoplankton Shaped by the Spatial Connectivity in a Large River Ecosystem: A Riverscape Perspective. PLOS ONE 7, e35891. https://doi.org/10.1371/journal.pone.0035891

Friedman, J.H., 1991. Multivariate Adaptive Regression Splines. Ann. Statist. 1–67. doi:10.1214/aos/1176347963

Fryirs, K.A., Brierley, G.J., 2012. Geomorphic analysis of river systems: an approach to reading the landscape. John Wiley & Sons.

Gabrisch, G., 2008. Create perpendicular lines to each segment of a shapefile, 1st ed.

García Balboa, J.L., Ariza López, F.J., 2007. Generalization-oriented Road Line Classification by Means of an Artificial Neural Network. GeoInformatica 12, 289–312. doi:10.1007/s10707-007-0026-z

Getmapping, n.d. Aerial Data - Infrared Imagery | Getmapping [WWW Document]. URL https://www.getmapping.com/products/high-resolution-aerial-imagery/aerial-data-colour-infrared-imagery#specifications (accessed 1.30.19).

Giddens, A., 2009. The politics of climate change. Cambridge, UK.

Gilvear, D., Bryant, R., 2003. Analysis of aerial photography and other remotely sensed data, in: Kondolf, G.M., Piâegay, H. (Eds.), Tools in Fluvial Geomorphology. Wiley, pp. 135–170.

Gleason, C.J., 2015. Hydraulic geometry of natural rivers. Progress in Physical Geography 39, 337–360. doi:10.1177/0309133314567584

Gleason, C.J., Smith, L.C., 2014. Toward global mapping of river discharge using satellite images and at-many-stations hydraulic geometry. Proceedings of the National Academy of Sciences 111, 4788–4791. doi:10.1073/pnas.1317606111

Gleyzer, A., Denisyuk, M., Rimmer, A., Salingar, Y., 2004. A fast recursive GIS algorithm for computing Strahler stream order in braided and nonbraided networks. JAWRA Journal of the American Water Resources Association 40, 937–946. doi:10.1111/j.1752-1688.2004.tb01057.x

Gómez-Gener, L., Obrador, B., von Schiller, D., Marcé, R., Casas-Ruiz, J.P., Proia, L., Acuña, V., Catalán, N., Muñoz, I., Koschorreck, M., 2015. Hot spots for carbon emissions from Mediterranean fluvial networks during summer drought. Biogeochemistry 125, 409–426. doi:10.1007/s10533-015-0139-7

Goodchild, M.F., Hunter, G.J., 1997. A simple positional accuracy measure for linear features. International Journal of Geographical Information Science 11, 299–306. doi:10.1080/136588197242419

Grayson, R.P., Holden, J., 2016. Improved automation of dissolved organic carbon sampling for organic-rich surface waters. Science of The Total Environment 543, Part A, 44–51. doi:10.1016/j.scitotenv.2015.10.149

Gregory, K.J., 2006. The human role in changing river channels. Geomorphology 79, 172–191. doi:http://dx.doi.org/10.1016/j.geomorph.2006.06.018

Gregory, K.J., 1997. Fluvial geomorphology of Great Britain. Chapman & Hall, London.

Güneralp, İ., Filippi, A.M., Hales, B., 2014. Influence of river channel morphology and bank characteristics on water surface boundary delineation using high-resolution passive remote sensing and template matching. Earth Surface Processes and Landforms n/a–n/a. doi:10.1002/esp.3560

Gurnell, A., 2014. Plants as river system engineers. Earth Surf. Process. Landforms 39, 4–25. doi:10.1002/esp.3397

Gustard, A., Bullock, A., Dixon, J.M., 1992. Low flow estimation in the United Kingdom. Institute of Hydrology, Wallingford, UK.

Haklay, M., 2010. How good is volunteered geographical information? A comparative study of OpenStreetMap and Ordnance Survey datasets. Environment and Planning B Planning and Design 682–703.

Halbedel, S., Koschorreck, M., 2013. Regulation of CO_2 emissions from temperate streams and reservoirs. Biogeosciences 10, 7539–7551. doi:10.5194/bg-10-7539-2013

Hannah, D.M., Demuth, S., van Lanen, H.A.J., Looser, U., Prudhomme, C., Rees, G., Stahl, K., Tallaksen, L.M., 2011. Large-scale river flow archives: importance, current status and future needs. Hydrological Processes 25, 1191–1200. doi:10.1002/hyp.7794

Hanson, P.C., Pace, M.L., Carpenter, S.R., Cole, J.J., Stanley, E.H., 2015. Integrating Landscape Carbon Cycling: Research Needs for Resolving Organic Carbon Budgets of Lakes. Ecosystems 18, 363–375. https://doi.org/10.1007/s10021-014-9826-9

Hartmann, J., Lauerwald, R., Moosdorf, N., 2014. A Brief Overview of the GLObal RIver Chemistry Database, GLORICH. Procedia Earth and Planetary Science 10, 23–27. doi:10.1016/j.proeps.2014.08.005

Harvey, A.M., 1991. The influence of sediment supply on the channel morphology of upland streams: Howgill Fells, Northwest England. Earth Surface Processes and Landforms 16, 675–684. doi:10.1002/esp.3290160711

Haunert, J.-H., Sester, M., 2007. Area Collapse and Road Centerlines based on Straight Skeletons. GeoInformatica 12, 169–191. doi:10.1007/s10707-007-0028-x

Hession, W.C., Pizzuto, J.E., Johnson, T.E., Horwitz, R.J., 2003. Influence of bank vegetation on channel morphology in rural and urban watersheds. Geology 31, 147–150. doi:10.1130/0091-7613(2003)031<0147:iobvoc>2.0.co;2

Hjulstrom, F., 1939. Transportation of detritus by moving water: Part 1. Transportation.

Horton, R.E., 1945. Erosional development of streams and their drainage basins; hydrophysical approach to quantitative morphology. Geological society of America bulletin 56, 275–370.

Hotchkiss, E.R., Hall Jr, R.O., Sponseller, R.A., Butman, D., Klaminder, J., Laudon, H., Rosvall, M., Karlsson, J., 2015. Sources of and processes controlling CO_2 emissions change with the size of streams and rivers. Nature Geosci 8, 696–699.

Huang, W., DeVries, B., Huang, C., Lang, M.W., Jones, J.W., Creed, I.F., Carroll, M.L., 2018. Automated Extraction of Surface Water Extent from Sentinel-1 Data. Remote Sensing 10, 797. https://doi.org/10.3390/rs10050797

Huete, A.R., 1988. A soil-adjusted vegetation index (SAVI). Remote Sensing of Environment 25, 295–309. doi:http://dx.doi.org/10.1016/0034-4257(88)90106-X

Hughes, R.M., Kaufmann, P.R., Weber, M.H., 2010. National and regional comparisons between Strahler order and stream size. Journal of the North American Benthological Society 30, 103–121. doi:10.1899/09-174.1

Hulme, M., 2010. Problems with making and governing global kinds of knowledge. Global Environmental Change 20, 558–564. doi:10.1016/j.gloenvcha.2010.07.005

Hunt, C.W., Snyder, L., Salisbury, J.E., Vandemark, D., McDowell, W.H., 2017. SIP CO_2: A simple, inexpensive surface water p CO_2 sensor. Limnol. Oceanogr. Methods n/a-n/a. doi:10.1002/lom3.10157

Iervolino, P., Guida, R., Iodice, A., Riccio, D., 2015. Flooding Water Depth Estimation With High-Resolution SAR. Geoscience and Remote Sensing, IEEE Transactions on 53, 2295–2307. doi:10.1109/TGRS.2014.2358501

Isikdogan, F., Bovik, A., Passalacqua, P., n.d. RivaMap: An automated river analysis and mapping engine. Remote Sensing of Environment. doi:10.1016/j.rse.2017.03.044

James, G., Witten, D., Hastie, T., Tibshirani, R., 2013. An introduction to statistical learning. Springer.

Jensen, J.R. (Ed.), 2013a. Remote Sensing of the Environment: An Earth Resource Perspective (Pearson New International Edition), 2nd ed. Pearson, Harlow.

Jensen, J.R., 2013b. Remote sensing of water, in: Jensen, J.R. (Ed.), Remote Sensing of the Environment: An Earth Resource Perspective (Pearson New International Edition). Pearson, Harlow, pp. 417–456.

Ji, L., Zhang, L., Wylie, B., 2009. Analysis of dynamic thresholds for the normalized difference water index. Photogrammetric Engineering and Remote Sensing 75, 1307–1317.

Jiang, Z., Huete, A.R., Didan, K., Miura, T., 2008. Development of a two-band enhanced vegetation index without a blue band. Remote Sensing of Environment 112, 3833–3845. doi:http://dx.doi.org/10.1016/j.rse.2008.06.006

Jollymore, A., Johnson, M.S., Hawthorne, I., 2012. Submersible UV-Vis Spectroscopy for Quantifying Streamwater Organic Carbon Dynamics: Implementation and Challenges before and after Forest Harvest in a Headwater Stream. Sensors 12. doi:10.3390/s120403798

Jones, J., 2015. Assessment of surface water bodies derived from Landsat.

Kempe, S., 1982. Long-term records of CO_2 pressure fluctuations in fresh waters. SCOPE/UNEP Sonderband 52, 91–332.

Khan, S., Hong, Y., Wang, J., 2012. Multispectral Satellite Data for Flood Monitoring and Inundation Mapping, in: Chang, N.B., Hong, Y. (Eds.), Multiscale Hydrologic Remote Sensing. CRC Press, Florida, pp. 251–268.

Klein, I., Gessner, U., Dietz, A.J., Kuenzer, C., 2017. Global WaterPack – A 250 m resolution dataset revealing the daily dynamics of global inland water bodies. Remote Sensing of Environment 198, 345–362. doi:10.1016/j.rse.2017.06.045

Kleinhans, M.G., 2010. Sorting out river channel patterns. Progress in Physical Geography 34, 287–326.

Kling, G.W., Kipphut, G.W., Miller, M.C., 1991. Arctic Lakes and Streams as Gas Conduits to the Atmosphere: Implications for Tundra Carbon Budgets. Science 251, 298–301. doi:10.1126/science.251.4991.298

Knighton, D., 1998. Fluvial forms and processes : a new perspective. Arnold.

Köhler, J., Hachoł, J., Hilt, S., 2010. Regulation of submersed macrophyte biomass in a temperate lowland river: Interactions between shading by bank vegetation, epiphyton and water turbidity. Aquatic Botany 92, 129–136. doi:10.1016/j.aquabot.2009.10.018

Kondolf, G.M., Montgomery, D.R., Piégay, H., Schmitt, L., 2003. Geomorphic Classification of Rivers and Streams, in: Tools in Fluvial Geomorphology. John Wiley & Sons, Ltd, pp. 171–204.

Kuhn, M., Johnson, K., 2013. Applied predictive modeling. Springer.

Lane, S.N., 2000. The Measurement of River Channel Morphology Using Digital Photogrammetry. The Photogrammetric Record 16, 937–961. doi:10.1111/0031-868X.00159

Lane, S.N., Richards, K.S., 1997. Linking river channel form and process: time, space and causality revisited. Earth Surface Processes and Landforms 22, 249–260.

Langerwisch, F., Walz, A., Rammig, A., Tietjen, B., Thonicke, K., Cramer, W., 2016. Climate change increases riverine carbon outgassing, while export to the ocean remains uncertain. Earth Syst. Dynam. 7, 559–582. doi:10.5194/esd-7-559-2016

Latapie, A., Camenen, B., Rodrigues, S., Paquier, A., Bouchard, J.P., Moatar, F., 2014. Assessing channel response of a long river influenced by human disturbance. CATENA 121, 1–12. doi:10.1016/j.catena.2014.04.017

Lauer, J.W., 2012. Channel planform statistics toolbox, 2.0. ed. NCED.

Lauerwald, R., Hartmann, J., Moosdorf, N., Kempe, S., Raymond, P.A., 2013. What controls the spatial patterns of the riverine carbonate system? — A case study for North America. Chemical Geology 337–338, 114–127. doi:10.1016/j.chemgeo.2012.11.011

Lauerwald, R., Laruelle, G.G., Hartmann, J., Ciais, P., Regnier, P.A.G., 2015. Spatial patterns in CO_2 evasion from the global river network. Global Biogeochem. Cycles 29, 534–554. doi:10.1002/2014GB004941

Lawlor, S.M., 2004. Determination of channel-morphology characteristics, bankfull discharge, and various design-peak discharges in western Montana (No. 2328-0328), Scientific Investigations Report 2004-5263. USGS.

Legleiter, C.J., Fonstad, M.A., 2012. An Introduction to the Physical Basis for Deriving River Information by Optical Remote Sensing, in: Fluvial Remote Sensing for Science and Management. John Wiley & Sons, Ltd, pp. 43–69.

Lehner, B., Döll, P., 2004. Development and validation of a global database of lakes, reservoirs and wetlands. Journal of Hydrology 296, 1–22. doi:http://dx.doi.org/10.1016/j.jhydrol.2004.03.028

Leigh, C., Boulton, A.J., Courtwright, J.L., Fritz, K., May, C.L., Walker, R.H., Datry, T., 2016. Ecological research and management of intermittent rivers: an historical review and future directions. Freshw Biol 61, 1181–1199. doi:10.1111/fwb.12646

Leopold, L.B., 1994. A View of the River. Harvard University Press.

Leopold, L.B., Maddock, T., 1953. The hydraulic geometry of stream channels and some physiographic implications.

Leopold, L.B., Wolman, M.G., 1957. River Channel Patterns: Braided, Meandering, and Straight.

Leopold, L.B., Wolman, M.G., Miller, J.P., 1964. Fluvial processes in geomorphology. WH Freeman and Co., San Francisco.

Lettenmaier, D.P., Alsdorf, D., Dozier, J., Huffman, G.J., Pan, M., Wood, E.F., 2015. Inroads of remote sensing into hydrologic science during the WRR era. Water Resources Research n/a–n/a. doi:10.1002/2015WR017616

Li, J., Wang, S., 2015. An automatic method for mapping inland surface waterbodies with Radarsat-2 imagery. International Journal of Remote Sensing 36, 1367–1384. doi:10.1080/01431161.2015.1009653

Li, W., Guo, Q., 2010. A maximum entropy approach to one-class classification of remote sensing imagery. International Journal of Remote Sensing 31, 2227–2235. doi:10.1080/01431161003702245

Li, X., Ling, F., Foody, G.M., Du, Y., 2016. Improving super-resolution mapping through combining multiple super-resolution land-cover maps. International Journal of Remote Sensing 37, 2415–2432. doi:10.1080/01431161.2016.1148288

Liu, S., Lu, X.X., Xia, X., Yang, X., Ran, L., 2017. Hydrological and geomorphological control on CO_2 outgassing from low-gradient large rivers: An example of the Yangtze River system. Journal of Hydrology 550, 26–41. doi:10.1016/j.jhydrol.2017.04.044

Liébault, F., Gomez, B., Page, M., Marden, M., Peacock, D., Richard, D., Trotter, C.M., 2005. Land-use change, sediment production and channel response in upland regions. River Research and Applications 21, 739–756. doi:10.1002/rra.880

Liébault, F., Piégay, H., 2001. Assessment of channel changes due to long-term bedload supply decrease, Roubion River, France. Geomorphology 36, 167–186. doi:http://dx.doi.org/10.1016/S0169-555X(00)00044-1

Love, M., Taylor, R.N., 2004. Fish passage evaluation at stream crossings (No. Part IX), California Salmonid Stream Habitat Restoration Manual. California Department of Fish and Wildlife, California.

Lowe, W.H., Likens, G.E., 2005. Moving Headwater Streams to the Head of the Class. BioScience 55, 196–197. doi:10.1641/0006-3568(2005)055[0196:MHSTTH]2.0.CO;2

Luke, A., Kaplan, B., Neal, J., Lant, J., Sanders, B., Bates, P., Alsdorf, D., 2015. Hydraulic modeling of the 2011 New Madrid Floodway activation: a case study on floodway activation controls. Natural Hazards 77, 1863–1887. doi:10.1007/s11069-015-1680-3

Mack, B., Roscher, R., Waske, B., 2014. Can I Trust My One-Class Classification? Remote Sensing 6, 8779–8802.

Malahlela, O.E., 2016. Inland waterbody mapping: towards improving discrimination and extraction of inland surface water features. International Journal of Remote Sensing 37, 4574–4589. doi:10.1080/01431161.2016.1217441

Manners, R.B., Schmidt, J.C., Scott, M.L., 2014. Mechanisms of vegetation-induced channel narrowing of an unregulated canyon river: Results from a natural field-scale experiment. Geomorphology 211, 100–115. doi:10.1016/j.geomorph.2013.12.033

Marcus, W.A., Fonstad, M.A., 2010. Remote sensing of rivers: the emergence of a subdiscipline in the river sciences. Earth Surface Processes and Landforms 35, 1867–1872. doi:10.1002/esp.2094

Marshall, M.R., Francis, O.J., Frogbrook, Z.L., Jackson, B.M., McIntyre, N., Reynolds, B., Solloway, I., Wheater, H.S., Chell, J., 2009. The impact of upland land management on flooding: results from an improved pasture hillslope. Hydrol. Process. 23, 464–475. doi:10.1002/hyp.7157

Martínez-Fernández, V., Solana-Gutiérrez, J., González del Tánago, M., García de Jalón, D., 2015. Automatic procedures for river reach delineation: Univariate and multivariate approaches in a fluvial context. Geomorphology. doi:10.1016/j.geomorph.2015.09.029

Martinis, S., Kersten, J., Twele, A., 2015. A fully automated TerraSAR-X based flood service. ISPRS Journal of Photogrammetry and Remote Sensing 104, 203–212. doi:10.1016/j.isprsjprs.2014.07.014

Marx, A., Dusek, J., Jankovec, J., Sanda, M., Vogel, T., van Geldern, R., Hartmann, J., Barth, J.A.C., 2017. A review of CO_2 and associated carbon dynamics in headwater streams: a global perspective. Rev. Geophys. n/a-n/a. doi:10.1002/2016RG000547

McAllister, M., Snoeyink, J., 2000. Medial axis generalization of river networks. Cartography and Geographic Information Science 27, 129–138.

McFeeters, S.K., 1996. The use of the Normalized Difference Water Index (NDWI) in the delineation of open water features. International Journal of Remote Sensing 17, 1425–1432. doi:10.1080/01431169608948714

McGuire, K., McDonell, J., 2007. Stable isotope tracers in watershed hydrology, in: Michener, R., Lajtha, K. (Eds.), Stable Isotopes in Ecology and Environmental Science. Blackwell Publishing, Oxford, pp. 334–374.

McKean, J., Nagel, D., Tonina, D., Bailey, P., Wright, C.W., Bohn, C., Nayegandhi, A., n.d. Remote Sensing of Channels and Riparian Zones with a Narrow-Beam Aquatic-Terrestrial LIDAR. Remote Sensing 1, 1065–1096. doi:10.3390/rs1041065

Memarsadeghi, N., Mount, D.M., Netanyahu, N.S., Le Moigne, J., 2007. A fast implementation of the ISODATA clustering algorithm. International Journal of Computational Geometry & Applications 17, 71–103.

Mennis, J., 2006. Mapping the Results of Geographically Weighted Regression. The Cartographic Journal 43, 171–179. doi:10.1179/000870406X114658

Merwade, V.M., 2007. An Automated GIS Procedure for Delineating River and Lake Boundaries. Transactions in GIS 11, 213–231. doi:10.1111/j.1467-9671.2007.01042.x

Mewse, C., 2016. That sweet spot between UAV and large format survey.

Miller, Z.F., Pavelsky, T.M., Allen, G.H., 2014. Quantifying river form variations in the Mississippi Basin using remotely sensed imagery. Hydrol. Earth Syst. Sci. 18, 4883–4895. doi:10.5194/hess-18-4883-2014

Mioc, D., Antón Castro, F., Dharmaraj, G., 2004. An algorithm for centerline extraction using natural neighbour interpolation, in: 20th ISPRS Congress.

Mnih, V., Hinton, G.E., 2010. Learning to Detect Roads in High-Resolution Aerial Images, in: Daniilidis, K., Maragos, P., Paragios, N. (Eds.), Computer Vision – ECCV 2010. Springer Berlin Heidelberg, pp. 210–223.

Montgomery, D.R., 1997. River management: What's best on the banks? Nature 388, 328–329.

Montgomery, D.R., Gran, K.B., 2001. Downstream variations in the width of bedrock channels. Water Resources Research 37, 1841–1846. doi:10.1029/2000WR900393

Morel, F.M., Hering, J.G., 1993. Principles and applications of aquatic chemistry. John Wiley & Sons.

Mount, N., Stott, T., 2008. A discrete Bayesian network to investigate suspended sediment concentrations in an Alpine proglacial zone. Hydrol. Process. 22, 3772–3784. doi:10.1002/hyp.6981

Mulholland, P.J., Helton, A.M., Poole, G.C., Hall, R.O., Hamilton, S.K., Peterson, B.J., Tank, J.L., Ashkenas, L.R., Cooper, L.W., Dahm, C.N., Dodds, W.K., Findlay, S.E.G., Gregory, S.V., Grimm, N.B., Johnson, S.L., McDowell, W.H., Meyer, J.L., Valett, H.M., Webster, J.R., Arango, C.P., Beaulieu, J.J., Bernot, M.J., Burgin, A.J., Crenshaw, C.L., Johnson, L.T., Niederlehner, B.R., O'Brien, J.M., Potter, J.D., Sheibley, R.W., Sobota, D.J., Thomas, S.M., 2008. Stream denitrification across biomes and its response to anthropogenic nitrate loading. Nature 452, 202–205. doi:10.1038/nature06686

Muslim, A.M., Foody, G.M., Atkinson, P.M., 2006. Localized soft classification for super-resolution mapping of the shoreline. International Journal of Remote Sensing 27, 2271–2285. doi:10.1080/01431160500396741

Myhre, G., Shindell, D., Bréon, F.-M., Collins, W., Fuglestvedt, J., Huang, J., Koch, D., Lamarque, J.-F., Lee, D., Mendoza, B., 2013. Anthropogenic and natural radiative forcing, in: Climate Change 2013: The Physical Science Basis. Contribution of Working Group I to the Fifth Assessment Report of the Intergovernmental Panel on Climate Change.

Myint, S.W., 2006. Urban vegetation mapping using sub-pixel analysis and expert system rules: A critical approach. International Journal of Remote Sensing 27, 2645–2665. doi:10.1080/01431160500534630

NASA, 2012. SWOT: Surface Water and Ocean Topography mission. California Institute of Technology, Pasadena, California.

Nazir, M., Awang, S., Shaaban, A., Yahaya, N., Jusoh, A., Arumugan, M., Ghani, A., 2016. Sediment Transport Dynamic in a Meandering Fluvial System: Case Study of Chini River. IOP Conference Series: Materials Science and Engineering 136, 012072.

Newson, M.D., Clark, M.J., Sear, D.A., Brookes, A., 1998. The geomorphological basis for classifying rivers. Aquatic Conservation: Marine and Freshwater Ecosystems 8, 415–430. doi:10.1002/(SICI)1099-0755(199807/08)8:4<415::AID-AQC276>3.0.CO;2-6

Newson, M.D., Large, A.R.G., 2006. "Natural" rivers, "hydromorphological quality" and river restoration: a challenging new agenda for applied fluvial geomorphology. Earth Surface Processes and Landforms 31, 1606–1624. doi:10.1002/esp.1430

Nickerson, B.G., 1988. Automated Cartographic Generalization For Linear Features. Cartographica: The International Journal for Geographic Information and Geovisualization 25, 15–66. doi:10.3138/4144-3U7G-MW01-1Q72

Nyberg, B., Buckley, S.J., Howell, J.A., Nanson, R.A., 2015. Geometric attribute and shape characterization of modern depositional elements: A quantitative GIS method for empirical analysis. Computers & Geosciences 82, 191–204. doi:10.1016/j.cageo.2015.06.003

Ogle, K., Barber, J.J., Barron-Gafford, G.A., Bentley, L.P., Young, J.M., Huxman, T.E., Loik, M.E., Tissue, D.T., 2015. Quantifying ecological memory in plant and ecosystem processes. Ecology Letters 18, 221–235. doi:10.1111/ele.12399

Okabe, A., Satoh, T., 2009. Spatial Analysis on a Network, in: Fotheringham, A.S., Rogerson, P.A. (Eds.), The SAGE Handbook of Spatial Analysis. SAGE Publications Ltd, London, pp. 443–465.

Öquist, M.G., Wallin, M., Seibert, J., Bishop, K., Laudon, H., 2009. Dissolved Inorganic Carbon Export Across the Soil/Stream Interface and Its Fate in a Boreal Headwater Stream. Environmental Science & Technology 43, 7364–7369. doi:10.1021/es900416h

Ordnance Survey, 2005. GB National Outlines [SHAPE geospatial data], Scale 1:250000. EDINA Digimap Ordnance Survey Service.

Ordnance Survey, 2016a. OS MasterMap Topography Layer user guide. Ordnance Survey.

Ordnance Survey, 2016b. OS VectorMap District: User guide and technical specification. Ordnance Survey.

Osborn, T.J., Gosling, S.N., Wallace, C.J., Dorling, S., 2015. The water cycle in a changing climate, in: 7th World Water Forum, Words Into Action. Faircount Media Group, London, pp. 14–19.

Pal, M., Foody, G.M., 2012. Evaluation of SVM, RVM and SMLR for accurate image classification with limited ground data. Selected Topics in Applied Earth Observations and Remote Sensing, IEEE Journal of 5, 1344–1355.

Palmer, S.C.J., Kutser, T., Hunter, P.D., 2015. Remote sensing of inland waters: Challenges, progress and future directions. Remote Sensing of Environment 157, 1–8. doi:10.1016/j.rse.2014.09.021

Parkhurst, D.L., Appelo, C., 1999. User's guide to PHREEQC (Version 2): A computer program for speciation, batch-reaction, one-dimensional transport, and inverse geochemical calculations, Water-Resources Investigations Report 99-4259. USGS, Denver, Colorado.

Passalacqua, P., Belmont, P., Foufoula-Georgiou, E., 2012. Automatic geomorphic feature extraction from lidar in flat and engineered landscapes. Water Resources Research 48, n/a–n/a. doi:10.1029/2011WR010958

Patton, P.C., Baker, V.R., 1976. Morphometry and floods in small drainage basins subject to diverse hydrogeomorphic controls. Water Resources Research 12, 941–952. doi:10.1029/WR012i005p00941

Pavelsky, T.M., 2014. Using width-based rating curves from spatially discontinuous satellite imagery to monitor river discharge. Hydrol. Process. 28, 3035–3040. doi:10.1002/hyp.10157

Pavelsky, T.M., Smith, L.C., 2008. RivWidth: A Software Tool for the Calculation of River Widths From Remotely Sensed Imagery. IEEE Geoscience and Remote Sensing Letters 5, 70–73.

Pearson, C., Reaney, S., Bracken, L., Butler, L., 2015. Investigating the potential to reduce flood risk through catchment-based land management techniques and interventions in the River Roe catchment, Cumbria, UK. Presented at the EGU General Assembly 2015, Vienna, Austria, p. 1001.

Pekel, J.-F., Cottam, A., Gorelick, N., Belward, A.S., 2016. High-resolution mapping of global surface water and its long-term changes. Nature 540, 418–422.

Peter, H., Singer, G.A., Preiler, C., Chifflard, P., Steniczka, G., Battin, T.J., 2014. Scales and drivers of temporal p CO_2 dynamics in an Alpine stream. J. Geophys. Res. Biogeosci. 119, 1078–1091. doi:10.1002/2013JG002552

Peterson, B.J., Wollheim, W.M., Mulholland, P.J., Webster, J.R., Meyer, J.L., Tank, J.L., Martí, E., Bowden, W.B., Valett, H.M., Hershey, A.E., McDowell, W.H., Dodds, W.K., Hamilton, S.K., Gregory, S., Morrall, D.D., 2001. Control of Nitrogen Export from Watersheds by Headwater Streams. Science 292, 86–90. doi:10.1126/science.1056874

Piao, S., Friedlingstein, P., Ciais, P., de Noblet-Ducoudré, N., Labat, D., Zaehle, S., 2007. Changes in climate and land use have a larger direct impact than rising CO_2 on global river runoff trends. Proceedings of the National Academy of Sciences 104, 15242–15247.

Piégay, H., Mathias Kondolf, G., Toby Minear, J., Vaudor, L., 2015. Trends in publications in fluvial geomorphology over two decades: A truly new era in the discipline owing to recent technological revolution? Geomorphology 248, 489–500. doi:10.1016/j.geomorph.2015.07.039

Piégay, H., Schumm, S.A., 2003. System Approaches in Fluvial Geomorphology, in: Tools in Fluvial Geomorphology. John Wiley & Sons, Ltd, pp. 103–134.

Powell, R.L., Matzke, N., De Souza, C., Clark, M., Numata, I., Hess, L.L., Roberts, D. A., 2004. Sources of error in accuracy assessment of thematic land-cover maps in the Brazilian Amazon. Remote Sensing of Environment 90, 221–234. doi:http://dx.doi.org/10.1016/j.rse.2003.12.007

Pulvirenti, L., Pierdicca, N., Chini, M., Guerriero, L., 2011. An algorithm for operational flood mapping from Synthetic Aperture Radar (SAR) data based on the fuzzy logic. Natural Hazard and Earth System Sciences. doi:10.5194/nhess-11-529-2011

Puttock, A.K., Cunliffe, A.M., Anderson, K., Brazier, R.E., 2015. Aerial photography collected with a multirotor drone reveals impact of Eurasian beaver reintroduction on ecosystem structure. J. Unmanned Veh. Sys. 3, 123–130. doi:10.1139/juvs-2015-0005

Quackenbush, L.J., 2004. A Review of Techniques for Extracting Linear Features from Imagery. Photogrammetric Engineering & Remote Sensing 70, 1383–1392.

R Core Team, 2017. R: A language and environment for statistical computing - Reference Index [WWW Document]. URL https://cran.r-project.org/doc/manuals/r-release/fullrefman.pdf (accessed 9.28.17).

Rantakari, M., Mattsson, T., Kortelainen, P., Piirainen, S., Finér, L., Ahtiainen, M., 2010. Organic and inorganic carbon concentrations and fluxes from managed and unmanaged boreal first-order catchments. Science of The Total Environment 408, 1649–1658. doi:10.1016/j.scitotenv.2009.12.025

Raven, P.J., Holmes, N.T.H., Dawson, F.H., Everard, M., 1998. Quality assessment using River Habitat Survey data. Aquatic Conservation: Marine and Freshwater Ecosystems 8, 477–499. doi:10.1002/(SICI)1099-0755(199807/08)8:4<477::AID-AQC299>3.0.CO;2-K

Raven, P.J., Holmes, N.T.H., Vaughan, I.P., Dawson, F.H., Scarlett, P., 2010. Benchmarking habitat quality: observations using River Habitat Survey on near-natural streams and rivers in northern and western Europe. Aquatic Conservation: Marine and Freshwater Ecosystems 20, S13–S30. doi:10.1002/aqc.1103

Rawlins, B.G., Clark, L., Boyd, D.S., 2014a. Using air photos to parameterize landscape predictors of channel wetted width. Earth Surface Processes and Landforms 39, 605–613. doi:10.1002/esp.3469

Rawlins, B.G., Palumbo-Roe, B., Gooddy, D.C., Worrall, F., Smith, H., 2014b. A model of potential carbon dioxide efflux from surface water across England and Wales using headwater stream survey data and landscape predictors. Biogeosciences 11, 1911–1925.

Raymond, P., Cole, J., 2001. Gas exchange in rivers and estuaries: Choosing a gas transfer velocity. Estuaries 24, 312–317. doi:10.2307/1352954

Raymond, P.A., Hartmann, J., Lauerwald, R., Sobek, S., McDonald, C., Hoover, M., Butman, D., Striegl, R., Mayorga, E., Humborg, C., Kortelainen, P., Durr, H., Meybeck, M., Ciais, P., Guth, P., 2013. Global carbon dioxide emissions from inland waters. Nature 503, 355–359. doi:10.1038/nature12760 http://www.nature.com/nature/journal/v503/n7476/abs/nature12760.html#supplementary-information

Regnauld, N., Mackaness, W.A., 2006. Creating a hydrographic network from its cartographic representation: a case study using Ordnance Survey MasterMap data. International Journal of Geographical Information Science 20, 611–631. doi:10.1080/13658810600607402

Regnier, P., Friedlingstein, P., Ciais, P., Mackenzie, F.T., Gruber, N., Janssens, I.A., Laruelle, G.G., Lauerwald, R., Luyssaert, S., Andersson, A.J., Arndt, S., Arnosti, C., Borges, A.V., Dale, A.W., Gallego-Sala, A., Godderis, Y., Goossens, N., Hartmann, J., Heinze, C., Ilyina, T., Joos, F., LaRowe, D.E., Leifeld, J., Meysman, F.J.R., Munhoven, G., Raymond, P.A., Spahni, R., Suntharalingam, P., Thullner, M., 2013. Anthropogenic perturbation of the carbon fluxes from land to ocean. Nature Geosci 6, 597–607.

Rennie, S., Adamson, J., Anderson, R., Andrews, C., Bater, J., Bayfield, N., Beaton, K., Beaumont, D., Benham, S., Bowmaker, V., Britt, C., Brooker, R., Brooks, D., Brunt, J., Common, G., Cooper, R., Corbett, S., Critchley, N., Dennis, P., Dick, J., Dodd, B., Dodd, N., Donovan, N., Easter, J., Eaton, E., Flexen, M., Gardiner, A., Hamilton, D., Hargreaves, P., Hatton-Ellis, M., Howe, M., Kahl, J., Lane, M., Langan, S., Lloyd, D., McElarney, Y., McKenna, C., McMillan, S., Milne, F., Milne, L., Morecroft, M., Murphy, M., Nelson, A., Nicholson, H., Pallett, D., Parry, D., Pearce, I., Pozsgai, G., Rose, R., Schafer, S., Scott, T., Sherrin, L., Shortall, C., Smith, R., Smith, P., Tait, R., Taylor, C., Taylor, M., Thurlow, M., Turner, A., Tyson, K., Watson, H., Whittaker, M., 2015a. UK Environmental Change Network (ECN) stream water chemistry data: 1992-2012 [WWW Document]. NERC Environmental Information Data Centre. URL https://doi.org/10.5285/5a715fd9-aefa-40cc-bbb6-56984b6db554 (accessed 4.11.16).

Rennie, S., Adamson, J., Anderson, R., Andrews, C., Bater, J., Bayfield, N., Beaton, K., Beaumont, D., Benham, S., Bowmaker, V., Britt, C., Brooker, R., Brooks, D., Brunt, J., Common, G., Cooper, R., Corbett, S., Critchley, N., Dennis, P., Dick, J., Dodd, B., Dodd, N., Donovan, N., Easter, J., Eaton, E., Flexen, M., Gardiner, A., Hamilton, D., Hargreaves, P., Hatton-Ellis, M., Howe, M., Kahl, J., Lane, M., Langan, S., Lloyd, D., McElarney, Y., McKenna, C., McMillan, S., Milne, F., Milne, L., Morecroft, M., Murphy, M., Nelson, A., Nicholson, H., Pallett, D., Parry, D., Pearce, I., Pozsgai, G., Rose, R., Schafer, S., Scott, T., Sherrin, L., Shortall, C., Smith, R., Smith, P., Tait, R., Taylor, C., Taylor, M.,

Thurlow, M., Turner, A., Tyson, K., Watson, H., Whittaker, M., 2015b. UK Environmental Change Network (ECN) stream water discharge data: 1993-2012 [WWW Document]. NERC Environmental Information Data Centre. URL https://doi.org/10.5285/f39f4588-0255-47b4-a61b-03848eb2f8c4 (accessed 4.11.16).

Revilla-Romero, B., Beck, H.E., Burek, P., Salamon, P., de Roo, A., Thielen, J., 2015. Filling the gaps: Calibrating a rainfall-runoff model using satellite-derived surface water extent. Remote Sensing of Environment 171, 118–131. doi:10.1016/j.rse.2015.10.022

Richey, J.E., Melack, J.M., Aufdenkampe, A.K., Ballester, V.M., Hess, L.L., 2002. Outgassing from Amazonian rivers and wetlands as a large tropical source of atmospheric CO_2. Nature 416, 617–620.

Ripley, B., 2016. Package "tree."

Riverdene Consultancy, 2016. Instructions for calculating the Habitat Modification Score using River Habitat Survey data [WWW Document]. URL http://www.riverhabitatsurvey.org/wp-content/uploads/2016/03/Habitat-Modification-Score-Rules-2003-RC.pdf (accessed 4.1.16).

Rodríguez-Cuenca, B., Alonso, M., 2014. Semi-Automatic Detection of Swimming Pools from Aerial High-Resolution Images and LIDAR Data. Remote Sensing 6, 2628–2646.

Rouse, J.W., Haas, R.H., Schell, J.A., Deering, D.W., Harlan, J.C., 1974. Monitoring the vernal advancement and retrogradation (greenwave effect) of natural vegetation. Texas A & M University, Remote Sensing Center.

Roux, C., Alber, A., Bertrand, M., Vaudor, L., Piégay, H., n.d. "FluvialCorridor": A new ArcGIS toolbox package for multiscale riverscape exploration. Geomorphology. doi:http://dx.doi.org/10.1016/j.geomorph.2014.04.018

Rowland, J.C., Shelef, E., Pope, P.A., Muss, J., Gangodagamage, C., Brumby, S.P., Wilson, C.J., 2016. A morphology independent methodology for quantifying planview river change and characteristics from remotely sensed imagery. Remote Sensing of Environment 184, 212–228. doi:10.1016/j.rse.2016.07.005

Ruhala, S.S., Zarnetske, J.P., 2016. Using in-situ optical sensors to study dissolved organic carbon dynamics of streams and watersheds: A review. Science of The Total Environment. doi:10.1016/j.scitotenv.2016.09.113

Sagin, J., Sizo, A., Wheater, H., Jardine, T.D., Lindenschmidt, K.-E., 2015. A water coverage extraction approach to track inundation in the Saskatchewan River Delta, Canada. International Journal of Remote Sensing 36, 764–781. doi:10.1080/01431161.2014.1001084

Salazar, S., Francés, F., Komma, J., Blume, T., Francke, T., Bronstert, A., Blöschl, G., 2012. A comparative analysis of the effectiveness of flood management measures based on the concept of "retaining water in the landscape" in different European hydro-climatic regions. Nat. Hazards Earth Syst. Sci. 12, 3287–3306. doi:10.5194/nhess-12-3287-2012

Schade, J.D., Bailio, J., McDowell, W.H., 2016. Greenhouse gas flux from headwater streams in New Hampshire, USA: Patterns and drivers. Limnol. Oceanogr. n/a-n/a. doi:10.1002/lno.10337

Schelker, J., Singer, G.A., Ulseth, A.J., Hengsberger, S., Battin, T.J., 2016. CO_2 evasion from a steep, high gradient stream network: importance of seasonal and diurnal variation in aquatic p CO_2 and gas transfer. Limnol. Oceanogr. 61, 1826–1838. doi:10.1002/lno.10339

Schlesinger, W.H., Melack, J.M., 1981. Transport of organic carbon in the world's rivers. Tellus 33, 172–187. https://doi.org/10.1111/j.2153-3490.1981.tb01742.x

Schumm, S.A., 1977. The Fluvial System. Wiley New York.

Schumm, S.A., 1967. Meander Wavelength of Alluvial Rivers. Science 157, 1549–1550.

Sear, D., Newson, M.D., Thorne, C.R., 2010. Guidebook of applied fluvial geomorphology. Thomas Telford.

Sharaf El Din, E., Zhang, Y., Suliman, A., 2017. Mapping concentrations of surface water quality parameters using a novel remote sensing and artificial intelligence framework. International Journal of Remote Sensing 38, 1023–1042. doi:10.1080/01431161.2016.1275056

Sharp, R., 2014. Investigating hillslope afforestation as a potential natural flood management strategy in the Eddleston Water catchment, Scottish Borders. The University of Edinburgh.

Sheldon, F., Bunn, S.E., Hughes, J.M., Arthington, A.H., Balcombe, S.R., Fellows, C.S., 2010. Ecological roles and threats to aquatic refugia in arid landscapes: dryland river waterholes. Marine and Freshwater Research 61, 885–895.

Sheng, Y., Shah, C.A., Smith, L.C., 2008. Automated image registration for hydrologic change detection in the lake-rich Arctic. Geoscience and Remote Sensing Letters, IEEE 5, 414–418.

Shields, F.D., Simon, A., Steffen, L.J., 2000. Reservoir effects on downstream river channel migration. Environmental Conservation 27, 54–66. doi:doi:null

Silva, J., Bacao, F., Dieng, M., Foody, G.M., Caetano, M., 2017. Improving specific class mapping from remotely sensed data by cost-sensitive learning. International Journal of Remote Sensing 38, 3294–3316. doi:10.1080/01431161.2017.1292073

Singh, V.P., 2003. On the theories of hydraulic geometry. International Journal of Sediment Research 18, 196–218.

Sivanpillai, R., Miller, S.N., 2010. Improvements in mapping water bodies using ASTER data. Ecological Informatics 5, 73–78. doi:http://dx.doi.org/10.1016/j.ecoinf.2009.09.013

Smith, L.C., Isacks, B.L., Bloom, A.L., Murray, A.B., 1996. Estimation of Discharge From Three Braided Rivers Using Synthetic Aperture Radar Satellite Imagery: Potential Application to Ungaged Basins. Water Resources Research 32, 2021–2034. doi:10.1029/96WR00752

Smith, M.J.D., Goodchild, M.F., Longley, P., 2007. Geospatial Analysis: A Comprehensive Guide to Principles, Techniques and Software Tools. Troubador Publishing Ltd.

Smits, A.P., Schindler, D.E., Holtgrieve, G.W., Jankowski, K.J., French, D.W., 2017. Watershed geomorphology interacts with precipitation to influence the magnitude and source of CO_2 emissions from Alaskan streams. J. Geophys. Res. Biogeosci. n/a-n/a. doi:10.1002/2017JG003792

Sofia, G., Tarolli, P., Cazorzi, F., Dalla Fontana, G., 2015. Downstream hydraulic geometry relationships: Gathering reference reach-scale width values from LiDAR. Geomorphology 250, 236–248. doi:10.1016/j.geomorph.2015.09.002

Spatial Ecology, 2014. Geospatial Modelling Environment, 0.7.3. ed.

Stanley, E.H., Casson, N.J., Christel, S.T., Crawford, J.T., Loken, L.C., Oliver, S.K., 2016. The ecology of methane in streams and rivers: patterns, controls, and global significance. Ecol Monogr 86, 146–171. doi:10.1890/15-1027

Stark, C.P., 2006. A self-regulating model of bedrock river channel geometry. Geophys. Res. Lett. 33, n/a-n/a. doi:10.1029/2005GL023193

Stavins, R.N., 1997. Policy instruments for climate change: how can national governments address a global problem. University of Chicago Legal Forum 293.

Strahler, A.N., 1957. Quantitative analysis of watershed geomorphology. Transactions of the American Geophysical Union 38, 913–920.

Strahler, A.N., 1956. The nature of induced erosion and aggradation. Man's Role in Changing the Face of the Earth 2, 621–638.

Strahler, A.N., 1952. Hypsometric (area-altitude) analysis of erosional topography. Geological society of America bulletin 63.

Sturt, M.M., Jansen, M. a. K., Harrison, S.S.C., 2011. Invertebrate grazing and riparian shade as controllers of nuisance algae in a eutrophic river. Freshwater Biology 56, 2580–2593. doi:10.1111/j.1365-2427.2011.02684.x

Su, Y.-F., Foody, G.M., Muad, A.M., Cheng, K.-S., 2012a. Combining pixel swapping and contouring methods to enhance super-resolution mapping. Selected Topics in Applied Earth Observations and Remote Sensing, IEEE Journal of 5, 1428–1437.

Su, Y.-F., Foody, G.M., Muad, A.M., Cheng, K.-S., 2012b. Combining Hopfield neural network and contouring methods to enhance super-resolution mapping. Selected Topics in Applied Earth Observations and Remote Sensing, IEEE Journal of 5, 1403–1417.

Sun, F., Sun, W., Chen, J., Gong, P., 2012. Comparison and improvement of methods for identifying waterbodies in remotely sensed imagery. International Journal of Remote Sensing 33, 6854–6875. doi:10.1080/01431161.2012.692829

Tal, M., Paola, C., 2010. Effects of vegetation on channel morphodynamics: results and insights from laboratory experiments. Earth Surface Processes and Landforms 35, 1014–1028. doi:10.1002/esp.1908

Tamminga, A., Hugenholtz, C., Eaton, B., Lapointe, M., 2015. Hyperspatial Remote Sensing of Channel Reach Morphology and Hydraulic Fish Habitat Using an Unmanned Aerial Vehicle (UAV): A First Assessment in the Context of River Research and Management. River Res. Applic. 31, 379–391. doi:10.1002/rra.2743

Tarolli, P., 2014. High-resolution topography for understanding Earth surface processes: Opportunities and challenges. Geomorphology 216, 295–312. doi:http://dx.doi.org/10.1016/j.geomorph.2014.03.008

Tatem, A.J., Lewis, H.G., Atkinson, P.M., Nixon, M.S., 2002. Super-resolution land cover pattern prediction using a Hopfield neural network. Remote Sensing of Environment 79, 1–14. doi:http://dx.doi.org/10.1016/S0034-4257(01)00229-2

Teodoru, C.R., Nyoni, F.C., Borges, A.V., Darchambeau, F., Nyambe, I., Bouillon, S., 2015. Dynamics of greenhouse gases (CO_2, CH_4, N_2O) along the Zambezi River and major tributaries, and their importance in the riverine carbon budget. Biogeosciences 12, 2431–2453. doi:10.5194/bg-12-2431-2015

Thomlinson, J.R., Bolstad, P.V., Cohen, W.B., 1999. Coordinating methodologies for scaling landcover classifications from site-specific to global: Steps toward validating global map products. Remote Sensing of Environment 70, 16–28. doi:http://dx.doi.org/10.1016/S0034-4257(99)00055-3

Thorne, C.R., 1998a. Stream reconnaissance handbook: geomorphological investigation and analysis of river channels. John Wiley & Sons Ltd.

Thorne, C.R., 1998b. River width adjustment II: Modeling. Journal of Hydraulic Engineering 124, 903–917.

Thorne, C.R., Allen, R.G., Simon, A., 1996. Geomorphological river channel reconnaissance for river analysis, engineering and management. Transactions of the Institute of British Geographers 469–483.

Thornton, M.W., Atkinson, P.M., Holland, D.A., 2007. A linearised pixel-swapping method for mapping rural linear land cover features from fine spatial resolution remotely sensed imagery. Computers & Geosciences 33, 1261–1272.

Ticehurst, C., Guerschman, J.P., Chen, Y., 2014. The Strengths and Limitations in Using the Daily MODIS Open Water Likelihood Algorithm for Identifying Flood Events. Remote Sensing 6, 11791–11809.

Tobler, W.R., 1970. A Computer Movie Simulating Urban Growth in the Detroit Region. Economic Geography 46, 234–240. doi:10.2307/143141

Tranvik, L.J., Cole, J.J., Prairie, Y.T., 2018. The study of carbon in inland waters—from isolated ecosystems to players in the global carbon cycle. Limnology and Oceanography Letters 3, 41–48. https://doi.org/10.1002/lol2.10068

Tranvik, L.J., Downing, J.A., Cotner, J.B., Loiselle, S.A., Striegl, R.G., Ballatore, T.J., Dillon, P., Finlay, K., Fortino, K., Knoll, L.B., Kortelainen, P.L., Kutser, T., Larsen, S., Laurion, I., Leech, D.M., McCallister, S.L., McKnight, D.M., Melack, J.M., Overholt, E., Porter, J.A., Prairie, Y., Renwick, W.H., Roland, F., Sherman, B.S., Schindler, D.W., Sobek, S., Tremblay, A., Vanni, M.J., Verschoor, A.M., von Wachenfeldt, E., Weyhenmeyer, G.A., 2009. Lakes and reservoirs as regulators of carbon cycling and climate. Limnol. Oceanogr. 54, 2298–2314. doi:10.4319/lo.2009.54.6_part_2.2298

Tucker, C.J., 1979. Red and photographic infrared linear combinations for monitoring vegetation. Remote Sensing of Environment 8, 127–150.

Tulbure, M.G., Broich, M., 2013. Spatiotemporal dynamic of surface water bodies using Landsat time-series data from 1999 to 2011. ISPRS Journal of Photogrammetry and Remote Sensing 79, 44–52. doi:10.1016/j.isprsjprs.2013.01.010

Turnpenny, J., Haxeltine, A., Lorenzoni, I., O'Riordan, T., Jones, M., 2005. Mapping actors involved in climate change policy networks in the UK. Tyndall Centre for Climate Change Research, Working Paper 66.

Tveite, H., 1999. An accuracy assessment method for geographical line data sets based on buffering. International Journal of Geographical Information Science 13, 27–47. doi:10.1080/136588199241445

UKTAG, 2003a. Guidance on the identification of small surface water bodies.

UKTAG, 2003b. Guidance on Typology for Rivers for Scotland, England and Wales (final working paper). UK Technical Advisory Group on the Water Framework Directive.

Ünsalan, C., Boyer, K.L., 2011. Remote Sensing Satellites and Airborne Sensors, in: Multispectral Satellite Image Understanding. Springer, London, pp. 7–15.

US Army Corps of Engineers Hydrologic Engineering Centre, n.d. HEC-GeoRAS, ArcGIS 10. ed.

USGS, 2016. Provisional Dynamic Surface Water Extent Overview [WWW Document]. URL http://remotesensing.usgs.gov/ecv/SWE_overview.php

Vachon, D., Prairie, Y.T., Cole, J.J., 2010. The relationship between near-surface turbulence and gas transfer velocity in freshwater systems and its implications for floating chamber measurements of gas exchange. Limnology and Oceanography 55, 1723.

Vanderbilt, V.C., Khanna, S., Ustin, S.L., 2007. Impact of pixel size on mapping surface water in subsolar imagery. Remote Sensing of Environment 109, 1–9. doi:10.1016/j.rse.2006.12.009

Verpoorter, C., Kutser, T., Tranvik, L., 2012. Automated mapping of water bodies using Landsat multispectral data. Limnol. Oceanogr.: Methods 10, 1037–1050.

Verpoorter, C., Kutser, T., Seekell, D.A., Tranvik, L.J., 2014. A global inventory of lakes based on high-resolution satellite imagery. Geophysical Research Letters 41, 6396–6402. doi:10.1002/2014GL060641

Vitousek, P.M., Mooney, H.A., Lubchenco, J., Melillo, J.M., 1997. Human Domination of Earth's Ecosystems. Science 277, 494–499. doi:10.1126/science.277.5325.494

Vogel, R.M., 2011. Hydromorphology. Journal of Water Resources Planning and Management 137, 147–149.

von Schiller, D., Marcé, R., Obrador, B., Gómez, L., Casas, J.P., Acuña, V., Koschorreck, M., 2014. Carbon dioxide emissions from dry watercourses. Inland Waters 4, 377–382.

Wallin, M.B., Grabs, T., Buffam, I., Laudon, H., Agren, A., Oquist, M.G., Bishop, K., 2013. Evasion of CO_2 from streams - the dominant component of the carbon export through the aquatic conduit in a boreal landscape. Glob Chang Biol 19, 785–797. doi:10.1111/gcb.12083

Wallin, M.B., Öquist, M.G., Buffam, I., Billett, M.F., Nisell, J., Bishop, K.H., 2011. Spatiotemporal variability of the gas transfer coefficient (K CO_2) in boreal streams: Implications for large scale estimates of CO_2 evasion. Global Biogeochemical Cycles 25, n/a–n/a. doi:10.1029/2010gb003975

Wang, Z., Müller, J.-C., 1998. Line generalization based on analysis of shape characteristics. Cartography and Geographic Information Systems 25, 3–15.

Wanninkhof, R., Mulholland, P.J., Elwood, J.W., 1990. Gas exchange rates for a first-order stream determined with deliberate and natural tracers. Water Resources Research 26, 1621–1630. doi:10.1029/WR026i007p01621

Ward, N.D., Bianchi, T.S., Medeiros, P.M., Seidel, M., Richey, J.E., Keil, R.G., Sawakuchi, H.O., 2017. Where Carbon Goes When Water Flows: Carbon Cycling across the Aquatic Continuum. Frontiers in Marine Science 4, 7. doi:10.3389/fmars.2017.00007

Warner, T.A., Nellis, M.D., Foody, G.M. (Eds.), 2009. The SAGE Handbook of Remote Sensing. SAGE Publications Ltd, London.

Wehrli, B., 2013. Biogeochemistry: Conduits of the carbon cycle. Nature 503, 346–347. https://doi.org/10.1038/503346a

Westaway, R.M., Lane, S.N., Hicks, D.M., 2003. Remote survey of large-scale braided, gravel-bed rivers using digital photogrammetry and image analysis. International Journal of Remote Sensing 24, 795–815. doi:10.1080/01431160110113070

Weyhenmeyer, G.A., Mackay, M., Stockwell, J.D., Thiery, W., Grossart, H.-P., Augusto-Silva, P.B., Baulch, H.M., de Eyto, E., Hejzlar, J., Kangur, K., Kirillin, G., Pierson, D.C., Rusak, J.A., Sadro, S., Woolway, R.I., 2017. Citizen science shows systematic changes in the temperature difference between air and inland waters with global warming. Scientific Reports 7, 43890.

Whipple, K.X., Hancock, G.S., Anderson, R.S., 2000. River incision into bedrock: Mechanics and relative efficacy of plucking, abrasion, and cavitation. Geological Society of America Bulletin 112, 490–503.

Whiteaker, T.L., Maidment, D.R., Gopalan, H., Patino, C., McKinney, D.C., 2007. Raster network regionalization for watershed data processing. International Journal of Geographical Information Science 21, 341–353. doi:10.1080/13658810600965255

Whittaker, A.C., Cowie, P.A., Attal, M., Tucker, G.E., Roberts, G.P., 2007. Bedrock channel adjustment to tectonic forcing: Implications for predicting river incision rates. Geology 35, 103–106. doi:10.1130/G23106A.1

Williams, G.P., 1986. River meanders and channel size. Journal of Hydrology 88, 147–164.

Williamson, A.N., 1974. Mississippi river flood maps from ERTS-1 digital data. Journal of the American Water Resources Association 10, 1050–1059. doi:10.1111/j.1752-1688.1974.tb00624.x

Wohl, E., 2014. Time and the rivers flowing: Fluvial geomorphology since 1960. Geomorphology 216, 263–282. doi:10.1016/j.geomorph.2014.04.012

Wohl, E., 2015. Of wood and rivers: bridging the perception gap. WIREs Water 2, 167–176. doi:10.1002/wat2.1076Carroll, M.L., Townshend, J.R., DiMiceli, C.M., Noojipady, P., Sohlberg, R.A., 2009. A new global raster water mask at 250 m resolution. International Journal of Digital Earth 2, 291–308. doi:10.1080/17538940902951401

Wolman, M.G., 1955. The natural channel of Brandywine creek, Pennsylvania. United States Geological Survey Professional Paper 271.

Xu, H., 2006. Modification of normalised difference water index (NDWI) to enhance open water features in remotely sensed imagery. International Journal of Remote Sensing 27, 3025–3033. doi:10.1080/01431160600589179

Yamazaki, D., O'Loughlin, F., Trigg, M.A., Miller, Z.F., Pavelsky, T.M., Bates, P.D., 2014. Development of the Global Width Database for Large Rivers. Water Resour. Res. 50, 3467–3480. doi:10.1002/2013WR014664

Yamazaki, D., Trigg, M.A., 2016. Hydrology: The dynamics of Earth's surface water. Nature 540, 348–349.

Yan, D., Wang, X., Zhu, X., Huang, C., Li, W., 2017. Analysis of the use of NDWIgreen and NDWIred for inland water mapping in the Yellow River Basin using Landsat-8 OLI imagery. Remote Sensing Letters 8, 996–1005. doi:10.1080/2150704X.2017.1341664

Yang, K., Li, M., Liu, Y., Cheng, L., Duan, Y., Zhou, M., 2014. River Delineation from Remotely Sensed Imagery Using a Multi-Scale Classification Approach. IEEE Journal of Selected Topics in Applied Earth Observations and Remote Sensing PP, 1. doi:10.1109/JSTARS.2014.2309707

Yu, L.L., Liang, L., Wang, J., Zhao, Y., Cheng, Q., Hu, L., Liu, S., Yu, L.L., Wang, X., Zhu, P., Li, X.X., Xu, Y., Li, C., Fu, W., Li, X.X., Li, W., Liu, C., Cong, N., Zhang, H., Sun, F., Bi, X., Xin, Q., Li, D., Yan, D., Zhu, Z., Goodchild, M.F., Gong, P., 2014. Meta-discoveries from a synthesis of satellite-based land-cover mapping research. International Journal of Remote Sensing 35, 4573–4588. doi:10.1080/01431161.2014.930206

Zadeh, L.A., 1965. Fuzzy sets. Information and Control 8, 338–353. doi:http://dx.doi.org/10.1016/S0019-9958(65)90241-X

Zolezzi, G., Luchi, R., Tubino, M., 2012. Modeling morphodynamic processes in meandering rivers with spatial width variations. Reviews of Geophysics 50, RG4005. doi:10.1029/2012RG000392

Zuur, A., Ieno, E.N., Walker, N., Saveliev, A.A., Smith, G.M., 2009. Mixed effects models and extensions in ecology with R. Springer Science & Business Media.

Zuur, A.F., Ieno, E.N., Elphick, C.S., 2010. A protocol for data exploration to avoid common statistical problems. Methods in Ecology and Evolution 1, 3–14. doi:10.1111/j.2041-210X.2009.00001.x

Glossary of Terms

active channel width	the width perpendicular to stream flow direction of the active channel; a geomorphic feature typically defined by the edge of permanent vegetation and a break in bank slope (Lawlor, 2004), defined during and above winter base flows (Love and Taylor, 2004)
ArcGIS	a proprietary geographical information system developed by ESRI.
at-a-station	variation in channel characteristics (e.g. width, depth, velocity) at a channel cross-section. Cf. *downstream hydraulic geometry*.
bankfull width	river width as measured when water is at the top of the channel banks.
baseflow index (BFI)	quantifies the relative proportion of river flow that is derived from stored sources.
bifurcation	occurs where a single-stem river splits into multiple channels.
catchment area	the upstream surface area of all land draining into a given point along a river network. Also known as: drainage area, watershed.
colour infrared (CIR)	false-colour imagery comprised of three bands between the wavelengths of 0.5 to 0.9 μm, two from the visible light spectrum (green and red) and a near-infrared (NIR) band.
contouring	an approach frequently used in GIS analysis to abstract otherwise complex or large datasets into something that is more easily communicable. For example, consumer-focused maps, especially those that are available in hard copy, represent elevation with a vector, or contour, which indicates elevation change, in place of the original continuous raster dataset that shows elevation for each point of an area's surface.
CO_2 evasion	the transfer of carbon dioxide from one sink to another. In the context of this study, from inland waters to the atmosphere. Also known as: vertical transfer, vertical export, degassing, efflux.
discharge	the amount of water flowing in a channel expressed as a volume per unit of time.

downstream hydraulic geometry (DHG)	variation in channel characteristics (e.g. width, depth, velocity) along the length of a stream. Cf. *at-a-station*.
effective width	coined by Smith *et al.* (1996) to refer to the mean width along a river reach.
ephemeral river	a river or stream that only flows in the event of high magnitude events such as significant rainfall, ice melting etc. Cf. *perennial river*.
fuzzy classification	determines the proportion of different land cover classes within a mixed pixel. C.f. *hard classification*.
geographical information system (GIS)	GIS can alternatively refer to the academic study of geographical information science.
Geographically Weighted Regression (GWR)	a form of regression analysis that incorporates geospatial variation to explain the response variable.
hard classification	assigns a pixel to the most prevalent land cover class. C.f. *fuzzy classification*.
hydraulic geometry	the relation of channel characteristics (width, depth, velocity) to discharge, either *at-a-station* or *downstream.*
hydromorphology	the conflation of fluvial geomorphology and hydrology to create a more holistic view of river systems.
inland waters	a general term referring to both *lotic* (streams and rivers) and *lentic* (lakes and reservoirs) freshwater systems.
intermittent river	a river or stream where flow is not continuous all year. This term generally refers to all temporary, seasonal, episodic, and *ephemeral* rivers. Cf. *perennial river*.
***k*-folds cross-validation**	a test of the predictive capacity of a model, where input data is randomly divided into a user-defined number of subsets, or k-folds, of roughly equal size. One fold is reserved for model validation, while the chosen model (e.g. OLS MLR) is fit using all other subsets (k - 1 folds). For example, in 10-fold cross-validation, nine subsets are used to fit the model, with the one remaining subset used for model validation. This process is repeated until each subset has acted as the validation dataset.
lentic	standing freshwaters (lakes and ponds). Cf. *lotic*.
limnology	the study of *inland waters*.
lotic	freshwater systems where a unidirectional flow is induced by gravity (rivers and streams). Cf. *lentic*.

one-class classification (OCC)	an approach where only a single class of interest is used as the basis for classification training data, whereas a conventional classification approach would attempt to capture an authoritative sample of every land cover class, which is neither necessary nor efficient in situations where these other classes are not pertinent to the study objectives.
ordinary least squares (OLS)	the most commonly used approach to linear regression which minimises the sum of squared deviations (squared residuals) from the regression line.
perennial river	a river or stream where there is continuous flow at some point within the channel all year round. Cf. *ephemeral river*, *intermittent river*.
R	a cross-platform, free for use software environment used for statistical computing, analysis, and modelling. See: https://www.r-project.org/
soft classification	see *fuzzy classification*
super-resolution mapping (SRM)	the enhancement of the imagery to produce an output map of finer spatial resolution than the input imagery.
surface water	refers to all waters present on the Earth's surface, in contrast to atmospheric water and groundwater.
thalweg	the point of lowest elevation in a channel's cross-section
variance inflation factor (VIF)	a commonly used approach for testing multicollinearity in regression analysis.
water surface width (WSW)	cross-sectional width measured at the air-water interface, perpendicular to the direction of flow, from water's edge to water's edge.
wetted width	see *water surface width*

Appendix

A.1 Workflow Diagrams

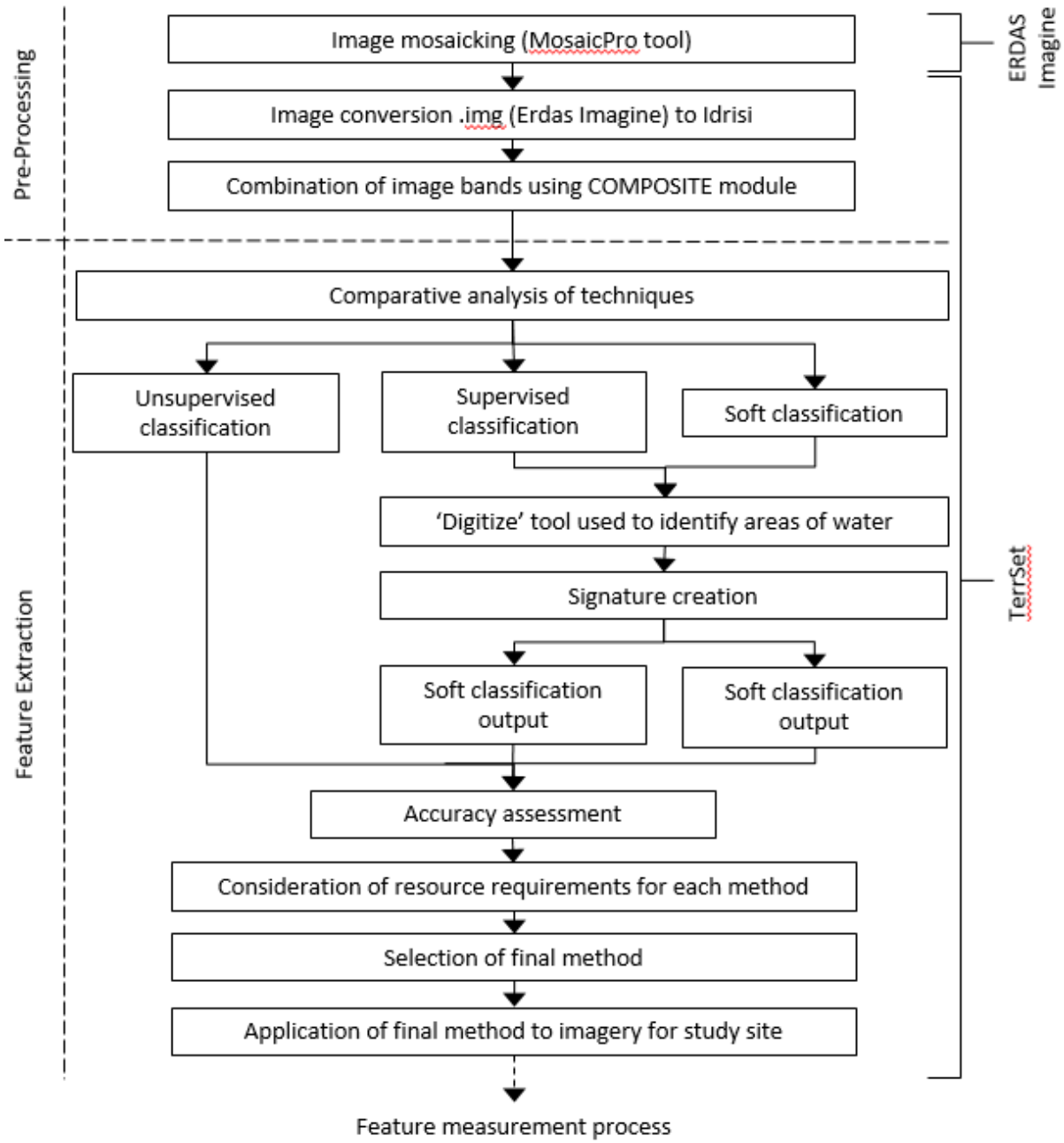


Figure A.1.1 Process for the comparative analysis of techniques for the extraction of surface waters from aerial imagery

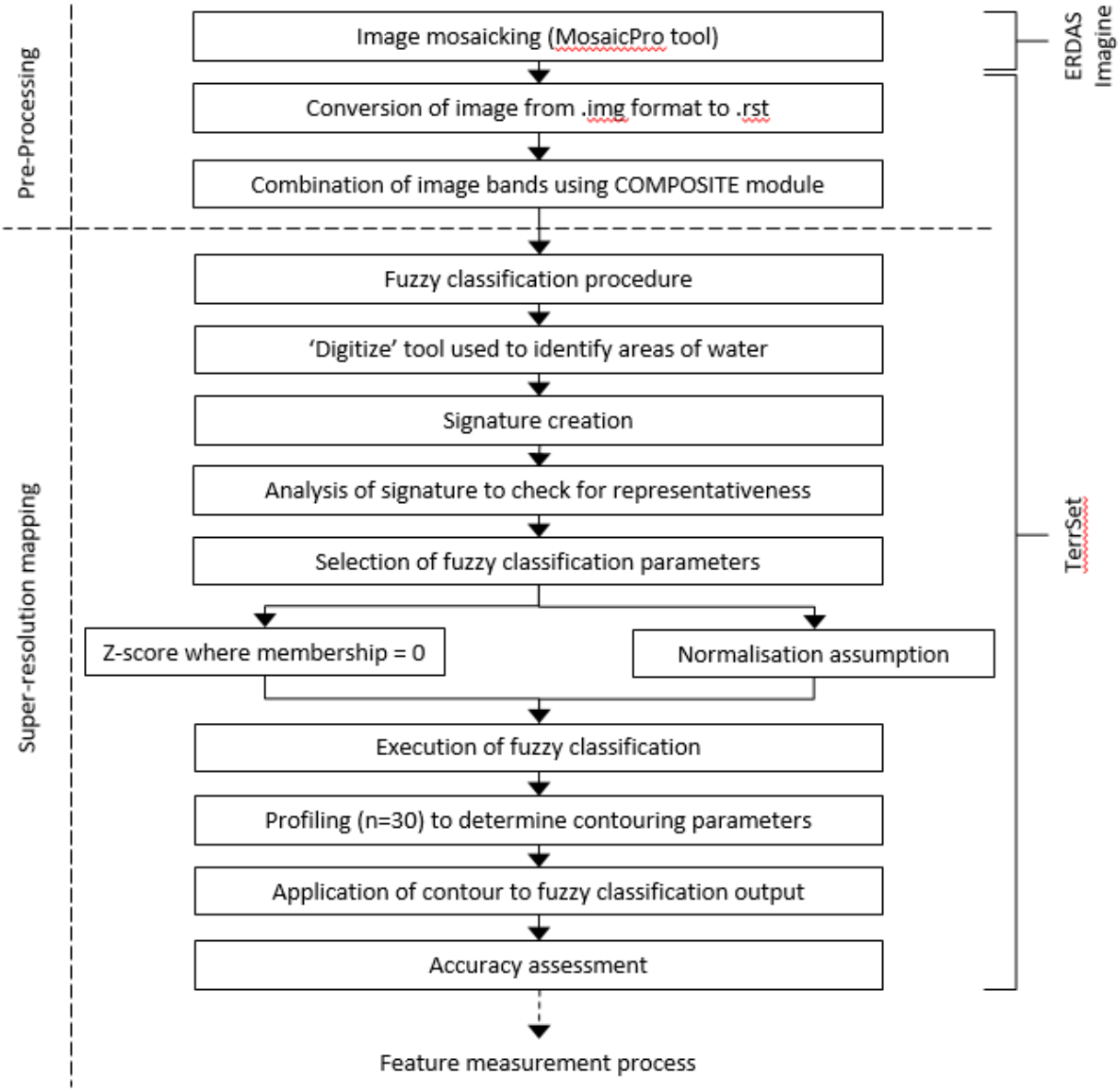


Figure A.1.2 Process for the super-resolution mapping of surface waters from aerial imagery

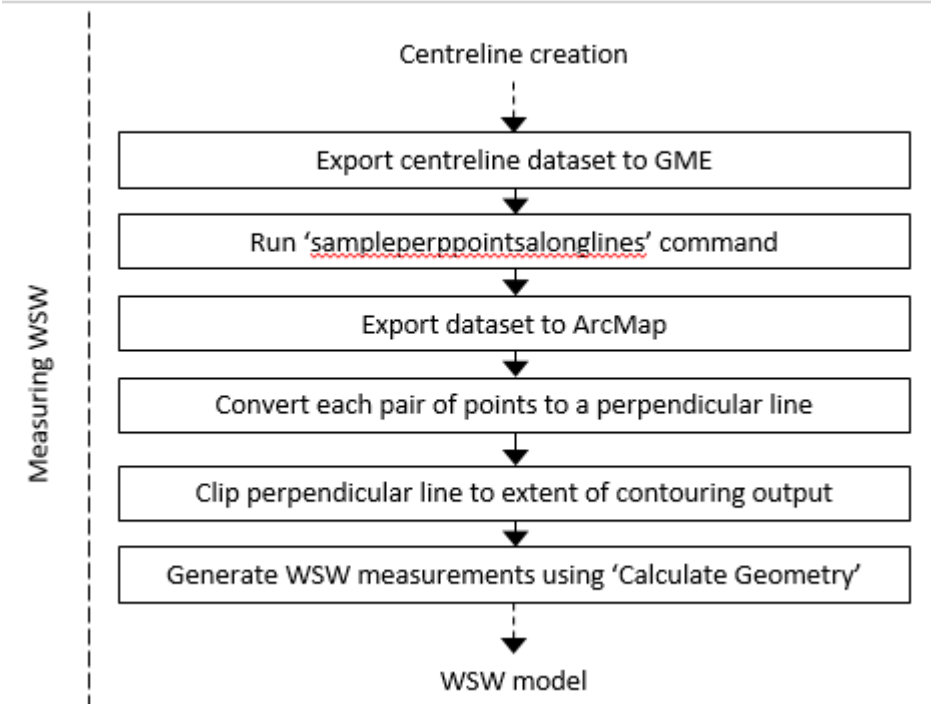


Figure A.1.3 Summary of the process for the measurement of SRM-derived surface waters

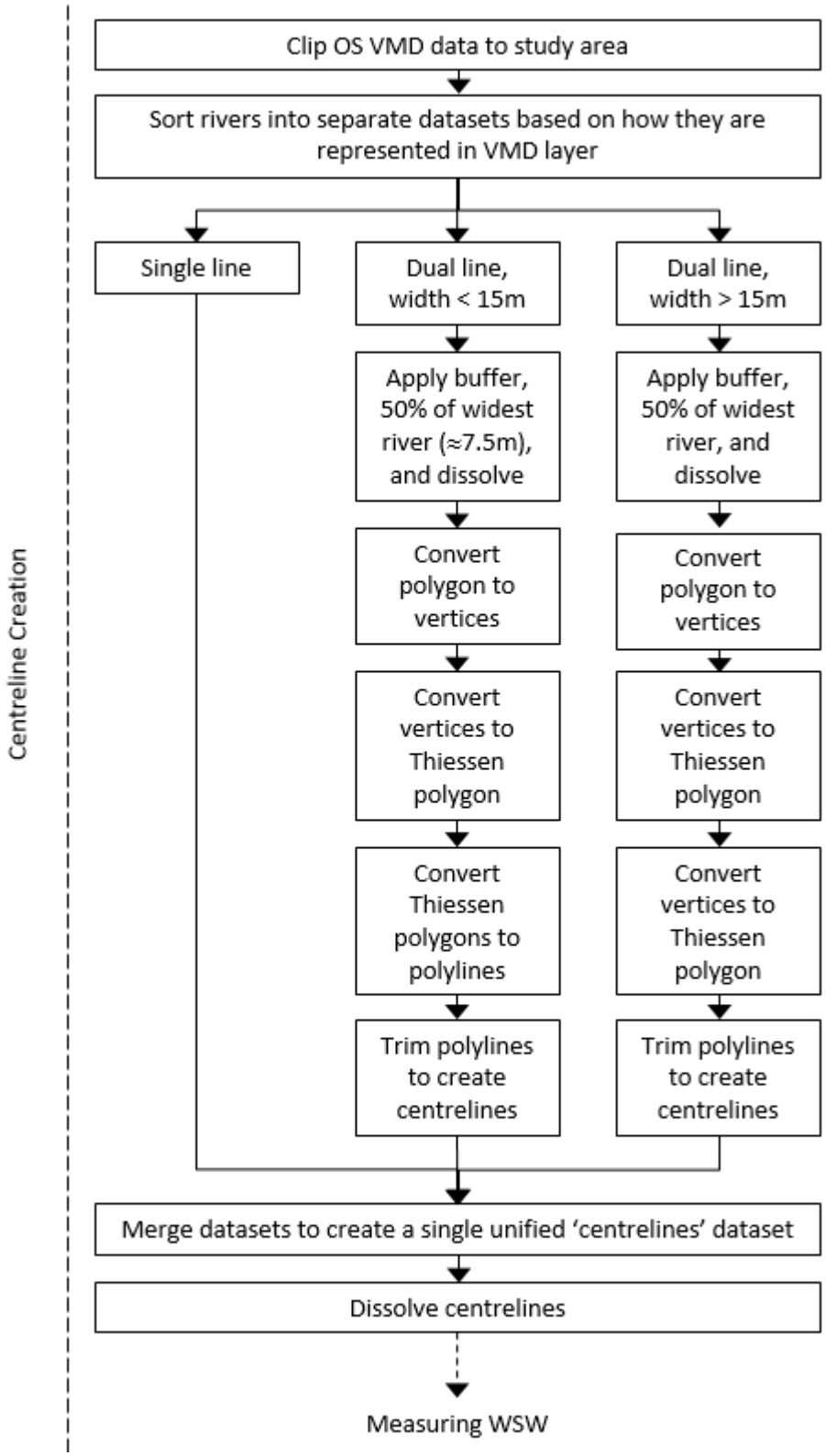


Figure A.1.4 Process for the creation of river centrelines

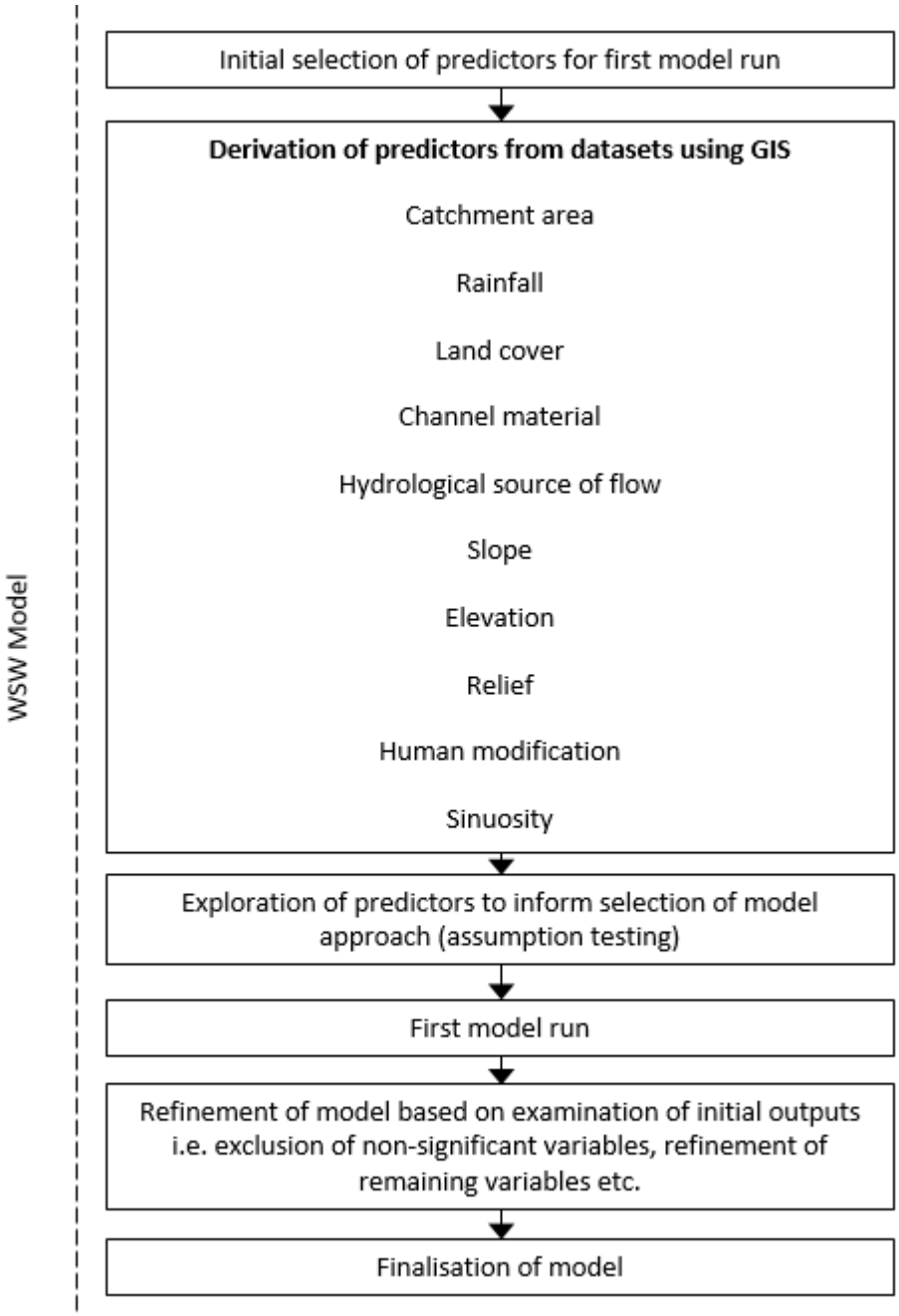


Figure A.1.5 Process for the predictive modelling of WSW

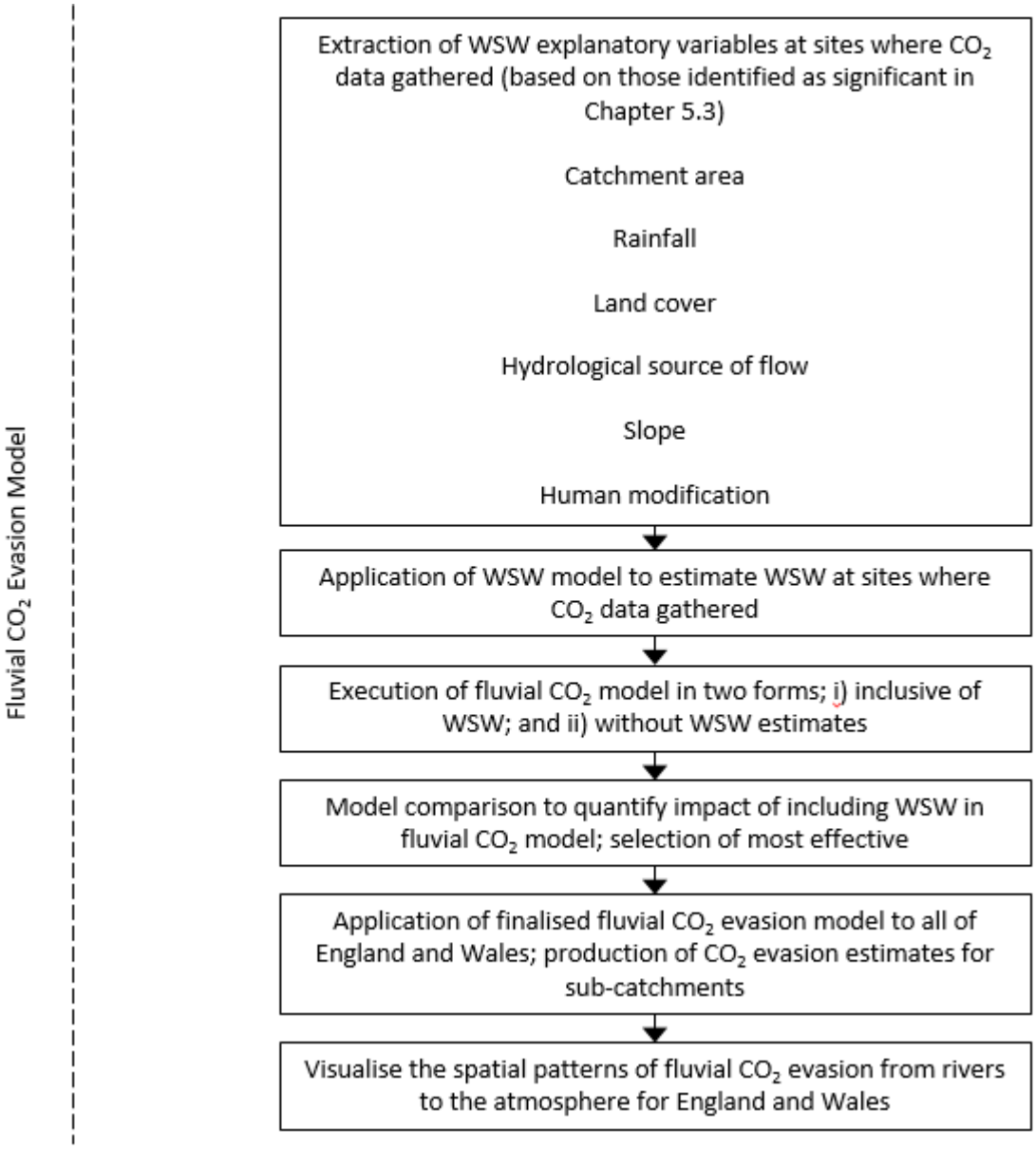


Figure A.1.6 Process for the estimation of fluvial CO_2 evasion in England and Wales

A.2 R plot(lm) output for minimal adequate multiple linear regression model of WSW

The below figures relate to Section 5.3 (p.134), which discussed results from the MLR process. The below were generated by running the plot(lm) function in R, a process which forms a significant part of the model verification process.

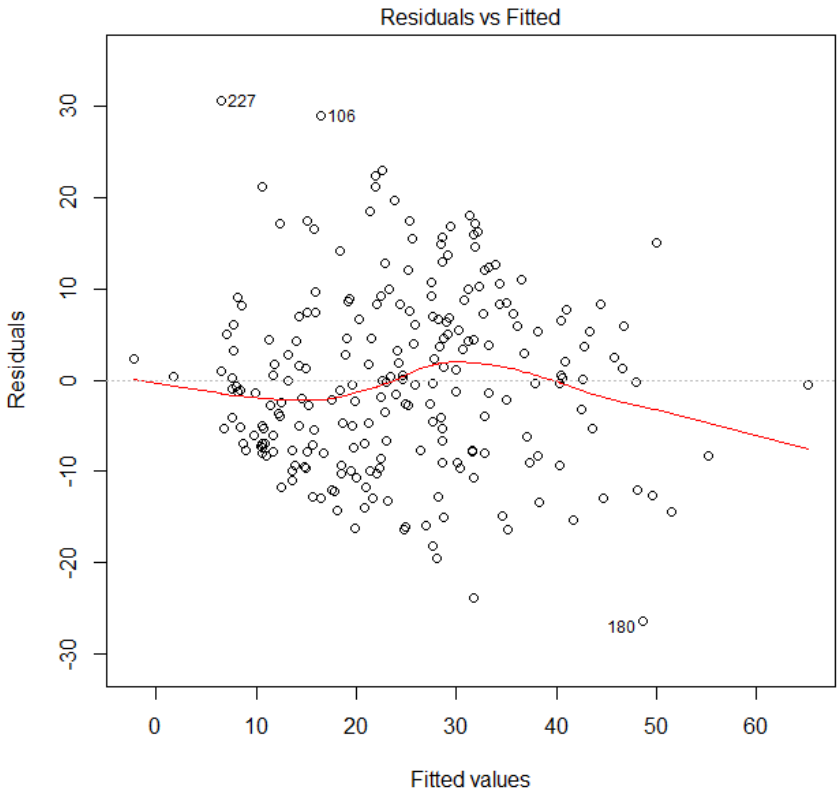


Figure A.2.1 Test for random distribution of residuals versus the fitted values for the minimal adequate MLR model of WSW

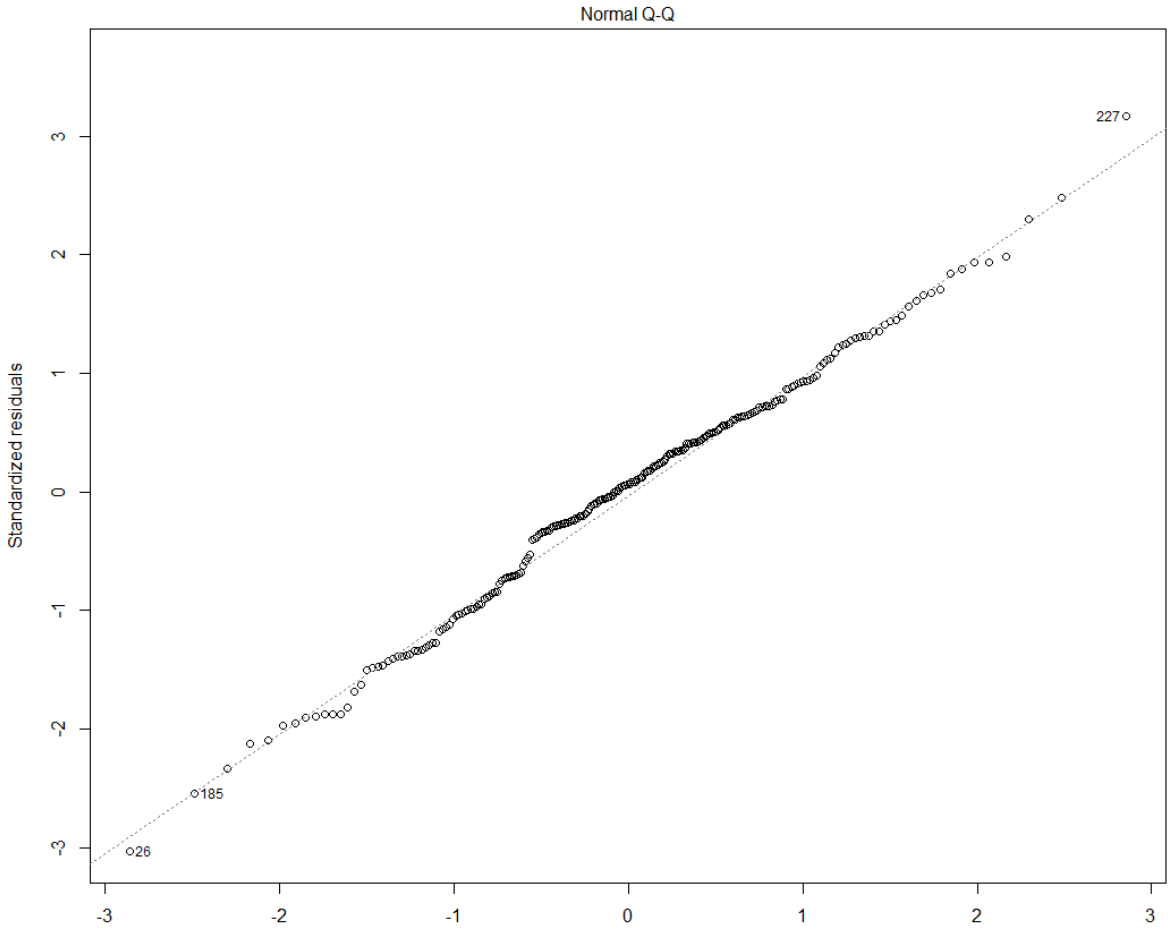


Figure A.2.2 Q-Q plot for the minimal adequate MLR model of WSW

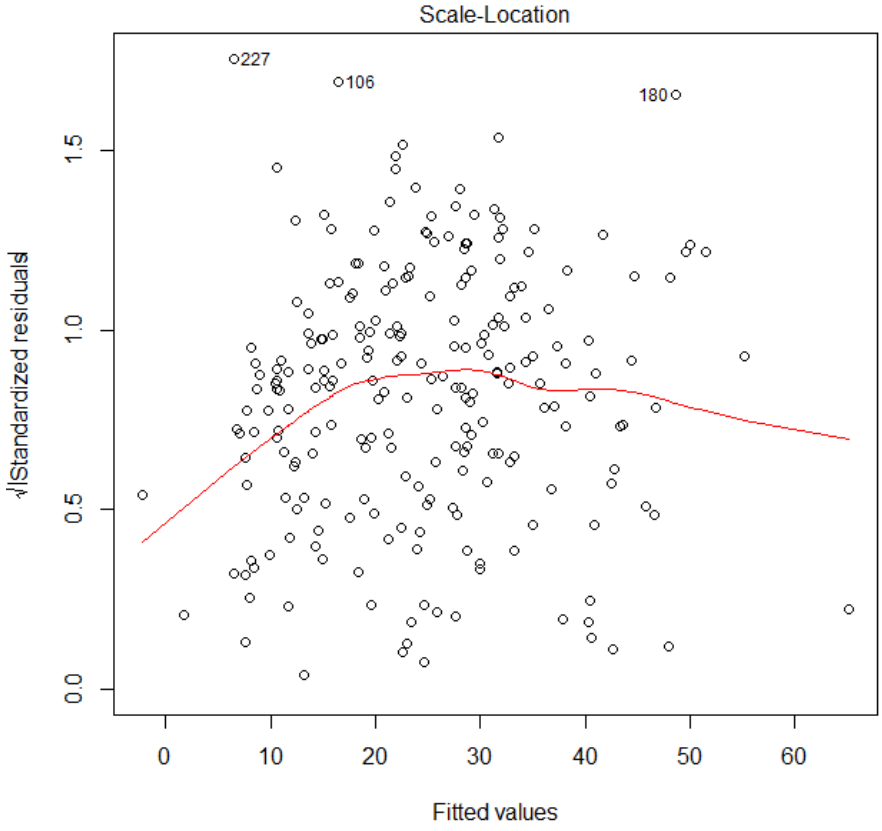


Figure A.2.3 Scale-location plot for the minimal adequate MLR model of WSW

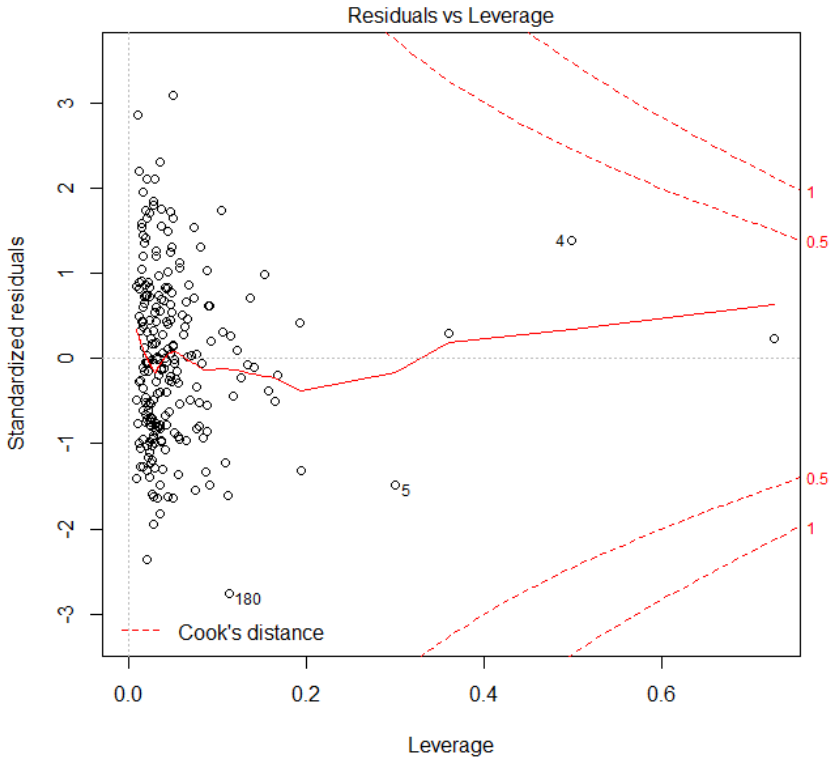


Figure A.2.4 Cook's distance plot for the minimal adequate MLR model of WSW